International Symposium on Physics of
New Quantum Phases in Superclean Materials

PSM2010

PROGRAM and ABSTRACTS

March 9–12, 2010
Hamagin Hall "VIA MARE"
Yokohama, Japan

http://kelvin.phys.s.u-tokyo.ac.jp/psm2010/

International Symposium on Physics of New Quantum Phases in Superclean Materials

PSM2010

国際シンポジウム

「スーパークリーン物質で実現する新しい量子相の物理（PSM2010）」

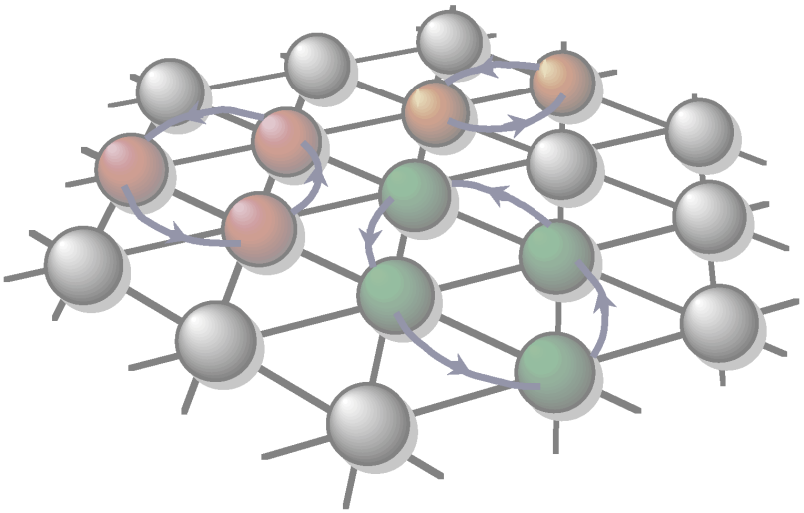

March 9-12, 2010

Hamagin Hall "VIA MARE"

Yokohama, Japan

Committees

Organizing Committee

Hiroshi Fukuyama	The University of Tokyo	: Chair
Osamu Ishikawa	Osaka City University	: Program Chair
Masatoshi Imada	The University of Tokyo	
Yoshiteru Maeno	Kyoto University	
Tsutomu Momoi	RIKEN	
Yuichi Okuda	Tokyo Institute of Technology	
Keiya Shirahama	Keio University	
Makoto Tsubota	Osaka City University	
Masahito Ueda	The University of Tokyo	
Nobuo Wada	Nagoya University	

Advisory Committee

Hidetoshi Fukuyama	Tokyo University of Science
Yasuhiro Iye	ISSP, University of Tokyo
Kimitoshi Kono	RIKEN
Anthony J. Leggett	University of Illinois at Urbana-Champaign
Takao Mizusaki	Toyota Physical and Chemical Research Institute
Douglas D. Osheroff	Stanford University

Local Arrangements

Tomohiro Matsui	The University of Tokyo
Yoriko Hayashi	The University of Tokyo
Naoki F. Kawai	The University of Tokyo
Kayoko Ogita	The University of Tokyo

Sponsors

Main sponsor : Grant-in-Aid for Scientific Research on Priority Areas
"Physics of New Quantum Phases in Superclean Materials"

Cosponsors : Global Center of Excellence for Physical Sciences Frontier
: Institute for the Physics and Mathematics of the Universe
: Japan Society for the Promotion of Science
: Yokohama Convention and Visitors Bureau

主　　催 : 文部科学省科学研究費補助金特定領域
「スーパークリーン物質で実現する新しい量子相の物理」

協　　賛 : 東京大学グローバル COE
: 数物連携宇宙研究機構
: 独立行政法人　日本学術振興会
: 財団法人　横浜観光コンベンション・ビューロー

PROGRAM

March 9 (Tuesday)

9:30-9:50 Opening

9:50-10:50 Session 1

9:50-10:20	Makoto Tsubota	**O1**	Quantum Turbulence and Nonlinear Phenomena in Quantum Fluids
10:20-10:50	Vanderlei S. Bagnato	**O2**	Excitations and Characterization of Quantum Turbulence in an Atomic Superfluid

10:50-11:10 Break

11:10-12:50 Session 2

11:10-11:40	Andrei I. Golov	**O3**	Turbulence in Superfluid ^{4}He at Low Temperatures: Experimental Advances
11:40-12:00	Hideo Yano	**O4**	Vortex Dynamics in Steady Quantum Turbulence of Superfluid ^{4}He at the Turbulent-to-Laminar Transition
12:00-12:20	Masahiko Machida	**O5**	Massively-Parallel Simulations for Quantum Turbulence：Current Development and New Insights
12:20-12:50	Yuichi Okuda	**O6**	Thermal and quantum crystallizations of ^{4}He in aerogel

12:50-14:10 Lunch

14:10-15:50 Session 3

14:10-14:40	Keiya Shirahama	**O7**	Towards a New Physics of Nanoscale Helium
14:40-15:00	Masaru Suzuki	**O8**	Superfluidity of ^{4}He Confined in One-dimensional Channel under Pressure
15:00-15:30	Nobuo Wada	**O9**	One-Dimensional Phonon State and Superfluidity of ^{4}He Fluid Nanotubes
15:30-15:50	Dai Hirashima	**O10**	Superfluid density in quasi-one-dimensional boson systems

15:50-16:20 Break

16:20-18:00 Session 4

16:20-16:50	Sébastien Balibar	**O11**	The enigma of supersolidity
16:50-17:20	Eun-Seong Kim	**O12**	Can supersolidity be suppressed in stiffened solid ^{4}He ?
17:20-17:40	Yutaka Sasaki	**O13**	Simultaneous Measurement of Torsional Oscillator and NMR of Extremely Diluted ^{3}He in Solid ^{4}He
17:40-18:00	Yoshiyuki Shibayama	**O14**	Non-Classical Rotational Inertia in Two-Dimensional ^{4}He Solid on Graphite

18:00-20:00 Poster Session (odd numbers)

March 10 (Wednesday)

9:30-10:50 Session 5

9:30-10:00	Masatoshi Imada	**O15**	Novel quantum phenomena emerging near quantum critical points -Achievements made by five-year project-
10:00-10:30	Thierry Giamarchi	**O16**	Localized spins systems as quantum simulators of interacting fermions and bosons
10:30-10:50	Yukitoshi Motome	**O17**	Spin-charge interplay in frustrated itinerant systems

10:50-11:10 Break

11:10-12:50 Session 6

11:10-11:40	Suchitra Sebastian	**O18**	Fermi surface reconstruction and approach to a metal-insulator QCP in the underdoped cuprates
11:40-12:00	Satoru Nakatsuji	**O19**	Quantum Criticality in the Valence Fluctuating Superconductor β-$YbAlB_4$
12:00-12:20	Kazuya Miyagawa	**O20**	Neutral-Ionic Phase Transition in TTF-CA under Pressure
12:20-12:50	John Saunders	**O21**	Anomalous "superfluid" response of ^{4}He films on graphite; a 2D supersolid ?

12:50-14:10 Lunch

14:10-15:50 Session 7

14:10-14:40	Douglas D. Osheroff	**O22**	**[PSM lecture]** Our Struggle to Understand Nuclear Spin Ordering in BCC Solid ^{3}He
14:40-15:10	Hiroshi Fukuyama	**O23**	Novel Quantum Phases in 2D ^{3}He on Graphite
15:10-15:30	Masao Ogata	**O24**	Phase Diagram of the Triangular *t-J* Model in the Doped-Mott Region: Effects of Ring Exchange Interactions
15:30-15:50	Takeo Takagi	**O25**	Stability of 4/7 Phase of He Adsorbed on Graphite

15:50-16:20 Break

16:20-18:00 Session 8

16:20-16:50	Tsutomu Momoi	**O26**	Magnon pairing and crystallization in the triangular-lattice ring-exchange model
16:50-17:20	Claire Lhuillier	**O27**	Exotic ground-states on the kagome lattice
17:20-17:40	Hirokazu Tsunetsugu	**O28**	Exotic Phases of Frustrated Systems
17:40-18:00	Yasuhiro Hatsugai	**O29**	Quantum/Spin liquids, geometrical phases and edge states

18:00-20:00 Poster Session (even numbers)

March 11 (Thursday)

9:30-10:50 Session 9

9:30-10:00	Masahito Ueda	**O30**	Topological Excitations in Bose-Einstein Condensates
10:00-10:30	Tin-Lun Ho	**O31**	Strongly Correlated "Materials" made out of Ultra Cold Atoms
10:30-10:50	Takuya Hirano	**O32**	Spin-dependent inelastic collisions in spin-2 Bose-Einstein condensates

10:50-11:10 Break

11:10-12:50 Session 10

11:10-11:50	Anthony J. Leggett	**O33**	**[PSM lecture]** Topological Quantum Computing in Fermi Superfluids and Strontium Ruthenate: Prospects and Problems
11:50-12:20	Shaun N. Fisher	**O34**	Experiments on a pure superfluid condensate: ^{3}He at ultralow temperatures
12:20-12:50	Suk Bum Chung	**O35**	Detecting the Majorana fermion surface state of ^{3}He-B through spin relaxation

12:50-14:00 Lunch

14:00-15:50 Session 11

14:00-14:30	Osamu Ishikawa	**O36**	New Features of Anisotropic Superfluid ^{3}He
14:30-14:50	Akira Yamaguchi	**O37**	Mechanical Spin Pump and Spin Relaxation in Superfluid ^{3}He-A_1
14:50-15:10	Rhuji Nomura	**O38**	Surface Andreev Bound States and Surface Majorana States on the Superfluid ^{3}He B Phase
15:10-15:30	Seiji Higashitani	**O39**	Boundary and Impurity Effects on Fourth Sound Propagation in Superfluid ^{3}He
15:30-15:50	Kazumasa Miyake	**O40**	Theory for *d*-Vector in Spin-Triplet Superconductor Sr_2RuO_4

16:30-19:00 Banquet

16:30	meeting at Osanbashi Yokohama International Passenger Terminal
17:00-19:00	Yokohama Bay Dinner Cruise

March 12 (Friday)

9:30-10:50 Session 12

9:30-10:00	Yoshiteru Maeno	**O41**	Novel Quantum Phenomena in Superconducting Sr_2RuO_4
10:00-10:20	Hiroshi Kambara	**O42**	Unconventional Local Transport Characteristics in Microfabricated Sr_2RuO_4-Ru eutectic crystals
10:20-10:40	Fumihiko Nakamura	**O43**	External-fields induced novel phenomena in Mott insulator Ca_2RuO_4

10:40-11:00 Break

11:00-11:50 Session 13

11:00-11:30	Alexander A. Golubov	**O44**	Odd-frequency pairing in superconducting heterostructures
11:30-11:50	Yukio Tanaka	**O45**	Odd-frequency pairing in spin-triplet superconductor junctions

11:50-12:20 Closing

Poster Presentations

Odd numbers: March 9 (Tuesday)
Even numbers: March 10 (Wednesday)

P1	Naoki F. Kawai	STM/STS Studies of Epitaxially Grown Graphene on SiC
P2	Tomohiro Matsui	Topological Dirac Fermion on Graphite
P3	Mitsuhiro Arikawa	Stability of zero-mode edge states with n=0 Landau level in graphene
P4	Kohei Sasaki	Pseudospin Phase Transitions during Crossing of Partially Filled Landau Levels in a Si Quantum Well
P5	Akira Fukuda	Commensurate-like to Incommensurate-like Phase Transition in the Layer Imbalanced Bilayer ν=1/3 Quantum Hall States under In-plane Magnetic Field
P6	Yangdong Zheng	Spin and Pseudospin Excitations in ν=2/3 Bilayer Quantum Hall Systems
P7	Anju Sawada	Superconductor-like Phenomenon in the Bilayer ν=1 Quantum Hall State
P8	Tomoki Morikawa	Activation energy gap in the ν_T=1 bilayer Quantum Hall States with small tunneling energy
P9	Toshikazu Arai	Anomaly in Edgemagneto-plasmon Resonance Line Width of Helium Surface State Electrons
P10	Shintaro Takayoshi	Ferromagnetic State and Spin Correlation Functions in Spin-1/2 Bose and Fermi Gases
P11	Masafumi Udagawa	Effects of spin-orbit coupling and electron correlation on Van-Vleck susceptibility in transition metal compounds
P12	Kiyohide Nomura	Theory of commensurate-incommensurate transition
P13	Shiro Sakai	Spectral structure of hole- and electron-doped cuprates: Roles of zeros of Green's function
P14	Hisatoshi Yokoyama	Variational Monte Carlo Studies of Hubbard-type Systems
P15	Kyoya Nakamikawa	Variational Monte Carlo study of partial Kondo screening in frustrated Kondo lattice systems
P16	Hiroaki Ishizuka	Electronic State of Charge Frustrated Systems with "Ice-rule" Constraint
P17	Junki Yoshitake	Self-organized cluster formation in frustrated multi-orbital systems
P18	Yu Yoshioka	Microscopic Origin of Nematic Phase
P19	Shigeki Onoda	Quantum Melting of Spin Ice to Spin Smectic
P20	Masahiko Hayashi	Topological Defects and Spectral Flow in the Dynamics of Electronic Condensate: The Case of Charge Density Waves
P21	Hiroshi Shinaoka	Soft Hubbard gaps under coexisting short-range interaction and disorder: application to electron transport in organic field-effect transistors

Odd numbers: March 9 (Tuesday)
Even numbers: March 10 (Wednesday)

P22	Masafumi Udagawa	Quantum criticality in an itinerant electron system coupled to ice-rule variables
P23	Shinji Watanabe	On Anomalous Criticalities in Paramagnetic Metals in Ce- and Yb-Based Systems
P24	Takahiro Misawa	Spin Fluctuation Theory for Quantum Tricritical Point: Applications to Heavy-Fermion Systems, $YbRh_2Si_2$, $CeRu_2Si_2$, and β-$YbAlB_4$
P25	Yosuke Matsumoto	Zero-Field Quantum Criticality in the Heavy Fermion Superconductor β-$YbAlB_4$
P26	Akiko Masaki	Mott Transition of Bose-Fermi Mixtures in Optical Lattices Induced by Attractive Interactions
P27	Kazushi Kanoda	Mott physics revealed by triangular-lattice organics
P28	Youhei Yamaji	Cofermion Theory for Changes in Fermi-Surface Topology of Doped Mott Insulators
P29	Shigeki Fujiyama	Orbital driven spin-Peierls transition in pyrochlore $Tl_2Rh_2O_7$
P30	Ryuichi Masutomi	Cyclotron resonance in the two dimensional metallic phase of Si/SiGe
P31	Daisuke Sato	Dimensional Crossover of ^{3}He Self-Condensation from 2D to 3D
P32	Hidehiko Ishimoto	Two-dimensional Solid ^{3}He in High Magnetic Fields
P33	Masashi Morishita	Thermal Conductivity of ^{3}He Solid Films on Graphite in Weak Magnetic Fields
P34	Masashi Morishita	Magnetization Measurements and Surface Observation of Grafoil Substrate
P35	Sachiko Nakamura	Towards Experimental Determination of the Structure of the 4/7 Phase in the Second-Layer Helium on Graphite
P36	Ryota Masumoto	Dynamical Transition and Self-Organized Criticality in Crystallization of ^{4}He in Aerogel
P37	Takehide Miura	Magnetic phase transitions of bcc solid ^{3}He
P38	Kota Takahashi	Phase diagram of S=1 bilinear-biquadratic chains with a single-ion anisotropy
P39	Taiyo Harada	Field-Induced Magnetic Orderings of S=1/2 Bond-Alternating Antiferromagnetic Chain F_5PNN
P40	Masahiro Sato	How to detect magnetic multipolar liquid phase in spin-1/2 frustrated ferromagnetic chains under magnetic field
P41	Kiyomi Okamoto	Anomalous Behavior of the Magnetization Plateau Width of an S=1/2 Isosceles Triangle Spin Nanotube
P42	Keigo Kobayashi	Analysis of Commensurate and Incommensurate State on Triangular Lattice Spin System with Transfer Matrix Method

P43	Takahiro Misawa	Chiral and BKT transitions in triangular-lattice Heisenberg models: Critical behavior near the $O(3)$ isotropic case
P44	Masanori Kohno	Quasiparticles in spatially anisotropic triangular antiferromagnets
P45	Tomoya Higo	Structural disorder effects of 2D triangular antiferromagnets isostructural to $NiGa_2S_4$
P46	Masafumi Tamura	Correlation between the Quantum Behavior and Lattice Anisotropy in a Frustrated Triangular Spin System, the $Pd(dmit)_2$ Salts
P47	Toru Sakai	Anomalous Magnetization Process of the S=1/2 Kagome Lattice Antiferromagnet
P48	Ryui Kaneko	Magnetic Properties of a Spatially Distorted Heisenberg Kagome Antiferromagnet
P49	Minoru Kubota	Quantized Vortex State and Torsional Oscillator Study on hcp ^{4}He under AC and DC Rotation
P50	Ryo Toda	Simultaneous Measurement of Torsional Oscillator and NMR of Extremely Diluted ^{3}He in Solid ^{4}He
P51	Keisuke Yamamoto	Successive phase transitions at finite temperatures toward the supersolid state in a three-dimensional extended Bose-Hubbard model
P52	Masaya Kunimi	Superflow of one-dimensional supersolid past an obstacle
P53	Takayuki Kogure	Supersolid Behaviors in Thin Solid ^{4}He Films Adsorbed on Nanoporous Media
P54	Aaron M. Koga	Torsional Oscillator Study for ^{4}He Growth on Graphite
P55	Tomoki Minoguchi	New dynamics of He-4 films on graphite -- Superfluid dynamics coupled with solid bilayer --
P56	Hajime Kobayashi	Mechanical Response of ^{4}He films Adsorbed on Graphite with a Quartz Tuning Fork
P57	Masahiro Wasai	Superfluid Transition of ^{4}He Film Pressurized by Bulk Liquid ^{3}He
P58	Takuya Oda	QCM Study of Superfluid Transition in ^{3}He-^{4}He Mixture Films
P59	Mitsunori Hieda	Vortex Dynamics of 2D Superfluid in ^{4}He and ^{3}He-^{4}He Films
P60	Mitsuaki Tsukamoto	Numerical Study of Bose-Hubbard Model in Restricted Geometry
P61	Taku Matsushita	Helium Fluid Adsorbed in 1.5 nm One-Dimensional Straight Pores
P62	Hajime Kiriyama	Path integral calculation of ^{4}He in quasi-one-dimensional channels
P63	Thomas E. Eggel	Quantum Phase Transition of ^{4}He in Nanoporous Gelsil Glass

P64	Yusuke Minato	Pore-size Dependence of Superfluidity of ^{4}He in 1D-Nanopores FSM
P65	Junko Taniguchi	Phase Diagram of ^{4}He Confined in 1D Nano-Porous Media
P66	Yuna Nakashima	State of ^{4}He Adsorbed in Three-Dimensional Nanopores of ZTC with 3D-period 1.4nm
P67	Kouhei Yamashita	Superfluid density of ^{4}He confined in nanopores
P68	Kazuhiro Sahashi	Quantum Clusters of Helium Formed in Nanocage in Na-Y Zeolite
P69	Shuichiro Kiyota	Size Effect on Superfluid Transition of ^{4}He Films in Thin Porous Gold
P70	Keiya Shirahama	Superfluid ^{4}He in a Porous-Alumina Nanopore Array
P71	Naoki Yamanaka	Quantum Superfluid Transition of ^{4}He Confined in a Regular Nanoporous Structure
P72	Yusuke Nago	Quantized Vortices Generated in Turbulent Region of Superfluid ^{4}He at High Temperatures
P73	Yusuke Nago	Generation of Quantum Turbulence in Superfluid ^{4}He using a Quartz Tuning Fork
P74	Ryu Numasato	Direct Energy Cascade in Two-Dimensional Compressible Quantum Turbulence
P75	Shoji Fujiyama	Analysis of vortex line density fluctuations and size distribution of quantum turbulence
P76	Daisuke Takahashi	Quantized vortex nucleation by 2D snowballs below the free surface of ^{4}He
P77	Yukie Miura	Detection Technique for Kelvin Waves on Vortex Lines in Superfluid ^{4}He
P78	Yusuke Fujihara	Superfluid Properties of Fermi Atoms in Optical Lattices
P79	Akihisa Koga	Polarized superfluid state in a fermionic optical lattice
P80	Emiko Arahata	Propagation of second sound in a superfluid Fermi gas in the unitary limit
P81	Yusuke Kato	Stability Criterion of Superfluidity with Dynamical Density Fluctuations
P82	Takashi Kashimura	Superfluid/ferromagnet/superfluid-junction and π-phase in a superfluid Fermi gas with population imbalance
P83	Hiroki Saito	Ferrofluidity in dipolar Bose-Einstein condensates
P84	Michikazu Kobayashi	Vortex Tiling in Spinor Condensates
P85	Hiroki M. Adachi	Textures and Vortices in *d*-Wave Fermi Condensates in Atomic Gases
P86	Tatsuyoshi Tanabe	Experimental study on the ground-state phase of ^{87}Rb spin-2 Bose-Einstein condensate

P87	Yoshihisa Taguchi	Mixing dynamics of binary ^{87}Rb Bose-Einstein condensates
P88	Satoshi Tojo	Controlling phase separation of binary Bose-Einstein condensates
P89	Ryosuke Shibato	Phase separation of multi-component Bose-Einstein condensates induced by a homonuclear Feshbach resonance
P90	Nobukuni Hamamoto	Cranked-Hartree-Fock-Bogoliubov theory for Fragmented Bose-Einstein Condensates
P91	Masaki Tezuka	Effect of confinement geometry on imbalanced Fermi condensates
P92	Norio Kawakami	Quantum-Quench Dynamics of Ultracold Fermions in Optical Superlattice
P93	Yuki Endo	Equilibrium Properties of a Trapped Dipolar Fermion at Finite Temperatures
P94	Seiichiro Suga	Three-component Fermionic Atoms in Optical Lattices
P95	Takeshi Ozaki	Excitation Spectrum of a Bose-Bose mixture in an Optical Lattice
P96	Shohei Watabe	Tunneling Problems of Excitations in Spin-1 Bose-Einstein Condensates
P97	Naoya Suzuki	Interface instabilities in two-component Bose-Einstein condensates
P98	Daisuke Takahashi	Transmission properties of Bogoliubov excitations near and at the critical current state
P99	Atsushi Motohashi	Thermalization of Atom-Molecule Bose gases in a Double-Well Potential
P100	Kenichi Kasamatsu	D-branes in Bose-Einstein condensates
P101	Pascal Naidon	Efimov physics with three lithium atoms
P102	Hiromitsu Takeuchi	Kelvin Helmholtz Instability in Atomic Bose-Einstein Condensates
P103	Shunji Tsuchiya	Theory of photoemission spectroscopy of Fermi gases in the BCS-BEC crossover
P104	Shintaro Taie	Ultracold Fermi Gases of Ytterbium in Optical Lattices
P105	Ken Obara	Frictional Motion of Superfluid ^{3}He Normal Fluid Component in Aerogel
P106	Ryusuke Kado	Phase Separation in A-like and B-like Phase of Superfluid ^{3}He in Aerogel
P107	Chiaki Kato	Fourth Sound Resonance of Superfluid ^{3}He in Slab Geometry
P108	Satoshi Murakawa	Measurements of Transverse Acoustic Impedance of Superfluid ^{3}He in Non-Unitary Phases at High Magnetic Fields
P109	Masamichi Saitoh	Magnetic Field Dependence of Dissipative Flow in Superfluid ^{3}He Films

P110	Takuto Kawakami	Singular and Half-Quantum Vortices in Superfluid ^{3}He-A between Parallel Plates
P111	Masatomo Kanemoto	Decaying Process of Persisitent Precessing Domain in Superfluid ^{3}He-B
P112	Takeshi Mizushima	Surface Andreev Bound States in Superfluid ^{3}He-B
P113	Satoshi Murakawa	Surface Majorana Cone of the Superfluid ^{3}He B Phase on a Partially Specular Wall
P114	Yasumasa Tsutsumi	Stable Textures and Majorana Zero Modes in Trapped *p*-Wave Resonant Superfluidity of Atomic Fermi Gases
P115	Takeshi Mizushima	Zero Energy Majorana States in Spinless Chiral *p*-wave Superfluids with Plural Vortices
P116	Yoshitomo Karaki	Low temperature magnetization hysteresis anomalies in Sr_2RuO_4
P117	Takuji Nomura	Effects of spin-orbit interaction on magnetism and spin-triplet superconductivity in Sr_2RuO_4
P118	Kenichi Tenya	Magnetization and Magnetocaloric Studies on the Spin-Triplet Superconductivity in Sr_2RuO_4
P119	Kenji Ishida	Nuclear-Magnetic-Resonance Measurements on Sr_2RuO_4 in a precisely Controlled Magnetic Field
P120	Hiroaki Ikeda	*ab* initio calculation of *d*-vector in spin-triplet superconductor Sr_2RuO_4
P121	Shunichiro Kittaka	Enhancement of T_c to 3 K by applying uniaxial pressure to Sr_2RuO_4
P122	Yasuhiro Asano	Surface Impedance of Spin-triplet NS junctions
P123	Ryoji Nakagawa	Interference between Sr_2RuO_4 and *s*-wave superconductors
P124	Youichi Yanase	Microscopic Theory of D-vector in Spin Triplet Superconductors
P125	Kenji Kobayashi	Interplay between Antiferromagnetism and Superconductivity in the Two-Dimensional Hubbard model within a Variational study
P126	Sadashige Matsuo	STM/STS Studies of Superconducting Ultra-Thin Indium Films on Graphite
P127	Markus Kriener	Superconductivity in the noncentrosymmetric system $Li_2(Pd_{1-x}Pt_x)_3B$
P128	Darren C. Peets	The Noncentrosymmetric *d*-Electron Superconductors $CaIrSi_3$ and $CaPtSi_3$
P129	Kenta M. Suzuki	Theoretical study on the field dependence of the FFLO state
P130	Yuki Fuseya	Meissner Effect of the Odd-Frequency Superconductivity
P131	Naoki Horie	Magnetic Field Induced Crossover in the Yb-based Heavy-Fermion System α-$YbAlB_4$

P132	Shingo Yonezawa	Heat Capacity Study of the Quasi-One-Dimensional Organic Superconductor $(TMTSF)_2ClO_4$ in Accurately Aligned Magnetic Fields
P133	Akihisa Okada	Effect of Long-Range Impurity Potential on Superconductivity
P134	Yuji Aoki	Pr site imperfection effect and doping effect on the spontaneous internal fields in the heavy fermion superconductor $PrOs_4Sb_{12}$
P135	Ryoichi Miyazaki	Heavy Fermion Superconducting Properties of the Filled Skutterudite $Pr(Os_{1-x}Ru_x)_4Sb_{12}$
P136	Kohta Saitoh	Noncontact Friction by Low Temperature Lateral Force Microscopy
P137	Tomohiro Ueno	Development of MRI Microscope
P138	Mariko Sakaki	Dielectric breakdown accompanied by structural change in a Mott insulator Ca_2RuO_4
P139	Satoshi Kashiwaya	Transport Properties of Sr_2RuO_4 Microdevices

Abstracts

Oral Presentations

O1

Quantum Turbulence and Nonlinear Phenomena in Quantum Fluids

Makoto Tsubota

Department of Physics, Osaka City University, Sumiyoshi-ku, Osaka 558-8585, Japan

We will report our activity on quantum turbulence and related nonlinear instability through the project entitled "Physics of New Quantum Phases in Superclean Materials".

In quantum condensed systems appear quantized vortices through the order parameters (macroscopic wave functions), and turbulence consisting of quantized vortices is called quantum turbulence (QT).

Quantized vortices and QT were discovered in superfluid helium in the 1950's, while they have become one of the most important themes in low temperature physics [1]. The recent striking output would be the confirmation of the Kolmogorov law (K41) of the energy spectra through the Gross-Pitaevskii model [2]. Nowadays QT is studied actively in superfluid ^{4}He and ^{3}He, even in cold atoms [3].

In this talk, we will first introduce the recent main motivations and the results in QT. Then we will discuss some current topics on nonlinear instability in quantum fluids. One is quantum Kelvin-Helmholtz instability (KHI) in two-component Bose-Einstein condensates [4]. KHI is well known in classical fluids, while we discuss characteristic phenomena of quantum KHI in quantum fluids. The other is realization of steady state in thermal counterflow QT in superfluid ^{4}He [5]. This system reminds us of the pioneering work by Schwarz [6], which had some difficulties. By considering the full interaction between vortices, we overcame the difficulties to obtain the steady state.

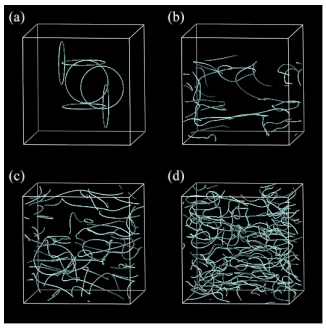

FIG.1: Formation of a steady state quantum turbulence in thermal counterflow.

[1] Progress in Low Temperature Physics, ed. W. P. Halperin and M. Tsubota (Elsevier, Amsterdam, 2008) Vol.16.
[2] M. Kobayashi and M. Tsubota, Phys. Rev. Lett. **94**, 065302 (2005): J. Phys. Soc. Jpn. **74**, 3248-3258 (2005).
[3] E. A. L. Henn *et al*., Phys. Rev. Lett. **103**, 045301 (2009).
[4] H. Takeuchi, N. Suzuki, K. Kasamatsu, H. Saito and M. Tsubota, arXiv:0909.2144.
[5] H. Adachi, S. Fujiyama and M. Tsubota, arXIv:0912.4822; Phys. Rev. B (in press).
[6] K. W. Schwarz, Phys. Rev. B **38**, 2398 (1988).

O2

EXCITATIONS AND CHARACTERIZATION OF QUANTUM TURBULENCE IN AN ATOMIC SUPERFLUID

[1]V. S. Bagnato, [1]E.A.L.Henn, [1]J.A.Seman, [2]G. Roati , [1]K.M.F. Magalhaes, ,
[1]R. Shiozaki, [1]M. Caracanas, [1]E. Ramos and [3]V. I. Yukalov

[1]Instituto de Física de São Carlos – Universidade de São Paulo
Av. Trabalhador Sancarlense, 400 - CP 369 – 13560-970 - São Carlos – SP – Brazil

[2]Permanent Institution – LENS – Florence –Italy
[3]Permanent Institution – Bogolubov Lab. Theoret. Physics – Dubna-Russia

In a recent achievement of our laboratory, we demonstrate the formation of vortices and anti-vortices all together. The evolution of such configuration with increasing the time of excitation as well as the amplitude of excitation, was a multiplication of vortices with a sudden proliferation characterizing the establishment of a turbulent regime on the sample. The dependence of the observed characteristics of the sample covering the possibilities of time and amplitude, generate a diagram showing regions of regular vortex formation , turbulent type configuration and finally a fragmentation of the cloud in small islands supposedly of superfluids. During the various regimes the free expansion of the cloud demonstrates to have peculiar behavior. The most impressive one is related to the expansion of the turbulent cloud, which keeps the original aspect ratio. We preset the beginning of the understanding for the behavior and a possible way to quantify the turbulence. On going experiments related to the fragmentation and decay of the turbulence are presented. Work supported by *FAPESP and CNPq* brazilian agencies. *Thanks to the students: P.Castilho, F. Jackson, P.E. S. Tavares, C. Castelo Branco. Special thanks to A. Fetter and M. Tsubota for valuable discussions.*

O3

Turbulence in Superfluid ^{4}He at Low Temperatures: Experimental Advances

A. I. Golov[1], P. M. Walmsley[1], H. E. Hall[1], P. Tompsett[1], A. A. Levchenko[2] and W. F. Vinen[3]

[1]*School of Physics and Astronomy, The University of Manchester, Manchester M13 9PL, United Kingdom*
[2]*Institute of Solid State Physics, Russian Academy of Sciences, Chernogolovka 142432, Russia*
[3]*School of Physics and Astronomy, University of Birmingham, Birmingham B15 2TT, United Kingdom*

Turbulence in superfluid helium, often called Quantum Turbulence (QT), is especially interesting in the limit of low temperatures (for ^{4}He, at $T < 0.4$ K), when thermal excitations become negligible [1]. The formulation sounds simple: a one-component incompressible inviscid liquid in which vorticity is confined to thin filaments (cores of quantized vortices), each contributing an identical velocity circulation of $h/m_4 = 10^{-3}$cm^2/s. These vortices advect with the local velocity which is induced by all of them. However, hydrodynamic interactions and especially reconnections between vortex lines make the dynamics rich and interesting. It is believed that, in ^{4}He, the dissipation of flow energy is only happening through phonon emission at extremely short scales of order 10 nm. The nature of the inertial cascade of energy from large to short length scales is of major interest. Some fundamental questions that require experimental verification are:
- does QT mimic classical "Richardson-Kolmogorov" cascade at large (quasi-classical) lengthscales?
- does it behave as wave turbulence (of Kelvin waves) at short (quantized) lengthscales?
- what are the nature of the cascade and its energy spectrum at intermediate lengthscales between these two; what is the role of interactions and reconnections, especially of emitted tiny vortex rings?
- how does the dissipation rate depend on polarization (either fluctuating or static)?
- are phonons the only/main mechanism of dissipation in ^{4}He?

One can see that QT, after being understood, has a potential to become an important benchmark type of turbulence along with the classical-hydrodynamic, magneto-hydrodynamic and wave turbulence.

For experimental progress with QT at sufficiently low temperatures, significant obstacles existed:
- how can one generate turbulences (as homogeneous as possible) of required spectra?
- how to measure meaningful parameters such as vortex line density, polarization, energy spectra?

Recently, we learned how to overcome both. The turbulence was generated either by an impulsive spin-down of a rotating container or by running a current of injected negative ions (that nucleate vortex loops/tangles and can also entrain liquid in large-scale motion) through the liquid. The detection of vortex tangles was through scattering off them of micron-size probe charged vortex rings. Also, measurements of the motion of charge trapped on vortex lines revealed important information about the dynamics of turbulence.

In this presentation, we will describe experimental observations for the following set-ups:
- free decay of quasi-classical turbulence (generated by large-scale flow) [2-4];
- free decay of "ultra-quantum" turbulence (that has negligible large-scale flow) [5];
- free decay of these two types of turbulence at steady rotation (i.e. with net polarization of the tangle);
- for a vortex tangle at steady rotation (i.e. a perturbed array of rectilinear vortex lines): different turbulent regimes as function of pumping intensity and frequency, emission of small vortex rings upon an impulsive perturbation;
- a new type of turbulent system, charged vortex tangle, that allows to apply body force and to detect the dynamics of drift and diffusive spreading of the tangle;
- strongly interacting polarized vortex rings at high densities, as precursor for tangle formation;
- multiply-charged vortex rings, with up to 11 electrons per ring.

[1] A.I.Golov, P.M.Walmsley, J. Low Temp. Phys. **156**, 51 (2009).
[2] P.M.Walmsley, A.I.Golov, H.E.Hall, A.A.Levchenko and W.F.Vinen, Phys. Rev. Lett. **99**, 265302 (2007).
[3] V.B.Eltsov, R.deGraaf, R.Hänninen, M.Krusius, R.E.Solntsev, V.S.L'vov, A.I.Golov and P.M.Walmsley, Progress in Low Temperature Physics (North-Holland, Amsterdam, 2008, B. Halperin and M. Tsubota eds.), Vol. **XVI**, pp. 45-146. Turbulent Dynamics in Rotating Helium Superfluids.
[4] P.M.Walmsley, A.I.Golov, H.E.Hall, W.F.Vinen, A.A.Levchenko, J. Low Temp. Phys. **153**, 127 (2009).
[5] P.M.Walmsley and A.I.Golov, Phys. Rev. Lett. **100**, 245301 (2008).

O4

Vortex Dynamics in Steady Quantum Turbulence of Superfluid ^{4}He at the Turbulent-to-Laminar Transition

H. Yano, Y. Nago, K. Andachi, Y. Miura, K. Obara, O. Ishikawa, and T. Hata

Graduate School of Science, Osaka City University, Osaka 558-8585, Japan

Turbulence can be easily generated by an oscillating structure due to the presence of vortex lines attached to it. This condition is convenient of turbulence generation, especially at very low temperatures [1]; however, it makes it difficult to study the dynamics of vortices at the turbulent transition. In the present work, we report the control of vortex lines attached to an oscillating object, using vibrating wires with different thicknesses, a cover box, control of cooling speed. Vibrating wires mostly without attached vortex lines enable to simplify the study of vortex dynamics at the turbulent transition [1-4].

Using these wires, we observed the lifetime of a turbulent state at the turbulent-to-laminar transition. The lifetime reveals an exponential distribution with a mean lifetime. We measured the lifetime for various powers injected in a turbulent state and find that the mean lifetime decreases exponentially with decreasing power (Fig. 1), following an equation of $\tau_0 \exp\left(P^2/P_0^2\right)$ shown as the solid line in Fig. 1. Here P is the injection power, and τ_0 and P_0 are the fitting parameters. This result suggests that the lifetime depends on the vortex line density in a turbulent state. We estimated τ_0 and P_0 to be 1.6 s and 0.88 pW, respectively. At powers below P_0 (the arrow in Fig. 1), a critical behavior emerges: the mean lifetime decreases steeply from the solid line.

Assuming a bottleneck of energy cascade in turbulence at a vortex line spacing [5], we find that the mean spacing of vortex lines produced at the critical power is equal to the amplitude of the wire vibration, suggesting that a vibrating wire stops generation of turbulence because of the absence of vortex lines in the path of the wire vibration. This is a reasonable conclusion, considering that seeds of vortices are necessary for turbulence generation [2,3]. Consequently, a bottleneck in the energy cascade exists at a vortex line spacing for turbulence generation by vibrating wires. This is the first observation of the bottleneck of energy cascade in steady quantum turbulence.

[1] H. Yano, N. Hashimoto, *et al.*, Phys. Rev. B 75 (2007) 012502.
[2] N. Hashimoto, H. Yano, *et al.*, Phys. Rev. B 76 (2007) 020504(R).
[3] R. Goto, S. Fujiyama, H. Yano, M. Tsubota, *et al.*, Phys. Rev. Lett. 100 (2008) 045301.
[4] H. Yano, T. Ogawa, A. Mori, Y. Miura, Y. Nago, *et al.* J. Low Temp. Phys. 156 (2009) 132.
[5] W.F. Vinen and J.J. Niemela, J. Low Temp. Phys. 128 (2002) 167.

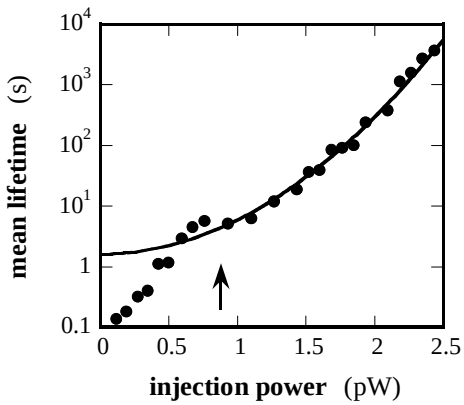

Fig.1: Mean lifetime of a turbulent state generated by a vibrating wire as a function of power injected in the turbulent state. The arrow indicates a critical power.

O5

Massively-Parallel Simulations for Quantum Turbulence : Current Development and New Insights

M. Machida,[1,2] N. Sasa,[1,2] T. Kano,[1,2] and M. Tsubota[3]

[1]*CCSE, Japan Atomic Energy Agency, 6-9-3 Higashi-Ueno, Taito-ku, Tokyo 110-0015*
[2]*CREST(JST), 4--1--8 Honcho, Kawaguchi, Saitama 332-0012*
[3] *Department of Physics, Osaka City University, Sumiyoshi-ku, Osaka 558-8585, Japan*

Turbulence is an important issue for not only physicists but also engineers. Especially, its understanding is crucial for wide engineering fields, e.g., construction of various power plants from nuclear to wind energy. The classical turbulent flow of normal fluids has still remained unsolved, while quantum fluids have offered a challenging target, "Quantum Turbulence", which may be more fundamental and accessible in a theoretical sense.

In Quantum Turbulence, there are interesting questions. The typical one is how the quantization effects affects the turbulent flow. In order to solve the problem, Kobayashi and Tsubota performed direct numerical simulations for a modified version of the Gross-Pitaevskii equation and found Kolmogorov spectrum as a statistical feature of the turbulent state similar to the classical turbulent flow [1]. Finally, they claimed that quantum turbulence is a quite clear prototype in understanding the inertial range, the Kolmogorov spectrum, the Richardson cascade process, and so on[1,2].

One of our research targets is to examine the picture in larger scale regimes and confirm the scale invariant property of the characteristic spectrum and the related structures as seen in the classical turbulence. In order to carry out the purpose, we constructed a code simulating the modified Gross-Pitaevskii equation[1] and perform large-scale parallel simulations [3]. Consequently, we succeeded in performing large-scale parallel simulations up to 2048^3 grids on the Earth Simulator. The simulation revealed that the universality seen in the spectrum holds on 256^3 to 2048^3. Thus, the theoretical expectation was fully confirmed by the large scale simulation. This is the first numerical confirmation in Quantum Turbulence. Moreover, we have visualized the vortex tangle image seen in the inertial range and found a self-similar structural picture of vortices [4]. The second target is to find out particularities of Quantum Turbulence. We found that the Kolmogorov spectrum breaks down above a high wave number, where a hump or plateau structure appears commonly from 256^3 to 2048^3[4]. The structure may be relevant to a concept, i.e., bottleneck effects in the energy cascade peculiar to Quantum Turbulence [4]. Since the bottleneck is currently an intensively investigated issue, the result may shed new light on Quantum Turbulence. In fact, we confirmed that the structure position is dependent on the input energy. This result indicates that the bottleneck position is given by the vortex density, which is almost consistent with a bottleneck scenario [4].

References

[1] M. Kobayashi and M. Tsubota, Phys. Rev. Lett. 94, 065302 (2005).

[2] See, e.g., M. Tsubota, J. Phys. Soc. Jpn. Vol.27, No.11, 111006(2008).

[3] N. Sasa, M. Machida and H. Matsumoto, J. of Low Temp. Phys. 138, 617 (2005).

[4] N.Sasa, T.Kano, M. Machida, V. S. L'vov, and M. Tsubota (in preparation).

O6

Thermal and quantum crystallizations of ^{4}He in aerogel

Y. Okuda, K. Ueno, R. Masumoto, and R. Nomura

Dept. of Condensed Matter Physics, Graduate School of Engineering Science, Tokyo Institute of Technology
O-okayama, Meguro-ku 152-8551, Japan

The way of the crystallization of ^{4}He in aerogel was found to show a dynamical phase transition due to the competition between thermal fluctuation and disorder: crystals grow via creep at high temperatures and via avalanche at low temperatures [1]. Here we report the growth velocity and the crystallization pressure of ^{4}He in both regions for the aerogel of 96 % porosity. In the creep region, crystal growth is faster at higher temperature and becomes slower with cooling. This temperature dependence is opposite to the bulk crystal growth. The velocity is well represented by the Arrhenius type temperature dependence. This is consistent with the expectation that crystal growth is via a thermally activated interface motion in the disordered media in the creep region. Growth velocity is the lowest at the transition temperature. In the avalanche region, it slightly increases with cooling and saturates at lower temperature. This temperature independent growth is presumably the result of the macroscopic quantum tunneling through the pinning sites distributed randomly. The crystallization pressure in aerogel is not just like a shift of the bulk crystallization pressure but has a maximum at the transition temperature.

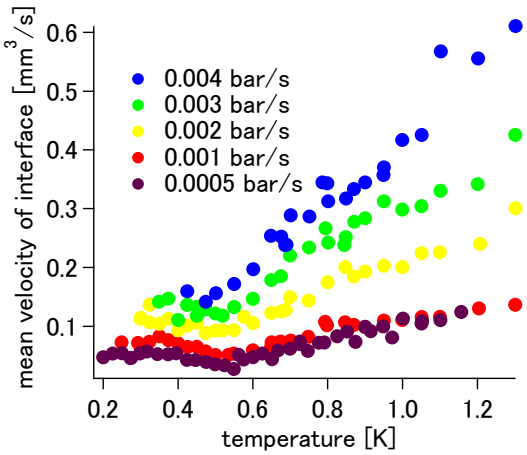

Fig.1 Mean growth velocity of the crystal in the 96 % aerogel plotted against temperature. The growth velocity shows the minimum at the temperature of the dynamical transition.

In the talk, I would also mention briefly the achievement of our group through the whole period of the project.

[1] Competition between thermal fluctuations and disorder in the crystallization of ^{4}He in aerogel, Nomura, A. Osawa, T. Mimori, K. Ueno, H. Kato and Y. Okuda, Phys. Rev. Lett. 101, 175703 (2008).

O7

Towards a New Physics of Nanoscale Helium

Keiya Shirahama

Department of Physics, Keio University, Yokohama 223-8522

Liquid and solid ^{4}He are the best-known examples of strongly correlated Bose system. When ^{4}He is confined in porous media with nanometer scale, the correlation and hence the quantum properties can be drastically altered. We have observed various new quantum phenomena in ^{4}He confined in nanoporous media. I will discuss our past and future studies, which aim at developing "nano-scale helium physics".

The most important phenomenon is the pressure - induced quantum phase transition (QPT) of ^{4}He in some nanoporous materials (Gelsil glass [1] and Hybrid Mesoporous Material (HMM-3) [2]). The QPT is closely related to the formation of Localized Bose-Einstein Condensates (LBEC) [1], in which the macroscopic superfluid coherence is destroyed. The LBEC state is probably caused by strong confinement of ^{4}He atoms in the nanopores or by disorder in the porous structure. The QPT behavior has been recently reproduced theoretically in a 3D quantum rotor model [3]. The LBEC state may be analogous to the pseudo-gap state in high-T_c cuprates, and to the insulating state in granular superconductors.

The ^{4}He – Gelsil system also shows interesting supersolid-like behaviors, both in confined solid [4] and in thin adsorbed solid [5], latter of which is understood as a manifestation of a quantum critical phenomenon.

If time permits, I will briefly discuss our recent study of superfluid properties of liquid ^{4}He confined in a regular 1D nanopore array provided by porous alumina, and future studies of the quantum critical phenomena by introducing new variable parameters that can be tuned near 0 K, such as static electric field, frequency in mechanical oscillators, and DC rotation. The ultimate goal of the former study using nanopore arrays is to realize a true superfluid Josephson junction using strongly – correlated liquid ^{4}He.

[1] K. Yamamoto *et al.*, Phys. Rev. Lett. **100** (2008) 195301; J. Phys. Soc. Jpn. 77 (2008) 013601; Phys. Rev. Lett. **93** (2004) 075302; K. Shirahama *et al.*, J. Phys. Soc. Jpn. **77** (2008) 111011. [2] N. Yamanaka *et al.*, in poster presentation. [3] T. Eggel, M. Oshikawa, in poster presentation. [4] H. Yoshimura *et al.*, in preparation. [5] T. Kogure *et al.*, in poster presentation. [6] R. Higashino *et al.*, in poster présentation.

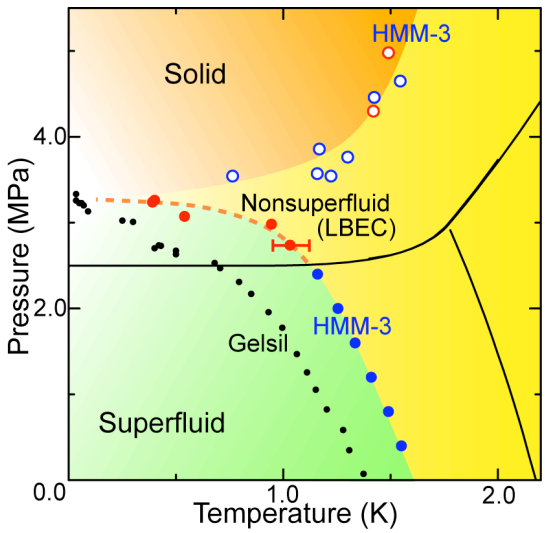

QPT behaviors in the P – T phase diagram: ^{4}He confined in a regular nanoporous material HMM-3 [2] and an irregular porous Gelsil glass [1]. Closed blue and red circles show superfluid T_c measured by a torsional oscillator and ultrasound, respectively.

O8

Superfluidity of ^{4}He Confined in One-dimensional Channel under Pressure

Masaru Suzuki and Junko Taniguchi

[1]*Department of Applied Physics and Chemistry, The University of Electro-Communications, 1-5-1 Chofugaoka, Chofu, Tokyo 182-8585, Japan*

Superfluidity of ^{4}He in restricted geometry has attracted the attention of many researchers for several decades. For a Gelsil glass with three-dimensionally (3D) connected pores of 2.5 nm in diameter, the superfluid transition temperature *T*c drops down to 1.4 K at zero pressure. Moreover, it is suppressed by pressurization monotonically, and approaches zero temperature at a critical pressure *P*c of 3.4 MPa. The dimensionality in restricted geometry can be easily controlled by changing the pore structure. One of the media suitable for this study is a FSM16 series, which posses a one-dimensional (1D) nano-meter size channel. It is of great interest to clarify the quantum properties in 1D channel.

We have carried out several experiments for ^{4}He confined in a FSM16 series under pressure. Figure 1 shows the results of torsional oscillator measurements for the 2.8-nm channel FSM16. The abscissa is the normalized temperature divided by $T\lambda$ of each pressure, while the frequency change $\Delta f'$ in the ordinate is corrected by the density of liquid ^{4}He. As seen, a rapid increase in the superfluid fraction in 1D channel takes place at *T*o of 0.9 K at low pressure, and is suppressed drastically by pressurization. Form heat capacity measurements, it was found that no anomaly at *T*o is observed while it shows a bump at the higher temperature. The obtained phase diagram for the 2.8-nm channel FSM16 from these measurements is similar to that of a Gelsil glass.

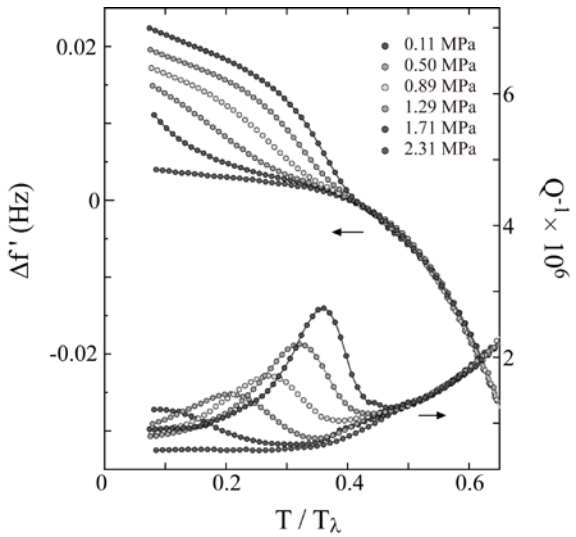

Fig. 1. Torsional oscillator measurements for the 2.8-nm channel FSM16.

[1] K. Yamamoto, H. Nakashima, Y. Shibayama, K. Shirahama, Phys. Rev. Lett. **93**, 075302 (2004).

O9

One-Dimensional Phonon State and Superfluidity of ^{4}He Fluid Nanotubes

N. Wada, T. Matsushita, M. Hieda, and D. S. Hirashima

Department of Physics, Graduate School of Science, Nagoya University, Nagoya 464-8602, Japan

We have studied ^{4}He and ^{3}He adsorbed in nanopores with regular structures. In these nano-extreme conditions, the ^{4}He Bose and ^{3}He Fermi fluids, respectively, are expected to exhibit the dimensionality of the pore connection and the interactions changed variously by the adsorption potentials from the pore walls and the helium densities [1].

In the three-dimensional (3D) nanopores of HMM-2 where pores 2.7nm in diameter are connected in 3D in the period 5.5nm, the ^{4}He fluid films formed in the 3D nanopores show the evidence of the 3D long-range-order transition; a sharp heat capacity (C) peak and superfluid onset appear at the same temperature (T_C=T_S), as shown in Fig.1(b)[2]. The ^{4}He fluid films formed in the 1D pores (FSM: d=2.8nm in diameter), however, indicate no 3DLRO; T_C << T_S, in Fig.1 (a).

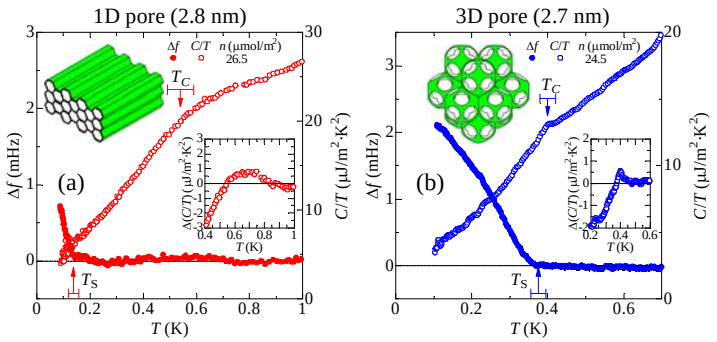

Fig.1. (a) Heat capacity anomaly (peak) at T_c and superfluid onset at T_S of ^{4}He in 1D pores of FSM (2.8nm), and (b) those in 3D pores, HMM-2(2.7nm, 3D period 5.4nm).

For FSM with d ≥1.8nm, ^{4}He fluid nanotube is formed in each 1D channel. The tube diameter d' is reduced from d by the solid ^{4}He layer thickness about 0.4nm, and the tube length L is about 300nm, the same as the FSM grain size. The 1D state of the fluid nanotube is defined when the thermal phonon wavelength $\lambda_{phonon} = hv_I/k_BT$, where v_I is the phonon velocity, is longer than $2\pi d'$. From the phonon heat capacity and the compressibility obtained from the pressure isotherm [1], v_I of the nanotube was estimated to be 50-150m/sec depending on the coverage. The ^{4}He fluid nanotubes with d'=1-2nm are actually in the 1D phonon state at the temperatures less than about 1K.

Superfluidity of the ^{4}He fluid nanotubes in the 1D phonon state was examined by the torsional oscillator [3,4]. Superfluid of the nanotubes was observed for the pore diameters above 1.8nm, as shown in Fig. 2. The bottom curves of d=2.8, 2.2, 1.8nm and that of d=1.5nm are the shift $\Delta F/S$ due to the superfluid on the grain surfaces of FSM. In the case of the large pores with d=4.7nm, the large $\Delta F/S$ come from the ^{4}He fluid nanotubes was observed whose temperature dependence is similar to the KT transition. The observed $\Delta F/S$ of the ^{4}He nanotubes become small for d=1.8 and 2.2nm. For the intermediate diameter d=2.4nm, $\Delta F/S$ of the nanotubes increases with decreasing T.

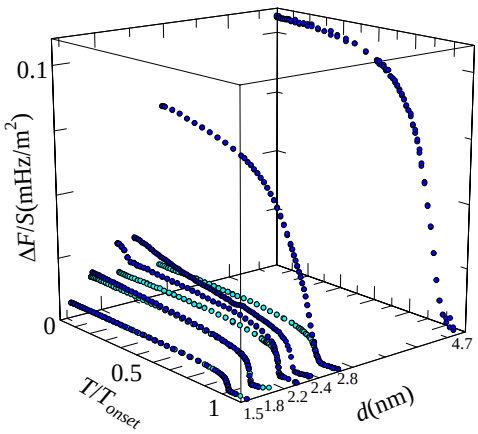

Fig.2. 1D pore diameter d dependence of the superfluid density observed by torsional oscillator. T_{onset}≈ 1K and other experimental conditions are almost the same except for d. Bottom curves for d=1.5, 1.8, and 2.8nm show the KT transition of the films on the grain surfaces of FSM.

The pore size d dependence of the superfluidity in the 1D phonon state (Fig.2) was well reproduced by the XY spin model calculation[5] for the tube with an asymmetry A= $L/2\pi d'$. For the large pores with A≈1, the usual KT transition is observed. For large A (small d or d'), the superfluid is still observed in the 1D state if the correlation is finite within the finite pore length L. The observed superfluid density increases with decreasing T, because the fluctuation by the phonon becomes small.

[1] N. Wada *et al.*, JLTP **157** (2009) 324.
[2] R. Toda *et al.*, PRL **99** (2007) 255301.
[3] H. Ikegami *et al.*, PRB **76**(2007) 144503.
[4] Y. Minato *et al.*, to be submitted.
[5] K. Yamashita and D. S. Hirashima, PRB **79** (2009) 014501.

O10

Superfluid density in quasi-one-dimensional boson systems

D. Hirashima and K. Yamashita[1]

[1]*Depertment of Physics, Nagoya University, Nagoya 464-8602, Japan*

Recently, Ikegami *et al*. [1] and Toda *et al*. [2] studied superfluid behavior of ^{4}He films adsorbed on the inner surface of nanopores FSM-16, using a torsional oscillator. They observed a finite frequency shift below a finite temperature T_s and confirmed that the signal came from the one-dimensional part of the system. The onset temperature T_s was found to be close to the Kosterlitz-Thouless (KT) transition temperature T_{KT}. This is a puzzling result and poses a problem such as what is really observed in a torsional oscillator experiment or the observability of superfluid behavior in (quasi-)one dimensional systems.

We study the superfluid density (helicity modulus) in the quasi-one-dimensional XY model and find that the helicity modulus is strongly reduced by phase slippage. We argue that the superfluid density observed in a torsional oscillator experiment is not proportional to the helicity modulus, but is the one that includes no contributions from phase slippage, and that is why a frequency shift can be observed from such a high temperature as the KT transition temperature. The definition of the superfluid density observed in experiments was also discussed by several authors [3]. We then briefly discuss superfluid density of ^{4}He filling nanopores [4]. These results must also be relevant to study of bosonic atomic gas trapped in a quasi-one-dimensional optical lattice.

[1] H. Ikegami *et al*., Phys. Rev. B **76**, 144503 (2007).
[2] R. Toda *et al*.,Phys. Rev. Lett. **99**, 255301 (2007).
[3] T.Minoguchi and Y. Nagaoka, Prog. Theor. Phys. **80**, 397 (1988); J. Machta and R. A. Guyer, J. Low. Temp. Phys. **74**, 231 (1989); N. V. Prokof'ev and B. V. Svistunov, Phys. Rev. B **61**, 11282 (2000).
[4] J. Taniguchi and M. Suzuki, J. Low Temp. Phys. 150, 347(2008)

O11

The enigma of supersolidity

Sébastien Balibar

Laboratoire de Physique Statistique, Ecole Normale Supérieure, Paris (France)

A "supersolid" is a solid where part of the mass is superfluid. This is paradoxical because, the mass being localized in a solid, it responds elastically to a shear stress. On the contrary, the atoms are indistinguishable and delocalized in a superfluid which consequently flows without dissipation. Since its discovery by Kim and Chan in 2004, supersolidity has been confirmed by 3 types of measurements in a dozen of laboratories but its origin is still mysterious. When Day and Beamish showed in 2007 that solid helium 4 was stiffer in its supersolid state than in its normal state, not softer, the whole phenomenon became even more surprising.

I will present possible interpretations of the experiments.

One of the main questions is whether supersolidity is due to the presence of disorder (dislocations, grain boundaries, helium 3 impurities...) in the solid samples or if disorder only enhances an intrinsic property of ideal helium 4 crystals, as proposed by P.W. Anderson. In 2009, our acoustic measurements have shown that there is a transition even in the absence of impurities. An experiment in ideal crystals with zero defects is in progress in our research group. I hope to know its answers by March 2010.

O12

Can supersolidity be suppressed in stiffened solid ^{4}He?

D. Y. Kim,[1] H. Choi,[1] W. Choi,[1] S. Kwon,[1] E. Kim,[1] and H. C. Kim[2]

[1]*Center for Supersolid & Quantum Matter Research and Department of Physics, KAIST, Daejeon 305-701, Korea.*

[2]*National Fusion Research Institute (NFRI), Daejeon 305-333, Korea.*

The observation of non-classical rotational inertia (NCRI) in solid helium has drawn attention because it was possibly the first experimental evidence of supersolid, a crystalline solid exhibiting superfluidity. Recently, shear modulus, μ, revealed anomalous behaviours that showed striking resemblance in the temperature, frequency, and ^{3}He concentration dependence to those of NCRI. The anomaly in μ can be understood with immobilization of dislocations by ^{3}He impurities without involving superfluidity. Extensive investigation on this phenomenon has shown that the anomaly in μ appears in hcp helium crystals irrespective of quantum statistics, while NCRI is found only in a bosonic solid. Here we report the first simultaneous measurement of shear modulus and NCRI in solid helium to elucidate the fundamental connection between them. Both emerge at remarkably similar temperatures, while no quantitative agreement between the increase of the shear modulus and the magnitude of NCRI is found. The most compelling observation is that NCRI can be reduced at very low stress fields in which ^{3}He impurities are still bound to dislocation lines, indicating that NCRI is suppressed by different excitations from dislocation stiffening.

O13

Simultaneous Measurement of Torsional Oscillator and NMR of Extremely Diluted ^{3}He in Solid ^{4}He

R. Toda,[1,2] W. Onoe,[1] P. Gumann,[2] M. Kanemoto, [1] K.Kosaka, [1]
T. Kakuda,[1] Y. Tanaka,[1] and Y. Sasaki[1,2]

[1]*Department of Physics, Graduate School of Science, Kyoto University, Sakyo-ku, Kyoto 606-8502, Japan*
[2]*Research Center for Low Temperature and Materials Sciences, Kyoto University, Sakyo-ku, Kyoto 606-8501, Japan*

Superfluid-like behavior of solid ^{4}He was discovered as missing rotational inertia, which is usually referred as non-classical rotational inertia (NCRI) by the torsional oscillator experiment [1]. Since then, a lot of theoretical and experimental studies have been done by many research groups. Among the many experimental results, the most peculiar observation is that the NCRI response and the onset temperature are affected strongly by the tiny amount of ^{3}He impurities [2]. The NCRI response disappears when solid ^{4}He contains just a hundred ppm of ^{3}He impurities. This is unreasonably small amount of impurities to destroy the phenomenon if we consider the NCRI as non-magnetic macroscopic phenomenon in solid ^{4}He like superfluid ^{4}He.

In order to study the physics in behind of this peculiar phenomenon, we have developed an apparatus to measure the torsional oscillator response and NMR response for the same solid ^{4}He with dilute ^{3}He impurities. NMR measurement of ^{3}He provides the information on the state of ^{3}He in solid ^{4}He. It is well known that in the solid mixture system, phase separation occurs at low temperature [3]. Below the phase separation temperature T_{PS}, ^{3}He atoms form clusters in solid ^{4}He. The clusters grow up slowly to a few μm in the case of a few % of ^{3}He sample [4]. In our torsional oscillator experiment, commercial grade ^{4}He (0.3 ppm of ^{3}He) at 3.6MPa shows the NCRI fraction of 0.06% at T=0. For the sample of ^{4}He with a few hundred ppm of ^{3}He at 3.6MPa, NCRI response is smashed away. These results are consistent with the observations by other groups. We did not observe any signature on the torsional oscillator frequency near T_{PS}. Thus the phase separation may not be related with NCRI response directly.

We have investigated the NMR properties of ^{3}He with this concentration as well as samples with 300ppm, 100ppm, and 10ppm of ^{3}He. Our results show that three different states of ^{3}He exist in solid ^{4}He below T_{PS}. One corresponds to the isolated ^{3}He atoms in solid ^{4}He. Since it has extremely long longitudinal relaxation time T_1 (over a day) at low temperature, we could not investigate the details of this state. Other two components grow up with time after cooling below T_{PS}. Thus both components of ^{3}He correspond to phase separated clusters in solid ^{4}He. The T_1 values of each component provide a distinction between each component (Fig.1). Both clusters disappear above T_{PS}. However, the (S) component, which is identified by shorter T_1, recovers much faster than the other (L) component, after the solid is cooled down below T_{PS} again. It suggests that the extra trapping potential works in the place where (S) exists, so that the ^{3}He atoms in (S) component stay in the same region even above T_{PS}. Such a trapping potential may come from the macroscopically disordered part of solid ^{4}He.

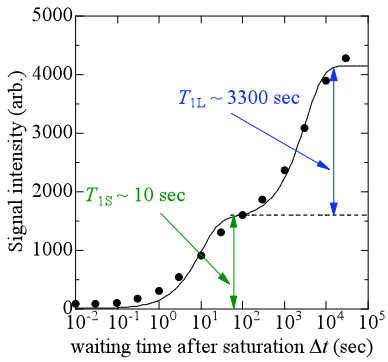

FIG.1: T_1 measurement at 8mK.

Strong ^{3}He impurity effect on NCRI exists below and above T_{PS}. But, it is unlikely that the isolated ^{3}He atoms, which locate separately with mean distance of 20 ^{4}He atoms for the case of 100ppm concentration, play a significant role in destroying NCRI response. However, if the NCRI response comes from the disordered part of solid ^{4}He, where some ^{3}He atoms are concentrated in, tiny amount of ^{3}He can play a significant role in destroying NCRI response.

[1] E. Kim and M. H. W. Chan, Nature **427**, 255 (2004)
[2] E. Kim, *et. al.*, Phys. Rev. Lett. **100**, 065301 (2008).
[3] D. O. Edwards and S. Balibar, Phys. Rev. B **39**, 4083 (1989)
[4] M. Poole and B. Cowan, J. Low Temp. Phys. **134**, 211 (2004).

*Present address: Department of Physics and Astronomy, Rutgers University, Piscataway, NJ 08854-8019, U.S.A

O14

Non-Classical Rotational Inertia in Two-Dimensional ^{4}He Solid on Graphite

Y. Shibayama,[1] H. Fukuyama,[2] and K. Shirahama[1]

[1]*Dept. of Physics, Keio University, 3-14-1 Hiyoshi, Kohoku-ku, Yokohama-shi, Kanagawa 223-8522, Japan*
[2]*Department of Physics, The University of Tokyo, 7-3-1 Hongo, Bunkyo-ku, Tokyo 113-0033, Japan*

In 2004, Kim and Chan [1] discovered non-classical rotational inertia (NCRI) in bulk solid ^{4}He and solid ^{4}He accommodated in porous media by torsional oscillator (TO) studies, and they interpreted the NCRI as superfluidity of solid ^{4}He, i.e. supersolidity. In an early theoretical work [2], supersolidity due to delocalized vacancies in bosonic quantum solid has been predicted. According to the theory, large zero-point fluctuation in quantum solid causes delocalized vacancies, which are named zero-point vacancies (ZPVs), in the solid, and in bosonic quantum solid the ZPVs exhibit Bose-Einstein condensation and superfluidity at low temperatures. However, recent experimental studies of annealing effects on NCRI in solid ^{4}He suggest that extrinsic crystal imperfections, which are independent of ZPVs, are strongly associated with the supersolid behaviors in solid ^{4}He [3].

As for ZPVs in quantum solid, a novel quantum phase due to mobile ZPVs has been proposed in two-dimensional (2D) ^{3}He solid on graphite at a density just below the registered 4/7 phase [4]. This suggests existence of mobile ZPVs also in 2D ^{4}He solid and superfluidity of the ZPVs. Moreover, Crowell and Reppy (CR) have found novel superfluid responses in 2D ^{4}He system on graphite by TO studies [5]. The superfluid responses may originate from supersolid state in 2D ^{4}He solid on graphite.

In order to search for the possible 2D supersolid state of ^{4}He, TO studies of ^{4}He films adsorbed on Grafoil were performed down to 10 mK [6]. In Fig.1, frequency shift Δf of the TO at 10 mK is shown as a function of the ^{4}He coverage $n_{4\mathrm{He}}$. Over 18.19 atoms/nm^2, a positive frequency shift with a small dissipation peak was observed below 200 mK. The size of Δf increases with the ^{4}He coverage. It reaches its maximum around 18.8 atoms/nm^2, and then turns to decrease. Over 19.0 atoms/nm^2, the shift increases with the coverage again. The reentrant feature in Δf is in agreement with the novel superfluid responses observed by CR [5]. In Fig.2, Δf at 15 mK of 18.68 atoms/nm^2 sample is shown as a function of the oscillation velocity. The Δf is suppressed over approximately 500 μm/s, which closely resembles to the suppression of NCRI in three-dimensional solid ^{4}He. On the other hand, the size of Δf of 21.47 atoms/nm^2 sample was independent of the velocity up to 1000 μm/s. The difference in oscillation velocity dependence of the frequency shift indicates the discrepancy in the origin of the observed frequency shift.

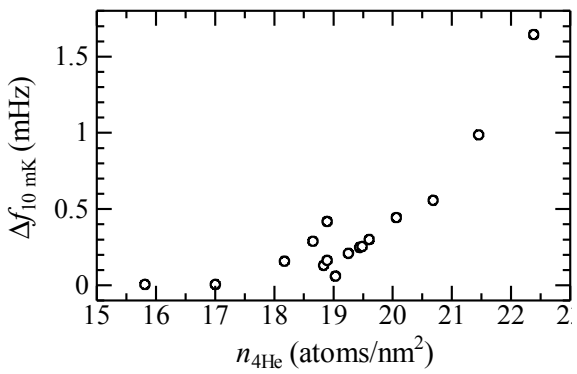

FIG.1: Δf at 10 mK as a function of ^{4}He coverage. The oscillation velocity is ca. 100 μm/s.

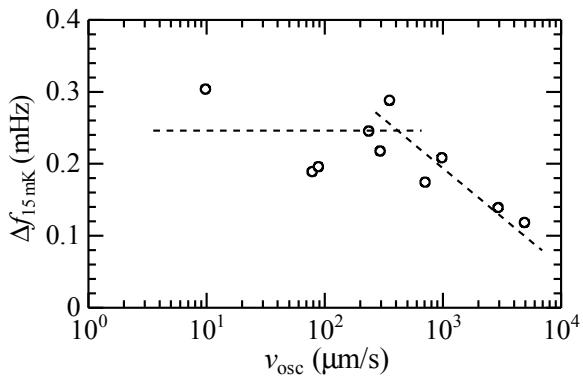

FIG.2: Oscillation velocity dependence of Δf for 18.68 atoms/nm^2 sample.

[1] E. Kim and M. H. W. Chan, Nature **427**, 225 (2004); Science **305**, 1941 (2004).
[2] A. F. Andreev and I. M. Lifshitz, Sov. Phys. JETP **29**, 1107 (1969).
[3] A. S. C. Rittner and J. D. Reppy, Phys. Rev. Lett. **97**, 165301 (2006).
[4] Y. Matsumoto *et al.*, J. Low Temp. Phys. **138**, 271 (2005).
[5] P. A. Crowell and J. D. Reppy, Phys. Rev. B **53**, 2701 (1996).
[6] Y. Shibayama *et al.*, J. Phys.: Conf. Ser. **150**, 032096 (2009).

O15

Novel quantum phenomena emerging near quantum critical points — Achievements made by five-year project—

M. Imada

Department of Applied Physics, University of Tokyo, Hongo, Bunkyo-ku Tokyo 113-8656, Japan

I first overview activities of our group, A01, "Novel quantum phenomena emerging near quantum critical points" and the outcome through the period of the project, achieved in collaboration of the groups of Kanoda-Miyagawa, Motome, Nakatsuji and Imada from 2005 through 2010. Our research covers scopes of both of unconventional quantum phase transitions and novel quantum phases.

On the quantum phase transitions, we have revealed the existence of a new universality class of quantum critical phenomena arising from the topological transition of the Fermi surface combined with strong interaction effects. This is realized in two examples, Lifshitz transition[1] and Mott transition[2]. It is characterized as the marginal quantum critical point (MQCP) emerging at the border between a finite-temperature critical line described by the Ising universality, and the topological critical line extending at zero temperature. For the Mott transition, the critical exponents of the MQCP gives good agreements with Mott transition for κ-$(ET)_2Cu[N(CN)_2]Cl$ revealed by Kanoda group[3].

Another unconventional quantum criticality appears in the proximity of continuous and first-order transitions as quantum tricriticality. The universality class of the quantum tricriticality has been elucidaed by extending the spin fluctuation theory[4]. The revealed universality class with quantitative estimates have accounted for puzzling experimental results for $YbRh_2Si_2$[5]. The coexistence of ferromagnetic and antiferromagnetic fluctuations is also consistent with experimental results of $CeRu_2Si_2$ by Suzuki and Onuki group [6] and β-$YbAlB_4$ revealed by Nakatsuji group[7].

On novel quantum phases, we have focused on several different types. One is quantum spin liquids discovered in the Mott insulator (or commensurate insulator) phase such as two-dimensional ^{3}He adsorbed on graphite as well as organic conductors, κ-$(ET)_2Cu_2CN_3$ [8] and EtMe3Sb[Pd(dmit)$_2$]$_2$[9] and has been shown to be stable numerically near the Mott transition[10].

Another novel phase we studied is non-Fermi liquids of metals separated from the conventional Fermi liquid by topological transitions of Fermi surface. Recently, this problem has been extensively studied in underdoped regions of the doped Mott insulator in connection to the high-*T*c cuprate superconductors and 2D ^{3}He slightly away from the 4/7 registered phase. In the Hubbard model, as a model for the cuprates, a cluster extension of the dynamical mean-field theory by Sakai has succeeded in reproducing the truncation of the Fermi surface as the Fermi arc or Fermi pocket as well as the pseudogap structure as observed in the underdoped region of the cuprates in collaboration with Motome [11]. A composite Fermion theory developed by Yamaji comprehensively accounts for these unconventional feature[12]. Two dimensional ^{3}He doped from the 4/7 phase contains essentially the same physics with a Fermi pocket formation of the "zero-point vacancy"[13,14]. Shinaoka has elucidated emergence and nature of soft-gap phase if effects of randomness coexist with correlation effects[15].

[1] Y. Yamaji, T. Misawa, and M. Imada, J.J. Phys. Soc. Jpn. **75** (2006) 094719; *ibid*. **76** (2007)063702.
[2] M. Imada, Phys. Rev. B **72** (2005) 075113; T. Misawa and M. Imada, Phys. Rev. B **75** (2007) 115121.
[3] F. Kagawa, K. Miyagawa and K. Kanoda, Nature **436** (2005) ; Nature Phys. **5** (2009) 880.
[4] T. Misawa *et al.*, J. Phys. Soc. Jpn. **77** (2008) 093712 and the presentation by T. Misawa in this conference.
[5] P. Gegenwart *et al*., Phys. Rev. Lett. **94** (2005) 076402; K. Ishida *et al*., Phys. Rev. Lett. **89** (2002) 107202; J. Custers, *et al*., Nature **424** (2003)524.
[6] D. Takahashi et al., Phys. Rev. B **67** (2003) 180407(R).
[7] S. Nakatsuji *et al.,* Nat. Phys. **4** (2008) 603.
[8[Y. Shimizu, K. Miyagawa, K. Kanoda, M. Maesato and G. Saito, Phys. Rev. Lett. **91** (2003) 107001.
[9] T. Itou, A. Oyamada, S. Maegawa, M. Tamura, and R. Kato: Phys. Rev. B **77** (2008) 104413.
[10] T. Kashima and M. Imada, J. Phys. Soc. Jpn.70 (2001) 3052; H. Morita *et al*.,J. Phys. Soc. Jpn. **71** (2002) 2109, T. Mizusaki and M. Imada: Phys. Rev. B **74** (2006) 014421.
[11] S. Sakai, Y. Motome and M. Imada, Phys. Rev. Lett. **102** (2009) 056404; Physica B **404** (2009) 3183 and the presentation by Shiro Sakai *et al*. in this conference.
[12] Youhei Yamaji and M. Imada, presentation in this conference.
[13] S. Watanabe and M. Imada, J. Phys. Soc. Jpn. **78** (2009) 033603; ibid. **76** (2007) 113603.
[14] Y. Matsumoto *et al.* J. Low Temp Phys. **138** (2005) 271; M. Neumann *et al*., Science **317** (2007) 1356.
[15] H. Shinaoka and M. Imada, Phys. Rev. Lett. **102** (2009) 016404; J. Phys. Soc. Jpn. **78** (2009) 094708.

O16

Localized spins systems as quantum simulators of interacting fermions and bosons

T. Giamarchi[1]

[1]*DPMC-MaNEP, University of Geneva, 24 Quai Ernest Ansermet, 1211 Geneva, Switzerland.*

Localized spin systems provide a fantastic laboratory to study the interplay between quantum effects and the interaction between excitations. Magnetic field and temperature allow an excellent control on the density of excitations and various very efficient probes such as neutrons and NMR are available. Localized spin systems can thus be used as ``quantum simulators" to tackle with great success questions that one would normally search in itinerant interacting quantum systems.

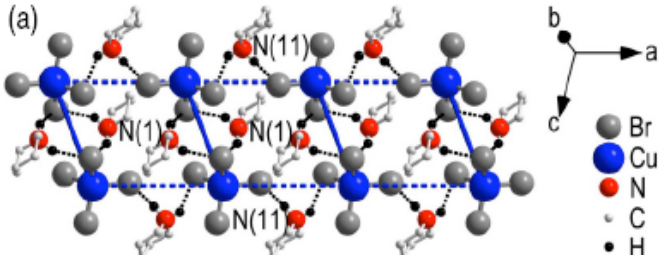

A spin ladder (HPIP or BPCB) that can be used to quantitatively test for luttinger liquid properties [3,4,5].

I will review these issues, focusing on two particular examples. In high dimensions, spin behave as interacting bosons and localized spins provide thus excellent realizations of Bose-Einstein condensates [1,2]. On the contrary if the spin exchange favors a low dimensional structure, such as a spin chain or a ladder, spins have a much more “fermionic” behavior and are described by the Luttinger liquid theory. Spin ladder systems thus offer a unique opportunity to test in very controlled way for such a Luttinger liquid physics [3,4,5].

Finally, how to describe the dynamical correlations at all energy scales, or how to go from this low dimensional case where the spins behave essentially as fermions, to the higher dimensional case where they behave as (essentially free) bosons, are very challenging, and experimentally relevant issues.

[1] T. Giamarchi and A. Tsvelik, Phys. Rev. B **59** 11398 (1999).
[2] T. Giamarchi, C. Ruegg and O. Tchernyshyov, Nat. Phys. **4** 198 (2008).
[3] M. Klanjsek et al., Phys. Rev. Lett. **101** 137207 (2008).
[4] C. Ruegg et al., Phys. Rev. Lett. **101** 247202 (2008).
[5] B. Thielemann et al., Phys. Rev. B **79** 020408(R) (2009).

O17

Spin-charge interplay in frustrated itinerant systems

Y. Motome

Department of Applied Physics, The University of Tokyo, 7-3-1 Hongo, Bunkyo-ku, Tokyo 113-8656, Japan

There have been growing interests in strongly-correlated electron systems on frustrated lattices. In these systems, a simple symmetry breaking is suppressed by frustration, yielding a chance to study the effect of enhanced fluctuations in charge and spin degrees of freedom at low temperatures. There, it is expected to have keen competition among different instabilities, such as insulator versus metal and magnetic order versus disorder, leading to some emergent properties in transport and magnetism. The purpose of our studies is to reveal such spin-charge coupled phenomena in correlated electron systems on frustrated lattices.

In this contribution, we present several topics from our recent theoretical studies on this issue:
(1) Chirality-driven heavy-mass behavior in the kagome Hubbard model (Fig. 1)
(2) Phase competition and phase separation in the pyrochlore double-exchange model (Fig. 2)
(3) Partial Kondo screening in frustrated Kondo systems
(4) Non-coplanar ordering and anomalous Hall effect in the triangular double-exchange model

These works have been done in collaboration with M. Udagawa, K. Nakamikawa, Y. Akagi (Univ. of Tokyo), and N. Furukawa (Aoyama Gakuin Univ., ERATO-MF).

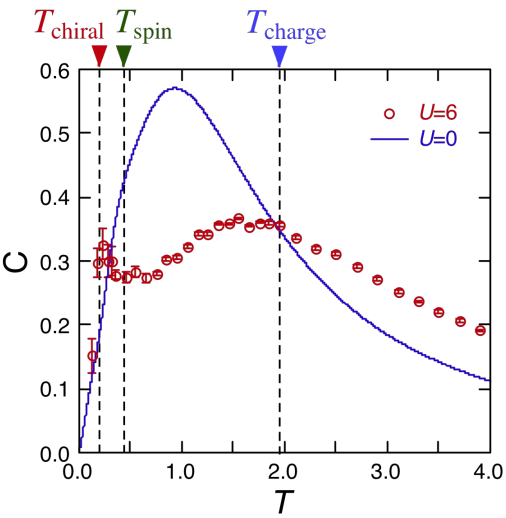

FIG.1: Temperature dependence of the specific heat of the kagome Hubbard model at half filling obtained by the cellular dynamical mean-field theory implemented with the continuous-time quantum Monte Carlo solver. T_{charge}, T_{chiral}, and T_{spin} are characteristic temperature scales of the charge, spin, and spin-chirality degrees of freedom, respectively, identified by the analysis of the cluster density matrix. The specific heat exhibits an additional sharp peak at T_{chiral}, indicating a formation of chirality-driven heavy-fermion state. (M. Udagawa and Y. Motome, submitted.)

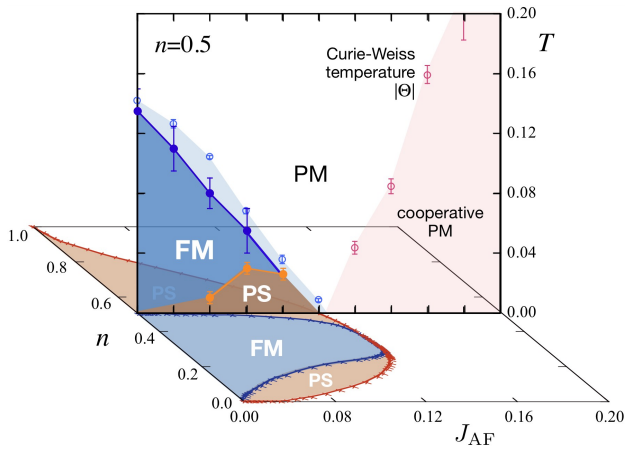

FIG.2: Phase diagram for the double-exchange model on the pyrochlore lattice as functions of the electron density n, the antiferromagnetic super-exchange coupling J_{AF}, and temperature T, obtained by Monte Carlo simulation. FM, PM, and PS are ferromagnetic metal, paramagnetic metal, and phase separation between the two, respectively. FM collapses as increasing J_{AF}, and finally is taken over by a peculiar PM state which exhibits almost T-independent transport and a large residual entropy with non-Fermi-liquid behavior.
(Y. Motome and N. Furukawa, submitted.)

O18

Fermi surface reconstruction and approach to a metal-insulator QCP in the underdoped cuprates

Suchitra Sebastian

Department. of Physics, University of Cambridge, The Old Schools, Trinity Lane Cambridge CB2 1TN,UK

Quantum oscillation measurements on the underdoped cuprate YBa2Cu3O6+x are presented over a wide magnetic field range up to 85T, and a broad temperature range between 100 mK and 20K. We show that Fermi Dirac statistics govern the elementary excitations even in this strongly correlated material in close proximity to the Mott insulating phase. The high resolution of these measurements enable multiple small sections of Fermi surface located at different locations in the Brillouin zone to be detected, indicating reconstruction by a long range order parameter. While the precise nature of this order parameter remains elusive, we demonstrate via our measurements that it must involve spin degrees of freedom. We further trace a single small section of Fermi surface toward the Mott insulating regime, and find a dramatic increase in effective mass at a metal-insulator quantum critical point (QCP), located under a local maximum in the YBCO superconducting dome. Possible mechanisms that drive this QCP, and their potential relation to enhanced superconducting temperatures are further investigated.

O19

Quantum Criticality in the Valence Fluctuating Superconductor β-$YbAlB_4$

S. Nakatsuji, Y. Matsumoto, T. Tomita, K. Kuga, and N. Horie

Institute for Solid State Physics, University of Tokyo, Kashiwa, 277-8581, Japan

Fermi liquid instabilities of metals at zero temperature are often ascribed to quantum critical soft modes of electronic spin degrees of freedom, leading to remarkably rich phenomena such as anomalous metallic behaviors and unconventional superconductivity. Archetypical examples have been found in heavy-fermion intermetallics, deriving from the competition between RKKY interaction and the Kondo screening. So far, all the quantum critical materials of this kind are known to have an almost integral valence to stabilize atomic local moments that is considered essential for the criticality. On the contrary, valence fluctuations generally promote the screening of local moments and consequently suppress the critical phenomena. In fact, no magnetic instability has been observed for the intermediate valence systems.

In this presentation, we show that the intermediate valence *f*-electron superconductor β-$YbAlB_4$ exhibits quantum criticality at practically zero field [1-4]. In particular, our high precision magnetization measurement has probed the quantum critical scaling properties down to far lower temperatures than the large energy scale of the local physics due to intermediate valence [4]. The observed power-law (B/T) scaling over three decades of temperature not only indicate unconventional quantum criticality, but places an upper bound on the critical magnetic field $B_c < 0.3$ mT.

Given this zero field quantum criticality, pressure and chemical doping are both important control parameters to induce possible magnetic quantum phase transitions in the material. We will present our recent results of the pressure and doping experiments to show the magnetic instability and the robust feature of the quantum criticality.

This is the work performed in collaboration with T. Tayama, Y. Shimura, T. Sakakibara, Y. Karaki, Y. Uwatoko, M. Okawa, and S. Shin at ISSP, Univ. of Tokyo.

[1] S. Nakatsuji, K.Kuga, Y. Machida, T. Tayama, T. Sakakibara, Y. Karaki, H. Ishimoto, S. Yonezawa, Y. Maeno, E. Pearson, G. G. Lonzarich, L.Balicas, H. Lee, and Z. Fisk, Nature Phys. **4**, 603-607 (2008).
[2] K. Kuga, Y. Karaki, Y. Matsumoto, Y. Machida, and S. Nakatsuji, Phys. Rev. Lett. **101**, 137004 (2008).
[3] M. Okawa, M. Matsunami, K. Ishizaka, R. Eguchi, M. Taguchi, A. Chainani, Y. Takata, M. Yabashi, K. Tamasaku, Y. Nishino, T. Ishikawa, K. Kuga, N. Horie, S. Nakatsuji, and S. Shin, arXiv:0906.4899.
[4] Y. Matsumoto, K. Kuga, Y. Karaki, T. Tomita, S. Nakatsuji, arXiv:0908.1242. ; Y. Matsumoto *et al.*, *preprint*.

O20

Neutral-Ionic Phase Transition in TTF-CA under Pressure

K. Miyagwa,[1] F. Iwase,[2] M. Hosoda,[1] R. Takehara,[1] T. Nishikawa[1], K. Kanoda[1] , H. Okamoto[3], K. Matsubayashi[4], and Y. Uwatoko[4]

[1]*Dept. of Physics, University of Tokyo, 7-3-1 Hongo, Bunkyo-ku, Tokyo 113-8656, Japan*
[2]*Institute for Molecular Science, 38 Nishigo-Naka, Myodaiji, Okazaki 444-8585, Japan*
[3]*Department of Advanced Materials Science, 5-1-5 Kashiwa-no-ha, Kashiwa-shi, Chiba 277-8561, Japan*
[3]*Institute for Solid State Physics, University of Tokyo,5-1-5 Kashiwa-no-ha, Kashiwa, Chiba 277-8581, Japan*

A neutral (N)-ionic(I) phase transition takes place in some semiconducting organic compounds of mixed-stack architecture composed of electron donor (*D*) and electron accepter (*A*) molecules. By cooling or pressurizing the neutral state, an electron moves from *D* to *A* and the ionic state appears. The TTF-CA is a typical N-I transition material, where TTF (*D* molecule) is tetrathiafulvalene and CA (*A* molecule) is *p*-chloranil.

At ambient pressure, the degree of charge transfer, ρ, from *D* to *A* in the neutral phase is about 0.3 [1]. With decreasing temperature, a first-order phase transition occurs at T_{NI} = 81 K and ρ increases to about 0.7 at low temperatures [1]; so, the system becomes more ionic (I-phase). Moreover, since the N-I phase transition is accompanied with dimerization of TTF and CA, a ferroelectricity appears in I-phase.

We investigate the electronic and lattice states of TTF-CA by $^{35/37}$Cl NQR and ^{1}H NMR and resistivity measurements in the wide pressure-temperature (*P*-*T*) region (Fig.1). The Cl NQR gives us information on the degree of charge transfer and lattice dimerization. The ^{1}H NMR can detect the fluctuations of spins and/or molecular motion. The resistivity reflects the nature of thermally excited carriers.

Below 8 kbar, the Cl NQR spectra shows that the N-I phase transition and dimerization occur simultaneously as already reported [2]. That is, a first order phase transition line divides N-phase and the dimeric I-phase in the pressure-temperature phase diagram. At around 8 kbar, however, the transition line seems to branch out into a N-I crossover line and a dimerization transition line, namely, in the higher pressure region, the charge transfer and the dimerization occur independently, and a non-dimeric I-phase is extended in a wide *P*-*T* region, as shown in Fig.1.

At room temperature, resistivity is measured under pressure sweep up to 82 kbar and is found to take a minimum around 8 kbar, where the N-I crossover occurs. This suggests that the N-I charge fluctuations contribute to charge carriers in this region.

At room temperature, the nuclear-lattice relaxation rate, $1/T_1$ at ^{1}H site is quite small (of the order of 10^{-4} s^{-1}) but increases with pressure in an accelerated manner. It seems that spin objects (like spin solitons) are generated in accordance with the N-I charge transfer.

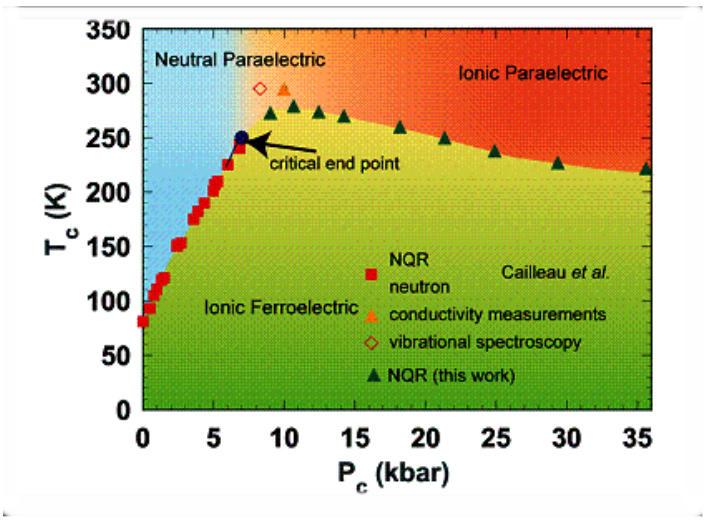

Fig.1 Pressure-Temperature dependence of TTF-CA

[1] C. S. Jacobsen and J. B. Torrance, J. Chem. Phys. **78**, 112 (1983); A. Girlando *et al*., ibid. **79**, 1075 (1983); Y. Tokura *et al*., Mole. Cryst. Liq. Cryst. **125**, 199 (1985); C. Katan *et al*., Phys. Rev. B 53, 12 112 (1996).
[2] M. H. Lemee-Cailleau *et al*., Phys. Rev. Lett. **79**, 1690 (1997)

O21

Anomalous "superfluid" response of ^{4}He films on graphite; a 2D supersolid ?

J Nyéki[1], A Phillis[1], J Parpia[2], B Cowan[1], and J Saunders[1]

[1]*Department of Physics, Royal Holloway University of London, Egham, Surrey, TW20 0EX, UK*

[2]*Department of Physics, Cornell University, Ithaca, NY 14853 USA*

The second layer of helium of ^{3}He adsorbed on graphite supports a two dimensional triangular super-lattice with respect to the underlying first helium layer. There is experimental and theoretical evidence that this Mott insulator is a quantum spin-liquid. In the case of ^{4}He we present evidence, from torsional oscillator measurements over the temperature range 1.5 mK to 3.5 K, for a corresponding two dimensional "superfluid" in this coverage range. The superfluid density has a highly anomalous temperature dependence. Both its inferred value at $T = 0$, and the characteristic onset temperature T^* are strong functions of the second layer density (equivalently the filling of the underlying triangular lattice). This result suggests that the new phase has additional broken symmetries which are responsible for the anomalous behaviour; the natural candidate is a supersolid. Indirect experimental evidence of likely breaking of translational invariance is provided by heat capacity measurements on ^{3}He doped ^{4}He films. However recent PIMC calculations of ^{4}He films [1] report that the possible triangular superlattice phases (4/7 or 7/12) are not stable, in contrast to previous findings [2].

We compare these results with those from a torsional oscillator control experiment on a ^{3}He film over the same coverage range. As part of this study the internal friction of the first solid helium layer has been measured for both isotopes, both for submonolayer and bilayer films. This data shows interesting features, which evolve in a systematic way, reflecting the evolving structure of the film. The fact that both internal friction and "superfluid" contributions to the torsional oscillator response must be taken into account is of note, particularly in the context of discussion of supersolidity in bulk helium.

[1] P Corboz, M Boninsegni, L Pollet and M Troyer, Phys. Rev. **B78**, 245414 (2008)
[2] M Pierce and E Manousakis, Phys. Rev. Lett. **81**, 156 (1998)

O23

Novel Quantum Phases in 2D ^{3}He on Graphite

Hiroshi Fukuyama

Department of Physics, The University of Tokyo, 7-3-1 Hongo, Bunkyo-ku, Tokyo 113-0033, Japan

Monatomic layer of helium three (^{3}He) physisorbed on graphite surface is one of the most fascinating quantum systems in two dimensions (2D). Particularly, in the second layer, where frequent intralayer particle exchanges are allowed though the atomic motions are still firmly confined into 2D, various interesting quantum phases are claimed to emerge [1]. Those are, for example, the gapless quantum spin-liquid phase [2,3], the ferromagnetic phase with tunable frustration [4] and the dimensional crossover of the self-condensation (gas-liquid transition) (Fig. 1) [5]. A more exotic and thus controversial one would be the zero-point vacancy phase [6]. The easy and fine tunability of particle density, i.e., inter-particle correlations, and the availability of atomically flat surface in exfoliated graphite substrates make this system suitable to study new quantum phases and correlation effects in strongly interacting Fermions in 2D.

I will review, in this talk, recent experimental investigations of this system measuring heat-capacity, magnetic susceptibility, resonance frequency shift and line broadening in cw-NMR, spin-spin relaxation time in pulsed-NMR [7] and magnetization curve [8] at temperatures down to 100 μK or in magnetic fields up to 11 T in a wide areal density region ranging from the second- to fourth- layer.

Despite such tunability and ideal two-dimensionality of this system, the previous experimental results obtained with Grafoil substrate, an exfoliated graphite, sometimes suffer from possible effects of surface heterogeneities. I will show how to discriminate those external effects from the intrinsic ones as well as our more recent attempts to solve this problem using a substrate of higher quality.

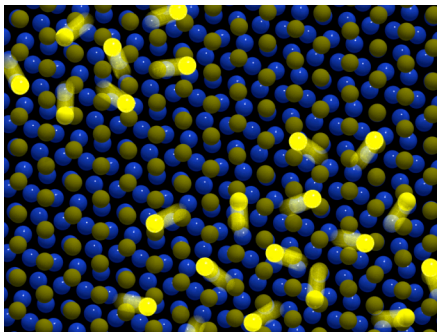

FIG.1: ^{3}He puddles (brighter spots) at the third-layer on graphite. The darker spots are the first- and second-layer helium atoms which do not form puddles.

[1] H. Fukuyama, J. Phys. Soc. Jpn. **77**, 111013 (2008) and references therein.
[2] K. Ishida, M. Morishita, K. Yawata and H. Fukuyama, Phys. Rev. Lett. **79**, 3451 (1997).
[3] R. Masutomi, Y. Karaki, and H. Ishimoto, Phys. Rev. Lett. **92**, 025301 (2004).
[4] D. Sato, S. Takayoshi, K. Obata, T. Matsui and H. Fukuyama, J. Low Temp. Phys. **158**, 544 (2010).
[5] D. Sato, D. Tsuji, S. Takayoshi, K. Obata, T. Matsui and H. Fukuyama, J. Low Temp. Phys. **158**, 201 (2010).
[6] Y. Matsumoto, D. Tsuji, S. Murakawa, H. Akisato, H. Kambara and H. Fukuyama, J. Low Temp. Phys. **138**, 271 (2005).
[7] S. Takayoshi, K. Obata, D. Sato, T. Matsui, and H. Fukuyama, J. Phys: Conf. Series **150**, 032104 (2009).
[8] H. Nema, A. Yamaguchi, T. Hayakawa and H. Ishimoto, Phys. Rev. Lett. **102**, 075301 (2009).

O24

Phase Diagram of the Triangular *t-J* Model in the Doped-Mott Region: Effects of Ring Exchange Interactions

Y. Fuseya,[1] and M. Ogata[2]

[1]*Dept. of Materials Engineering Science, Osaka University, Toyonaka, Osaka 560-8531, Japan*
[2]*Department of Physics, University of Tokyo, 7-3-1 Hongo, Bunkyo-ku, Tokyo 113-0033, Japan*

We study a triangular *t-J* model with multiple-spin ring exchange interactions (*K*) using exact diagonalization of small clusters as a model of monolayer liquid ^{3}He [1]. A new phase is found in the vicinity of the ferromagnetic phase in the doped-Mott region (Fig. 1(b)). The competition between the ferromagnetic two-spin exchange interaction, *J*, and the ring exchange interaction, *K*, generates a phase of possible "spin-charge (mass) separation". By considering the hole motion between the four-site plaquettes (Fig. 2), we can understand that the holes (mass) can move without disturbing the surrounding spin system so much, which is a similar situation with the one-dimensional electron system [1]. The triangular *t-J-K* model, therefore, naturally unravels the mysterious double-peaked heat capacity observed in monolayer liquid ^{3}He adsorbed on a graphite [2,3]. Our results suggest that doping a gapless spin-liquid yields a "spin-charge (mass) separated" state. These results open a new possibility of doped-Mott systems.

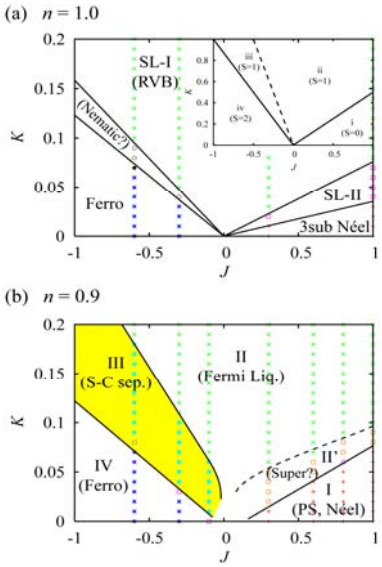

Fig. 1: Phase diagram of the triangular *t-J-K* model for (a) n=1 and (b) n=0.9 with N_a=20. The inset is the phase diagram of the four-spin plaquette.

[1] Y. Fuseya and M. Ogata, J. Phys. Soc. Jpn. **78**, (2009) 013601.
[2] Y. Matsumoto *et al.*, J. Low Temp. Phys. **138** (2005) 271.
[3] Y. Matsumoto *et al.*, unpublished.

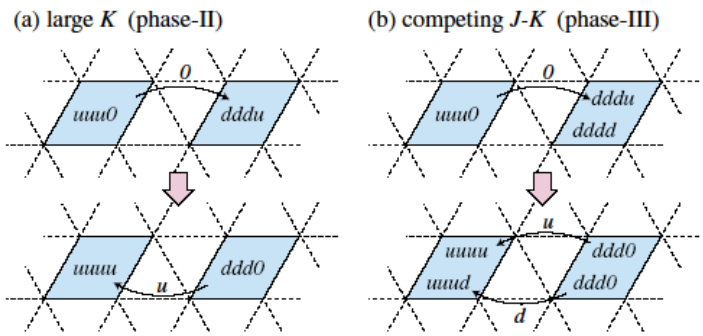

Fig. 2: Illustration of hole motion between the four-site plaquettes (shaded region) for (a) the large-*K* region and (b) the competing *J* and *K* region [1].

O25

Stability of 4/7 Phase of He Adsorbed on Graphite

T. Takagi

Dept. of Applied Physics, Fukui University, 9-1 Bunkyo-3, Fukui-city, Fukui, 910-8507, Japan

Stability of a 4/7 phase of He particles adsorbed on graphite was studied by path integral Monte Carlo simulation. The first layer and the second layer are constructed by ^{4}He and ^{3}He, respectively. We removed ^{3}He particles from the second layer of 4/7 phase and made vacancies on the triangular lattice. For these systems, we checked the stability of the phase for various densities of vacancies. The stability was determined by measuring Binder parameter of the system, and found that the system is stable less than 2% of the vacancy doping. The shape of the vacancy is not clear observing of the particle density profile in the real space, so a band width of the hole might be wide. Next we added additional particles into the second layer of 4/7 phase. In the case of adding 1% of excess particles into interstitial position of the lattice, the 4/7 structure was destroyed. We increased the particle density of the second layer with keeping the triangular lattice shape, and measured chemical potential of the second layer. To determine the critical density of the second layer which causing the third layer promotion, we also measured the chemical potential of the third layer. From obtained chemical potentials of each layer, we found that the third layer promotion occurs at the areal density 7.3 nm^{-2}.

O26

Magnon pairing and crystallization in the triangular-lattice ring-exchange model

T. Momoi,[1] K. Kubo,[2] and P. Sindzingre[3]

[1]*Condensed Matter Theory Laboratory, RIKEN,2-1 Wako, Saitama 351-0198, Japan*
[2]*Department of Physics and Mathematics, Aoyama Gakuin University, Sagamihara 229-8558, Japan*
[3]*Laboratoire de Physique Theorique de la Matiere Condensee, UMR 7600 of CNRS, Universite P. et M. Curie, case 121, 4 Place Jussieu, 75252 Paris Cedex, France*

We theoretically investigated unique magnetic behavior induced by ring-exchange interactions, aiming at microscopic understanding of anomalous magnetism observed in the 2nd layer of solid ^{3}He films on graphite [1]. As nuclear magnetism of solid ^{3}He is known to be well described with ring-exchange interactions, we extensively studied the ring-exchange model with two-, four-, five-, and six-spin interactions. Previous theoretical studies of this model found a spin gapped ground state [2] and a half-magnetization plateau [3] in strong four-spin exchange regime, whereas formation of nematic or triatic order was discovered in the proximity of the ferromagnetic (FM) phase boundary [4]. The parameter sets used in both studies were somewhat far from the estimated values [5].

To make a quantitative comparison with experiments and reveal magnetic behavior, we studied the ring exchange model in a wide parameter space. We found that a half-magnetization plateau (m/m_{sat}=1/2) appears in a wide parameter region, extending near to an FM phase boundary. Near the experimentally estimated parameter point, this magnetization plateau ends up to an edge and hence can be very narrow, as observed in a recent magnetization measurement [6]. In parameter regime close to the edge of the magnetization plateau, magnons prefer forming two-magnon bound states, giving rise to a nematic ordered state. We used magnon instability arguments from both fully polarized (FM) state and *uuud* half-magnetization plateau state, complemented with exact diagonaliation analysis of finite-spin systems.

[1] K. Ishida, M. Morishita, K. Yawata, and H. Fukuyama, Phys. Rev. Lett. **79**, 3451 (1997); R. Masutomi, Y. Karaki, and H. Ishimoto, Phys. Rev. Lett. **92**, 025301 (2004).
[2] G. Misguich, B. Bernu, C. Lhuillier, and C. Waldtmann, Phys. Rev. Lett. **81**, 1098 (1998); Phys. Rev. B **60**, 1064 (1999).
[3] T. Momoi, H. Sakamoto, and K. Kubo, Phys. Rev. B **59**, 9491 (1999).
[4] T. Momoi, P. Sindzingre, and N. Shannon, Phys. Rev. Lett. **97**, 257204 (2006).
[5] E. Collin, S. Triqueneaux, R. Harakaly, M. Roger, C. Bauerle, Yu. M. Bonkov, and H. Godfrin, Phys. Rev. Lett. **86**, 2447 (2001)
[6] H. Nema, A. Yamaguchi, T. Hayakawa, and H. Ishimoto, Phys. Rev. Lett. **102**, 075301 (2009).

O27

Exotic ground-states on the kagome lattice

C. Lhuillier,[1] L. Messio,[1] O. Cepas,[2] G. Misguich,[3] P. Sindzingre[1]

[1] *L.P.T.M.C., Université Pierre-et-Marie-Curie, Paris 6, F-75252 Paris cedex 05, France*
[2] *The Institut Néel, CNRS et Université Joseph Fourier, BP 166, F-38042 Grenoble cedex 9, France*
[3] *Institut de Physique Théorique, CEA, IPhT, CNRS, URA 2306, F-91191 Gif-sur-Yvette, France.*

It has been known for a long time that the pure Heisenberg model on the kagome lattice is a very special system, with a T=0 extensive degeneracy for classical spins and an elusive ground-state for $S=1/2$ spins [1]: I will give a brief account of the most recent results and open questions about this phase [1, 2,3].

Experimental outburst of compounds with the kagomé lattice structure has lead us to investigate the various small magnetic cell structures compatible with the lattice. Their order parameters, equal time structure factor and powder average will be shortly presented as well as microscopic Hamiltonians that may favor some of these specific phases.

Depending on microscopic models, Kagomé lattices may harbor a large family of non planar chiral classical orders. Some of these chiral states survive quantum fluctuations [4] and give rise to finite temperature phase transitions with subtle interplay between chirality variable and the Z_2 defects of the spin structure [5].

Depending on incoming new results I may want to revisit very shortly the multi-spin exchange phase diagram on the triangular lattice and its relevance to the physics of ^{3}He layers.

[1] P. Sindzingre *et al*., EPL **88**, 27009 (2009) *and refs. therein.*
[2] O. Cepas *et al*., Phys. Rev. B **78**, 140405 (2008)
[3] L. Messio *et al*., Phys. Rev. B *(in print)*
[4] J.-C. Domenge *et al*., Phys. Rev. B **77**, 172413 (2008)
[5] L. Messio *et al*., J. Phys. Rev. B **78**, 054435 (2008).

O28

Exotic Phases of Frustrated Systems

H. Tsunetsugu,[1] T. Ohashi,[2] T. Momoi,[3] N. Kawakami,[4] and M. E. Zhitomirsky[5]

[1]*Institute for Solid State Physics, University of Tokyo, Kashiwa, Chiba 277-8581, Japan*
[2]*Department of Physics, Osaka University, Toyonaka, Osaka 560-0043, Japan*
[3]*Condensed Matter Theory Laboratory, RIKEN, Wako, Saitama 351-0198, Japan*
[4]*Department of Physics, Kyoto University, Kyoto 606-8502, Japan*
[5]*CEA, INAC, Service de Physique Statistique, Magnetisme et Supraconductivite, F-38054 Grenobel, France*

Systems with competing interactions provide a good possibility of exotic emergent new state of condensed matter, and a spin liquid state in ^{3}He film is a typical example. In this presentation, I review our theoretical works on frustrated itinerant systems as well as quasi-1D frustrated quantum spin systems. First, I summarize our results of dynamical mean-field theory (DMFT) calculations for the Hubbard model on an anisotropic triangular lattice [1], and discuss the unusual reentrant metal-insulator transition observed in the organic compound κ-$(ET)_2Cu[N(CN)_2]Cl$ [2]. It is found that frustration effects lead to high-temperature part of metal-insulator crossover, while the low-temperature part is due to enhanced spin fluctuations in the intermediate metallic phase. Secondly, I review our analytical investigation on quantum spin systems with competing ferro- and antiferromagnetic exchange interactions, which may lead to the formation of bound magnon pairs in high magnetic field [3]. This is a spin nematic state [4], where ordinary spin dipole vanishes and spin quadrupole is the order parameter characterizing breaking of O(2) spin rotation symmetry. We develop an analytical approach to study the static and dynamical properties of the magnon-pair condensate near saturation field [5]. The representation of the condensate wavefunction describes a coherent state of magnon pairs and allows us to calculate various static characteristic quantities. The energy dispersion of quasiparticle excitations has a small gap. The developed theory predicts the high-field spin nematic phase in the frustrated quasi-1D compound $LiCuVO_4$ [6].

[1] T. Ohashi, T. Momoi, H. Tsunetsugu, and N. Kawakami, Phys. Rev. Lett. **100** (2008) 076402; Prog. Theor. Phys. Suppl. **176** (2008) 97.
[2] F. Kagawa et al., Phys. Rev. B **69** (2004) 064511.
[3] N. Shannon, T. Momoi, and P. Sindzingre, Phys. Rev. Lett. **96** (2006) 027213; T. Hikihara, L. Kecke, T. Momoi, and A. Furusaki, Phys. Rev. B **78** (2008) 144404.
[4] H. H. Chen and P. M. Levy, Phys. Rev. Lett. **27** (1971) 1383; A. F. Andreev and I. A. Grishchuk, Sov. Phys. JETP **60** (1984) 267.
[5] H. Tsunetsugu and M. E. Zhitomirsky, unpublished.
[6] M. Enderle et al, Europhys. Lett. **70** (2005) 237; M. G. Banks et al., J. Phys.: Cond. Matt. **19** (2007) 145227.

O29

Quantum/Spin liquids, geometrical phases and edge states

Y. Hatsugai

Institute of Physics, University of Tsukuba, 1-1-1 Tennodai, Tsukuba-shi, Ibaraki 305-8571, Japan

Strong quantum effects in low dimensional electron systems prevent formation of conventional order and result in realization of exotic phases without characteristic symmetry breaking. Such a class of states is a quantum/spin liquid where any local order parameters do not play fundamental roles. Various kinds of quantum Hall states are typical examples. Today we have a long list of states which belong to this class. It includes Haldane spin chains, spin ladders with/without ring exchanges, orthogonal dimers as Shastry-Sutherland antiferromagnets, half-filled Kondo insulators, quantum spin Hall systems and so on.

A quantum state with spontaneous breaking of continuous symmetry is supplemented by gapless excitations as the Nambu-Goldston modes. However for these quantum liquids, we do not have sufficient reasons to guarantee existence of gapless excitations. It is then natural to have a gapped quantum ground state where absence of the low energy excitation implies that they do not respond against for usual small external perturbation. As a result, a featureless quantum ground state is realized.

Even in such a situation, they are apparently interesting states and we realized wide variety among them. Therefore something to distinguish and characterize the states is required and can be quite useful. A concept of the topological orders were used here based on topological field theories about decades ago which should be compared with a standard local field theory which describes criticality by diverging local fluctuations. Recently we have noticed that geometrical phases which are intrinsic for quantum systems are useful for a description of such featureless quantum liquids [1]. Although the geometrical phase does not affect expectation values of classical (hermite) observables, it can be measured by interferences between the quantum states. The geometrical phase is a quantum observable. The Berry phase is a typical one that is defined by using a fictitious vector potential (Berry connection), which is essentially an overlap $\langle \Phi | \Phi' \rangle$ between infinitesimally different two states. We are proposing to use this Berry phases to characterize the quantum liquids and gave classifications for several class of the systems [2]. Recently we also apply the strategy to characterize the BEC-BCS crossover of the cold atoms [3] and two dimensional dimers. Also this geometrical phase is generalized for a time reversal invariant system with Kramers degeneracy where the quaternion is fundamental like the complex number is crucial for the standard Berry phase [4].

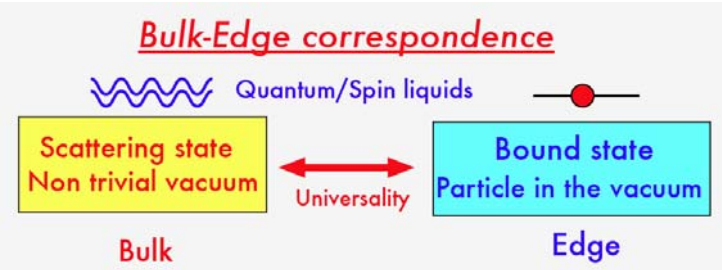

Although the bulk looks like featureless, the gapped quantum/spin liquids with boundaries show characteristic local physics by appearance of edge states. The edge states reflect non trivial topological properties of the bulk. This *bulk-edge correspondence* is also a fundamental property of the quantum/spin liquids as topological insulators. We demonstrate this for various quantum liquid systems, which include graphene and anisotropic superconductors [5] (see also above figure).

We summarize our contribution for the project, "Physics of New Quantum Phases in Superclean Materials (PSM)", as described above and present some of recent results.

[1] Y. Hatsugai, J. Phys. Soc. Jpn. 73, 2604 (2004), 74, 1374(2005), 75, 123601 (2006).
[2] For example, M. Arikawa, S. Tanaya, I. Maruyama and Y. Hatsugai, Phys. Rev. B79, 205107 (2009).
[3] M. Arikawa, I. Maruyama and Y. Hatsugai, in preparation.
[4] Y. Hatsugai, arXiv:0909.4831, to appear in New J. Phys., special issue of topological insulators.
[5] Y. Hatsugai, Phys. Rev. Lett. 71, 3697 (1993), Solid.State Comm. 149, 1061 (2009).

O30

Topological Excitations in Bose-Einstein Condensates

Masahito Ueda

Department of Physics, University of Tokyo, Tokyo, Japan
Email: ueda @phys.s.u-tokyo.ac.jp

Spinor and/or dipiolar Bose-Einstein condensates can host a rich variety of topological excitations due to their internal degrees of freedom and anisotropic nature of the interaction. In this talk, I will review our group's activities on these topics such as the Kibble-Zurek mechanism [1], knot excitations [2], non-Abelian vortices [3], and ferrofluidity [4].

This work was done in collaboration with Yuki Kawaguchi, Hiroki Saito, Michikazu Kobayashi, and Muneto Nitta.

[1] H. Saito, *et al*., Phys. Rev. A **76**, 043613 (2007).
[2] Y. Kawaguchi, *et al.*, Phys. Rev. Lett. **100**, 180403 (2008).
[3] M. Kobayashi, *et al*., Phys. Rev. Lett. **103**, 115301 (2009).
[4] H. Saito, *et al.*, Phys. Rev. Lett. **102**, 230403 (2009).

O31

Strongly Correlated ``Materials'' made out of Ultra Cold Atoms

Tin-Lun Ho

The Ohio State University, Enarson Hall 154W 12th Avenue, Columbus, Ohio 43210, USA

At present, there is a worldwide effort to use ultra-cold atoms to simulate intractable quantum models for condense matter systems. It is hope that these super-clean systems, should they be successfully simulated, will provide us with the solutions of some longstanding problems, as well as a whole host of new quantum systems. In this talk, we shall discuss the current situation of this world wide effort, the serious challenges it faces, the successes so far -- including impressive experimental success of producing synthetic gauge fields, as well as the exciting prospects ahead.

O32

Spin-dependent inelastic collisions in spin-2 Bose-Einstein condensates

S. Tojo,[1] T. Hayashi,[1] T. Tanabe,[1] T. Hirano[o],[1] Y. Kawaguchi,[2] H. Saito,[3] M. Ueda[2]

[1]*Department of Physics, Gakushuin University, Tokyo 171-8588, Japan*
[2]*Department of Physics, University of Tokyo, Tokyo 113-0033, Japan*
[3]*Department of Applied Physics and Chemistry, University of Electro-Communications, Tokyo 182-8585, Japan*

The field of cold collisions has attracted extensive interest and has grown explosively since the early days of atom cooling and trapping [1]. The development of novel techniques for cooling and manipulating atoms have led to a deeper understanding of physics of collisions: e.g., evaporative cooling enabled Bose-Einstein condensates (BECs) to be realized and opened the field of ultracold collisions, while the evaporative cooling process itself relies on the nature of collisions. In an optical trap, the spin degrees of freedom of atoms are liberated enabling a rich variety of spinor BECs physics to be studied. Spin-2 BECs have attracted much interest in recent years and there have been several experimental studies of spin-2 systems; investigation of their magnetic phases [2], of multiply charged vortices [3], and the phase separation between binary BECs [4].

In this work, we have observed the time dependence of spin populations in spin-2 two component condensates initially populated in all possible sets of magnetic sublevels as shown in Fig.1 at 3 G of the magnetic field which suppresses the spin-changing collision between different magnetic sublevels in same hyperfine states [5], and compared the results with our theoretical model. By analogy with the scattering length in elastic collisions, two-body inelastic collisions are described by two parameters, b_0 and b_2, which correspond to channels with the total spins of 0 and 2, respectively. We experimentally determine these two parameters from the loss rates of single-component BECs of $|F=2, m_F=1>$ and $|F=2, m_F=0>$. We calculated the time evolution of the number of atoms in two-component BECs using the values of b_0 and b_2 by the Gross-Pitaevskii equation including the effect of a magnetic field gradient [6]. The results agreed well with the experimental results.

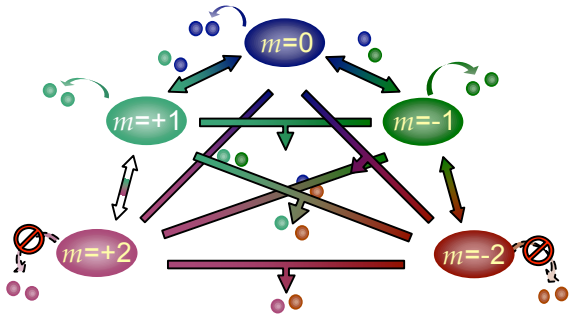

Fig.1: Inelastic collision channels for all combinations of m and m' in a spin-2 BEC.

A detailed understanding of the relative-population dependence and the spin-state dependence of inelastic collisions are key issues in the future study of spinor BECs, such as the determination of the magnetic ground state of spin-2 ^{87}Rb BEC and observation of novel quantum vortices.

[1] As review, J. Weiner, V.S. Bagnato, S. Zilio, and P.S. Julienne, Rev. Mod. Phys. **71**, 1 (1999).
[2] M. Ueda and M. Koashi, Phys. Rev. A **65**, 063602 (2002); H. Saito and M. Ueda, *ibid.* **72**, 053628 (2005).
[3] T. Isoshima, M. Okano, H. Yasuda, K. Kasa, J.A. M. Huhtamäki, M. Kumakura, and Y. Takahashi, Phys. Rev. Lett. **99**, 200403 (2007); T. Kuwamoto, H. Usuda, S. Tojo, and T. Hirano, J. Phys. Soc. Jpn (in press).
[4] D.S. Hall, M.R. Matthews, J.R. Ensher, C.E. Wieman, and E.A. Cornell, Phys. Rev. Lett. **81**, 1539 (1998); K.M. Mertes, J.W. Merrill, R. Carretero-Gonzalez, D.J.Frantzeskakis, P.G. Kevrekidis, and D.S. Hall, *ibid.* **99**, 190402 (2007).
[5] T. Kuwamoto, K. Araki, T. Eno, and T. Hirano, Phys. Rev. A **69**, 063604 (2004); S. Tojo, A. Tomiyama, M. Iwata, T. Kuwamoto, and T. Hirano, Appl. Phys. B **93**, 403 (2008).
[6] S. Tojo, T. Hayashi, T. Tanabe, T. Hirano, Y. Kawaguchi, H. Saito, and M. Ueda, Phys. Rev. A **80**, 042704 (2009).

O33

Topological Quantum Computing in Fermi Superfluids and Strontium Ruthenate: Prospects and Problems

Anthony J. Leggett

Department of Physics and Center for Advanced Study, University of Illinois at Urbana–Champaign, Urbana, Illinois 61801–3080, USA

One of the most promising systems for the possible implementation of topologically protected quantum systems is a system of "half-quantum vortices" ("HQV's") occurring in a ($p + ip$) Fermi superfluid such as is believed to be realized in the A phase of superfluid ^{3}He and probably in Sr_2RuO_4 ("SRO"). However, the success of this operation requires, as a minimum, (a) that in the relevant systems the Cooper pairs indeed form in the ($p + ip$) phase (b) that the HQV's can be stabilized and manipulated (c) that the "Majorana fermions" which have been postulated to occur on these half-quantum vortices really exist.

In this talk I will first briefly review the current evidence for the ($p + ip$) state and comment on some ambiguities concerning the appropriate many-body wave function to describe it, then comment on the current situation regarding the existence of HQV's.

Finally I will point out that a "Majorana fermion" is nothing more nor less than a quantum superposition of a "real" (Bogoliubov-Dirac) fermion and a "pure annihilator", and attempt to use a variant of a toy model due to Kitaev to discuss its occurrence in a HQV.

O34

Experiments on a pure superfluid condensate: ^{3}He at ultralow temperatures.

Shaun N. Fisher

Department of Physics, Lancaster University, Bailrigg, Lancaster, LA1 4YW, United Kingdom

Superfluid ^{3}He is almost perfectly pure and can be cooled to such low temperatures that the normal fluid fraction becomes entirely negligible. The few remaining thermal (quasiparticle) excitations travel ballistically in a potential determined by the superfluid condensate. The excitations are readily detected by mechanical oscillators providing highly sensitive thermometry, and we have developed techniques to produce and measure beams of ballistic quasiparticles. The excitations have a large cross-section for Andreev reflection from superfluid defects such as quantum vortices. This allows us detect vortices directly and offers a technique for imaging quantum turbulence and other superfluid structures. We discuss some recent experiments and analogies with classical physics and cosmology.

O35

Detecting the Majorana fermion surface state of ^{3}He-B through spin relaxation

Suk Bum Chung

Department of Physics, Stanford University, Stanford, California 94305, USA

The concept of the Majorana fermion has been postulated more than eighty years ago; however, this elusive particle has never been observed in nature. The non-local character of the Majorana fermion can be useful for topological quantum computation. Recently, it has been shown that the 3He-B phase is a time-reversal invariant topological superfluid, with a single component of gapless Majorana fermion state localized on the surface. Such a Majorana surface state contains half the degrees of freedom of the single Dirac surface state recently observed in topological insulators. We show here that the Majorana surface state can be detected through an electron spin relaxation experiment. The Majorana nature of the surface state can be revealed though the striking angular dependence of the relaxation time on the magnetic field direction, $1/T_1 ¥propto sin^2 ¥theta$ where $¥theta$ is the angle between the magnetic field and the surface normal. The temperature dependence of the spin relaxation rate can reveal the gapless linear dispersion of the Majorana surface state. We propose a spin relaxation experiment setup where we inject an electron inside a nano-sized bubble below the helium liquid surface.

O36

New Features of Anisotropic Superfluid ^{3}He

O. Ishikawa

Department. of Physics, Graduate School of Science, Osaka City University, 3-3-138 Sugimoto, Sumiyoshiu-ku, Osaka 558-8585, Japan

Anisotropic superfluid ^{3}He shows very interesting properties when it is confined in restricted spaces, like narrow cylinder, thin film between parallel plates and aerogel of silica strands.

The constraint that angular momentum of the Copper Pairs must be perpendicular to the surface of the container or objects plays an important role on forming texture in the real sample space. This texture is a spatial configuration of the angular part of order parameter vector. In narrow cylinders of 0.1 mm and 0.2 mm diameter, the Mermin-Ho texture was observed by using the rotating cryostat. The Mermin-Ho texture is also a quantum vortex with no singular vortex core structure. It was shown that the Mermin-Ho texture has one circulation quantum and four CUV vortices (Continuous Unlocked Vortex) can invade into a narrow cylinder of 0.2 mm diameter from bulk liquid at angular velocity of 12 rad/s and that the sign of the vorticity of Mermin-Ho vortex changes by reverse rotation.

The energy loss of flowing fluid in hydrodynamic regime is usually attributed to viscosity of fluid and turbulent flow at high Reynolds number. Beside two factors, quantized vortex passing across the flow is another type of energy loss in quantum fluid. In aerogel, the fourth sound experiment reveals a new type of energy loss mechanism in superfluid B-like phase. Fourth sound is a wave in which only density deviation of superfluid component can propagate in confined spaces. Aerogel grows directly in narrow pores inside packed silver fine powders. The energy loss of fourth sound with aerogel becomes smaller than that without aerogel. The drag force acting on the normal component due to aerogel strands can explain the experimental results well. Theoretical argument shows that the midgap state of quasiparticles below the energy gap of bulk liquid plays an important role on this frictional motion.

The very stable coexisting phenomena of the A-like and the B-like phases are observed in the cylindrical shape of aerogel of 97.5 % porosity. Using Magnetic Resonance Imaging (MRI), it was found that the B-like phase appears in the central part of cylinder surrounded by the A-like phase with decreasing temperatures. The phase boundary between the A-like phase and the B-like phase seems to be pinned by aerogel, but this pinning is so strong that the phase boundary can not move easily by changing temperature. As a result we observed a large hysteresis of the fraction of both phases and we could controlled any fraction of phase by a turn around of temperature sweeping.

O37

Mechanical Spin Pump and Spin Relaxation in Superfluid ^{3}He-A$_1$

A. Yamaguchi1[1,2], Y.Aoki,[1] S.Murakawa[3], H. Ishimoto[1] and H. Kojima[4]

[1]*Institute for Solid State Physics, University of Tokyo, 5-1-5 Kashiwanoha, Kashiwa-shi, Chiba 277-8581, Japan*
[2] *University of Hyogo, 3-2-1 Kouto, Kamigoricho, Akogun, Hyogo, 678-1297, Japan*
[3]*Department of Condensed Matter Physics, Tokyo Institute of Technology,*
2-12-1 O-okayama, Meguro-ku, Tokyo 152-8551, Japan
[4]*Serin Physics Laboratory, Rutgers University*

When liquid He-3 is placed in high magnetic field, a unique superfluid A$_1$ phase emerges with its almost totally spin-polarized pairing state splitting the null field transition temperature into two transitions. The unique magneto-hydrodynamics of the A$_1$ superfluid exhibit a magnetic fountain effect. The effect in which the gradients in pressure and magnetic field in the chemical potential are balanced has been applied extensively to investigate the intrinsic spin relaxation. In addition, if the spin-polarized superfluid is forced through a superleak into a small chamber, it is possible to increase the polarization of liquid He-3 dramatically in the chamber.

We have constructed a device using a glass capillary array as the superleak and a flexible membrane as an electrostatically actuated pneumatic pump, and carried out experiments to observe the accumulated spin density in the small chamber and to investigate the spin relaxation [1]. The change in spin density was deduced from the measured differential pressure. Measurements in 5 tesla indicate that the superfluid polarization increased by 40% from that produced by the static field. The observed increase in the spin relaxation time compared to the magnetic fountain experiments is explained by the increase of polarization.

[1] A. Yamaguchi, Y. Aoki, S. Murakawa, H. Ishimoto and H. Kojima, Phys. Rev. B 80, 052507 (2009)

O38

Surface Andreev Bound States and Surface Majorana States on the Superfluid ^{3}He B Phase

R. Nomura, S. Murakawa, Y. Wada, M. Wasai, K. Akiyama, Y. Tamura, M. Saitoh, Y. Aoki, and Y. Okuda

Department of condensed Matter Physics, Tokyo Institute of Technology, 2-12-1 Ookayama, Meguro-ku, Tokyo 152-8551, Japan

One of the universal features in unconventional superconductors and superfluids is the appearance of the surface Andreev bound states (SABS) in the vicinity of an interface. SABS are the low-lying quasiparticle excitations resulting from the interference of the Andreev reflected quasiparticles. Recently, it was pointed out that SABS can be recognized as the gapless edge states on a topologically non-trivial BCS states, as the quantum Hall and quantum spin Hall systems have the edge states. SABS are Majorana fermions satisfying the equivalence of particles and antiparticles. SABS of the superfluid ^{3}He B phase on a specular wall have a linear dispersion and form the surface Majorana cone[1, 2, 3].

Figure 1 shows theoretical calculation of the surface density of states (SDOS) of the B phase in various boundary conditions[4], which are represented by the specularity factor S. Bandwidth Δ^* of SABS is the narrowest in the diffusive scattering limit $S = 0$ and becomes broader as increasing S. Zero-energy weight of SDOS is the maximum at $S = 0$ and decreases as increasing S. In the specular scattering limit $S = 1$, SDOS has a linear energy dependence which is nothing but the Majorana cone.

We have shown that complex transverse acoustic impedance $Z = Z' + iZ''$ is a good probe for SABS and gives spectroscopic details of SDOS[5, 6]. S can be controlled *in situ* by coating the wall with ^{4}He and be evaluated by the measurement of Z in the normal state.

In the temperature dependence $Z(T)$, a clear kink in Z' and a peak in Z'' appear at a particular temperature T^*. $Z(T)$ is well reproduced theoretically and it is found that the kink and the peak are weak singularities appearing at T^* at which the condition $\omega = \Delta + \Delta^*$ is met, where ω is the angular frequency of the measurement. As increasing S by the coating, we observed that Δ^* becomes broader as the theory predicted. In large S region ($S > 0.4$), $\Delta^*/\Delta \sim 1$ and the gap is filled by the SABS band[7].

In the coated case at $S > 0$, we observed a new peak in $Z(T)$ at a temperature lower than T^*. Z at various S is shown in Fig. 2 as a function of the scaled energy. The low-energy or low-temperature peak is absent at $S = 0$ and it becomes prominent as S increases. The theory reproducing this peak showed that the reduction of the zero-energy SDOS is the origin of the peak[8,9]. Growth of the peak is a strong experimental indication of the Majorana cone of the ^{3}He B phase on the specular wall.

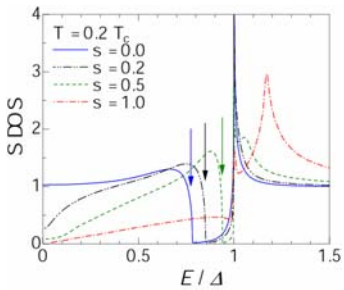

Fig. 1. Surface density of states of the ^{3}He B phase. The arrows indicate Δ^*.

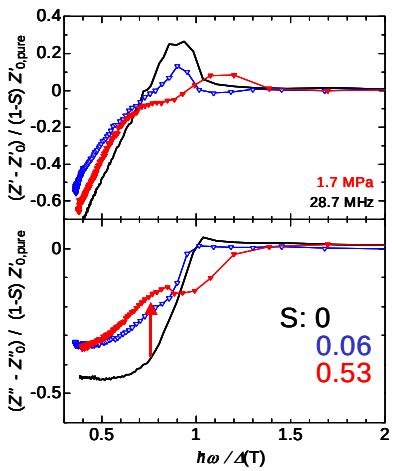

Fig. 2 Z as a function of the scaled energy. Z_0 is the value in the normal state just above T_c. Growth of the new peak is indicated by the arrow.

[1] A. Schnyder *et al.*, Phys. Rev. B **78**, 195125 (2008).
[2] X.-L. Qi *et al.*, Phys. Rev. Lett. **102**, 187001 (2009).
[3] S. B. Chung and S.-C. Zhang, Phys. Rev. Lett. **103**, 235301 (2009).
[4] Y. Nagato *et al.*, J. Low Temp. Phys, **149**, 294 (2007)
[5] Y. Aoki *et al.*, Phys. Rev. Lett. **95**, 075301 (2005)
[6] M. Saitoh *et al.*, Phys. Rev. B **74**, 220505(R) (2006)
[7] Y. Wada *et al.*, Phys. Rev. B **78**, 214516 (2008)
[8] S. Murakawa *et al.*, Phys. Rev. Lett. **103**, 155301 (2009)
[9] K. Nagai *et al.*, J. Phys. Soc. Jpn. **77**, 111003 (2008).

O39

Boundary and Impurity Effects on Fourth Sound Propagation in Superfluid ^{3}He

S. Higashitani, Y. Nagato, and K. Nagai

Graduate School of Integrated Arts and Sciences, Hiroshima University, Kagamiyama 1-7-1, Higashi-Hiroshima 739-8521, Japan

As was shown by Einzel and Parpia [1], normal liquid ^{3}He in a narrow channel filled with a high porosity aerogel can exhibit two distinct steady flow behaviors, depending on the relative importance between the boundary effect and the impurity effect. One is the Hagen-Poiseuille (HP) flow characterized by a parabola flow profile and a flow conductance proportional to the square of the channel width. The other is the Drude type flow in which the flow velocity is almost constant across the channel and the flow conductance is dominated by the momentum relaxation due to impurity scattering. Similar flow phenomena are expected for the normal-fluid component in superfluid ^{3}He. As a result, there are two possible mechanisms responsible for the fourth sound propagation in superfluid ^{3}He impregnated in aerogel, i.e., the boundary effect causing the HP flow of the viscous normal fluid and the impurity effect giving rise to friction between the normal-fluid component and the aerogel; the normal-fluid component is clamped to the channel wall in the former case and to the aerogel in the latter case. Thus, there arises a renewed interest in the superfluid dynamics: Which law (HP or Drude) governs the fourth sound propagation in the superfluid ^{3}He-aerogel system? We show that the formulas for the energy loss of the fourth sound in the above two pictures have distinct forms, as in the case of the flow conductance in normal liquid ^{3}He. We also show from analysis of the fourth sound resonance experiment by the Osaka City University group that the normal-fluid dynamics in the aerogel (99 % porosity) obeys not the conventional HP law but the Drude law.

[1] D. Einzel and J. M. Parpia, Phys. Rev. Lett. **81**, 3896 (1998).

O40

Theory for *d*-Vector in Spin-Triplet Superconductor Sr_2RuO_4

K. Miyake

Department of Materials Engineering Science, Graduate School of Engineering Science, Osaka University, 1-3 Machikaneyama-cho, Toyonaka-shi, Osaka 560-8531, Japan

In this five years research project, we have investigated a structure and its physical consequence of ***d***-vector in Sr_2RuO_4, spin triplet superconductor. I report the results of this investigation, which resolves a puzzle of the structure of ***d***-vector and the anomalous ^{17}O-NQR relaxation rate in the superconducting state.

1) Microscopic model of Sr_2RuO_4:

Since the energy level of 4*d* electron is deeper than that of 3d or 5d, the 4d electrons have stronger hybridization with 2*p* electrons at O site, giving rise to a considerable part (about 1/3) of the density of states from 2*p* orbital at the Fermi level. Therefore, the Hubbard model (which takes into account only the Coulomb interaction U_{dd} and neglects the 2*p* degrees of freedom and so the Coulomb interaction U_{pp}) is not enough as a microscopic model for Sr_2RuO_4, but the model should be extended the so as to take into account U_{pp}. On this extended model, we derived the pairing interaction by the the 3rd order perturbation theory following Nomura-Yamada theory [1] and showed that the Cooper pair wave function of the type ($\sin k_x + i \sin k_y$) is stabilized in contrast to the type of $\sin k_x \cos k_y$ or $\cos k_x \sin k_y$ which is stabilized in the case of Hubbard model. Then, by taking the atomic spin-orbit interaction and the Hund's rule coupling at Ru site perturbatively, the stable direction of ***d***-vector is shown to be in the *ab*-plane [2], which resolves the puzzle of Knight shift measurements [3].

2) Anomalous ^{17}O-NQR relaxation rate due to internal Josephson oscillations through pair spin-orbit interaction:

Among remaining puzzles in spin-triplet superconductor Sr_2RuO_4, I present a possible resolution for the anomalous relaxation of ^{17}O NQR from the viewpoint that its anomalous behavior [4] is a manifestation of the internal Josephson mode associated with the spin-orbit coupling of the relative motion of Cooper pairs [5].

Supposing the spin-triplet superconducting state of Sr_2RuO_4, the spin-orbit (SO) coupling associated with relative motion in Cooper pairs is calculated by extending the method for the dipole-dipole coupling given by Leggett in the superfluid ^{3}He [6]. It is shown that the SO coupling works only in the equal-spin pairing (ESP) state to make the pair angular momentum $\hbar\boldsymbol{L}$ and the pair spin angular momentum $i\boldsymbol{d}\times\boldsymbol{d}^*$ parallel with each other. The SO coupling gives rise to the internal Josephson effect in a chiral ESP state as in superfluid A-phase of ^{3}He with a help of an additional anisotropy arising from SO coupling of atomic origin which works to direct the ***d***-vector into the *ab*-plane. This resolves the problem of the anomalous relaxation of ^{17}O-NQR and the structure of ***d***-vector in Sr_2RuO_4 by applying the theory of Leggett and Takagi for dynamical spin susceptibility by internal Josephson oscillations [7].

References

[1] T. Nomura and K. Yamada, J. Phys. Soc. Jpn. **69**, 3678 (2000); **71**, 1993 (2002).
[2] Y. Yoshioka and K. Miyake, J. Phys. Soc. Jpn. **78**, 074701 (2009).
[3] H. Murakawa, K. Ishida, K. Kitagawa, Z. Q. Mao, and Y. Maeno, Phys. Rev. Lett. **93**, 167004 (2004); H. Murakawa, K. Ishida, K. Kitagawa, H. Ikeda, Z. Q. Mao, and Y. Maeno, J. Phys. Soc. Jpn. **76**, 024716 (2007); K. Ishida, private communications
[4] H. Mukuda, K. Ishida, Y. Kitaoka, K. Miyake, Z. Q. Mao, Y. Mori and Y. Maeno, Phys. Rev. B **65**, 132507 (2002).
[5] K. Miyake, J. Phys. Soc. Jpn. **79**, No.2 (2009), in press.
[6] A. J. Leggett, Rev. Mod. Phys. **47**, 331 (1975).
[7] A. J. Leggett and S. Takagi, Ann. Phys. **106**, 79 (1977).

O41

Novel Quantum Phenomena in Superconducting Sr_2RuO_4

Y. Maeno

Department of Physics, Kyoto University, Kyoto 606-8502, Japan

We review our recent activities in confirming the detailed structure of the order parameter of Sr_2RuO_4 and establishing various novel phenomena expected for chiral spin-triplet superconductivity. The layered unconventional superconductor Sr_2RuO_4 is a superclean material in the sense that the quasiparticle mean-free path can be made as large as thirty time the coherence length [1]. The accumulated experimental evidence on Sr_2RuO_4 indicates that the time reversal symmetry (TRS) of the superconducting order parameter is broken. This broken TRS is attributable to a chiral order parameter consisting of two-component orbital wave function and equal-spin pairing (ESP) state. Such chiral *p*-wave state is considered as a two-dimensional analogue of the superfluid ^{3}He-A phase [2].

We have mainly taken two approaches in our investigations. In the first approach, the efforts have been directed toward resolving some of the issues concerning the chiral spin-triplet interpretation [3, 4]. In addition, the direction of the *d*-vector has been re-examined both experimentally [5] and theoretically [6].

In the second approach, novel phenomena associated with boundaries with other materials have been studied. In particular, it was revealed that eutectic crystals consisting of Sr_2RuO_4 with Ru or with $Sr_3Ru_2O_7$ exhibit unusual superconducting behavior [7, 8]. Moreover, micro-fabricated eutectic samples with the enhanced roles of boundaries and edges were shown to exhibit superconducting interference and hysteresis [9, 10]. Theoretically, notable progress has been made by recognizing the emergence of "odd-frequency" pairing states at the boundaries involving a spin-triplet superconductor [11]. It has also been recognized that micron-size crystals are useful in extracting novel features of the superconducting order parameter of Sr_2RuO_4 [12].

The results presented are mainly obtained by collaborations with K. Ishida, H. Kambara, S. Kashiwaya, K. Miyake, Y. Tanaka, S. Yonezawa, S. Kittaka, T. Nakamura, R. Nakagawa, H. Taniguchi, M. Sigrist, and H. Kaneyasu.

[1] A.P. Mackenzie and Y. Maeno, Rev. Mod. Phys. **75**, 657 (2003).
[2] T.M. Rice and M. Sigrist, J. Phys.: Condens. Matter. **7**, L643 (1996).
[3] S. Kittaka *et al.*, Phys. Rev. B **80**, 174514 (2009).
[4] J. R. Kirtley *et al.*, Phys. Rev. B **76**, 014526 (2007).
[5] K. Ishida *et al*., J. Phys. Chem. Solids **69,** 3108 (2008).
[6] Y. Yoshioka and K. Miyake, J. Phys. Soc. Jpn. **78**, 074701 (2009).
[7] S. Kittaka *et al.*, Phys. Rev. B **78**, 103705 (2009).
[8] S. Kittaka et al., Phys. Rev. B **77**, 214511 (2008).
[9] H. Kambara *et al.*, Phys. Rev. Lett. **101,** 267003 (2008).
[10] R. Nakagawa *et al*., to appear in Physica C (2010).
[11] Y. Tanaka and A. A. Golubov, Phys. Rev. Lett. **98**, 037003 (2007); Tanaka, *et al.*, Phys. Rev. Lett. **99**, 037005 (2007), Asano *et al.*, Phys. Rev. Lett. **99**, 077005 (2007).
[12] J. Jang, R. Budakian, and Y. Maeno, arXiv: 0908.2673.

O42

Unconventional Local Transport Characteristics in Microfabricated Sr_2RuO_4-Ru eutectic crystals

H. Kambara,[1] S. Kashiwaya,[1] H. Yaguchi,[2] Y. Asano,[3] Y. Tanaka,[4] and Y. Maeno[5]

[1] *National Institute of Advanced Industrial Science and Technology (AIST), Tsukuba 305-8568*
[2] *Department of Physics, Faculty of Science and Technology, Tokyo University of Science, Noda 278-8510*
[3] *Department of Applied Physics, Hokkaido University, Sapporo 060-8628*
[4] *Department of Applied Physics, Nagoya University, Nagoya 464-8603*
[5] *Department of Physics, Kyoto University, Kyoto 606-8502*

Strontium ruthenate Sr_2RuO_4 (SRO) is an attractive material because of rich internal degrees of freedom in the superconducting state, the so-called spin-triplet chiral *p*-wave state ($p_x \pm ip_y$) with broken time reversal symmetry [1]. So far, several experiments (μSR, Kerr effect, Josephson junction) suggest the possible existence of chiral domain in SRO, although a direct evidence of the chiral domain with scanning Hall probe or SQUID detection is absent. Here we have adopted microfabrication technique with a focused ion beam to SRO-Ru eutectic crystal, and succeeded in making a microbridge to investigate local transport characteristics without averaging over the bulk property [2]. We have observed quite anomalous voltage-current (*V-I*) and differential resistance-current (*dV/dI-I*) characteristics of the microbridge (Fig. 1). Namely, (i) voltage decreases at certain thresholds with increasing current, and as a result, (ii) the hysteresis loop shows the opposite direction compared to usual Josephson junctions. These features are too unusual to explain without taking account of internal degrees of freedom in the superconducting state. Assuming the existence of chiral domain and domain wall motion under dc current, the anomalous transport phenomena are explainable.

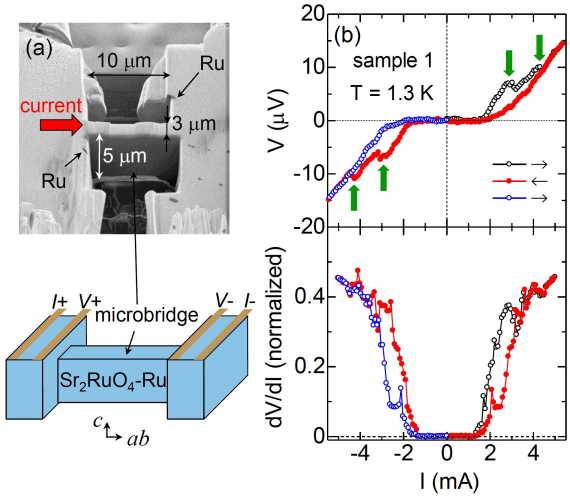

FIG.1: (a) Scanning ion microscope image of microbridge of Sr_2RuO_4-Ru. (b) Anomalous *V-I* (upper) and *dV/dI-I* (lower) characteristics obtained dc and ac methods, respectively. The bold arrows denote anomalous voltage drops.

[1] A. P. Mackenzie and Y. Maeno, Rev. Mod. Phys. **75**, 657 (2003).
[2] H. Kambara, S. Kashiwaya, H. Yaguchi, Y. Asano, Y. Tanaka, and Y. Maeno, Phys. Rev. Lett. **101**, 267003 (2008).

O43

External-fields induced novel phenomena in Mott insulator Ca_2RuO_4

Fumihiko Nakamura

ADSM, Hiroshima University, Higashi-Hiroshima 739-8530, Japan.

A 4d electron Mott insulator Ca_2RuO_4 (CRO) shows versatile phase transitions in external fields. We introduce here two attractive our findings as follows: Firstly, pressure phase diagram of this system is unique and quite different from that of the doped system. Pressurised CRO displays versatile quantum phenomena, ranging from an antiferromagnetic Mott insulator to superconductivity via a ferromagnetic (FM) quasi-2D metal. In particular, it is amazingly that the superconductivity occurs in the vicinity of a FM critical point [1]. Secondly, we show that application of quite small electric-field of ~40V/cm induces the transition from the Mott insulating to the quasi two-dimensional metallic state at 295K. The breakdown phenomenon is accompanied by a structural transition. Thus, we can fully expect that our findings of the breakdown at quite weak threshold-field will make a great impact on not only basic physics but also application to an electronic device.

[1] P. L. Alireza *et al*., Journal of Physics: Condensed Matter, 22 (2010) 052202.

O44

Odd-frequency pairing in superconducting heterostructures

A.A. Golubov,[1] Y. Asano,[2] Y. Tanaka[3]

[1] *Faculty of Science and Technology, University of Twente, 7500 AE, Enschede, The Netherlands*
[2] *Department of Applied Physics, Hokkaido University, Sapporo 060-8628, Japan*
[3] *Dept. of Applied Physics, Department of Applied Physics, Nagoya University, Nagoya 464-8603, Japan*

We present theory of odd-frequency pairing in superconducting heterostructures, where quite generally, the odd-frequency pairing component is induced near interfaces. General description of superconducting proximity effect in a normal metal or a ferromagnet attached to an unconventional superconductor (S) is given within quasiclassical kinetic theory for various types of symmetry state in S. As an example, we consider a junction between a diffusive normal metal (DN) and a p-wave superconductor (even-frequency spin-triplet odd-parity symmetry), where the pairing amplitude in a DN belongs to an odd-frequency spin-triplet even-parity symmetry class. Further application of the model is the Josephson effect in SFS junctions where F is fully polarized ferromagnet. Relevance to recent experiments on unconventional junctions is discussed.

O45

Odd-frequency pairing in spin-triplet superconductor junctions

Y. Tanaka,[1] Y. Asano[2], A.A. Golubov[3] and S. Kashiwaya[4]

[1]*Dept. of Applied Physics, Department of Applied Physics, Nagoya University, Nagoya 464-8603, Japan*
[2] *Department of Applied Physics, Hokkaido University, Sapporo 060-8628, Japan*
[3]*Faculty of Science and Technology, University of Twente, 7500 AE, Enschede, The Netherlands*
[4]*National Institute of Advanced Industrial Science and Technology, Tsukuba 305-8568, Japan*

Based on a general theory of proximity effect [1], we have studied about proximity effect in proximity effect in junctions between diffusive normal metals (DN) and superconductors [2]. It is revealed when the superconductor has a spin-triplet state odd-parity pairing realized in Sr_2RuO_4, the resulting symmetry in DN is always odd-frequency spin-triplet s-wave [2]. The resulting quasiparticle density of state in DN has a zero energy peak [3]. The presence of the odd-frequency pairing in DN can explain anomalous proximity effect [3], Josephson effect [4] in spin-triplet superconductor junctions. We discuss how to detect anomalous proximity effect via T-shaped junction [5] and anomalous magnetic response of the present system[6].

[1] Y. Tanaka, A.A. Golubov, S. Kashiwaya and M. Ueda, Phys. Rev. Lett. 99, 037005 (2007).
[2]Y. Tanaka and A.A. Golubov, Phys. Rev. Lett. 98 037003 (2007).
[3]Y. Tanaka and S. Kashiwaya, Phys. Rev. B, 70, 012507 (2004); Y. Tanaka, S. Kashiwaya and T. Yokoyama, Phys. Rev. B 71, 094513 (2005).
[4]Y. Asano, Y. Tanaka and S. Kashiwaya, Phys. Rev. Lett., 96, 097007 (2006).
[5]Y. Asano, Y. Tanaka, A.A. Golubov and S. Kashiwaya, Phys. Rev. Lett. **99**, 067005 (2007).
[6] Y. Tanaka, Y. Asano, A. A. Golubov, and S. Kashiwaya, Phys. Rev. B **72**, 140503 (2005); Y. Asano, Y. Tanaka and AA. Golubov, unpublished.

Poster Presentations

Odd numbers: March 9 (Tuesday)

Even numbers: March 10 (Wednesday)

P1

STM/STS Studies of Epitaxially Grown Graphene on SiC

N. F. Kawai, T. Matsui and Hiroshi Fukuyama

Department of Physics, The University of Tokyo, 7-3-1 Hongo, Bunkyo-ku, Tokyo 113-0033, Japan

Graphene, an sp^2-bonded carbon monolayer sheet, is the first truly two-dimensional material when it is suspended only at edges. Owing to the honeycomb crystalline structure and the linear dispersion, graphene shows many novel properties, e.g., extremely high mobility, anomalous quantum Hall effect, Klein tunneling, and so on [1]. Recently, epitaxially grown graphene samples with large area and high crystallinity become available by thermal decomposition of SiC substrate. This method attracts much attention from the viewpoint not only of basic research but also of application because of its compatibility with the lithography technique and the future possibility of graphene-based electronic devices.

Previously, we have studied unique electronic properties of the quasi two-dimensional electron system at *bulk* graphite surfaces such as the "graphite edge state" localized at the zigzag edge (Fig.1) [2], the zero-energy Landau levels [3] and real space imaging of the localized/delocalized electronic wave-functions near defects [4] with the scanning tunneling microscopy/spectroscopy (STM/STS) technique at low temperatures [5]. These properties are characteristic of the graphene stack. As natural extension, we are now investigating properties of a few layers of graphene in which they will appear much more distinctly and probably new features as well.

Epitaxial graphene samples were synthesized by heating 6H- or 4H-SiC (0001) single crystals up to T = 1600 K in UHV. Uniform growth of graphene layers of large area was confirmed with low-energy electron diffraction (LEED) and STM (Fig. 2) after each heating sequence. Fig. 3a shows a preliminary tunneling spectrum of a bilayer graphene sample measured at T = 2 K in zero magnetic field. This shares several common features with the previous data by other workers [6]. However, the spectrum at B = 6 T (Fig. 3b) shows no clear Landau-level peak structure, which might be due to the graphene/SiC interface effect. We also discuss preliminary STM/STS results on thicker graphene layers synthesized at the SiC (000-1) surface where the interface effect should be negligibly small.

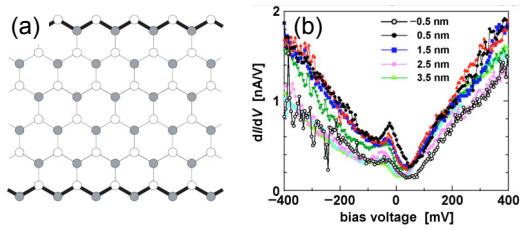

Fig.1: (a) Graphite zigzag edge. (b) Tunnel spectra near a zigzag step edge at graphite surface: U_g = -0.1 V, T = 77 K, in UHV [2].

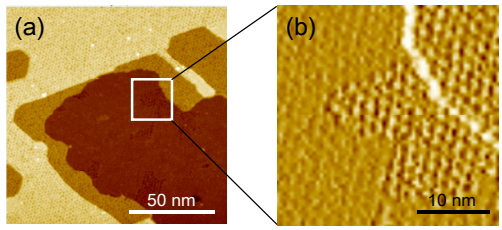

Fig.2: (a) STM image of epitaxially grown graphene layer at 6H-SiC (0001) surface and (b) its gradient image: U_g = -1 V, T = 80 K, in UHV.

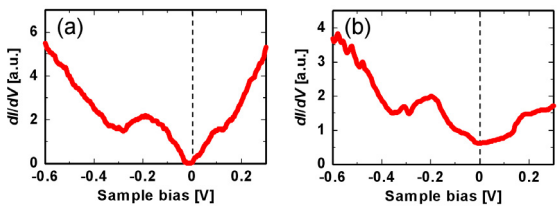

Fig.3: Tunnel spectra of bilayer graphene at 4H-SiC (0001) surface at (a) B = 0 T and (b) B = 6 T: T = 2 K, in UHV.

[1] A. H. Castro Neto *et al.*, Rev. Mod. Phys. **81**, 109 (2009).
[2] Y. Niimi *et al.*, Appl. Surf. Sci. **241**, 43 (2005); Phys. Rev. B **73**, 085421 (2006).
[3] T. Matsui *et al.*, Phys. Rev. Lett. **94**, 226403 (2005).
[4] Y. Niimi *et al.*, Phys. Rev. Lett. **97**, 236804 (2006); *ibid.* **102**, 026803 (2009).
[5] H. Kambara, T. Matsui, Y. Niimi, and H. Fukuyama, Rev. Sci. Instrum. **78**, 073703 (2007).
[6] P. Lauffer *et al.*, Phys. Rev. B **77**, 155426 (2008).

P2

Topological Dirac Fermion on Graphite

T. Matsui,[1] K. Tagami,[2] M. Tsukada,[3] and Hiroshi Fukuyama[1]

[1]*Department of Physics, The University of Tokyo, 7-3-1 Hongo, Bunkyo-ku, Tokyo 113-0033, Japan*
[2]*Advanced Corporation, 1-9-20, Akasaka, Minato-ku, Tokyo 107-0052. Japan*
[3]*WPI-AIMR, Tohoku University, 2-1-1 Katahira, Aoba-ku, Sendai 980-8577, Japan*

Since the experimental success to fabricate Graphene, a monolayer sheet of graphite, the unique characters of Dirac fermion (DF) start to attract a big interest. Its energy band has a linear *k*-dispersion and, therefore, is characterized by Dirac equation including relativistic properties. In addition to Graphene, a typical material with DF, some other materials are also paid many attentions recently because of their topologically appeared DFs. Graphite is a well known quasi two-dimensional (2D) material and one of the good candidates which have the topological Dirac fermion (TDF). The Fermi surface of graphite is located along the Brillouin zone edge (*H-K-H*), and it shows the linear band dispersion around *H* point, while it is parabolic around *K* point like the conventional 2D carriers, namely Schrödinger fermions (SFs), which can be dealt with Schrödinger equation. Since the wave function amplitude becomes zero at *H* point, the carriers at *H* point can be localized at surfaces. Consequently, the TDF can be expected on the surface of graphite.

Here, we observed the TDF on the surface of graphite with scanning tunneling microscopy and spectroscopy (STM/S), a measurement probe sensitive to surfaces, in magnetic fields. The observed surface density of states (DOS) show many peaks which are originated from the Landau levels on graphite surfaces.[1] The field (*B*) dependencies of the peaks are usually very complicated reflecting the irregular structure of graphite in *z* direction with many stacking faults. However, the detailed analysis suggests that there certainly are peaks which have the square-*B* dependence, and more surprisingly, they also depend on square of the Landau index *n*. Different from the (*n*+1) *B* dependence for conventional SFs, such square-*nB* dependence is characteristic to DFs. Considering that they are the levels of TDF, the Fermi velocity (v_F) would be (1.07 ± 0.05) x 10^6 m/s which is comparable to the v_F of DF reported for Graphene.

This result is verified by theoretical calculations with the Green's function method, which had successfully reproduced the observed peak structures of the surface DOS of graphite.[1] Figure 1(b) shows the *B* dependence of Landau levels on the top surface layer (*l* = 1) of graphite with infinite thickness. As indicated with solid lines, Landau levels with square-*B* dependence can be found in higher energies. It is also confirmed that these peaks depend on square-*n* with v_F = 1.01 x 10^6 m/s. Moreover, these peaks are localized especially on the surface. The DOS on each graphite layer of top (*l* = 1) to 4th (*l* = 4) from the surface are calculated and shown in fig. 1(a). The square-*B* dependent levels denoted with filled circles are appeared every second layers reflecting the two layers periodicity of graphite stacking. The levels from the *K* point become stronger and dominant on the deeper layers. These calculations clearly show that graphite has TDF originated from *H* point and its properties can be observed obviously on the surfaces.

[1] T. Matsui *et al*., Phys. Rev. Lett. **94**, 226403 (2005).

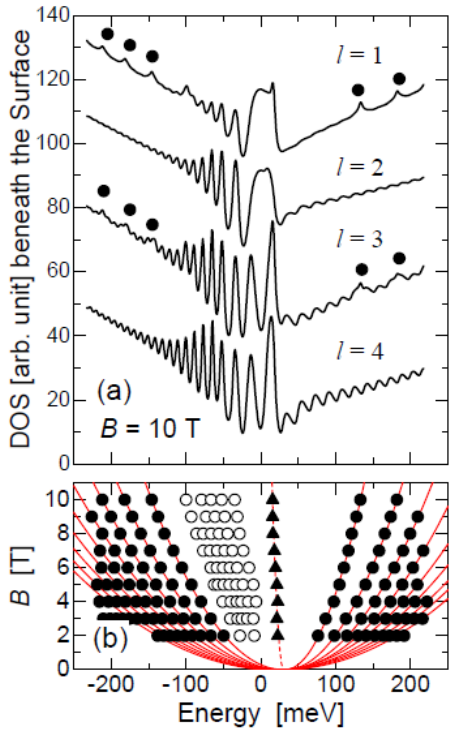

FIG.1 (a) The DOS calculated on each layer from the surface of graphite with infinite thickness in *B* = 10 T. *l* = 1 corresponds to the top surface layer and *l* = 2, 3, 4 to the 2nd, 3rd and 4th layer from the surface. The Landau levels denoted with filled circles show the square-*B* dependence, which are found to appear on every second layers. (b) The field dependence of peaks appeared in the surface DOS, i.e. the DOS of *l* = 1 in (a). The peaks in higher energies (filled circles) clearly show the square-*B* dependence as indicated with solid lines.

P3

Stability of zero-mode edge states with *n* =0 Landau level in graphene

M. Arikawa,[1] H. Aoki,[2] and Y. Hatsugai[1]

[1]*Institute of Physics, University of Tsukuba, 1-1-1 Tennodai, Tsukuba 305-8571, Japan*
[2]*Department of Physics, University of Tokyo, 7-3-1 Hongo, Bunkyo-ku, Tokyo 113-0033, Japan*

The anomalous quantum Hall effect (QHE) experimentally observed in graphene arises from the chiral symmetry of the honeycomb lattice, which in turn gives rise to the "massless Dirac" dispersion and the associated n =0 Landau level in magnetic fields. Since the edge and bulk states should be intimately related in QHE, here we focus on the edge state of the graphene. We have previously shown that an edge mode exists at E =0, and that, although the spectrum is embedded in the bulk Landau level, the charge is accumulated along a zigzag edge with an appreciable charge re-distribution involving the bulk states which we have called a "topological compensation"[1].

In real graphene, small but finite second-neighbor hopping exists, which degrades the chiral symmetry in the bipartite lattice. In the absence of magnetic fields, this not only shifts the Dirac point away from E =0 but also makes the edge mode near the zigzag boundary no longer flat (FIG. 1(b)). In a magnetic field ($\propto\phi$), the n =0 Landau level is also shifted from E=0 (FIG. 1(c)), but retains the delta-function-like singularity for a bond randomness that models ripples [2]. Here we have found that the edge mode is again embedded in the n =0 bulk Landau level *despite* the broken chiral symmetry due to the second-neighbor hopping, where the charge is accumulated along the zigzag edge. Hence the behavior of the zero mode has turned out to significantly differ from the case of zero magnetic field, which is related to the stability of topological compensation [1]. The charge density accumulated along the zigzag edge can be measured with an STM imaging in magnetic fields.

[1] M. Arikawa, Y. Hatsugai and H. Aoki, Phys. Rev. B **78**, 205401 (2008); J. Phys.: Conf. Ser. **150**, 022003 (2009).
[2] T. Kawarabayashi, Y. Hatsugai and H. Aoki, in preparation.

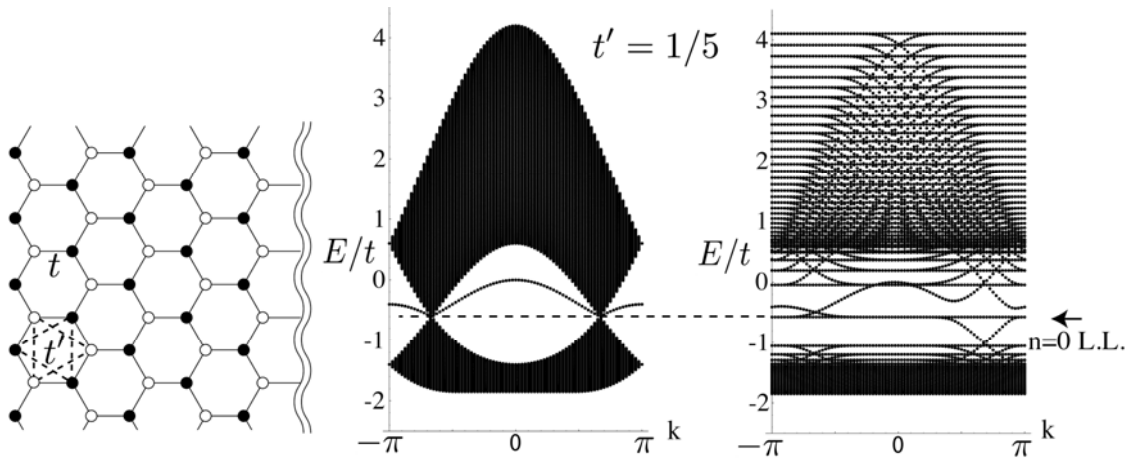

FIG.1(a) Zigzag edge (b) Energy dispersion(ϕ=0) (c) Energy dispersion(ϕ=1/41)

P4

Pseudospin Phase Transitions during Crossing of Partially Filled Landau Levels in a Si Quantum Well

K. Sasaki[1], R. Masutomi[1], K. Toyama[1], K. Sawano[2], Y. Shiraki[2], T. Okamoto[1]

[1]*Department of Physics, University of Tokyo*
[2]*Research Center for Silicon Nano-Science, Tokyo City University*

In a perpendicular magnetic field, two-dimensional electrons form Landau levels (LLs), which are separated by the cyclotron energy. On the other hand, the total magnetic field leads to the Zeeman effect, which splits each LL into two separate sublevels. Since the Zeeman energy is proportional to the total magnetic field (B_{tot}) and the cyclotron energy to the perpendicular magnetic field ($B_{\perp}$), we can control two energies separately by tilting the angle of the 2D system. We focus on the point where two LLs coincide (LL crossing) by controlling energy levels. Two energy levels which have different spins and different orbital wave functions nearly degenerate here. Some preceding researches revealed the nature of LL crossing when one of the coincidence LLs is completely filled. In such a situation, the system behaves as an Ising ferromagnet. During the LL crossing, the electrons having different pseudospins form Ising ferromagnetic domains and a sharp peak is observed in a longitudinal resistivity [1]. On the other hand, there are less experiments of a crossing of partially filled LLs.

In this work we investigate crossing of partially filled LLs. We intend to make clear the ground state in this region. We use Si/SiGe heterostructure two-dimensional electron system.

We observed a pronounced dip in the longitudinal resistivity and a Hall resistivity change during the LL crossing process (Figure 1). The dip in the longitudinal resistivity has a different origin from the peak structure observed in the experiment of the fully filled LL crossing. We also found a hysteresis behavior around the resistivity dip (Figure 2). The hysteresis can be explained as a consequence of a first order pseudospin phase transition. We consider that there exists a pseudospin-unpolarized state during the LL crossing and the pseudospin-unpolarized state is the origin of the resistivity dip.

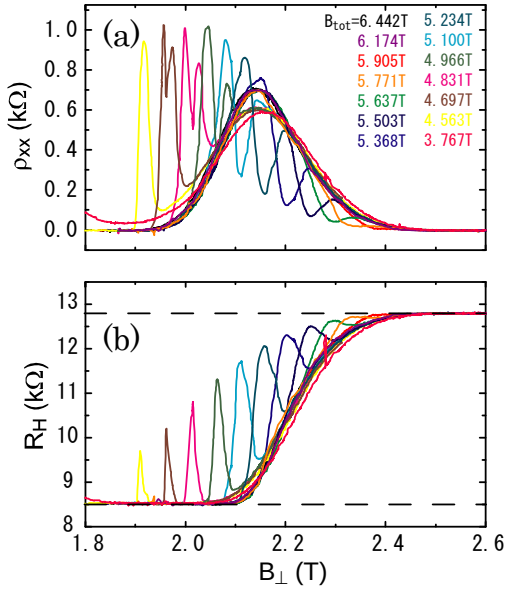

Figure.1: (a) Longitudinal resistivity and (b) Hall resistivity versus perpendicular component of magnetic field $B_{\perp}$ at 70mK. Results of different total magnetic fields are shown.

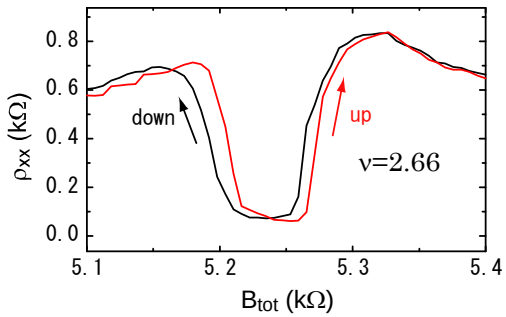

Figure.2: A hysteresis around a longitudinal resistivity dip at 70mK.

[1] K. Toyama, *et al.*, Phys. Rev. Lett. **101**, 016805 (2008).

P5

Commensurate-like to Incommensurate-like Phase Transition in the Layer Imbalanced Bilayer ν=1/3 Quantum Hall States under In-plane Magnetic Field

A. Fukuda[1], T. Sekikawa[2], K. Iwata[2], Y. Ogasawara[2], T. Arai[3] and A. Sawada[3]

[1] *Department of Physics, Hyogo College of Medicine, Nishinomiya 663-8501, Japan*
[2] *Graduate School of Science, Department of Physics, Kyoto Univ., Kyoto 606-8502, Japan*
[3] *Research Center for Low Temperature and Materials Sciences, Kyoto Univ., Kyoto 606-8501, Japan*

The single-layer fractional quantum Hall state (FQHS) at Landau level filling factor ν = 1/3 is interpreted as the ν = 1 integer quantum Hall state (IQHS) of composite fermions (CFs), where one CF consists of one electron and two flux quanta. On the other hand, the bilayer ν = 1 IQHS, where two two-dimensional electron systems are separated by barrier and the layer degree of freedom (pseudospin) plays an essential role, supports the presence of an interlayer phase coherence. This system is also viewed as an ideal pseudospin ferromagnet. In addition, when an in-plane magnetic field $B_{//}$ is applied, the bilayer ν = 1 system undergoes the commensurate (C) - incommensurate (IC) phase transition[1]. Recently we reported the occurrence of a new class of quantum phase called "pseudospin soliton lattice" between the C and IC phase in the balanced ν = 1 bilayer IQHS[2], which indicates the presence of the phase coherence modulated by the in-plane magnetic field. We aspire for the finding of the soliton lattice also in the ν = 1/3 FQHS to clarify the existence of the interlayer phase coherence even in the weekly interacting CFs. Firstly, the similarity of the bilayer ν = 1/3 FQHS to the ν = 1 IQHS and the applicability of the CF model even in the in-plane magnetic fields attracts our interests. We already reported the preliminary results in the balanced ν = 1/3 FQHS[3]. Additionally we have already investigated effects of the layer imbalance in the bilayer ν = 1 IQHS. Therefore, not only the presences of the soliton lattice but also the effects of the layer imbalance on the C-IC phase transition in the bilayer ν = 1/3 FQHS is worth investigating.

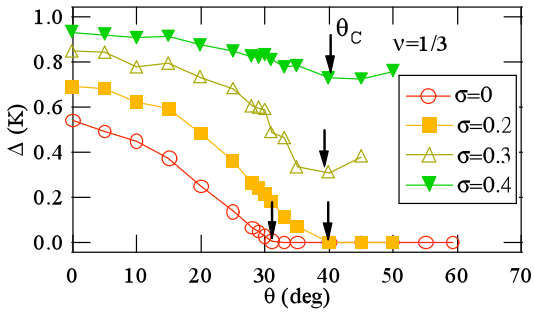

Fig.1 Activation energy Δ as a function of tilting angle θ for various layer density imbalance parameter σ

In this report, we carried out the detailed magnetotransport experiments, especially focused on the activation energy measurements, in the bilayer ν = 1/3 FQHS. We used the GaAs/AlGaAs double-quantum-well sample with the tunneling energy 11 K, provided by NTT basic research laboratory. Activation energy Δ is derived from the temperature T dependence of magnetoresistance $R_{xx} = R_0\exp(-\Delta/2kT)$, where k is the Boltzmann constant. The in-plane field $B_{//}$ is applied by rotating the sample *in situ* at low temperatures in the total magnetic fields B_{tot} with tilting angle $\theta = \sin^{-1}(B_{//}/B_{tot})$. In Fig. 1, we show Δ in the ν = 1/3 bilayer FQHS as a function of θ for various layer imbalance parameter $\sigma \equiv (n_f - n_b) / (n_f + n_b)$, where n_f and n_b is the electron density in the front and back layer, respectively. The total density n_T is fixed at 0.6×10^{11} cm^{-2}. At small σ (0 and 0.2), Δ steeply degreases as θ is increased and FQHSs collapse above the critical tilting angle θ_C. These behaviors of Δ at $\theta < \theta_C$ are similar to the C phase in the bilayer ν = 1 IQHS. At large σ (0.3 and 0.4), with increasing θ, Δ drops initially. However, Δ stays finite even above θ_C, which means the IC-like phase appears in the ν = 1/3 layer-imbalanced bilayer FQHS. In the symposium, we will report the transition from the C-like phase to the IC-like phase of the ν = 1/3 layer-imbalanced bilayer FQHS in detail.

[1] S. Q. Murphy *et al.*, Phys. Rev. Lett. **72**, 728 (1994).
[2] A. Fukuda *et al.*, Phys. Rev. Lett. **100**, 016801 (2008).
[3] A. Fukuda *et al.*, Physica E **40**, 1261 (2008).

P6

Spin and Pseudospin Excitations in the ν=2/3 Bilayer Quantum Hall Systems

Y. D. Zheng,[1] T. Morikawa,[2] A. Fukuda,[3] S. Tsuda,[2] T. Arai,[1] and A. Sawada[1]

[1]*Research Center for Low Temperature and Materials Sciences, Kyoto University, Kyoto 606-8501, Japan*
[2]*Graduate School of Science, Department of Physics, Kyoto University, Kyoto 606-8502, Japan*
[3]*Department of Physics, Hyogo College of Medicine, Mukogawacho 1-1, Nishinomiya, Hyogo 663-8501, Japan*

Bilayer quantum Hall (QH) systems have four energy levels in one Landau level, corresponding to the spin and pseudospin (layer) degrees of freedom. At the filling factor ν=2/3 and ν=2, the ground state is quite nontrivial since there are several ways to fill electrons into two energy levels in the lowest Landau level, depending on the interlayer/intralayer Coulomb interactions, Zeeman energy, interlayer tunneling energy and bias energy *etc*. It has been elucidated that there are three phases, the SP-PU phase (spin-polarized & pseudospin-unpolarized), the SU-PP phase (spin-unpolarized & pseudospin-polarized) and the SP-PP phase (spin-polarized & pseudospin-polarized) in such systems.[1][2] The ν=2/3 state is a fractional QH effect (FQHE) state dealt with the composite-fermion (CF) picture, while the ν=2 state is an integral QH effect (IQHE) state merely being a electron system.[3] The excitation modes of the spin and pseudospin in the ν=2/3 and the ν=2 state could be considered as the skyrmion mode, the vortex mode and the meron mode, must have the peculiar features in each phase. The elementary excitations in the ν=2 state have been studied theoretically[4] and experimentally[5]-[7] so far, however, few researches are reported about the spin and pseudospin excitations in the ν=2/3 state.

The purpose of this study is to investigate the spin and pseudospin excitations, especially the excited skyrmions in the different phases of the ν=2/3 bilayer QH states by measuring the magnetoresistance and the thermal activation energy Δ, the case of the ν=2 will also be investigated at the same time for comparison. In this report, we present the preliminary experimental results and give some interpretations from the theoretical standpoint. The sample used in the measurements has a GaAs/AlGaAs double-quantum-well structure with small interlayer tunneling energy Δ_{SAS} about 1 K. We carry out the magnetotranseport measurements (magnetoresistance and Hall resistance) in temperature range from 50 mK to 1.5 K for several total electron densities n_T and layer density imbalance parameters $\sigma = (n_f - n_b) / n_T$, under perpendicular and titled magnetic fields. The Δ is calculated from the temperature dependence of the magnetoresistance. The total magnetic fields B_{tot} and the σ dependences of the Δ reveal the characteristic of the spin and pseudospin skyrmions, respectively. FIG.1 shows the image plots of the magnetoresistance R_{xx} around ν=2 and ν=2/3 QH states as a function of n_T and σ, the SP-PU phase, the SU-PP phase and the SP-PP phase could be distinguished distinctly from these plots.

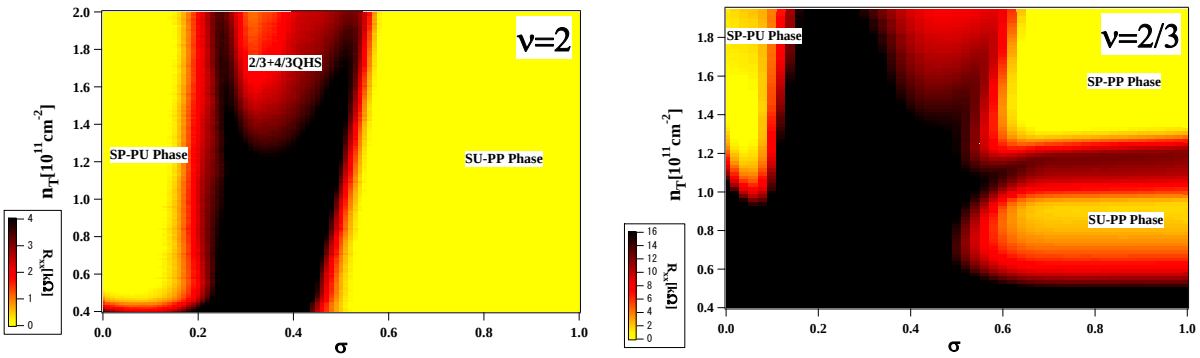

FIG.1: Image plots of the magnetoresistance R_{xx} around the ν=2 and the ν=2/3 quantum Hall states without in-plane magnetic fields as a function of the total electron density n_T and the layer density imbalance parameter σ at T=60 mK.

[1] S. Das Sarma *et al.*: Phys. Rev. **B 58**, 4672 (1998).
[2] N. Kumada *et al.*: Phys. Rev. **B 69**, 155319 (2004).
[3] B. I. Halperin *et al.*: Phys. Rev. **B 47**, 7312 (1993).
[4] Z. F. Ezawa: *Quantum Hall Effects, Field Theoretical Approach and Related Topics*, Chapter 26 (World Scientific, Singapore, 2000)
[5] A. Sawada *et al.*: Phys. Rev. Lett. **80**, 4534 (1998).
[6] N. Kumada *et al.*: J. Phys. Soc. Jap. **69**, 3178 (2000).
[7] A. Fukuda *et al.*: Phys. Rev. **B 73**, 165304 (2006).

P7

Superconductor-like Phenomenon in the Bilayer ν=1 Quantum Hall State

A. Sawada,[1] A. Fukuda,[2] S. Tsuda[3], T. Arai[1], K. Iwata[3], D. Terasawa[4], M. Morino[4]
S. Kozumi[4] and Y. Ogasawara[3]

[1]*Research Center for Low Temperature and Materials Sciences, Kyoto Univ., Kyoto 606-8501, Japan*
[2] *Department of Physics, Hyogo College of Medicine, Nishinomiya 663-8501, Japan*
[3]*Graduate School of Science, Kyoto University, Kyoto 606-8502, Japan*
[4]*Graduate School of Science, Tohoku University, Sendai 980-8578, Japan*

Bilayer ν=1 quantum Hall (QH) system closely resembles the superconductor junction in the presence of the interlayer phase coherence. The Hall current flows as the dc Josephson current between the two layers. Strong interlayer Coulomb interactions lead to a broken-symmetry state with spontaneous interlayer phase coherence.

The commensurate-incommensurate (C-IC) phase transition at the ν=1 QH state occurs in association with the change in the phase symmetry induced by the in-plane magnetic field $B_{//}$. We investigate an anomalous magnetotransport of the bilayer ν=1 QH state in tilted magnetic fields using samples with tunneling energies Δ_{SAS}~11 K. We find a magnificent peak in magnetoresistance R_{xx} around the C-IC transition point [1, 2]. To investigate the peak, we measured activation energy gap Δ from the temperature dependence of R_{xx}. In Fig. 1, we plot Δ at the exact ν=1 filling point around the C-IC phase transition point at σ=0 for various values of N_{tot} [1]. We construct a phase diagram for the bilayer ν=1 QH state in the $B_{//}$-N_{tot} plane at T=130 mK (Fig. 2) [2]. The C-IC phase boundaries are obtained by collecting ($B_{//}$, N_{tot}: solid circles) where R_{xx} starts to increase. We divide the IC phase for $B_{//} > B_{//}^{C}$ into two regions, that is, the nondissipative and dissipative regions. The boundaries between the two regions are defined by ($B_{//}$, N_{tot}: solid squares) that gives a local minimum of the derivative of R_{xx} with respect to N_{tot}. In the narrow sphere named "soliton" phase, the magnetoresistance increases anomalously due to the backscattering of electrons against a thermally fluctuating magnetic flux lattice in the QH regime. The soliton phase is very similar to the mixed state of the type-Ⅱ superconductors.

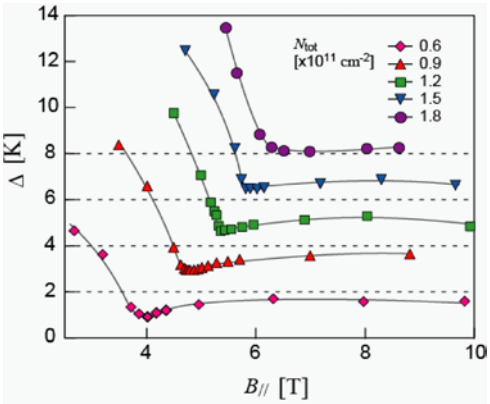

Fig. 1 Activation energy gap Δ of the double-layer ν= 1QH state at σ= 0 for several values of n_{tot} as a function of $B_{//}$.

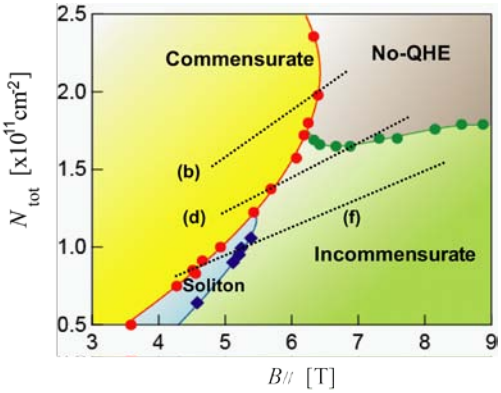

Fig. 2 Phase diagram of the bilayer ν=1 QH state at σ =0 as a function of the in-plane magnetic field and the total electron density at T=130 mK.

In another experiments, we expect the occurrence of the Josephson-like plasma oscillation due to the fluctuations of the electron densities of each layer [3]. To detect the plasma oscillation, the sample should be cooled down to about 50 mK in a dilution refrigerator, and irradiated with microwave through a superconductive coaxial cable. We are searching the resistively detected resonance due to the Josephson-like plasma oscillation.

[1] D. Terasawa *et al.*, Phys. Rev. **B** *in press*.
[2] A. Fukuda *et al.*, Phys. Rev. Lett. 100, 016801 (2009).
[3] Z. F. Ezawa, Phys. Rev. B51, 11152 (1995).

P8

Activation energy gap in the ν_T=1 bilayer Quantum Hall States with small tunneling energy

T. Morikawa[1], Y. D. Zheng[1], A. Fukuda[2], S. Tsuda[1], T. Arai[3], and A. Sawada[3]

[1]*Graduate School of Science, Department of Physics, Kyoto University, Kyoto 606-8502, Japan*
[2]*Department of Physics, Hyogo College of Medicine, Mukogawacho 1-1, Nishinomiya, Hyogo 663-8501, Japan*
[3]*Research Center for Low Temperature and Materials Sciences, Kyoto University, Kyoto 606-8501, Japan*

We are interested in the bilayer Quantum Hall states (BQHS), which show a variety of fascinating phenomena. The total Landau filling factor ν_T=1 BQHS can be viewed as various ways such as Bose-Einstein condensation of composite bosons, the superfluidity of counter-flowing excitons, or pseudospin (layer degree of freedom) ferromagnetism. One of the most interesting physics is to investigate effects of the tunneling energy Δ_{SAS} and layer density imbalance on the macroscopic phase coherence in the ν_T=1 BQHS.

Our group had been studying ν_T=1 BQHS using a sample with relatively large tunneling energy Δ_{SAS}=11K, including the effects of the layer imbalance.[1] Recently, we have been carrying out transport experiments using a sample with small tunneling energy Δ_{SAS}=1K, where an intrinsic macroscopic phase coherence is more essential.

In this symposium, we report results of transport experiments using a sample with Δ_{SAS}=1K. The sample is consisted of GaAs/AlGaAs double quantum wells and the low temperature mobility is 1.9×10^6cm^2/Vs. Owing to the front and back gate, we can control the electron density of each layer independently. We have measured magnetororesistance R_{xx} for several total electron densities n_T and layer density imbalance parameter σ ($\sigma\equiv(n_f-n_b)/(n_f+n_b)$), where n_f (n_b) is the density of front (back) layer. We have also collecting R_{xx} data for several temperatures T. From these data, we derive thermal activation energy Δ, using the Arrehnius relationship $R_{xx}\propto\exp(-2\Delta/kT)$, where k is the Boltzmann constant. The σ dependence of Δ at the fixed n_T is illustrated in Fig.1. We can see that the activation energy becomes smallest at the balanced state (σ=0). The n_T dependence of Δ at the fixed σ is also plotted in Fig.2. The activation energy has a peak at $n_T=0.68\times10^{11}$cm^{-2}.

We also have been trying to study the effects of the in-plane magnetic fields to the activation energy in the ν_T=1 BQHS with Δ_{SAS}=1K. The stepping motor in dilution refrigerator enables us to rotate the sample *in situ* at low temperatures. We expect the occurrence of the commensurate–incommensurate (C-IC) phase transition due to the modulation of the interlayer phase coherence by the in-plane fields. The C-IC transition is caused by the competition between the interlayer tunneling energy and the exchange energy. We will compare the behavior of the C-IC transition between sample with Δ_{SAS}=1K and that with Δ_{SAS}=11K.

[1] Y.Ogasawara *et al.*, J. Phys. **150**, 022068 (2009).

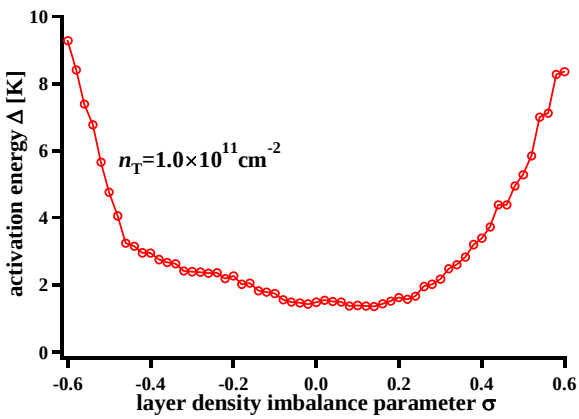

Fig.1: Activation energy as a function of σ at the fixed $n_T=1.0\times10^{11}$cm^{-2} using the sample with Δ_{SAS}=1K.

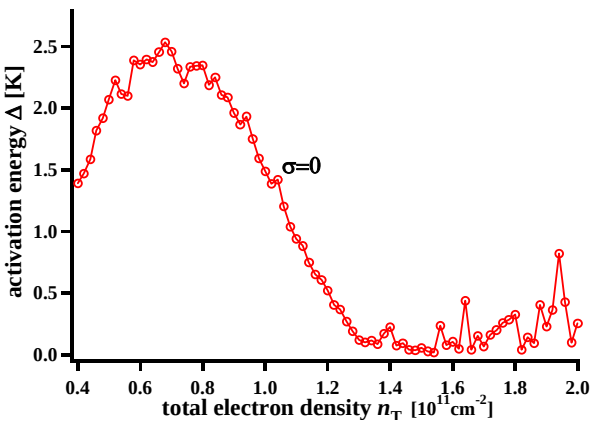

Fig.2: Activation energy as a function of n_T at the balanced state (σ=0) using the sample with Δ_{SAS}=1K.

P9

Anomaly in Edgemagneto-plasmon Resonance Line Width of Helium Surface State Electrons

T. Arai[1], S. Yamanaka[2], R. Nishinakagawa[3], H. Yayama[2], A. Fukuda[4], and A. Sawada[1]

[1]*Research Center for Low Temperature and Materials Sciences, Kyoto University, Kyoto 606-8501, Japan*
[2]*Department of Physics, Kyushu University, 6-10-1 Hakozaki, Higashi-ku, Fukuoka 812-8581, Japan*
[2]*Department of Physics, Kyoto University, Kitashirakawa-Oiwakecho, Sakyo-ku, Kyoto 606-8502, Japan*
[2]*Department of Physics, Hyogo College of Medicine, Nishinomiya 663-8501, Japan*

Two-dimensional electron gas (2DEG) formed on liquid helium surface is often referred as "classical Coulomb liquid" since its Fermi energy is much smaller than typical experimental temperature of dilution refrigerator. The average Coulomb interaction energy can be over 100 times larger than the thermal kinetic energy. Extremely clean surface of liquid helium provides an ideal stage to experimentally investigate the dynamics of Coulomb liquid. The only known scatterers are helium vapor atoms and ripplons. The number of these scatterers decreases as the temperature is lowered. Therefore, in the presence of strong magnetic field, Landau level broadening induced by scatterings is very small and all electrons are confined in a narrow range of kinetic energy.

Edgemagneto-plasmon (EMP) is an electron density wave, which occurs when perpendicular magnetic field is present. EMP propagates within a narrow strip near the edge, while density in the bulk is uniform. We employed EMP resonance technique to study the dynamics of 2DEG on helium. From the analysis of EMP line shapes, we are able to extract information of magnetoconductivity tensor and electronic structure near the edge [1]. We measured EMP frequencies and line widths at various lateral confinement potentials by changing the voltage of so-called guard electrode surrounding 2DEG. FIG. 1 shows measured EMP frequency and line width as a function of guard electrode potential (V_G). At strong lateral confinement (large $|V_G|$), measured frequency is high and line width is broad. This can be understood within the simple model of EMP [1]. For large $|V_G|$, 2DES is compacted into a small area so that EMP wavelength is short and 2DES density drop near the edge is steep. At this condition, it is known that EMP resonance shows high frequency and broad line width. Measured line widths of this region quantitatively agree with theory [2]. For small $|V_G|$, where lateral confinement is weak, we observed unexpected line broadening as shown in FIG. 1(b), while the behavior of resonance frequency is smooth. In order to find out the origin of the EMP line broadening, we measured EMP spectra at various conditions. The results were the following. The broadening is sensitive to the confinement potential configuration. Broad signals appear when lateral confinement is weak. The broadening is diminished at high temperatures above 1 K. Varying magnetic field within 2.2 – 6.4 T makes small differences. According to our results, we propose that an EMP oscillation mode switching takes place at the point where line width takes minimum. The EMP is the conventional mode with fixed 2DES boundary in the strong confinement region, while an EMP mode accompanied by boundary deformation [2] occurs in the weak confinement region.

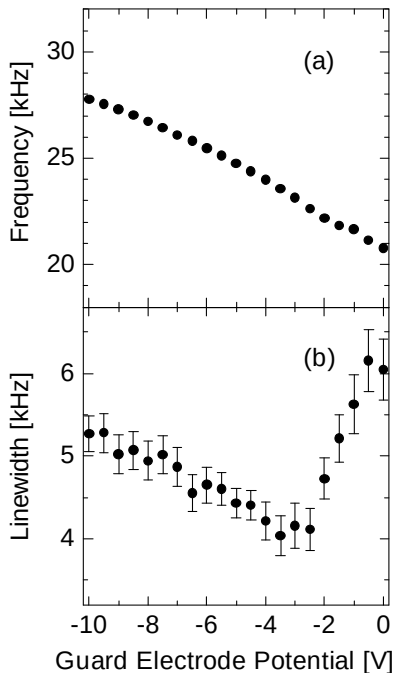

FIG. 1: Measured EMP resonance frequency (a) and line width (b) at T = 0.55 K, n = 2.5×10^{12} m^{-2}, B = 6.4 T. For -3 V < V_G, unexpected broadening is observed.

[1] V.A.Volkov, S.A. Mikhailov, in *Modern Problems in Condensed Matter Sciences*, Vol. **27.2**, North-Holland, Amsterdam, 1991, p.855 (Chapter 15)
[2] Yu. P. Monarkha, Low Temp. Phys. **21**, 458 (1995)

P10

Ferromagnetic State and Spin Correlation Functions in Spin-1/2 Bose and Fermi Gases

Shintaro Takayoshi[1], Masahiro Sato[2] and Shunsuke Furukawa[3,2]

[1]*Institute for Solid State Physics,University of Tokyo, 5-1-5 Kashiwanoha, Kashiwa-shi, Chiba 277-8581, Japan*
[2]*Condensed Matter Theory Laboratory, RIKEN, 2-1 Hirosawa, Wako-shi, Saitama 351-0198, Japan*
[3]*Department of Physics,University of Toronto, 60 St. George Street, Toronto, Ontario M5S 1A7, Canada*

Internal degrees of freedom generally enrich physical properties of many-body systems. For example, various kinds of magnetism are caused by the spin degrees of freedom in electron systems. We study two-component (i.e., spin-1/2) hard-core Bose/Fermi gases on a one-dimensional lattice, as the simplest case with internal degrees of freedom. Such systems could be realized using ultra-cold atoms [1]. Moreover, they are known to appear as effective theories in some frustrated magnetic systems [2] and other quantum systems [3]. Here, we focus on the situation where the two components are convertible. In this case, it is naturally expected that a spontaneous population imbalance (i.e., ferromagnetic state) is induced by a sufficiently strong repulsion between the components. Many physicists actually have argued related phenomena such as phase separation in mixture of two-species atoms. However, any corresponding theory and accurate predictions have been still lacking in spite of the simplicity of the phenomenon. In fact, it is known well that the bosonization theory cannot capture the imbalanced phase [1]. Furthermore, recent strong coupling theories for SU(2) symmetric spin-1/2 boson gases [4] also cannot cover the phase transition.

We therefore study the basic features of the ferromagnetic phase transition and state [5] by combining analytical approaches with powerful numerical methods (iTEBD method [6] and numerical diagonalization). As a result, it is shown that (1) the universality class of the transition changes, depending strongly on the existence of the inter component hopping and (2) the low-energy physics in the imbalanced phase is described by a single-component Tomonaga-Luttinger liquid. We also determine the accurate global phase diagram as in Fig. 1.

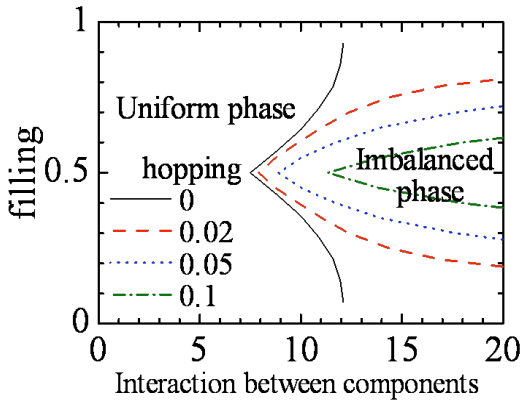

Fig. 1. Ground-state phase diagram of the 1D two-component gas system.

Furthermore, we investigate the low-energy properties of the ferromagnetic phase by calculating the two-spin correlation functions via iTEBD method [7].

In this conference, we will explain in detail our results for the above two-component gases.

[1] M.A. Cazalilla and A.F. Ho, Phys. Rev. Lett. **91**, 150403 (2003); A.Kolezhuk, arXiv:0903.1647.
[2] A. Kolezhuk and T. Vekua, Phys. Rev. B **72**, 094424 (2005); M. Sato and T. Sakai, Phys. Rev. B **75**, 014411 (2007).
[3] A. Tokuno and M. Sato, Phys. Rev. A **78**, 013623 (2008); K.Yang, Phys. Rev. Lett.(2004).
[4] S. Akhanjee and Y. Tserkovnyak, Phys. Rev. B **76**, 140408(R) (2007); M.Zvonarev, V.Cheianov, and T.Giamarchi, Phys. Rev. Lett. **99**, 240404 (2007); Phys. Rev. Lett. **103**, 110401 (2009); K.A. Matveev and A, Furusaki, Phys. Rev. Lett. **101**, 170403 (2008).
[5] S. Takayoshi, M. Sato, and S. Furukawa, arXiv:0911.3157.
[6] G.Vidal, Phys. Rev. Lett. **98**, 070201 (2007).
[7] M. Sato and S. Takayoshi, in preparation.

P11

Effects of spin-orbit coupling and electron correlation on Van-Vleck susceptibility in transition metal compounds

M. Udagawa,[1] and Y. Yanase[2]

[1]*Department of Applied Physics, The University of Tokyo, 7-3-1 Hongo, Bunkyo-ku, Tokyo 113-8656, Japan*
[1]*Department of Physics, The University of Tokyo, 7-3-1 Hongo, Bunkyo-ku, Tokyo 113-0033, Japan*

The paramagnetism of metallic systems has two origins. One is the Pauli susceptibility (χ_P), which is roughly proportional to the density of states at the Fermi level. The other is the Van Vleck susceptibility (χ_{VV}), which exists only in the systems where the magnetization is not conserved. χ_{VV} is expected to be large for 4d and 5d transition metal compounds, and rare-earth systems, since orbital moments and large spin-orbit coupling make the magnetization non-conservative in these systems. The most remarkable and sometimes confusing property of χ_{VV} is that a broad range of energy scales contributes to χ_{VV}. Namely, the relevant energy range is not limited to the neighborhood of Fermi level. Therefore, χ_{VV} remains finite, even when an energy gap opens at the Fermi level.

This characteristic property of χ_{VV} plays a crucial role in several experimental situations. In Knight shift experiment to determine the parity of superconducting order parameter, a finite χ_{VV} is a serious obstacle. The invariant Knight shift across the superconducting transition is sometimes attributed to the large χ_{VV} [1]. For the correct interpretation of the experiment, an accurate evaluation of χ_{VV} is desired. χ_{VV} also seems to be important to 5d transition metal compounds. Recently, large paramagnetic susceptibilities are reported for a series of Ir compounds, with tiny specific heat coefficients, resulting in huge Wilson ratios. At first sight, this seems contradictory, since any kinds of spin excitations should also contribute to specific heat. This contradiction, however, can be resolved by assuming a large χ_{VV}, since χ_{VV} originates from the polarization of ground state. However, the origin of anomalous enhancement of χ_{VV} still remains a question.

Despite the relevance in many experimental situations, χ_{VV} has not drawn much theoretical interests, so far. In particular, the effects of electron correlation has not been studied, except for several analyses for rare-earth systems[2,3]. In this contribution, motivated by the growing interest in χ_{VV} in 4d and 5d systems, we have studied the effect of electron correlation on χ_{VV}, focusing on the transition metal compounds.

We consider Sr_2RuO_4 as a model system, due to its relatively simple orbital structure and the interest in the Knight shift experiment of this material [4,5]. We adopt the multi-orbital Hubbard model, and calculate the magnetic susceptibility of this model with the dynamical mean-field theory. As an impurity solver, we use the iterative perturbation theory, which is adequate only for weakly correlated systems, but it requires small computational cost and is adequate for investigating large parameter space spanned by inter- and intra- orbital electron interaction (U,U',J). To separate the contribution from χ_P and χ_{VV}, we use the formulation due to Kontani and Yamada[2]. We also consider the case of large spin-orbit coupling, with the application to Ir compounds in mind.

We find that the correlation enhancement of χ_P and χ_{VV} are dominated by different mechanisms. For small spin-orbit coupling (λ), χ_P shows large enhancement in the region where spin fluctuation is developed. On the other hand, χ_{VV} tends to be large, accompanied by the strong orbital fluctuation. In general, correlation enhancement of χ_{VV} is smaller than that of χ_P in this region. On the other hand, for intermediate λ, χ_{VV} shows large enhancement due to electron correlation. The large enhancement of χ_{VV} results from the mixing of spin and orbital degrees of freedom, which make the spin moment non-conservative. The large χ_{VV} for intermediate λ may underlie the large paramagnetic susceptibility of Ir compounds, with the huge Wilson ratio.

[1] A. M. Clogston et al., Rev. Mod. Phys. **36**, 170 (1964).
[2] H. Kontani and K. Yamada, J. Phys. Soc. Jpn. **65**, 172 (1995).
[3] T. Mutou and D. Hirashima, J. Phys. Soc. Jpn. **65**, 366 (1995).
[4] K. Ishida et al., Nature **396**, 658 (1998).
[5] H. Murakawa et al., Phys. Rev. Lett. **93**, 167004 (2004).

P12

Theory of commensurate-incommensurate transition

K. Nomura

Dept. of Physics, Kyushu University, 6-10-1 Hakozaki , Higashi-ku, 812-8581, Fukuoka, Japan

Phenomena of the commensurate-incommensurate (C-IC) transitions are observed in many cases, such as in the quantum S=1 bilinear-biquadratic chain, the crossover between the Tomonaga-Luttinger-liquid and the high-temperature paramagnetic region, classical ANNNI models, and spin systems on the triangular lattice.

We have proposed a mechanism to explain the onset of the incommensurability [1], considering singularity in the complex plane. And we have verified the validity of our phenomenological theory, applying it for the C-IC transition in the S=1 bilinear-biquadratic chian [2].

We also talk the C-IC change of the classical NNNI spin chain, the simplest case of ANNNI spin models. We find that the asymmetry of the transfer matrix is related with the C-IC change.

[1] K. Nomura, J. Phys. Soc. Jpn., Vol.72, (2003) 476
[2] T. Murashima and K. Nomura, Phys. Rev. B 73, (2006) 214431

P13

Spectral structure of hole- and electron-doped cuprates: Roles of zeros of Green's function

S. Sakai,[1] Y. Motome,[2] and M. Imada[2]

[1]*Institute for Solid State Physics, Vienna University of Technology, 1040 Vienna, Austria*
[2]*Department of Applied Physics, University of Tokyo, 7-3-1 Hongo, Bunkyo-ku, Tokyo 113-8656, Japan*

Angle-resolved photoemission spectroscopy (ARPES) has revealed various anomalous features in the nomal state of high-T_c cuprates, such as pseudogap, Fermi arc, and kinks in dispersion. They remain to be a central issue of correlated electron physics. We here propose that the anomalies are understood in a unified fashion from the itinerancy/locality duality of electrons.

In terms of quantum field theory the itinerancy is described by zero-energy poles of the electron Green's function G in the momentum space. On the other hand, the locality is described by low-energy poles of the selfenergy, i.e., *zeros* of G, which are not taken into account in the conventional theory for metals.

By analyzing the electronic structure incorporating both poles and zeros of G, we show that the interference of the two singularities comprehensively reproduces the ARPES anomalies. We apply a cluster dynamical mean-field theory to the two-dimensional Hubbard model in the lightly-doped region to the Mott insulator.

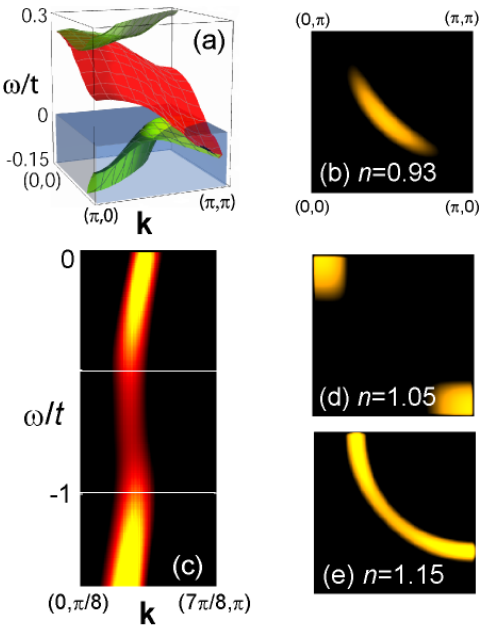

Fig. (a) Low-energy pole (bright green) and zero (dark red) surfaces in a hole-doped Mott insulator. (b) Fermi arc in a lightly hole-doped region. (c) Waterfall in the spectra. (d)(e) Doping evolution of the spectral weight around the Fermi level in electron-doped cases. (a) and (c) are calculated at zero temperature while (b), (d) and (e) at finite temperatures. t is the nearest-neighbor transfer integral, ω is the energy from the Fermi level, and **k** is the momentum.

Figure (a) shows the low-energy pole-zero structure in the momentum-energy space, calculated for 7% hole doping [1]. We see a pseudogap characterized by the zero surface crossing the Fermi level. The zero surface pushes down the pole surface below it, leaving an island of poles above the Fermi sea. This structure leads to several important consequences. *(i) Opening of a pseudogap in the entire Brillouin zone.* This is distinctive from the previous scenarios based on preformed pair and d-density wave ordering because they assume d-wave gaps in the zero temperature limit. Our result is, however, consistent with ARPES data when considering that ARPES looks the $\omega<0$ region only. *(ii) Spectral asymmetry as to the Fermi level.* This is more pronounced around the nodes than the antinodes, in accord with ARPES observation. *(iii) Back-bending behavior of the dispersion around antinode*, as observed by ARPES. This is due to the proximity to the zeros. *(iv) Emergence of Fermi arc at finite temperatures* [Fig. (b)]. This is because a large scattering around the zero surface suppresses the spectral intensity of the Fermi pocket (island) on the side closer to the zeros [1,2].

Moreover, at higher binding energies we find a waterfall behavior [Fig. (c)], which is similar to that discovered in the cuprates. We also extend our study to electron doping and find that the Fermi surface emerges from around the antinode [Fig. (d)] and then evolves into the normal Fermi surface [Fig. (e)]. This is consistent with the ARPES data. The spectra at n=1.05 can be understood by the presence of a zero surface around (0,0). Thus we propose that zeros of G hold a key to the comprehensive understanding of the various spectral anomalies observed in the cuprates [3].

[1] S. Sakai, Y. Motome, and M. Imada, Phys. Rev. Lett. **102**, 056404 (2009); Physica B **404**, 3183 (2009).
[2] T. D. Stanescu and G. Kotliar, Phys. Rev. B **74**, 125110 (2006).
[3] S. Sakai, Y. Motome, and M. Imada, in preparation.

P14

Variational Monte Carlo Studies of Hubbard-type Systems

H.Yokoyama[1] and K. Kobayashi[2]

[1]*Dept. of Physics, Tohoku University, Aramaki-Aoba, Aoba-ku, Sendai, 980-8578, Japan*
[2]*Department of Natural Science, Chiba Institute of Technology, Shibazono, Narashino, 275-0023, Japan*

In this project, using an optimization or correlated variational Monte Carlo method, we have addressed correlated systems: (1) Superfluid-Insulator (Mott) transition in S=0 Bose Hubbard models on the square and triangular lattices. (2) A crossover of superconducting mechanisms between BCS and Bose-Einstein-condensation types in the attractive Hubbard model. (3) Superconducting properties of the repulsive Hubbard model on a square lattice with the diagonal transfer, keeping the cuprate superconductors in mind. .

In connection with the item (3), in this presentation, we first discuss the interplay between *d*-wave superconductivity and antiferromagnetism which is motivated by a NMR study which pointed out the coexistence of the two orders in a single CuO_2 plane. In our calculations for the *t-t'-U* Hubbard model, the phase diagram has rich structure as compared to the *t-J* model, in which the antiferromagnetic state for doped systems always has a *d*-wave superconducting order; according to the model parameters, our phase diagram has regions, in which the two phases coexist and are mutually exclusive [1].

As a second topic, we address the so-called two-gap problem of cuprates. From the variational Monte Carlo calculations, we show that the antinodal region in the **k** space is important not only for the pseudogap but for the superconducting gap. Thus, simple dichotomy of electrons in the **k** space is not correct. We would like to point out that so-called pseudogap possibly stems from the inhomogeneous nature of the cuprate superconductors. Details will be explained in the presentation.

[1] K. Kobayashi and H. Yokoyama, to appear in J. Phys. Chem. Solids (2010).
[2] H. Yokoyama, M. Ogata and K. Kobayashi, to appear in Physica C (2010).

P15

Variational Monte Carlo study of partial Kondo screening in frustrated Kondo lattice systems

K. Nakamikawa, Y. Yamaji, M. Udagawa, and Y. Motome

Department of Applied Physics, The University of Tokyo, 7-3-1 Hongo, Bunkyo-ku, Tokyo 113-8656, Japan

The study of Kondo lattice systems has a long history. Intensive studies have been carried out for the quantum criticality, non-Fermi-liquid behavior, and superconductivity, all of which emerge from the competition between the Kondo singlet formation and the RKKY interaction. Geometrical frustration may bring another interesting aspects to this competition. In frustrated localized spin systems, a partial ordering has been observed under keen competition between exchange interactions; the system is spontaneously separated into magnetic and non-magnetic sublattices to avoid frustration. Recently, similar but different partial ordering phenomena have been observed in several rare-earth materials, such as the triangular-lattice system UNi_4B [1], and the distorted-kagome-lattice systems CePdAl and TbNiAl [2,3], where the Kondo screening appears to vanish local magnetic moments on a specific sublattice selectively. The origin of this partial Kondo screening has been explored by mean-field analyses on a Blume-Emery-Griffiths type effective model, and phase diagrams including partially-ordered phase were obtained [4]. However, the previous theoretical studies do not fully incorporate the effect of quantum fluctuation and the correlation between conduction electrons and localized moments. In order to further elucidate the possibility of partial Kondo screening and the resulting peculiar magneto-transport phenomena, more elaborate treatments are highly desired.

For this purpose, we investigate the ground-state properties of the Kondo lattice model and its effective model at half filling, the Kondo necklace model [5], defined on a frustrated triangular lattice. We employ the variational Monte Carlo method combined with multi-variable optimization [6]. The method enables to obtain the ground state in high precision, taking account of the quantum effects which were not fully considered in the previous studies.

As a result, for the Kondo necklace model, we find that the partial ordering takes place in the intermediate region between the Kondo singlet phase and a magnetically ordered phase. The partially-ordered state is a realization of the partial Kondo screening: It is composed of enhanced Kondo singlets on 1/3 of lattice sites and magnetic states on the remaining Honeycomb lattice. This result illuminates the crucial role of quantum fluctuation on the partial ordering, since the mean-field theory [5] does not reproduce this intermediate phase. Moreover, we show that the partial Kondo screening is further stabilized by introducing the Ising anisotropy in the antiferromagnetic coupling between localized spins. For the Kondo lattice model, which includes itinerant electrons explicitly, we also find that a partial Kondo screening state remains at half filling for a finite Ising-like exchange interaction, qualitatively consistent with the results for the Kondo necklace model. In this case, interestingly, the partially-ordered state accompanies a charge disproportionation along with the partial Kondo screening. We discuss the relation between the partial Kondo screening and the charge disproportionation.

[1] S. A. M. Mentink et al., Phys. Rev. Lett **73** (1994) 1031.
[2] A. Dönni *et al*,.J. Phys.: Cond. Mat. **8** (1996) 11213.
[3] A. Oyamada *et al*., Phys. Rev. B **77** (2008) 064432.
[4] R. Ballou, J. Alloys and Compounds **275-277** (1998) 510, and references therein.
[5] S. Doniach, Physica **91B** (1997) 231.
[6] D. Tahara and M. Imada, J. Phys. Soc. Jpn. **77** (2008) 114701.

P16

Electronic State of Charge Frustrated Systems with "Ice-rule" Constraint

H. Ishizuka, M. Udagawa, and Y. Motome

Dept. of Applied Physics, University of Tokyo, 7-3-1 Hongo, Bunkyo-ku, Tokyo, 113-8656, Japan

Recently, charge frustration attracts considerable attentions, since it underlies many intriguing phenomena, such as electronic ferroelectricity, multiferroicity, and novel metallic state in quantum melting of charge order [1]. In particular, a class of systems under "ice rule" draws special interests. The ice rule is a local constraint, originally derived from the local correlation between neighboring hydrogen bonds in the water ice I_h. [2]. Magnetite Fe_3O_4 is a typical material in this class, for which it has been argued that the ice rule imposed on the configuration of Fe^{2+} and Fe^{3+} plays a crucial role on the metal-insulator transition. Recent discovery of a magnetic analogue, the spin-ice materials [3], has much improved the understanding of the ice-rule physics, however, it is not fully understood how the ice-rule systems are affected by coupling to other degrees of freedom, such as lattice distortion and conduction electrons. In this contribution, we investigate the interplay between the ice-rule variables and itinerant electrons to clarify how the Fermi statistics and quantum kinetic motion of electrons affect macroscopic properties of ice-rule systems.

For this purpose, we consider a simple spinless-fermion system with onsite potential, defined on tetrahedron-based corner-sharing lattices, such as pyrochlore and checkerboard lattice:

$$H = -t \sum_{<i,j>} (c_i^+ c_j + h.c.) + \sum_i U_i c_i^+ c_i$$

where $U_i = \pm U/2$ satisfies the "ice rule" local constraint: two of four sites in a tetrahedral unit cell have a potential $+U/2$ and the remaining two sites being $-U/2$ (FIG.1). We investigate the effect of this local constraint in comparison with that of randomly-distributed potentials, by direct diagonalization of the Hamiltonian matrix. In particular, we focus on two topics: (i) how the "ice-rule" local constraint affects global electronic states and (ii) how the kinetic motion of electrons lifts the macroscopic degeneracy of ground states left out by "ice rule".

As to (i), we find several significant differences in the density of states between "ice-rule" and random averaging. The difference of electronic state shows up dramatically in the optical conductivity of the region where U is large: A characteristic sharp peak exists for random configurations, whereas it is suppressed for the ice-rule configurations (FIG.1). This is a hallmark of the ice-rule frustration.

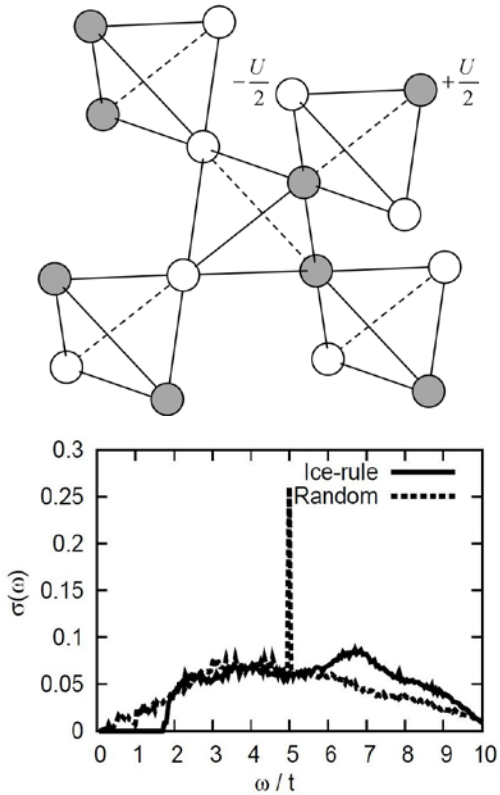

FIG. 1: (Top) Example of potential configuration satisfying "ice rule" (bottom) Optical conductivity at $U/t=5$.

On the other hand, as to (ii), we find that the energy difference is surprisingly small between different ice-rule configurations of the pyrochlore model. This comes from the fact that the lowest order perturbation to the ice-rule manifold is of fifth order in t/U. The result implies that the kinetic motion of electrons does not lift the macroscopic degeneracy down to extremely low temperature.

[1] J. van den Brink and D. Khomskii, J. Phys. Cond. Mat. **20** (2008) 43421.
[2] J. D. Bernal and R. H. Fowler, J. Chem. Phys. **1** (1933) 515; L. Pauling, J. Am. Chem. Soc. **57** (1935) 2680.
[3] M. J. Harris *et al.*, Phys. Rev. Lett. **79** (1997) 2554; A. P. Ramirez *et al.*, Nature **399** (1999) 333.

P17

Self-organized cluster formation in frustrated multi-orbital systems

J. Yoshitake and Y. Motome

Department of Applied Physics, The University of Tokyo, 7-3-1 Hongo, Bunkyo-ku, Tokyo 113-8656, Japan

In geometrically frustrated systems, a simple-minded long-range ordering is severely suppressed, resulting in highly degenerate low-energy states. At lowest temperature, however, nature disfavors residual entropy, in accord with the third law of thermodynamics, and the ground state is reached by some kind of symmetry breaking in most of real materials. The process of lifting degeneracy is diverse. A particularly interesting example is found in cluster formation. There, in order to avoid the frustration between nearest neighbors, a cluster in a somewhat larger length scale is self-organized. For example, a trimerization occurs in the triangular-lattice system $LiVO_2$ [1] and the pyrochlore-slab system $SrV_xGa_{12-x}O_{19}$ (SVGO) [2]. Even larger-size clusters have also been observed, such as the heptamer in AlV_2O_4 [3,4] and the octamer in $CuIr_2S_4$ [5]. In particular, SVGO and AlV_2O_4 are intriguing because they retain magnetic moments coexisting with the spin-singlet clusters. In these systems, not only spin but also orbital and/or charge degrees of freedom are expected to play a crucial role, however, the microscopic mechanism is not fully explored so far.

In this contribution, we study the mechanism of cluster formation with focusing on the effects of coupling to orbital degree of freedom and lattice distortion, through the analysis of the multi-orbital Hubbard model coupled to phonon degrees of freedom. Specifically, we consider the three-orbital Hubbard models corresponding to the three-fold degenerate t_{2g} orbitals, including the trigonal crystal field splitting and the Peierls-type electron-phonon coupling. We employ the Hartree-Fock approximation to obtain the ground state of these models with treating the lattice distortions classically and adiabatically.

Firstly, we consider the pyrochlore-slab models to search for the mechanism of trimerization in SVGO [2]. For d^2 configuration, we find instability toward trimerization in the two kagome planes with leaving magnetic moments in the intervening triangular plane, consistent with the experiments in SVGO. This trimerization can be attributed to the formation of bonding-orbitals which is assisted by the strong orbital anisotropy and the Peierls coupling. On the other hand, for the d^3 configuration, which corresponds to $SrCr_8Ga_4O_{19}$ (SCGO), Mott insulating states with several types of magnetic ordering are stabilized in a broad parameter range, instead of the trimer state. This result is consistent with the fact that SCGO is a frustrated magnetic insulator with S=3/2 [6].

Secondly, we carried out the same analysis for the pyrochlore models to consider the heptamer formation in AlV_2O_4. As a result, in the case of $d^{2.5}$ configuration corresponding to AlV_2O_4, the model reproduces well the heptamer formation. The obtained state well explains the spin and orbital ordering anticipated in the experimental results of AlV_2O_4. This heptamer formation is also attributed to the formation of bonding-orbitals as in the case of the trimerization in SVGO. It is found that the trigonal distortion also plays an important role in stabilizing the heptamer. On the other hand, for $d^{1.5}$ configuration, the tendency to clustering is largely suppressed, consistent with the absence of long-range order in LiV_2O_4, which shows Fermi liquid behavior with anomalously large quasiparticle mass [7].

[1] J. B. Goodenough, '*Magnetism and the Chemical Bond*' (John Wiley and Sons, New York-London, 1963): J. B. Goodenough, G. Dutta, and A. Manthiram, Phys. Rev. B **43** (1991) 10170.
[2] J. Miyazaki *et al*,. Phys. Rev. B **79** (2009) 180410(R).
[3] Y. Horibe *et al*., Phys. Rev. Lett. **96** (2006) 086406.
[4] K. Matsuda, N. Furukawa, and Y. Motome, J. Phys. Soc. Jpn. **75** (2006) 124716.
[5] P. G. Radaelli *et al*., Nature **416** (2002) 155.
[6] X. Obradors *et al*., Solid State Commun. **65** (1988) 189.
[7] S. Kondo *et al*., Phys. Rev. Lett. **78** (1997) 3729.

P18

Microscopic Origin of Nematic Phase

Y. Yoshioka, K. Miyake

Division of Materials Physics, Department of Materials Engineering Science, Graduate School of Engineering Science, Osaka University, Toyonaka 560-8531, Japan

In recent years, a novel phase in the bilayer ruthenate $Sr_3Ru_2O_7$ under the external magnetic field has been extensively studied.

Theoretically, several authors suggest that the appearance of this phase, called nematic phase, can be explained by considering Fermi surface deformation due to electron-electron correlations.[1,2] If the chemical potential is close to the van Hove filling, considering Zeeman magnetic field and the interaction with *d*-wave symmetry, two first order metamagnetic transitions can be caused by increasing the magnetic field. In the region sandwiched between these two transitions, the Fermi surface has a lower rotational symmetry than that of the crystal, that is, the nematic phase is realized.

We discuss a microscopic origin of the interaction with *d*-wave symmetry.

[1] Hae-Young Kee and Yong Baek Kim, Phys. Rev. B **71**, 184402 (2005).
[2] H. Yamase and Andrey A. Katanin, J. Phys. Soc. Jpn. **76**, 073706 (2007).

P19

Quantum Melting of Spin Ice to Spin Smectic

Shigeki Onoda and Yoichi Tanaka

Condensed Matter Theory Laboratory, RIKEN, Wako 351-0198, Saitama, Japan

A quantum melting of the spin ice is proposed for pyrochlore-lattice magnets $Pr_2TM_2O_7$ (*TM* =Ir, Zr, and Sn). The quantum pseudospin-1/2 model is derived from the strong-coupling perturbation of the f-p electron transfer in the basis of atomic non-Kramers magnetic doublets. The ground states are characterized by a cooperative ferroquadrupole and pseudospin chirality in the cubic unit cell, forming a magnetic analog of smectic liquid crystals. Then, pinch points observed for spin correlations in the spin ice are replaced with the minima. The relevance to experiments including the recently discovered chiral spin state in $Pr_2Ir_2O_7$ is discussed.

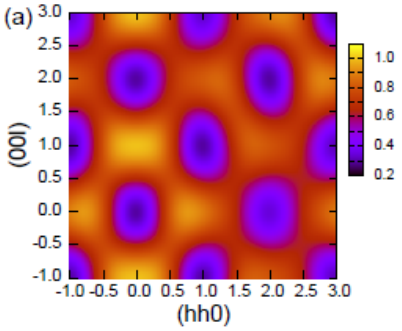

Fig.1: Spin correlation profile in the proposed state

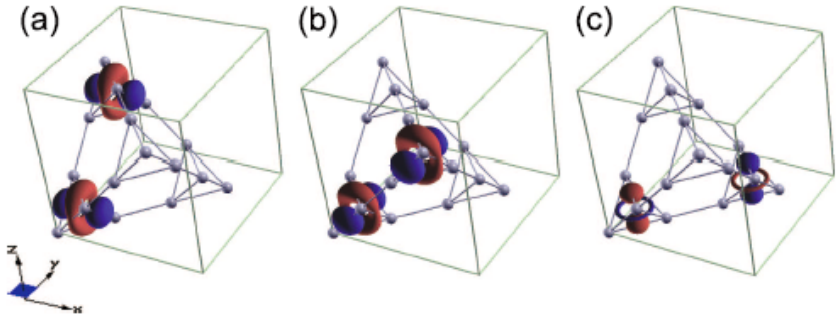

Fig.2: Cooperative quadrupole correlation in the spin smectic state.

[1] S. Onoda and Y. Tanaka, AriXive:09.072536.
[2] Y. Machida, S. Nakatsuji, S. Onoda, T. Tayama, and T. Sakakibara, Nature **463**, 210 (2010).

P20

Topological Defects and Spectral Flow in the Dynamics of Electronic Condensate: The Case of Charge Density Waves

M. Hayashi[1] and H. Ebisawa[2]

[1]*Faculty of Eudcation and Human Studies, Akita University, 1-1 Tegatagakuen-machi, Akita 010-8502*
[2] *Institute of Liberal Arts and Sciences, Tohoku University, 41 Kawauchi, Aoba-ku, Sendai 980-8576*

Topological defects play important roles in both equilibrium and non-equilibrium properties of the condensed systems, such as superconductivity and superfluidity. They mediate the transition from order to disorder at the critical point and also determine the rigidity of the order when the system is driven by external forces. Topological singularities at the center of the difects have been considered to have crucial effects on the dynamics of the defect itself, such as the case of vortices in superconductivity.

The dislocations in the charge density wave (CDW) condensate are also intriguing objects which dominate the phase transition and dynamical processes, including quenched non-equilibrium phase transition. Until quite recently, experimantally obtained CDW systems have had impurities which supress the free motion of the condensate and the dynamics have been well described by classical diffusional motion. However there are several reports of mesoscopic clean samples which show different dynamics from dirty ones. Some even report quantum effects in CDW's. Therefore it may be of interest to investigate the dynamics characteristic to clean CDW's.

In this paper, we discuss the time-dependent Ginzburg-Landau (GL) equation for CDW condensate. We develope a new framework taking account of the effects of quasiparticles explicitly and discuss the dynamics of dislocations. Our method enables to treat the so-called spectral flow behavior: when the dislocation travels across the one-dimensional chains of CDW, two quasiparticles (electrons or holes) including spin are created from the condensate (*i.e.*, the vacuum of CDW). This process, if not treated properly, violates the gauge invariance of the theory, since it creates charge from the vacuum.

In this paper, we propose a new framework to accommodate this spectral flow effect in the analysis of sliding conduction of CDW. The time-dependnt GL equation of the order parameter $\Delta(x,t)$ can be given in the following form,

$$\tau\left(\frac{\partial}{\partial t}-\frac{2\pi i}{e}j_{qp}\right)\Delta=\xi_0^2\left(\frac{\partial}{\partial x}+\frac{2\pi i}{e}\rho_{qp}\right)^2\Delta+\left(1-\tilde{t}\right)\Delta-\frac{|\Delta|^2}{\Delta_0^2}\Delta$$

where τ is the relaxation time, ξ_0 is the coherence length, $\tilde{t}$ is temperature normalized by critical temperature, and Δ_0 is the order parameter at $\tilde{t}=0$. ρ_{qp} and j_{qp} are the charge density and current of the quasi-particles, respectively. Some microscopic basis of this equation will also be discussed. By numerically solving this equation along with the diffusion equation of quasiparticles and Maxwell equation, we discuss the quasiparticle distribution and the elestic deformation of condensate during the sliding. We also address the effects of dislocations in the non-equilibrium phase transition.

[1] M. Hayashi, in *Quantum Coherence and Decoherence*, Eds, Y. A. Ono and F. Fujikawa, (Elsevier, 1999) p.273.
[2] M. Hayashi and H. Ebisawa, Physica C (to be published).

P21

Soft Hubbard gaps under coexisting short-range interaction and disorder: application to electron transport in organic field-effect transistors

H. Shinaoka[1] and M. Imada[2]

[1] *Institute for Solid State Physics, The University of Tokyo*, 5-1-5 *Kashiwanoha, Kashiwa, Chiba 277-8581, Japan*
[2]*Department of Applied Physics, The University of Tokyo, 7-3-1 Hongo, Bunkyo-ku, Tokyo 113-0033, Japan*

Recently, we have reported a theoretical study of the Anderson-Hubbard model under coexisting short-range interaction (on-site repulsion) and disorder. [1,2] We determined the ground-state phase diagram and investigated the single-particle density of states (DOS) for three dimensions within the unrestricted Hartree-Fock approximation. One might naively expect that, even for the interacting case, the DOS remains nonzero at the Fermi energy in the insulating phases because of localized impurity states induced by disorder. We, however, found that the DOS vanishes toward the Fermi energy all over the insulating phases for the interacting case. Because only the short-range interaction is present in this model, this unconventional soft gap (*soft Hubbard gap*) cannot be explained within the conventional theory[3] owing formation of soft gaps to the long-range part of the Coulomb interaction and excitonic effects.

To clarify the origin of the soft Hubbard gap, we proposed a phenomenology, which predicts the scaling of the DOS as

$$A(E) = \alpha \exp\left[-\left\{-\gamma \log\left(\frac{|E - E_{\mathrm{F}}|}{\Delta_0}\right)\right\}^d\right].$$

Here d is the spatial dimensions, E_{F} is the Fermi energy, and Δ_0 (> 0) is the energy scale of the soft gap ($|E\text{-}E_{\mathrm{F}}| < \Delta_0$). The positive constants α, γ depend on the localization length and electron density. Indeed, this predicted scaling is in perfect agreement with the numerical data. In contrast to the conventional theory by Efros and Shklovskii (ES), the present phenomenology owes the formation of the soft Hubbard gap to a multi-valley energy landscape or spin-glass freezing, which may be characteristic to correlated random systems.

In this talk, we analyze experimental data for organic field-effect transistors of κ-(BEDT-TTF)$_2$Cu[N(CN)$_2$]Br published by Y. Kawasugi *et al.*[4] The DC transport measurement is a useful and effective tool for investigating the DOS at low energies with high resolution in insulating phases. Indeed, we found that the temperature dependence of the DC resistivity is consistent with the present theory for two dimensions (d=2), indicating the coexistence of electron correlation and disorder. Although the DC resistivity finally crosses over to ES–type variable-range hopping (VRH) at lower energies, the ES-type VRH regime was found to be restricted to lower and lower energies toward the metal-insulator transition, being consistent with the divergence of the dielectric constant at the metal-insulator transition.

[1] H. Shinaoka and M. Imada, Phys. Rev. Lett. **102** 016404, (2009).
[2] H. Shinaoka and M. Imada, J. Phys. Soc. Jpn. **78** 094708, (2009).
[3] A. L. Efros and B. I. Shklovskii, J. Phys. C **8**, L49, (1975).
[4] Y. Kawasugi, H. M. Yamamoto, N. Tajima, T. Fukunaga, K. Tsukagoshi and R. Kato, Phys. Rev. Lett. **103**, 116801 (2009).

P22

Quantum criticality in an itinerant electron system coupled to ice-rule variables

M. Udagawa, H. Ishizuka, and Y. Motome

Department of Applied Physics, The University of Tokyo, 7-3-1 Hongo, Bunkyo-ku, Tokyo 113-8656, Japan

"Ice rule" is seen in a broad range of systems in condensed matter physics. It imposes a configurational constraint on two-state variables defined at neighboring four lattice sites so that two out of four are in the opposite state to the other two. The ice rule plays an important role not only in the most well-known material, the water ice I_h [1], but the charge frustrated system, magnetite Fe_3O_4 [2] and spin ice materials, such as $Ho_2Ti_2O_7$ [3] and $Dy_2Ti_2O_7$ [4]. Under the ice-rule constraint, the ground state is disordered and retains macroscopic degeneracy. Nevertheless, the ice-rule configuration is not completely random but cooperative in nature because of a hidden gauge structure. Indeed it exhibits a power-law spatial correlation in the ice-rule variables.

An interesting question is how this cooperative ice-rule texture affects the electronic properties when the system is itinerant. It is known that electrons sometimes exhibit critical behavior in peculiar spatial structure, such as in quasicrystals. So far, several theoretical studies have been carried out on this issue, e.g., a proton diffusion in ice I_h and a charge fractionalization in the pyrochlore systems, however, the effect of ice-rule configurations is yet to be fully explored.

In this contribution, we address this issue in one of the simplest models which describe fermions interact with ice-rule variables, an extended Falicov-Kimball model

$$H = -t\sum_{<i,j>}(c_i^+ c_j + H.c.) + U\sum_i n_i^c\left(n_i^f - \tfrac{1}{2}\right) + V\sum_{<i,j>} n_i^f n_j^f ,$$

where c_i annihilates a spinless fermion at site i, and the number of immobile particle takes $n_i^f = 0$ or 1. We consider this model on a family of tetrahedron-based lattices, such as the pyrochlore lattice (fig. a), in the ice-rule limit: $<n_i^f>= 1/2$ and $V\rightarrow\infty$, where the immobile particles distribute with satisfying the ice rule, i.e., two out of four sites are occupied in every tetrahedron (fig. a).

We find that this model is *exactly solvable* on a loop-less variant of the tetrahedron-based lattices, a tetrahedron Husimi cactus (THC) (fig. b). We clarify the ground-state phase diagram including a "charge ice" insulator in which the fermions are localized in the ice-rule configuration (fig. c). The exact solution reveals that a non-Fermi-liquid behavior emerges at a quantum critical point where the charge ice melts as decreasing the interaction. We also compare the exact solution with the numerical results for the pyrochlore and checkerboard lattices, and find that our Husimi cactus model captures the essential physics of itinerant electrons under the ice rule.

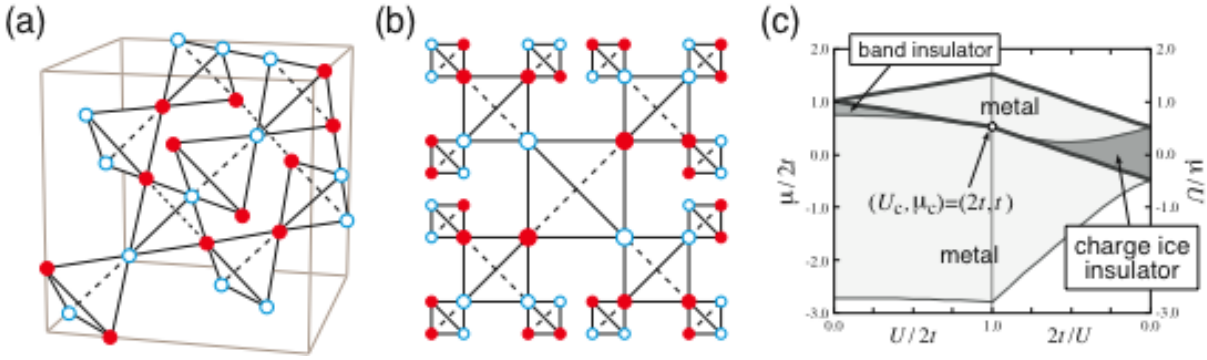

Figure: Examples of ice-rule configuration on (a) a pyrochlore lattice and (b) a tetrahedron Husimi cactus (THC). The sites with $n_I^f = 1$ (0) are shown with filled (empty) circles. (c) The exact ground-state phase diagram of the extended Falicov-Kimball model on THC in the ice-rule limit.

[1] L. Pauling, J. Am. Chem. Soc. **57**, 2680 (1935).
[2] P. W. Anderson, Phys. Rev. **102**, 1008 (1956).
[3] M. J. Harris et al., Phys. Rev. Lett. **79**, 2554 (1997).
[4] A. P. Ramirez et al., Nature **399**, 333 (1999).

P23

On Anomalous Criticalities in Paramagnetic Metals in Ce- and Yb-Based Systems

S. Watanabe and K. Miyake

Division of Materials Physics, Department of Materials Engineering Science, Graduate School of Engineering Sceience, Osaka University, Toyonaka, Osaka 560-8531, Japan

Recently, anomalous quantum critical behavior has been observed in Ce- and Yb-based metals, which does not follow the conventional theory for critical phenomena of spin fluctuations. In β-$YbAlB_4$ [1] and $YbRh_2Si_2$ [2], it was reported that uniform spin susceptibility exhibits diverging behavior toward zero temperature in spite of no evidence of existence of ferromagnetism, offering a theoretical challenge. Furthermore, non-Fermi-liquid (NFL) region extended in a wide pressure region in β-$YbAlB_4$ [1] is also in sharp contrast to the conventional V-shaped NFL region. The enhancement of uniform spin susceptibility has been also observed in paramagnetic-metal phases of $YbAuCu_4$ and $Ce_{0.9-x}La_xTh_{0.1}$, suggesting that these anomalies are not specific to the special materials, but seem rather general in paramagnetic metals in Ce- and Yb-based systems.

In this presentation, we discuss that the proximity of the quantum critical point of a first-order valence transition (VQCP) of Ce or Yb ion is a possible origin of these anomalies. We demonstrate how the VQCP is controlled by pressure and magnetic field [3,4] and how its proximity affects physical quantities [3-5]. The robust NFL region in β-$YbAlB_4$ under pressure is also shown to be naturally explained by this viewpoint [6].

[1] S. Nakatsuji, *et al*., Nature Phys. **4**, 603 (2008); Y. Matsumoto *et al*., arXiv:0908.1242.
[2] P. Gegenwart *et al*., Phys. Rev. Lett. **94**, 076402 (2005).
[3] S. Watanabe, A. Tsuruta, K. Miyake and J. Flouquet, Phys. Rev. Lett. **100**, 236401 (2008).
[4] S. Watanabe, A. Tsuruta, K. Miyake and J. Flouquet, J. Phys. Soc. Jpn. **78**, 104706 (2009).
[5] S. Watanabe and K. Miyake, arXiv:0906.3986.
[6] S. Watanabe, A. Tsuruta, K. Miyake and J. Flouquet, Physica B **404**, 2942 (2009).

P24

Spin Fluctuation Theory for Quantum Tricritical Point: Applications to Heavy-Fermion Systems, $YbRh_2Si_2$, $CeRu_2Si_2$, and β-$YbAlB_4$

T. Misawa, Y. Yamaji, and M. Imada

Department of Applied Physics, University of Tokyo, 7-3-1 Hongo, Bunkyo-ku, Tokyo, 113-8656, Japan
JST, CREST, Hongo, Bunkyo-ku, Tokyo 113-8656

Recent experimental results on quantum critical phenomena point out that physical properties do not follow the prediction of scalings by the conventional spin fluctuation theory[1,2,3]; i.e., critical exponents of thermodynamic and transport properties do not follow this standard theory, whereas in other cases the critical region is unexpectedly wide. In a number of compounds, this breakdown of the standard theory has been suggested in connection with the proximity of the first-order transition and the effects of inhomogeneities. When continuous transition switches over to the first-order transition or phase separations, a tricritical point necessarily emerges as the boundary of these two. The purpose of our study is certainly related to this motivation for elucidating physics under the proximity of first-order transitions and phase separations with the interplay of quantum fluctuations.

In this study, we propose a phenomenological spin fluctuation theory for antiferromagnetic quantum tricritical point (QTCP) [4,5], where a first-order phase transition changes into a continuous one at zero temperature. Under magnetic fields, ferromagnetic quantum critical fluctuations develop around the antiferromagnetic QTCP in addition to antiferromagnetic ones, which is in sharp contrast with the conventional antiferromagnetic quantum critical point. For itinerant electron systems, we show that the temperature dependence of critical magnetic fluctuations around the QTCP are given as $\chi_Q \propto T^{-3/2}$ ($\chi_0 \propto T^{-3/4}$) at the antiferromagnetic ordering (ferromagnetic) wave number $q = Q$ ($q = 0$). The convex temperature dependence of χ_0^{-1} is the characteristic feature of the QTCP, which is never seen in the conventional spin fluctuation theory. We propose a general theory of quantum tricriticality that has nothing to do with the specific Kondo physics itself, and solves puzzles of quantum criticalities widely observed in heavy-fermion systems such as $YbRh_2Si_2$ [6], $CeRu_2Si_2$[7], and β-$YbAlB_4$ [8]. For $YbRh_2Si_2$, our theory successfully reproduces quantitative behaviors of the experimental ferromagnetic susceptibility and the magnetization curve by choosing the phenomenological parameters properly. The quantum tricriticality is also consistent with singularities of other physical properties such as specific heat, nuclear magnetic relaxation time $1/T_1T$, and Hall coefficient. For $CeRu_2Si_2$ and β-$YbAlB_4$, we point out that the quantum tricriticality is a possible origin of the anomalous diverging enhancement of the uniform susceptibility observed in these materials.

[1] G. R. Stewart: Rev. Mod. Phys. **73** (2001) 797.

[2] H. v. Löhneysen *et al*.: Rev. Mod. Phys. **79** (2007) 1015.

[3] P. Gegenwart, Q. Si, and F. Steglich: Nature Phys. **4** (2008) 186.

[4] T. Misawa, Y. Yamaji, and M. Imada: J. Phys. Soc. Jpn. **77** (2008) 093712.

[5] T. Misawa, Y. Yamaji, and M. Imada: J. Phys. Soc. Jpn. **78** (2009) 084707.

[6] P. Gegenwart *et al*.:Phys. Rev. Lett. **94** (2005) 076402.

[7] D. Takahashi *et al*.:Phys. Rev. B **67** (2003) 180407(R).

[8] S. Nakatsuji *et al.*:Natuere Physics **4** (2008) 603.

P25

Zero-Field Quantum Criticality in the Heavy Fermion Superconductor β-$YbAlB_4$

Y. Matsumoto, K. Kuga, Y. Karaki, T. Tomita, N. Horie, T. Sakakibara, Y. Shimura, S. Nakatsuji

Institute for Solid State Physics, University of Tokyo, Kashiwa, 277-8581, Japan

Heavy fermion (HF) systems have attracted much interest as prototypical systems to study unconventional superconductivity and non-Fermi-liquid (NFL) states. In fact, a number of unconventional superconductors have been found in Ce ($4f^1$) based intermetallic HF systems near a quantum critical point. On the other hand, recent studies by our group revealed the first Yb ($4f^{13}$) based HF superconductivity with the transition temperature T_c = 80 mK in the new compound β-$YbAlB_4$ [1, 2]. Interestingly, pronounced NFL behaviors appear above T_c in the transport and thermodynamic properties [1]. The magnetic field dependence of the NFL behaviors indicates that the system is a rare example of a pure metal that displays quantum criticality at ambient pressure and under zero magnetic field [1]. Furthermore, recent hard x-ray photoemission spectroscopy (HXPES) measurements revealed intermediate valence of $Yb^{+2.75}$ where we normally expect a Fermi liquid ground state with moderate quasiparticle effective mass [3]. The system provides the first unique example of quantum criticality in the mixed valent system.

Here we present clear experimental evidences that indicate the zero-field quantum criticality in β-$YbAlB_4$. We employed the high resolution magnetization measurements down to 20 mK[4], and found that the magnetization in quantum critical region satisfies a following scaling equation, $-dM/dT = B^{-1/2}f(T/B)$ over wide ranges of magnetic fields (0.3 mT < B < 1 T) and temperatures (20 mK < T < 2 K). This T/B scaling strongly suggests B_c = 0 within the experimental resolution of ~ 0.2 mT, which is comparable to the Earth's magnetic field. In addition, this indicates unconventional quantum criticality. Furthermore, magneto-caloric effect obtained by using magnetization and specific heat data exhibit clear diverging behaviors toward zero temperature, which also supports the zero-field quantum criticality. In the presentation, we will further discuss the T-B phase diagram of the system and how the large temperature scale of the valence fluctuation (200 K) may be renormalized to a small effective Kondo temperature of ~ 10 K.

[1] S. Nakatsuji, K.Kuga, Y. Machida, T. Tayama, T. Sakakibara, Y. Karaki, H. Ishimoto, S. Yonezawa, Y. Maeno, E. Pearson, G. G. Lonzarich, L.Balicas, H. Lee, and Z. Fisk, Nature Phys. **4**, 603-607 (2008).
[2] K. Kuga, Y. Karaki, Y. Matsumoto, Y. Machida, and S. Nakatsuji, Phys. Rev. Lett. **101**, 137004 (2008).
[3] M. Okawa, M. Matsunami, K. Ishizaka, R. Eguchi, M. Taguchi, A. Chainani, Y. Takata, M. Yabashi, K. Tamasaku, Y. Nishino, T. Ishikawa, K. Kuga, N. Horie, S. Nakatsuji, and S. Shin, arXiv:0906.4899.
[4] Y. Matsumoto, K. Kuga, Y. Karaki, T. Tomita, S. Nakatsuji, arXiv:0908.1242. ; Y. Matsumoto *et al.*, *preprint*.

P26

Mott Transition of Bose-Fermi Mixtures in Optical Lattices Induced by Attractive Interactions

A.Masaki and H. Mori

Dept. of Physics, Tokyo Metropolitan University, 1-1 Minamiohsawa, Hachiohji-shi Tokyo 192-0397, Japan

Single-band Bose-Fermi Hubbard model, often used for theoretical analysis, have successfully described the systems in optical lattices in many cases. However remarkable phenomena which cannot be explained with this model have been observed in recent experiments of Bose-Fermi mixtures in optical lattices[1-3]: When the Bose-Bose interactions were repulsive and the Bose-Fermi interactions were attractive, the boson component lost its coherence as the fermion component was introduced.

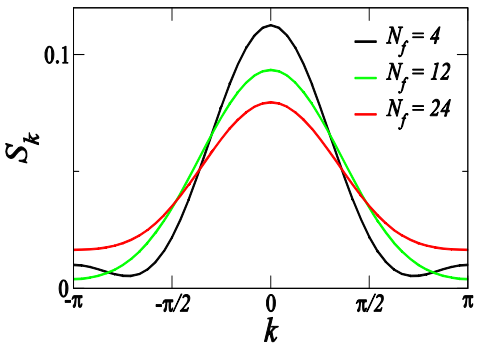

FIG. 1: Boson momentum distribution with different number of fermions.

Lühmann et al., [4] discussed that this could be attributed to the boson self-trapping effect caused by the attractive boson-fermion interactions. The more bosons reside in a well of the lattice potential, the more squeezed the wave function, taking account of higher bands, of the fermions in the well is and the deeper the effective lattice potential for both the bosons and the fermions becomes. However their calculation was not sufficient to account for the many-body effect.

The Bose-Fermi interactions play an important role in the many body mixture systems. In the present study we considered higher-order effects of the Bose-Fermi interactions in the optical lattice potential, which actually affected the bosonic and fermionic hopping terms in the Hamiltonian. We introduced a modified Bose-Fermi-Hubbard model with the hopping terms changed effectively by the number density of the bosons and the fermions.

To extract various physical properties of our Hamiltonian directly, we performed Quantum Monte Carlo Simulations and studied the fermion-inducing Mott transition of the bosons. We found that the superfluidity in uniform systems and the visibility of bosonic momentum distribution in trapped system varied with the total number of the bosons and that of the fermions. Also we discuss the validity of our calculation for repulsive interaction case.

[1] K. Günter et al., Phys. Rev. Lett. **96**, 180402 (2006).
[2]S. Ospelkaus et al., Phys. Rev. Lett. **96**, 180403 (2006).
[3]Th. Best et al., Phys. Rev. Lett. **102**, 030408 (2009).
[4]D.-S. Lühmann et al., Phys. Rev. Lett. **101** 050402 (2008).

P27

Mott physics revealed by triangular-lattice organics

K. Kanoda,[1] Y. Kurosaki,[1] T. Furukawa,[1] H. Hashiba,[1] H. Oike,[1] F. Kagawa,[1] K. Miyagawa,[1] Y. Shimizu,[2] H. Taniguchi,[3] S. Yamashita,[4] Y. Nakazawa[4]

[1]*Department of Applied Physics, University of Tokyo, Tokyo, Japan*
[2]*Institute for Advanced Research, Nagoya University, Nagoya, Japan*
[3]*Department of Physics, Saitama University, Saitama, Japan*
[4]*Department of Chemistry, Osaka University, Osaka, Japan*

Mott transition is a metal-insulator transition induced by electron-electron Coulomb interaction and essentially a phenomenon in the charge degrees of freedom. When the lattice is triangular, antiferromagnetically interacting spins suffer from geometrical frustration against ordering. So, the correlated electrons on triangular lattice in the vicinity of Mott transition are in an intriguing situation where both the charge and spin degrees of freedom possibly exhibit quantum fluctuations. The family of layered organic conductors, κ-$(ET)_2X$, whose bandwidth is comparable with the Coulomb repulsive energy and controllable by pressure, are model systems of interacting electrons on anisotropic triangular lattice [1]. In this symposium, we summarize our project achievements in our experimental study on κ-$(ET)_2X$ in the light of the above mentioned issues.

First, we present the spin-liquid behavior and Mott transition in κ-$(ET)_2Cu_2(CN)_3$, which is a half-filled band system with nearly isotropic triangular lattice [2]. This material shows no indication of magnetic ordering down to 30 mK. The spins are likely in a quantum liquid state. The nature of the spin liquid is controversial; the measurements of specific heat and NMR relaxation rate point to the gapless feature of elementary excitations, while thermal conductivity suggests the gapped excitations. It is noted that the Wilson ratio estimated from the low-temperature values of spin susceptibility and specific heat coefficient is 1-2, which implies that the spin objects follow the degenerate Fermi statistics irrespective of the insulating state; they are possibly spinons. Noticeably, this system shows a magnetic and thermodynamic anomaly around 5-6 K. This anomaly is featured by a kink in NMR relaxation rate $1/T_1$ and enhanced broadening of spectra, and persistent under pressures up to 0.3 kbar, where Mott transition occurs. The metallic phase neighboring the spin liquid above 0.3 GPa is a conventional metal characterized by $1/T_1T$= constant, which is in contrast with the pseudo-gapped behavior observed in the metallic phase neighboring the antiferromagnet.

Second, we show the anomalous magnetic and transport properties of the model systems of doped triangular lattices, κ-$(ET)_4Hg_{3-\delta}X_8$ [X=Br, Cl], where the missing content δ of Hg in the anion layers contributes to the hole doping into the ET layers with half-filled band [3]. In both materials, $1/T_1T$ is anomalously enhanced on cooling down to 10K for X=Br and 1K for X=Cl without magnetic ordering; in the Cl compound, the NMR enhancement factor, K_α, amounts to as much as 10^4, implying that the system is in a quantum critical region of magnetic ordering or spin liquid. The contactless conductivity measurement for κ-$(ET)_4Hg_{2.89}Br_8$ showed that T_c has a dome shape against pressure as reported previously, the superconductivity at low pressures is inhomogeneous, and the Fermi liquid crosses over to a non-Fermi liquid at a temperature which is increased with pressure. We argue these results in terms of doped-Mott insulator, which may be a doped spin liquid instead of the doped antiferromagnet like cuprates.

Third, the pressure-driven Mott criticality in κ-$(ET)_2Cu[N(CN)_2]Cl$, which was previously studied by transport measurements, has been investigated from the spin degrees of freedom [4]. We measured ^{13}C NMR $1/T_1$ under temperature and pressure variations around the endpoint of the 1st order Mott transition and found that $1/T_1$ shows a critical behavior with the same exponent as conductivity does. This result can be understood in terms of critical density variation of holons and doublons, provided that they work as charge carriers and spin extinguishers.

[1] K. Kanoda, J. Phys. Soc. Jpn. **75**, 051007 (2006).
[2] Y. Shimizu *et al*., Phys. Rev. Lett. **91**, 107001 (2003); Phys. Rev. B **73**, 140407 (2006); submitted
[3] Y. Kurosaki *et al*., Physica B, **404**, 3138 (2009) ; H. Oike *et al*., Physica B. **404**, 376 (2009).
[4] F. Kagawa *et al*., Nature. Phys. **5,** 880 (2009).

P28

Cofermion Theory for Changes in Fermi-Surface Topology of Doped Mott Insulators

Y. Yamaji and M. Imada

Department of Physics, The University of Tokyo, 7-3-1 Hongo, Bunkyo-ku, Tokyo 113-0033, Japan

We propose that pseudogap phenomena [1] and Fermi-arc formation [2] experimentally observed in underdoped cuprate superconductors are consequences of *topological changes in the Fermi surface*, which emerge in proximity to Mott insulating states. To develop a physically unequivocal theory and explain how the topological changes occur, we start from one of the simplest theory for correlated electron systems, namely, the slave-boson mean-field theory for the Hubbard model [3] on a square lattice. Our crucial step is to further take into account the charge dynamics and fluctuations. The extra charge fluctuations seriously modify low-energy single-particle spectra of doped Mott insulators near the Fermi level: An electron added around an empty site (or a hole added around a doubly occupied site) constitutes *composite fermion*, called *holo-electron* (or *doublo-hole*) at low energy in distinction from the normal quasiparticles. These unexplored composite fermions substantiate the extra charge fluctuation. We show that the quasiparticles hybridize with the holo-electrons and doublo-holes. The resultant hybridization gap is identified as the pseudogap observed in the underdoped region of the high-T_c cuprates. Because the Fermi level crosses the top (bottom) of the low-energy band formed just below (above) the hybridization gap in the hole-doped (electron-doped) case, it causes a Fermi-surface reconstruction, namely, a topological change in the Fermi surface forced by the penetration of zeros of the quasiparticle Green function. The pseudogap, and the resultant formation of pocket or arc of the Fermi surface reproduce the experimental results for the cuprate superconductors in the underdoped region.

Here we show the results for the electron density n=0.95, next-nearest-neighbor hopping t'=0.25t, and on-site Coulomb repulsion U=12t, where the energy unit t is the nearest-neighbor hopping, as is illustrated in FIG.1: Fig.1(a) shows the reconstructed band dispersion (thick solid curves). Around so-called antinodal points (π, 0), the hybridization gap is clearly seen. The reconstructed Fermi surface, namely, Fermi pocket is shown in Fig.1(b). The spectral function at the Fermi level (ω=0) is also shown in Fig.1(c), which is consistent with experimentally observed Fermi arcs.

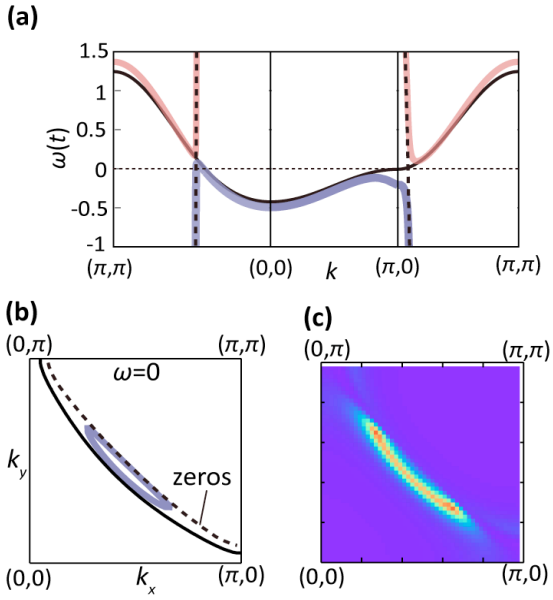

FIG.1: Results for n=0.95, t'=0.25t, and U=12t.
(a) Band dispersions and zero surface calculated for hole-underdoped case (hole concentration, x=0.05). Thin solid (black) curve gives the bare band dispersion of quasiparticles, and thin dashed (black) curve represents the zero surface induced by cofermions. Thick (blue and red) solid curves stand for reconstructed bands.
(b) Bare and reconstructed Fermi surface, and zero surface at ω=0.
(c) Spectral function at ω=0 with broadening factor η=0.05t.

[1] As a review, M. R. Norman, D. Pines, and C. Kallin, Adv. Phys. **54**, 715 (2005).
[2] As a review, A. Damascelli, Z. Hussain, and Z.-X. Shen, Rev. Mod. Phys. **75**, 473 (2003).
[3] G. Kotliar and A. E. Ruckenstein, Phys. Rev. B **57**, 1362 (1987).

P29

Orbital driven spin-Peierls transition in pyrochlore $Tl_2Rh_2O_7$

Shigeki Fujiyama,[1] Ayako Yamamoto,[1]
M. Yoshida,[2] M. Takigawa[2], and H. Takagi[1,3]

[1]*Magnetic Materials Laboratory, RIKEN, ASI, Wako, Saitama 351-0198, Japan*
[2]*Institute for Solid State Physics, University of Tokyo,*
[3]*Department of Advanced Materials, University of Tokyo*

Antiferromagnetic spin coupling confined in Pyrochlore lattice is known to emerge unconventional quantum electronic states at low temperatures. Many transition metal pyrochlore materials have been studied so far. There remains an open question in the mechanism of metal insulator transition: it is still unsettled whether MIT can occur without structural change and concomitant relaxation of geometrical frustration.

The 4d transition metal based pyrochlores provide a playgroud to study MIT in spin-orbital-lattice composite system. One famous example is $Tl_2Ru_2O_7$ (S = 1, L = 1), which realizes low temperature nonmagnetic state evidenced by Tl NMR. Here, high temperature cubic lattice is elongated along the <110> direction at MIT (~ 130 K), and one dimensional Haldane spin coupling is theoretically proposed as the origin of this nonmagnetic state. (S. Lee et al. Nat. Materials (2006))

We synthesized $Tl_2Rh_2O_7$ (S = 1/2, L = 1, T_{MIT} ~ 100 K) and t_{2g}-half-filled $Hg_2Ru_2O_7$ (S = 3/2, T_{MIT} ~ 110 K) and performed powder X-ray diffraction and Tl, Hg NMR to compare the electronic states with that of $Tl_2Ru_2O_7$.

In spite of the similarlity of the MIT temperatures of these three materials, various characters of lattice distortions and magnetic ground states were observed. A nonmagnetic ground state in associated with <110> lattice distortion was observed for $Tl_2Rh_2O_7$ while $Hg_2Ru_2O_7$ shows a classical antiferromagnetic state with <111> distortions. When comparing with $Hg_2Ru_2O_7$, we can consider the orbital degree of freedom plays a key role to determine the fates of the lattices and electronic states. We need other mechanism than Haldane spin coupling to realize singlet ground state for S=1/2 $Tl_2Rh_2O_7$. We propose orbital-driven Peierls instability as the origin of the observed nonmagnetic state of this material.

P30

Cyclotron resonance in the two dimensional metallic phase of Si/SiGe

R. Masutomi,[1] A. Sekine,[1] K. Sasaki,[1] K. Sawano,[2] Y. Shiraki,[2] and T. Okamoto[1]

[1]*Department of Physics, University of Tokyo, 7-3-1 Hongo, Bunkyo-ku, Tokyo 113-0033, Japan*
[2]*Research Center for Silicon Nano-Science, Advanced Research Laboratories, Tokyo City University, 8-15-1 Todoroki, Setagaya-ku, Tokyo 158-0082, Japan*

A metal-insulator transition (MIT) in two dimensional systems has attracted much attention because it conflicts with the scaling theory of localization in two dimensions [1]. In 1994, Kravchenko and collaborators observed an apparent MIT in Si metal-oxide-semiconductor field-effect transistor (MOSFETs). Subsequently the metallic behavior of the resistivity is studied in a variety of semiconductor systems. Most of the MIT occur in the region where electron-electron interaction becomes important. Some models have been proposed to explain a wealth of experimental data. However, its origin remains unclear and controversial. In this work, we report cyclotron resonance (CR) measurements on two dimensional electrons in a Si quantum well. The scattering time τ_{CR} obtained from the CR signal is compared with the transport scattering time τ_t.

We used a heterostructure sample with a 20-nm-thick strained Si channel sandwiched between relaxed $Si_{0.8}Ge_{0.2}$ layers [2]. The 2DES has a high mobility of 43 m^2/Vs at electron density $N_s = 2.3 \times 10^{15}$ m^{-2} and 0.4 K. The sample was mounted inside a wave-guide with a 6 mm bore inserted into a pumping ^3He cryostat. CR measurements for Si/SiGe have been performed in the frequency of 100 GHz using a Gunn oscillator. The CR signal was detected by a carbon bolometer immersed in liquid ^3He.

Plotted in Fig. 1(a) are the temperature dependence of τ_{CR} and τ_t, where τ_{CR} is obtained from the half width at half maximum of the CR signal and τ_t is the transport scattering time related to the zero-field conductivity σ_0 ($\tau_t = m^*\sigma_0/e^2N_s$). Both τ_{CR} and τ_t exhibit a metallic temperature dependence at $N_s = 1.2 \times 10^{15}$ m^{-2}. Fig. 1(b) shows N_s dependence of τ_{CR} and τ_t at 0.4 K. For our sample, the critical electron density N_c of the MIT is almost 0.5×10^{15} m^{-2}. In the vicinity of the MIT, τ_t decreases rapidly with decreasing N_s, while τ_{CR} dose not change so much. The observed result cannot be explained in terms of the single particle picture.

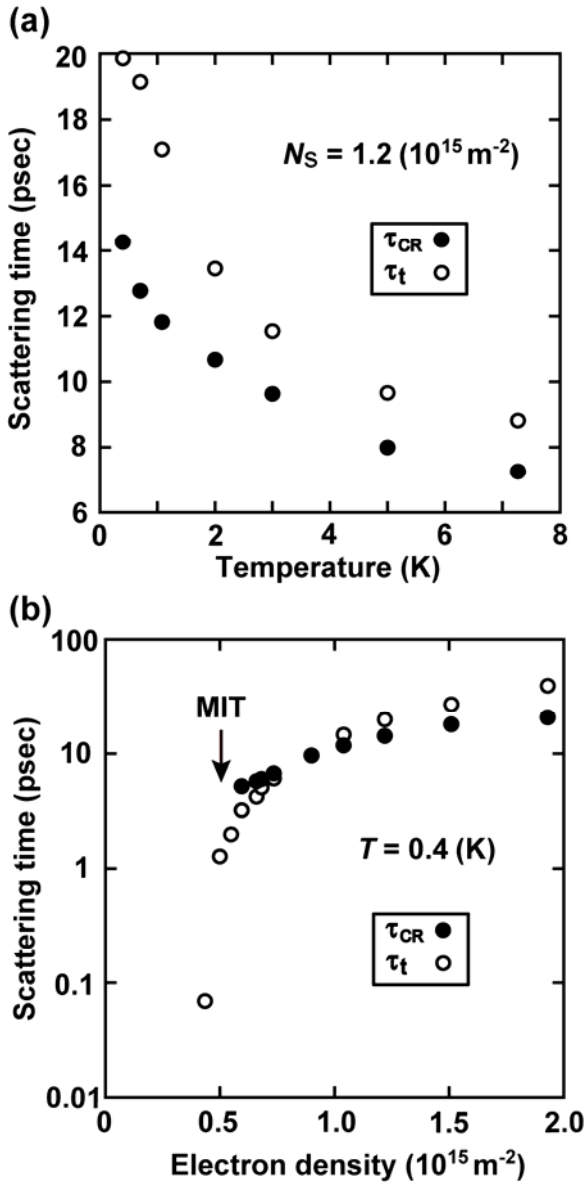

FIG.1: Temperature (a) and density (b) dependence of τ_{CR} and τ_t.

[1] E. Abrahams *et al.*, Phys. Rev. Lett. **42**, 673 (1979).

[2] A. Yutani and Y. Shiraki, Semicond. Sci. Technol. **11**, 1009 (1996); J. Cryst. Growth **175/176**, 504 (1997).

P31

Dimensional Crossover of ^{3}He Self-Condensation from 2D to 3D

D. Sato, K. Naruse, T. Matsui, and Hiroshi Fukuyama

Department of Physics, The University of Tokyo, 7-3-1 Hongo, Bunkyo-ku, Tokyo 113-0033, Japan

It has been long believed that, for ^{3}He atoms in strict two-dimensions (2D), there is no critical point, i.e., no gas-liquid transition, both theoretically [1] and experimentally [2]. This is because the large zero-point energy and hard-core repulsion inhibit self-condensing. However, a weakly-bound liquid state with an areal density of about 2 nm^{-2} is suggested for ^{3}He in the confinement potential of graphite substrate from the variational Monte Carlo calculation taking account of delocalization of the wave function perpendicular to the 2D plane [3]. In the previous experiments for a few layers of ^{3}He adsorbed on graphite [2], the existence of a liquid phase of very low-density below 1 nm^{-2} is not excluded. It is an interesting question to ask whether we can observe the dimensional crossover of self-condensation when we change the number of ^{3}He layers adsorbed on graphite.

In this work, we measured heat capacities (C) of the 2nd, 3rd and 4th layer of ^{3}He on graphite in a wide temperature range ($0.1 \leq T \leq 80$ mK) to seek for a possible low density self-condensed phase, a *paddle* phase, in each layer. Fig. 1 shows the temperature dependence of the measured heat capacities for the 2nd layer ^{3}He of ρ_{2nd} = 0.5 nm^{-2}. They show the $C = \gamma T$ behaviour below 20 mK, which is characteristic of degenerated Fermi fluid. The γ value ($= \pi k_B^2 m^* A/(3\hbar)$) is nearly the same as that of the ideal Fermi gas uniformly spreading over the whole surface, where m^* is the effective mass and A is the total surface area. On the other hand, as shown in Fig. 2, the measured γ value of the 3rd layer ^{3}He decreases linearly with decreasing 3rd layer density (ρ_{3rd}) below 1.3 nm^{-2}, indicating a liquid phase of about 1 nm^{-2} [4]. A similar density dependence of γ is observed in the 4th layer. Therefore, our experimental results suggest that we have observed the dimensional crossover of ^{3}He self-condensation with the threshold confinement potential between -20 K (2nd layer on graphite) and -6 K (3rd layer).

[1] M.D. Miller and L.H. Nosanow, J. Low Temp. Phys. **32**, 145 (1978).
[2] D.S. Greywall, Phys. Rev. B **41**, 1842 (1990); D.S. Greywall and P.A. Busch, Phys. Rev. Lett. **65**, 64 (1990).
[3] B. Brami, F. Joly and C. Lhuillier, J. Low Temp. Phys. **94**, 63 (1994).
[4] D. Sato, D. Tsuji, S. Takayoshi, K. Obata, T. Matsui and H. Fukuyama, J. Low Temp. Phys. **158**, 201 (2010).

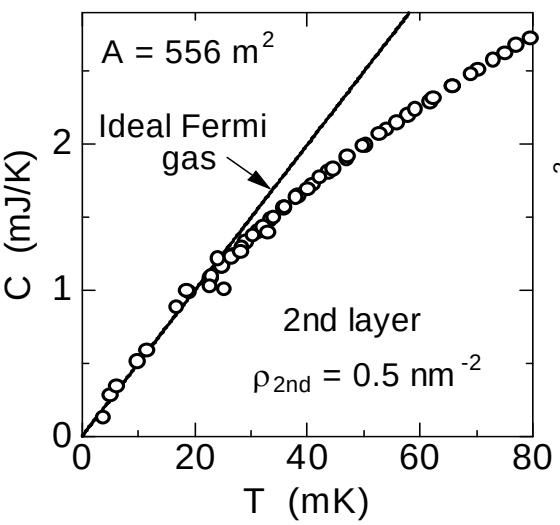

FIG.1: Heat capacity data for the 2nd layer ^{3}He on graphite of low density (ρ_{2nd} = 0.5 nm^{-2}).

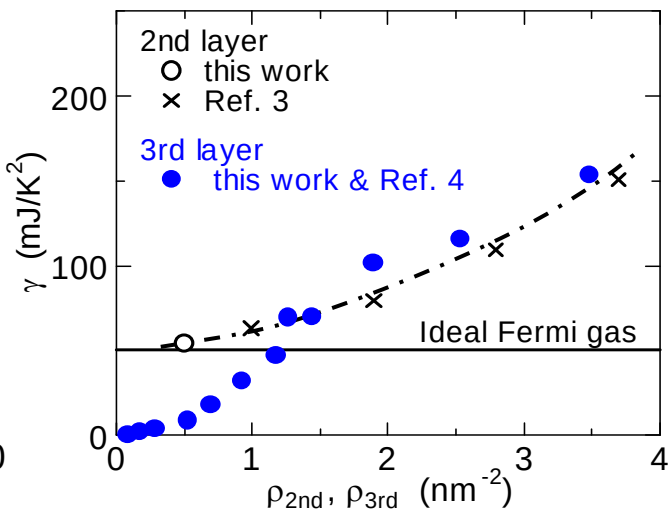

FIG.2: Density dependences of γ for the 2nd and 3rd layer ^{3}He on graphite.

P32

Two-dimensional Solid ^{3}He in High Magnetic Fields

H.Nema[1], A.Yamaguchi[2] and H.Ishimoto[3]

Institute for Solid State Physics, University of Tokyo, Kashiwa, Chiba 277-8581, Japan

^{3}He film adsorbed on graphite surface offers an ideal two-dimensional anti-ferromagnetic *S=1/2* quantum spin system on a triangular lattice. Competition between ferromagnetic and anti-ferromagnetic interaction arising from various multiple spin exchanges makes it strongly frustrated. The ground state in such a frustrated quantum spin system is one of the most interesting issues in condensed matter physics. Recent experiments on the anti-ferromagnetic solid ^{3}He in the second layer (so called 4/7 phase) indicate a gapless spin liquid ground state [1][2], whereas there still exists a controversy on whether the spin gap is finite or not. We have been trying to clarify the magnetic properties of this system up to very high magnetic fields [3]. Here we report a precise magnetization measurement with uhf NMR below 1 mK over the wide magnetic field region up to 11 T. As shown in Fig.1, the magnetization curve has a narrow plateau at half of the saturation magnetization between 1.2 T and 2.2 T, and reaches full saturation at around 10 T [4]. This fact is clearly consistent with a stable **uuud** state in the certain magnetic field region. Moreover there seem to exist another kinks at around 1/4 and 2/3 of the saturation magnetization. The observed behavior is discussed in the multiple spin exchange model [5] and a minimal model based on the Hubbard Hamiltonian [6].

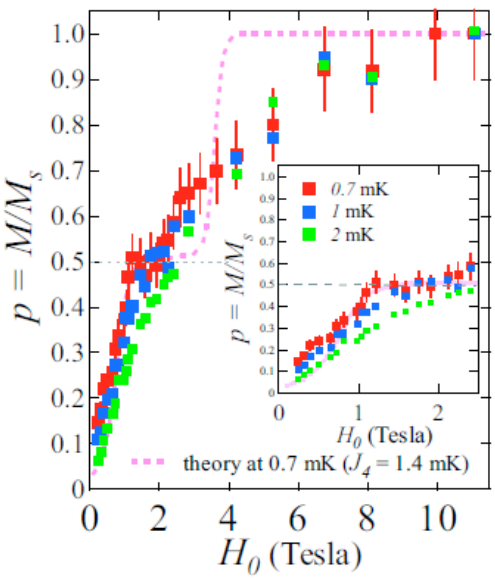

Fig.1 Magnetization curve of 4/7 phase

Present address
[1] Department of physics, Osaka City University
[2] Graduate School of Material Science, University of Hyogo
[3] Riken

[1] K.Ishida *et al*., Phys. Rev. Lett. **79** (1997) 3451.
[2] R.Masutomi *et al*., Phys. Rev. Lett. **92** (2004) 025301.
[3] Y.Yamaguchi *et al*., J. Low Temp. Phys **148** (2007) 755.
[4]H.Nema *et al*., Phys. Rev. Lett. **102** (2009) 075301.
[5] G.Misguich *et al*., Phys. Rev. Lett. **81** (1998) 1098.
T. Momoi *et al*., Phys. Rev. **B59** (1999) 9491 .
[6] S.Watanabe *et al*., J.Phys. Soc.Jpn. **76** (2007) 113603.

P33

Thermal Conductivity of ^{3}He Solid Films on Graphite in Weak Magnetic Fields

M. Morishita

Graduate School of Pure and Applied Sciences, University of Tsukuba, Tsukuba 305-8751, Japan

Mechanism of thermal relaxation between ^{3}He thin films and graphite substrates has not been understood yet. Previous thermal conductivity measurements between ^{3}He films and graphite substrate have revealed that heat flows along the ^{3}He solid films over a long distance and then flows into the graphite substrate at some local spots [1]. In this presentation, results of recent thermal conductivity measurements in weak magnetic fields up to 600 Oe will be reported. Examples of the measured thermal conductance (κ), and the divided values by heat capacity (C), κ/C, are shown in FIG. 1 and FIG. 2, respectively. Although thermal conductivity (κ) shows complicated magnetic-filed and temperature variation as shown in FIG. 1, κ/C show almost no magnetic-field variation between 150 and 600 Oe as shown in FIG. 2. These observations strongly suggest that heat is transferred along the solid ^{3}He films by quasiparticles. κ/C shows clear minima at some temperature around 1 mK, which depends on the areal density. Above and below this temperature, quasiparticles are thought to be phonons and spin excitations, respectively. The local spots where heat is transferred between the ^{3}He solid film and the graphite substrate are supposed to be magnetic and non-magnetic impurity clusters in graphite substrate.

[1] M. Morishita, J. Low Temp. Phys. **148**, 767 (2007).

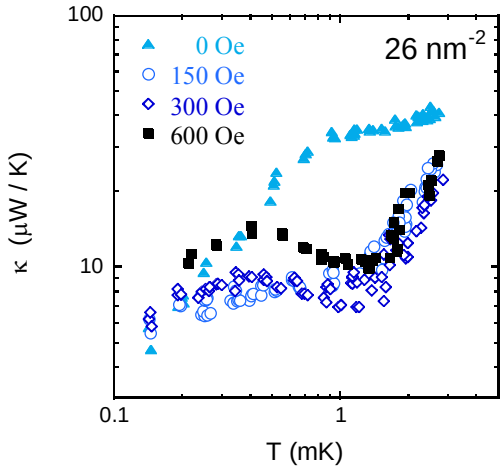

FIG.1: Thermal conductance between the graphite substrate and the ^{3}He solid film with areal density of 26 nm^{-2}.

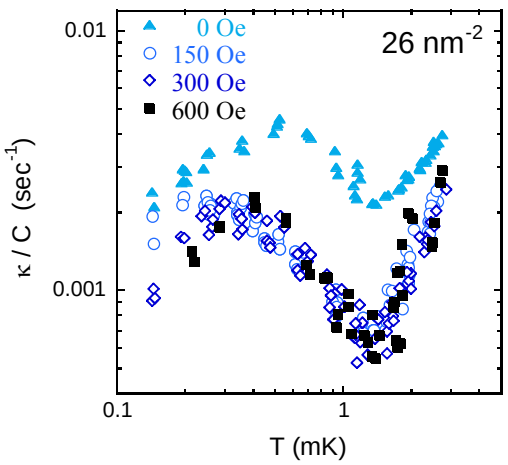

FIG.2: Ratio of thermal conductance (κ) and heat capacity (C) of the ^{3}He solid film with areal density of 26 nm^{-2}.

P34

Magnetization Measurements and Surface Observation of Grafoil Substrate

M. Morishita

Graduate School of Pure and Applied Sciences, University of Tsukuba, Tsukuba 305-8751, Japan

Important roles of impurity clusters in graphite substrate in heat transfer mechanisms between ^{3}He films and graphite substrate have been suggested. At sub-mK temperature range, especially, magnetic impurity clusters of large diameter about several-hundreds-nm are thought to play important role. Existence of such large clusters might be questionable. For the actual graphite substrate, Grafoil, although contents of some impurities have been reported from the ash analysis [1], configuration of impurities has not been clarified. In this report, results of surface observations of Grafoil by a scanning electron microscope (SEM), analyses by energy dispersive X-ray spectroscopy (EDS), and magnetization measurements are shown. Impurity clusters with diameter of 1~10 μm containing Al, Ca, Si, Fe, etc. are observed at exfoliated surfaces of Grafoil. Ferromagnetism is also observed after subtraction of a diamagnetic contribution. The saturation magnetization is several times larger than that of HOPG [2], and coincide with the amount of magnetic impurities reported from the ash analysis [1].

[1] The data sheets of Grafoil by Union Carbide Corporation.
[2] P. Esquinazi *et al*., Phys. Rev. B **66**, 024429 (2002).

P35

Towards Experimental Determination of the Structure of the 4/7 Phase in the Second-Layer Helium on Graphite

S. Nakamura, K. Matsui, T. Matsui and Hiroshi Fukuyama

Department of Physics, The University of Tokyo, 7-3-1 Hongo, Bunkyo-ku, Tokyo 113-0033, Japan

The 4/7 commensurate phase in the second layer ^{3}He adsorbed on graphite is an ideal model system for two-dimensional frustrated quantum antiferromagnet [1]. The same phase of ^{4}He at densities slightly lower than the stoichiometry is a candidate of *supersolid* [2]. The existence of the 4/7 phase was first proposed for ^{3}He to account for the magnetic anomalies in heat capacity and magnetization measurements below 10 mK [1]. The heat-capacity anomalies observed previously at high temperatures, i.e., T = 1 K (^{3}He) and 1.5 K (^{4}He), also support the order-disorder transition around the 4/7 density [1]. On the other hand, the neutron diffraction experiment failed to confirm directly this structure due to the technical problems [1]. A recent PIMC calculation for ^{4}He claimed the absence of the 4/7 phase [3]. Therefore, further and unambiguous experimental information on the structure of the low density second-layer He on graphite is highly desirable.

In this presentation, we show details of construction of the experimental apparatus for new heat-capacity measurements with ZYX, an exfoliated graphite substrate, to study the nature of the prospective order-disorder transition in the low-density second-layer ^{3}He and ^{4}He on graphite. All of the previous heat-capacity measurements have been done using Grafoil substrate whose micro-crystallite size is ten times smaller than ZYX. Moreover, it is considered that about 15% of the total He atoms adsorbed on Grafoil are trapped in surface heterogeneities showing amorphous properties. By use of ZYX, we thus will be able to distinguish whether the high-T heat-capacity anomalies at T = 1 and 1.5 K are critical behavior due to the phase transition or merely broad maxima representing some specific energy scale.

Fig.1: Calorimeter with ZYX substrate.

We also show detailed designs of low-energy electron diffraction (LEED) experiments using natural graphite as an adsorption substrate to obtain direct structural information on the 4/7 phase. The usefulness of the LEED technique has already been proved in the previous experiments on 2D solids of rare gas atoms and hydrogen molecules at temperatures down to 5 K [4]. However, special cares must be taken in the case of measurements of 2D He since they should be performed at much lower temperatures than 1 K. As shown in Fig. 2, we will (1) install the LEED optics at the bottom of a cryogen-free dilution refrigerator and cool it to T = 70 K, (2) use a tilted electron gun, (3) suppress the incident current density below 1 pA for a spot diameter ≈ 2 mm and (4) improve the detection sensitivity with two micro channel plates (MCP) and a delay-line detector (DLD). These careful designs will allow us to perform the LEED measurements in the continuous mode at equilibrium sample temperatures below 0.3 K.

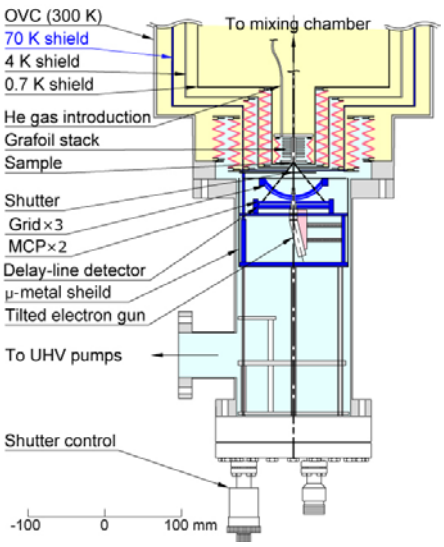

Fig.2: Ultra-low temperature LEED apparatus.

[1] H. Fukuyama, J. Phys. Soc. Jpn. **77**, 111013 (2008) and reference therein.
[2] Y. Shibayama, H. Fukuyama and K. Shirahama, J. Phys. **150**, 032096 (2009).
[3] P. Corboz, M. Boninsegni, L. Pollet and M. Troyer, Phys. Rev. B **78**, 245414 (2008).
[4] J. Cui and S. C. Fain, Jr., Phys. Rev. B **39**, 8628 (1989).

P36

Dynamical Transition and Self-Organized Criticality in Crystallization of ^{4}He in Aerogel

R. Masumoto, K. Ueno, R. Nomura and Y. Okuda

Department of Condensed Matter Physics, Tokyo Institute of Technology, 2-12-1 Oookayama, Meguro-ku, Tokyo 152-8550, Japan

Dynamical transition in the way of crystallization of ^{4}He in aerogel was observed as a function of temperature: ^{4}He crystals inside the aerogel grew via creep at high temperatures and via avalanche at low temperatures owing to the competition between thermal fluctuation and quenched disorder[1].

Variable volume cell was employed to investigate the temperature dependence of the dynamics. The crystals were not made by the ordinary blocked capillary method with cooling but by a compression of the sample cell over the bulk melting pressure at constant temperatures. The cell had optical windows so that we could visualize the dynamics directly. Aerogel is so transparent that it is suitable for the visualization of the dynamics within it.

Crystal has a greater density than liquid so that the extra mass has to be transported in the crystallization process. ^{4}He crystals did not grow from the outer surface of the aerogel but nucleated at various sites inside the aerogel. The aerogel was in a glass tube and had a contact with the outer bulk crystals only on its upper surface. This means that crystallization in aerogel does not occur by the forced invasion of outer bulk ^{4}He crystals but by a process of the bulk crystals once being melted, transported to increase the pressure of the liquid in the aerogel and re-crystallized there[2]. The profiles of some nucleated crystals are drawn in the figure.

In the creep region, crystal growth was faster at higher temperature and became slower with cooling. This is consistent with the expectation that crystal growth is via a thermally activated interface motion in the disordered media in the creep region. This temperature dependence is opposite to the bulk crystal growth. Growth velocity was the lowest at the transition temperature. In the avalanche region, it slightly increased with cooling and saturated at lower temperature. This temperature independent growth is presumably a result of a macroscopic quantum tunneling through the disordered potentials or instability by the compression.

The crystallization pressure in aerogel was not just like a shift of the bulk crystallization pressure but had a maximum at the transition temperature. This observation was possible because we made the constant temperature measurement, not the blocked capillary method. This anomalous crystallization pressure in the aerogel is likely to reflect the growth velocity: the lower was the growth velocity, the higher was the crystallization pressure.

Distribution of the avalanche size was analyzed. The avalanche size distributed over a large scale and followed a power low. The system was in a scale invariant critical state without any fine-tuning of the experimental parameters. It can be concluded that the low temperature avalanche region is in the self-organized critical state.

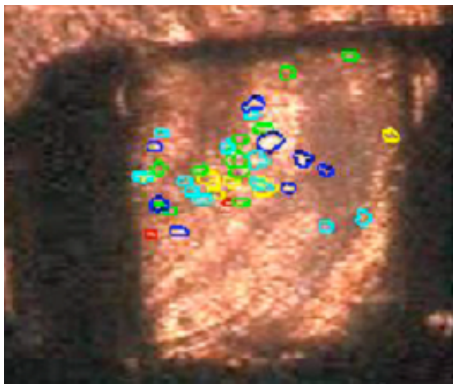

[1] R. Nomura, A. Osawa, T. Mimori, K. Ueno, H. Kato and Y. Okuda, Phys. Rev. Lett. **101**, 175703 (2008)

[2] K. Ueno, R. Masumoto, T. Mimori, A. Osawa, R. Nomura and Y. Okuda, J. Low Temp. Phys. **158**, 490 (2010)

P37

Magnetic phase transitions of bcc solid ^{3}He

T. Miura and K. Kubo

Department of Physics, Aoyama Gakuin University, 5-10-1 Fuchinobe, Sagamihara, Kanagawa, 229-8558, Japan

At low temperatures and under the external magnetic field bcc solid helium3 exhibits two peculiar magnetic orderings, the uudd and the cnaf structures[1]. It is well known that the phase transitions from the uudd phase to both the cnaf and the paramagnetic phases are discontinuous. Also the transition between the cnaf and the paramagnetic phases is known to be continuous at a high magnetic field. At a low magnetic field and close to the triple point the transition was reported to be discontinuous and a tricritical point is expected to exist on the phase boundary between the cnaf and the paramagnetic phases[2,3,4]. So far few theoretical investigations were elaborated on the properties of the phase transitions between the cnaf and the paramagnetic phases and the nature of this phase transition seems to be not well clarified[5,6].

We studied this problem by using Monte Carlo simulations of the classical spin model on the bcc lattice. The spins are assumed to interact through multiple ring exchanges. We studied the nature of the phase transition by examining the energy histograms of the states generated by Monte Carlo steps. For a parameter set of the three-spin and the planar and the folded four-spin exchanges suggested by Roger et. al.[7], we found that the energy histogram shows two peaks near the phase transition at low magnetic field while it has only one peak at high magnetic field. This implies that the transition changes from a discontinuous to a continuous one by increasing the magnetic field.

We will report our results for other values of parameters and compare them with the phase diagram obtained by experiments.

[1] D.D. Osheroff, M.C. Cross and D.S. Fisher, Phys. Rev. Lett. **44** (1980) 792.

[2] D.D. Osheroff, Physica 109 & 110 (1982) 1461.

[3] A. Sawada, H. Yano, M. Kato, K. Iwahashi and Y. Masuda, Phys. Rev. Lett. **56** (1986) 1587.

[4] J.S. Xia, W. Ni and E.D. Adams, Phys. Rev. Lett. **70** (1993) 1481.

[5] Z. Sun and J.H. Hetherington, J. Low Temp. Phys. **86** (1992) 303.

[6] J. DuBois and P. Kumar, J. Low Temp. Phys. **98** (1995) 37.

[7] M. Roger, J.H. Hetherington and J.M. Delrieu, Rev. Mod. Phys. **55** (1983) 1.

P38

Phase diagram of *S*=1 bilinear-biquadratic chains with a single-ion anisotropy

K. Takahashi,[1] K. Hijii,[2,3] and K. Nomura[1]

[1]*Department of Physics, Kyushu University, Fukuoka 812-8581, Japan*
[2]*Department of Physics, Graduate School of Science, University of Tokyo, Bunkyo-ku, Tokyo 113-0033, Japan*
[3]*Core Research for Evolutional Science and Technology (CREST), Japan Science and Technology Agency (JST), 4-1-8 Honcho Kawaguchi, Saitama, 332-0012, Japan*

We study the one-dimensional *S*=1 bilinear-biquadratic (BLBQ) chains with a single-ion anisotropy, which is described by the following Hamiltonian

$$H(\theta,D)=\sum_{j=1}^{L}[\cos\theta(\boldsymbol{S}_j\cdot\boldsymbol{S}_{j+1})+\sin\theta(\boldsymbol{S}_j\cdot\boldsymbol{S}_{j+1})^2]-D\sum_{j=1}^{L}(S_j^z)^2, \qquad (1)$$

where $\boldsymbol{S}_j$ is a spin-1 operator, D is the parameter controlling a single-ion anisotropy and L is system size (L: even). This model appears magnetic materials and ultracold alkali atoms in optical lattice, and theoretically it is discussed by Kolezhuk [1].

We discuss the ground state phase diagram of this model numerically by twisted boundary condition level spectroscopy method [2]. We determine the phase boundaries among the dimerized phase, Neel phase and XY2 phase (the XY2 phase is predicted by Schulz [3]). Our phase diagram is summarized in Fig.1. The phase transition between XY2 phase and Neel phase is Berezinskii-Kosterlitz-Thouless transition and the phase transition between Neel phase and dimerized phase belongs to Gaussian universality class. When $\theta=-\pi/2$, it is exactly known the followings. In $D=0$ case, the ground state phase is the dimerized phase and this Hamiltonian has SU(3) symmetry. In $D=\infty$ case, the ground state phase is XY2-Neel transition line and this Hamiltonian has SU(2) symmetry. From our results of numerical calculation, for $\theta=-\pi/2$ and finite D>0, we find exact symmetry differ from previously identified symmetries.

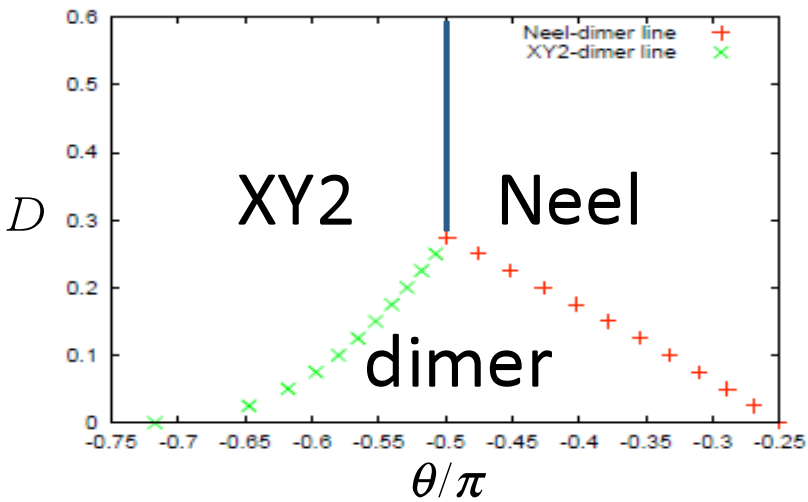

Fig. 1. Phase diagram of $S=1$ BLBQ chains (1) in the region of $-3\pi/4 \le \theta \le -\pi/4$ and $0 \le D \le 0.6$.

[1] A. Kolezhuk, Phys. Rev. B **78**, 144428 (2008).
[2] K. Nomura and A. Kitazawa, J. Phys. A: Math. Gen. **31** 7341 (1998).
[3] H. J. Schulz, Phys. Rev. B **34** 6372 (1986).

P39

Field-Induced Magnetic Orderings of S=1/2 Bond-Alternating Antiferromagnetic Chain F_5PNN

T.Harada ,[1] T.Matsushita ,[1] N.Wada ,[1] S.Nishihara ,[2] and Y.Hosokoshi[2]

[1]*Department of Physics , Nagoya University, Furo-cho, Chikusa-ku, Nadoya 464-8602, Japan*
[2]*Department of Physical Science, Osaka Prefecture University, Osaka 599-8511, Japan*

F_5PNN (pentafulorophenyl nitronyl nitroxide) consists of bond-alternating antiferromagnetic chains of S=1/2, of which ground state is the non-magnetic state of singlet dimers. In zero field, an energy gap (spin gap) exists between the ground state (spin singlet state) and the excited states (spin triplet states). As magnetic field increases, the spin gap becomes smaller. Then the spin gap vanishes between H_{c1} (~3T) and H_{c2} (~6.5T), where the field-induced magnetic ordering is caused by inter-dimer interaction. Since the long-range order does not exist because of large fluctuation, the ordering in 1D chain of dimers is short-ranged. At much lower temperatures, 3DLRO occurs by small inter-chain interaction. F_5PNN has been so far studied by measurements of heat capacity[1], dielectric constant[2] and so on. In the heat capacities, sharp peaks due to 3DLRO are observed at T~0.2K between 3 and 6.5T. Broad peaks suggesting 1DSRO are partly observed in 0.3K<T<0.7K. The 3DLRO is also observed as peaks in the dielectric constant.

In this work, we have measured the AC magnetic susceptibility of F_5PNN. The magnetic susceptibilities in various magnetic fields are shown in Fig.1. In H<3T, where the spin gap remains, the magnetic susceptibility exponentially decreases toward $T\rightarrow 0$. On the other hand, between 3 and 6T in the gapless region, a peak of the magnetic susceptibility is observed at each magnetic field. In Fig.2, the peak temperatures are plotted as a function of magnetic field. The ordering temperatures observed in heat capacity (3DLRO [▲], 1DSRO [△]) and dielectric constant [○] are plotted together. Since peaks of the AC susceptibilities are observed at higher temperatures than the 3DLRO transition temperatures, they clearly indicate preceding 1DSRO. Thus, development of 1DSRO in F_5PNN can be observed by peaks in magnetic susceptibilities. Field dependence of the observed susceptibility also reflects one-dimensionality of the system. As seen in Fig.1, in the vicinity of H_{c1} or H_{c2}, the magnetic susceptibility shows divergent behavior, which is characteristic of 1D spin gap systems and agrees with 1D XY model. Recently these orderings are of interest about correspondence between 1DSRO and Tomonaga-Luttinger liquid, and that between 3DLRO and Bose-Einstein condensation of magnons.

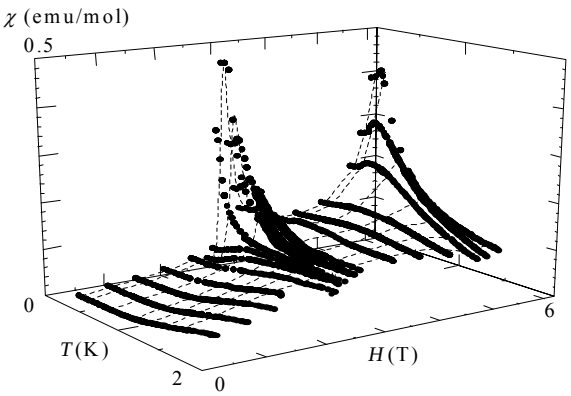

Fig.1 Temperature dependences of the magnetic susceptibility at various magnetic fields.

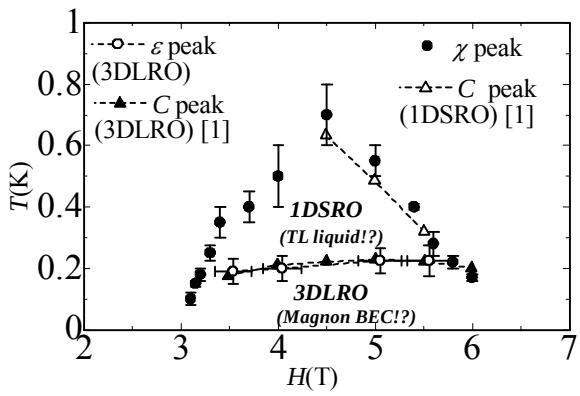

Fig.2 Magnetic field versus temperature phase diagram.

[1] Y.Yoshida et al., Phys. Rev. Lett. **94,** 037203 (2005)
[2] T.Matsushita et al., AIP Conf. Proc. **850**, 1029 (2006)

P40

How to detect magnetic multipolar liquid phase in spin-1/2 frustrated ferromagnetic chains under magnetic field

Masahiro Sato,[1] Toshiya Hikihara,[2] and Tsutomu Momoi,[1] and Akira Furusaki[1]

[1]*Condensed Matter Theory Laboratory, RIKEN, Wako, Saitama 351-0198, Japan*
[2]*Department of Physics, Hokkaido University, Sapporo 060-0810, Japan*

Over the last couple of years, magnetic multipolar orders have been predicted to emerge in some realistic magnetic models [1]. Many experimentalists have continuously searched such kinds of new orders, especially, in frustrated magnetic compounds. Quite recently, it has been shown that magnetic multipolar correlators exhibit quasi long range order in the wide region of the field-induced Tomonaga-Luttinger (TL) liquid in the frustrated spin-1/2 chains with ferromagnetic nearest-neighbor coupling J_1 and antiferromagnetic second-nearest-neighbor coupling J_2 [2]. This J_1-J_2 model could describe magnetic properties of several quasi one-dimensional edge-sharing cuprates such as $LiCuVO_4$ and $LiCu_2O_2$ [3]. In fact, the low-field ordered phases of $LiCuVO_4$ [4] can be well explained by using the phase diagram of the J_1-J_2 spin chain [2].

Despite of the active research of multipolar orders, their evidence or signature has never been reported yet. A main reason would be the fact that any experimental way of probing them has not been established well. Actually, it is generally difficult to obtain any direct evidence for multipolar orders because for this purpose it is necessary to see proper four or more spin correlations and usual magnetic experiments can observe only two-point ones. Instead of the direct measurement of multi spin correlations, we here propose an effective experimental way of characterizing the multipolar liquid phases in the J_1-J_2 spin chains. Namely, we have found some features in the NMR spectra of the multipolar phases: The NMR relaxation rate $1/T_1$ in the high-field multipolar TL liquids decreases with lowering temperature [5] and $1/T_1$ in the nematic liquid monotonically decreases as a function of applied field [6]. These behaviors are quite different from those of the standard TL liquid phase in usual one-dimensional magnets, and it would be used as a clear signature of the multipolar liquid phases.

In this conference, we will explain in detail these features of the multipolar TL liquids in the frustrated spin-1/2 chains.

References

[1] See, for example, N. Shannon et al., Phys. Rev. Lett. 96, 027213 (2006); T. Momoi et al., Phys. Rev. Lett. 97, 257204 (2006).
[2] T. Hikihara, et al., Phys. Rev. B 78, 144404 (2008); J. Sudan, et al., Phys. Rev. 80, 140402(R) (2009).
[3] See, for example, M. Hase et al., Phys. Rev. B 70, 104426 (2004).
[4] F. Schrettle et al., Phys. Rev. B 77, 144101 (2008).
[5] M. Sato et al., Phys. Rev. B 79, 060406(R) (2009).
[6] M. Sato et al., in preparation.

P41

Anomalous Behavior of the Magnetization Plateau Width of an S=1/2 Isosceles Triangle Spin Nanotube

K. Okamoto,[1] T. Sakai,[2,3] M. Sato,[4] K. Okunishi,[5] and C. Itoi[6]

[1]*Deparment of Physics, Tokyo Institute of Technology, Oh-okayama, Meguro-ku, Tokyo 152-8551, Japan*
[2]*Japan Atomic Energy Agency, SPring-8, Sayo, Hyogo 679-5148, Japan*
[3]*Department of Material Science, University of Hyogo, Kamigori, Hyogo 678-1297, Japan*
[4]*Condensed Matter Theory Laboratory, RIKEN, Wako, Saitama 351-0198, Japan*
[5]*Department of Physics, Niigata University, Niigata 950-2181, Japan*
[6]*Department of Physics, Nihon University, Kanda-Surugadai, Chiyoda-ku, Tokyo 101-8308, Japan*

The spin nanotubes have various interesting magnetic properties due to their unique structures and frustrations. Let us consider the S=1/2 isosceles triangle spin nanotube sketched in Fig.1. All the coupling are supposed to be antiferromagnetic. Hereafter we set J_r =1 and $\alpha = J_r'/ J_r$. We have recently obtained the zero-field phase diagram of this model on the J_1–α plane [1].

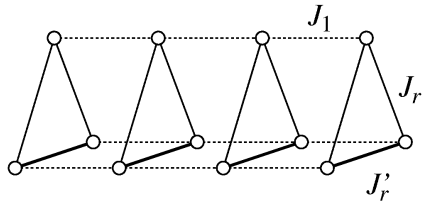

FIG.1

In this report we discuss the magnetization plateau at 1/3 of the saturation magnetization (1/3 plateau). We can expect the existence of the 1/3 plateau when $J_1 << 1$, because the ground state of the unit isosceles triangle has S^z =1/2 which is 1/3 of the saturation value. The DMRG result for the behavior of the magnetization plateau width W normalized by the saturation field H_s as a function of α for the J_1=0.1 case is shown by the solid line in Fig.2. We can see the anomalous increase of W around α=1. Since the ground state of the unit isosceles triangle changes at α=1, the change of the plateau formation mechanism is expected around α=1. In usual cases, however, near the mechanism changing point, the width of the magnetization plateau decreases, of which typical behavior is shown by the dashed line in Fig.1. Thus we have found a new, anomalous and exotic behavior of W, which is completely opposite to the usual cases. More detailed DMRG calculation revealed that the translational symmetry along the leg direction and the reflection symmetry is spontaneously broken in the plateau-width-increasing region. That is, the expectation values $\langle S^z \rangle$ of the spins change as 0.46, -0.04, 0.46, -0.04, …, along one base leg, and –0.04, 0.46, -0.04, 0.46, …, along the other base leg.

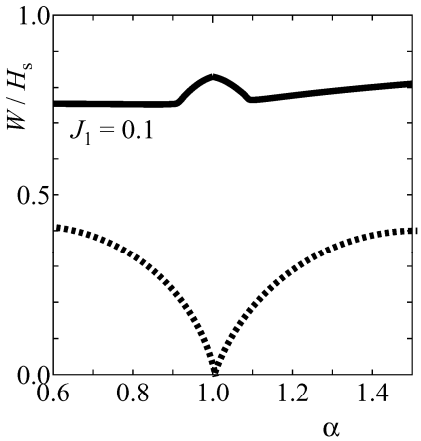

FIG.2

We have derived the effective Hamiltonian which is valid in the $J_1 << 1$ case. By use of this effective Hamiltonian we have succeeded to explain the mechanism for the anomalous behavior of W, and also reproduce the change of $\langle S^z \rangle$ quantitatively, 0.46 – 0.12, 0.46, -0.12,… Further we have found other models which show anomalous increases of the spin gaps (which is nothing but the magnetization plateaux at zero magnetization) similar to Fig.2. near the changing point of the spin gap formation mechanisms.

[1] T. Sakai *et al.*, Phys. Rev. B **78**, 184415 (2008).

P42

Analysis of Commensurate and Incommensurate State on Triangular Lattice Spin System with Transfer Matrix Method

K.Kobayashi and K.Nomura

Departmentt of Physics, Kyushu University, 6-10-1 Hakozaki, Higashi-ku, Hukuoka-shi, Hukuoka 812-8581, Japan

Generally, a correlation function of spin lattice system decays exponentially in disordered phase. But sometimes correlation function is displayed as a product of exponential and periodic function, such as

$<S_0 S_r> \sim \exp(-cr)\cos(qr)$

(c:constant,q:wavenumber,r:distance). So, this system becomes commensurate state (q=2\pi* rational number) or incommensurate state(other cases).

We study commensurate and incommensurate state[1][2] on triangular lattice[3] with transfer matrix method. Hamiltonian H is

$H = (J_1 S_{i,j} S_{i,j+1} + J_2 S_{i,j} S_{i+1,j} + J_3 S_{i,j} S_{i-1,j+1})$,

where J_1, J_2, J_3 are coupling constants, and spin $S_{i,j}$ is satisfied for a periodic boundary condition.

In this case transfer matrix T is

$T_{a,b} = (\exp(- \backslash beta\ H))_{a,b}$

(\beta = Boltzmann constant) . When T is a symmetric matrix, its all eigenvalues are real number, so the system becomes ferromagnetic or antiferromagnetic along its transfer direction. On the other hand, when it is an asymmetric matrix, its eigenvalues can contain complex pairs other than real values, so the system can become both commensurate and incommensurate state.

For $J_1 = J_2 = J_3$ case, there is an exact result by [3], and correlations are commensurate(q=2\pi / 3). For $J_1 = J_2$ and different J_3 case, it is observed that correlations are incommensurate in the lattice direction[1][2].

In this study, we discovered a special direction along which the transfer matrix is symmetric on the triangular spin lattice system. Our proof can be applied to XY model[4] on the triangular lattice and so on.

References

[1]J.Stephenson,J.Math.Phys.11,413(1970)
[2]J.Stephenson,J.Math.Phys.11,420(1970)
[3]G.H.Wannier,Phys.Rev.79,357(1950)
[4]S.Miyashita and H.Shiba,J.Phys.Soc.Jpn.53,1145(1984)

P43

Chiral and BKT transitions in triangular-lattice Heisenberg models: Critical behavior near the *O*(3) isotropic case

T. Misawa and Y. Motome

Department of Applied Physics, The University of Tokyo, 7-3-1 Hongo, Bunkyo-ku, Tokyo 113-8656, Japan

Antiferromagnetic Heisenberg model on the triangular lattice is one of the most fundamental models for geometrically frustrated systems. In its quantum version, feasibility of a spin-liquid phase is intensively explored from both experimental and theoretical points of view. Even in the classical spin systems, there still remain fundamental problems unresolved. For example, it is not clear yet how the anisotropy in the spin rotational symmetry affects the finite-temperature properties of the system, in particular, how the chiral and Berezinskii-Kosterlitz-Thouless (BKT) transition temperatures behave in the vicinity of the *O*(3) isotropic point. This is an important problem for interpreting experimental results because the spin anisotropy inevitably exists in real triangular antiferromagnets. In this study, we shed new light on this problem by using the nonequilibrium relaxation (NER) method [1] focusing on singularities of both the spin and vector chirality relaxation time.

In Fig. 1, we show the phase diagram for the Heisenberg model with anisotropic exchange interactions on the triangular lattice determined by the NER method. Approaching the isotropic Heisenberg point (λ=1) from both the *XY* and Ising anisotropic cases, we find that the chiral and all the BKT transitions are clearly discernable down to very small anisotropy of 0.1%. The results reveal that the phase diagram shows a characteristic "V shape", which suggests that the anisotropy is a relevant perturbation. In the isotropic Heisenberg case, we find that the system exhibits singular behaviors, such as a BKT-like criticality in a divergently-wide temperature range and an apparent quasi long-range ordering of the vector chirality (see Fig.2). We discuss the relation between our findings and the Z_2 vortex transition predicted for the isotropic point [2,3]. We also discuss the relevance of our results to peculiar behavior of the relaxation time observed experimentally in triangular antiferromagnets such as $NiGa_2S_4$ [4].

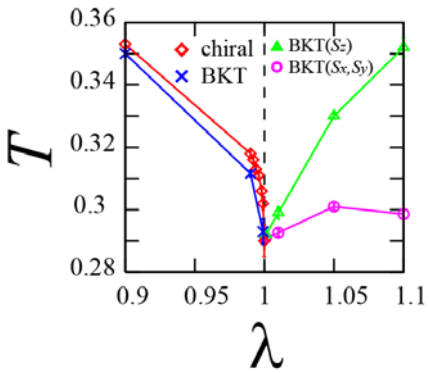

FIG.1: Phase diagram for the anisotropic Heisenberg model as a function of the exchange anisotropy λ determined by the NER method. For the *XY* anisotropy (λ<1), the chiral and BKT transition temperatures are shown by diamonds and crosses, respectively. For the Ising anisotropy (λ >1), two BKT transition temperatures as to S^z and S^x, S^y components are plotted by triangles and circles, respectively. The lines are guides for the eye.

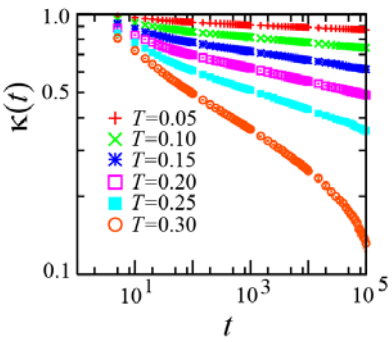

FIG.2: Relaxation of the vector chirality $\kappa(t)$ at the isotropic Heisenberg point (λ=1). The vector chirality $\kappa(t)$ exhibits a power-law decay down to T=0.05 in the range of Monte Carlo step t that we reached. This behavior apparently shows that a BKT-like transition occurs in the vector chiral degree of freedom at a finite temperature.

References

[1] Y. Ozeki and N. Ito, J. Phys. A: Math. Theor. **40** (2007) R149-R203.
[2] S. Miyashita and H. Kawamura, J. Phys. Soc. Jpn. **54** (1985) 3385.
[3] H. Kawamura, A. Yamamoto, and T. Okubo: J. Phys. Soc. Jpn **79** (2009) 023701.
[4] S. Nakatsuji *et al.*: Science **309** (2005) 1697.

P44

Quasiparticles in spatially anisotropic triangular antiferromagnets

Masanori Kohno

International Center for Materials Nanoarchitectonics, National Institute for Materials Science, 1-1 Namiki, Tsukuba 305-0044, Japan

The spectral properties of the spin-1/2 antiferromagnetic Heisenberg model on an anisotropic triangular lattice are investigated by using a weak-interchain-coupling approach combined with exact Bethe-ansatz solutions [1,2]. We found that the spectral features can be classified according to the sign of the Fourier transform of the interchain coupling $J'(\boldsymbol{k})$. In the momentum regime with $J'(\boldsymbol{k})=0$, the spectral properties of one-dimensional (1D) chains strongly persist even though the interchain coupling J' is not so small. Thus, the spectral features of the two-dimensional (2D) antiferromagnet in this momentum regime are characterized by quasiparticles (QPs) of 1D chains. For $J'(\boldsymbol{k})<0$, bound states of 1D QPs emerge below the continuum of 1D chains. For $J'(\boldsymbol{k})>0$, antibound states of 1D QPs above the continuum or a broad continuum with suppressed spectral weights appear. These bound or antibound states behave as QPs which dominate the spectra of spatially anisotropic frustrated antiferromagnets.

In the absence of a magnetic field, the dominant excitation spectra are explained in terms of the QP called triplon, which can be regarded as the bound states of spinons [1]. The triplon shows a gapless excitation from the spin-singlet ground state. Thus, it carries spin quantum number $S=1$ in contrast with conventional magnons created from magnetically ordered ground states with broken SU(2) symmetry.

In a magnetic field, the spectral properties are characterized by the QPs which can be regarded as bound or antibound states of 1D QPs in a magnetic field, i.e., psinon (ψ), anti-psinon (ψ^*), and the QP representing a 2-string (σ) in the Bethe ansatz [3]. For the longitudinal dynamical structure factor $S^{zz}(\boldsymbol{k},\omega)$, the bound states of ψ and ψ^* dominate the excitation spectra, which cause the instability toward the spin-density-wave (SDW)-type incommensurate ordering at the gapless point $\boldsymbol{k}=(\pi\pm2\pi m,k_y)$ for $J'(\boldsymbol{k})<0$ (m is the magnetization per site). This behavior is contrasted with that of the spin-wave theory, where ordering is caused by in-plane fluctuations (XY-type), and the ordering momentum is close to $k_x=\pi$, which does not shift so significantly as a function of m. For $S^{+-}(\boldsymbol{k},\omega)$, the bound states of 2 ψ's characterize the spectral features. For $S^{+-}(\boldsymbol{k},\omega)$, there are three kinds of dominant QPs. One is the QP originating from the $1\psi^*$ mode of 1D chains, which is responsible for the resonant mode at $\boldsymbol{k}=0$ and reduces to the conventional 2D magnon above the saturation field. The in-plane fluctuations around $k_x=\pi$ are accounted for by the bound states of 2 ψ^*'s. Also, the bound states of σ and ψ originating from 2-string solutions of the Bethe ansatz play an important role for the high-energy properties, whose behaviors cannot be explained by the linear spin-wave theory or low-energy effective theory [2].

Unusual spectral features observed in the spatially anisotropic triangular antiferromagnet Cs_2CuCl_4 are quantitatively explained in terms of the above QPs in a unified manner as shown in Fig. 1 [1,2].

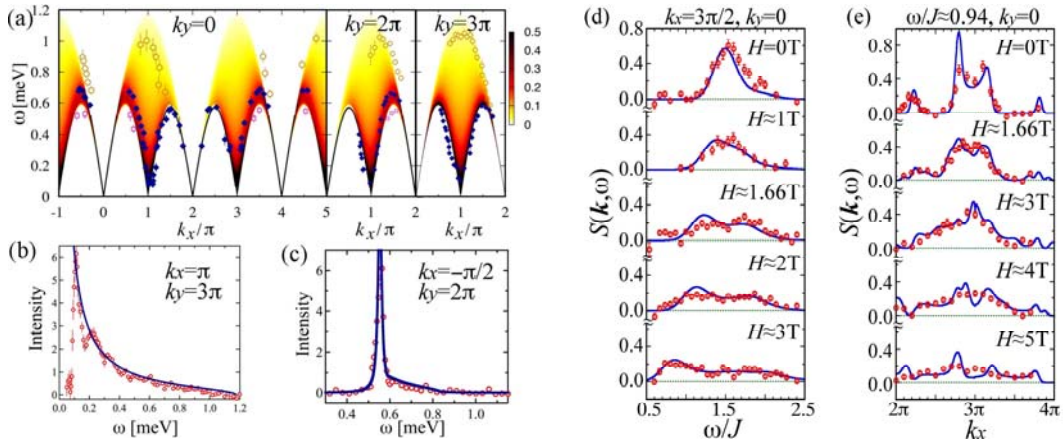

Fig. 1. Comparisons of dynamical structure factor $S(\boldsymbol{k},\omega)$ with experimental results on Cs_2CuCl_4.

[1] M. Kohno, O. A. Starykh, and L. Balents, Nature Phys. **3**, 790 (2007).
[2] M. Kohno, Phys. Rev. Lett. **103**, 197203 (2009).
[3] M. Kohno, Phys. Rev. Lett. **102**, 037203 (2009).

P45

Structural disorder effects of 2D triangular antiferromagnets isostructural to $NiGa_2S_4$

T. Higo,[1] M. Mernerd,[2] J. Y. Chan,[2] H. Sawa,[3] E. Nishibori,[3] and S. Nakatsuji[1]

[1]*Institute for Solid State Physics, Univ. of Tokyo,*
[2]*Department of Chemistry, Louisiana State University*
[3]*Department of Applied Physics, Nagoya Univ.*

Geometrically frustrated magnets have attracted great interest for the possible emergence of novel spin-disordered states such as spin liquid and glass. In two dimensions (2D), the triangular lattice is one of the simplest forms of geometrically frustrated lattice with a single magnetic ion in a unit cell, and has been extensively studied to search for spin-disordered states [1]. $NiGa_2S_4$ is the first example of low spin antiferromagnets on an exact triangular lattice [2, 3]. Despite a strong antiferromagnetic coupling with the Weiss temperature $|\theta_W| \sim 80$ K, this magnet does not form a conventional three-dimensional antiferromagnetic order at least down to $T = 0.08$ K. Instead, microscopic resonance experiments [4, 5] have clarified unusual bulk critical slowing down across $T^* = 8.5$ K that has a highly extended critical regime down to a characteristic freezing temperature $T_0 \sim 3$ K. In this temperature regime, spins retain slow dynamics with micro-second order time scale [6]. Below T_0, the results of nuclear relaxation rates and the specific heat suggest an existence of antiferromagnetic spin-wave-like excitations in two dimensions without a long-range order.

In order to further clarify the ground state of $NiGa_2S_4$, we have searched for isostructural compounds to $NiGa_2S_4$, with structural disorder, chemical pressure and different spin sizes. Then, we have succeeded in growing single crystals of $Ni_{0.7}Al_2S_{3.7}$ ($S = 1$), $Co_{0.5}Al_{0.5}(Co_{0.25}Al_{0.75})_2S_4$ ($S = 3/2$), and $Fe_{0.5}Al_{0.5}(Fe_{0.25}Al_{0.75})_2S_4$ ($S = 2$), $Mn_{0.5}Al_{0.5}(Mn_{0.25}Al_{0.75})_2S_4$ ($S = 5/2$) for the first time. $Ni_{0.7}Al_2S_{3.7}$ has a deficiency at the Ni-site about 30 %, ”magnetic site vacancy type”. In $M_{0.5}Al_{0.5}(M_{0.25}Al_{0.75})_2S_4$ (M = Co, Fe, Mn), there is a mixing between M and Al ions in a quasi-2D cation sublattice, ”site disorder type”. These two types compounds show different physical properties. Below the freezing temperature of 4 K, the magnetic specific heat C_M of the ”magnetic site vacancy type” $Ni_{0.7}Al_2S_{3.7}$ forms a broad peak and exhibits a T^2-dependence below 1 K. This is in sharp contrast with a T-dependence C_M due to the local nature of spin fluctuations in a canonical spin-glass, as actually observed for the ”site disorder type” systems $M_{0.5}Al_{0.5}(M_{0.25}Al_{0.75})_2S_4$ (M = Co, Mn). This data suggests a linearly dispersive mode in two dimensions as has been seen in $NiGa_2S_4$.The structural disorder, chemical pressure, and spin size effects will be discussed in the presentation.

[1] M. F. Collins, and O. A. Petrenko, *Can. J. Phys*. **75**, 605 (1997).
[2] S. Nakatsuji, Y. Nambu, H. Tonomura, O. Sakai, S. Jonas, C. Broholm, H. Tsunetsugu, Y. Qiu, and Y. Maeno, *Science* **309**, 1697 (2005).
[3] S. Nakatsuji, Y. Nambu, and S. Onoda, *J. Phys. Soc. Jpn*. **79**, 011003 (2010).
[4] H. Takeya, K. Ishida, K. Kitagawa, Y. Ihara, K. Onuma, Y. Maeno, Y. Nambu, S. Nakatsuji, D. E. MacLaughlin, A. Koda, and R. Kadono, *Phys. Rev B* **77**, 054429 (2008).
[5] D. E. MacLaughlin, Y. Nambu, S. Nakatsuji, R. H. Heffner, L. Shu, O. O. Bernal, and K. Ishida, *Phys. Rev B* **78**, 220403(R) (2008).
[6] Y. Nambu and S. Nakatsuji, in preparation.

P46

Correlation between the Quantum Behavior and Lattice Anisotropy in a Frustrated Triangular Spin System, the $Pd(dmit)_2$ Salts

M. Tamura,[1,2] T. Yamamoto,[1,3] R. Kato[1] and K. Yakushi[4]

[1]*Condensed Molecular Materials Lab., RIKEN, Wako 351-0198, Japan*
[2]*Dept. of Phys., Faculty of Science and Technology, Tokyo Univ. of Science, Noda 278-8510, Japan*
[3]*Dept. of Chem., Faculty of Science, Osaka University, Toyonaka 560-0043, Japan*
[4]*Institute for Molecular Science, Okazaki 444-8585, Japan*

Variety of unconventional quantum states have been found in a series of molecule-based Mott insulators, the $Pd(dmit)_2$ salts [1]. In the salts, the spin-1/2 units $[Pd(dmit)_2]_2^-$ are arranged in a two-dimensional triangular fashion. The low-temperature physical behavior varies with the anisotropy of the triangular lattice, which is controllable by the counter cation. Therefore, this series affords frustration-controlled quantum spin systems. In a most frustrated case, the $EtMe_3Sb$ salt, neither magnetic long-range order nor spin gap is detected down to 14 mK by NMR; a so-called spin-liquid state is thus concluded for this salt [2]. By contrast, Neel-like antiferromagnetic order is stabilized in considerably anisotropic cases (the Me_4P and Me_4As salts). The first example of two-dimensional valence-bond order, which is accompanied by the lattice alternation as well as a spin-Peierls phase in one-dimension, has been found in the monoclinic $EtMe_3P$ salt below 25 K [3]. This peculiar phase appears due to suppression of the antiferromagnetic order by frustration. Pressure-induced superconductivity has been observed in contact with this valence-bond order phase. The Et_2Me_2Sb salt undergoes a valence transition, assisted by the HOMO-LUMO two-level electronic states of the dimeric unit, $[Pd(dmit)_2]_2^-$ [4].

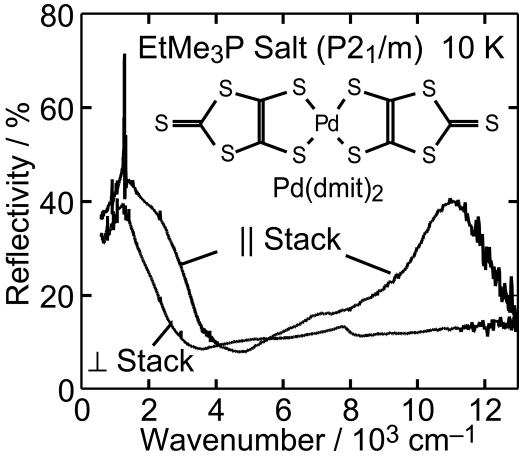

FIG. 1: Infrared reflectivity spectra of the monoclinic EtMe3P salt in the valence-bond order state.

In order to clarify the role of the frustration, experimental estimation of the anisotropy is specifically desired. For this purpose, we have adopted polarized infrared reflectance spectroscopy on the single crystal samples, from which the anisotropy of the infrared conductivity can be obtained. An example of the results is shown in Fig. 1. The prominent peak near 11,000 cm^{-1} is due to the local intradimer excitation, evidencing the HOMO-LUMO two-level state of the dimeric unit. The low-energy portion of the spectra below 4,000 cm^{-1} indicates the lattice anisotropy and the charge gap. From the result, it follows that the two-dimensional lattice anisotropy and the charge gap of this salt are considerably small. This is consistent with the suppression of the antiferromagnetic order by sufficiently strong frustration in this salt. More details of the analysis of the spectral data will be presented and discussed in the symposium.

[1] M. Tamura and R. Kato, Sci. Technol. Adv. Mater. **10**, 024304 (2009).
[2] T. Itou *et al.*, Phys. Rev. B 77 (2008) 104413.
[3] M. Tamura *et al*, J. Phys. Soc. Jpn. 75 (2006) 093701.
[4] M. Tamura *et al.*, Chem. Phys. Lett., 411 (2005) 133.

P47

Anomalous Magnetization Process of the S=1/2 Kagome Lattice Antiferromagnet

T. Sakai,[1,2,3] and H. Nakano[2]

[1]*Japan Atomic Energy Agency, SPring-8, Kouto 1-1-1, Sayo Hyogo 679-5148, Japan.*
[2]*Department of Material Science, Univ. of Hyogo, Kouto 3-2-1, Kamigori Hyogo 678-1297, Japan.*
[3]*JST TRIP, Japan*

The S=1/2 Kagome lattice aintiferromagnet is one of interesting highly frustrated spin systems. It is believed that no long-range order is realized even at zero temperature, due to strong frustration and large quantum fluctuation. Some recent numerical exact diagonalization studies indicated a plateau-like behavior of the magnetization curve at the 1/3 height of the saturation moment[1,2]. However, the magnetization curve of this system exhibits a shape which is quite different from typical magnetization plateaux. In order to clarify the anomalous behavior around the 1/3 height of the saturation magnetization, we calculate the derivative of magnetization with respect to the external field by the numerical exact diagonalization, as well as the magnetization curve[3]. It reveals a quite different behavior between the lower and higher field regions of some critical magnetic field corresponding to the 1/3 of the saturation. About the critical field, the derivative of the magnetization exhibits a diverging behavior at the lower-field side, while it is very small (maybe zero) at the higher-field side. For typical magnetization plateaux, the derivative diverges in one-dimensional systems, while it is finite in two-dimensional ones. The behavior does not change in each case of the dimensions irrespective of the difference of the lower- or higher-field sides. In the present case, the behavior of the derivative at the lower-field side seems like that of a one-dimensional system, while the derivative at the higher-field side behaves as a two-dimensional one. Since this is a quite unique field-induced phenomenon, we call it a 'magnetization ramp' (Fig. 1), to distinguish it from the typical magnetization plateaux. The present result suggests that a kind of one-dimensional spin liquid is possibly realized at the lower-field side of the critical field. We will also discuss about the relation to the magnetization step, which was observed at the magnetization measurement of the real S=1/2 Kagome lattice antiferromagnets; volborthite and vesignieite[4].

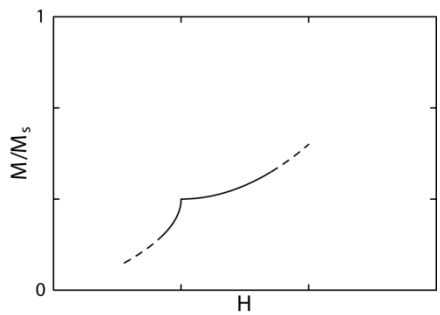

Fig. 1 Magnetization ramp.

[1] K. Hida: J. Phys. Soc. Jpn. **70**, 3673 (2001).
[2] A. Honecker et. al.: J. Phys.: Condens. Matter, **16**, S749 (2004).
[3] H. Nakano and T. Sakai, in preparation.
[4] Y. Okamoto et al.: J. Phys. Soc. Jpn. **78**, 033701 (2009).

P48

Magnetic Properties of a Spatially Distorted Heisenberg Kagome Antiferromagnet

R. Kaneko, T. Misawa, and M. Imada

Department of Applied Physics, The University of Tokyo, 7-3-1 Hongo, Bunkyo-ku, Tokyo 113-8656, Japan

In frustrated system, perturbations such as temperatures, quantum fluctuations, and magnetic fields lift the macroscopic degeneracy and sometimes induce nontrivial phase transitions. One of the most intensively studied frustrated systems is a Heisenberg antiferromagnet on a kagome lattice. Recent studies on the ideal Heisenberg kagome lattice compound, volborthite, show unconventional three steps in the magnetization curve [1]. These steps are different from the conventional magnetization process for pure kagome antiferromagnets [2,3] and the origin of these steps is still not clear [4].

To understand the magnetization process on volborthite, we focus on the spatial anisotropy in volborthite as shown in Fig.1. For volborthite, it is believed that $J_2 > J_1$ [5]. In the classical antiferromagnetic Heisenberg model on the distorted kagome lattice, we clarify how the spatial anisotropy affects the magnetization process.

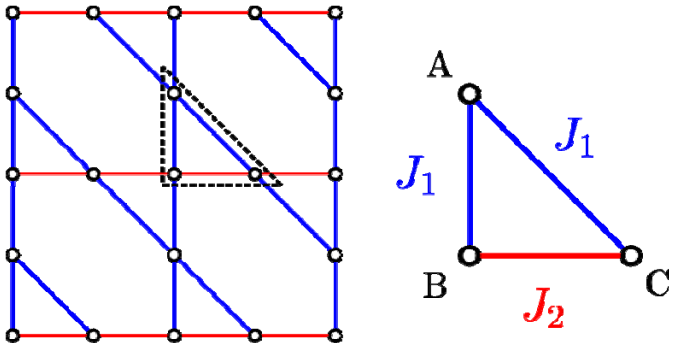

Fig.1: A distorted kagome lattice. Lattice points labeled by A, B, and C represent relative positions in each unit cell (dashed-line triangle). J_1 and J_2 denote exchange constants.

By using a Monte Carlo method, we find a distortion-induced magnetization step at low temperatures and magnetic fields. Also, we have observed a sudden change of spin structure factor around the transition. This first-order transition induced by spatial anisotropy may correspond to the experimentally observed unconventional steps.

[1] H. Yoshida *et al.*, J. Phys. Soc. Jpn. **78**, 043704 (2009).
[2] K. Hida, J. Phys. Soc. Jpn. **70**, 3673-3677 (2001).
[3] M. E. Zhitomirsky, Phys. Rev. Lett. **88**, 057204 (2002).
[4] F. Wang, A. Vishwanath, and Y. B. Kim, Phys. Rev. B **76**, 094421 (2007).
[5] P. Sindzingre, arXiv:0707.4264 (2007).

P49

Quantized Vortex State and Torsional Oscillator Study on hcp ^{4}He under AC and DC Rotation

Nobutaka Shimizu,[1] Sergey Nemirovskii,[2] Akira Kitamura[3], Yoshinori Yasuta[1], and Minoru Kubota[1]

[1]*Institute for solid State Physics, University of Tokyo, Kashiwanoha 5-1-5, Kashiwa, 277-8581, Japan*
[2]*Institute of Thermophysics, Lavrentyev ave. 1, 630090 Novosibirsk, Russian*
[3] *Graduate School of Science and Technology, Niigata Univ. Niigata 950-2181, Japan*

In the late 1960's, Proposals for the supersolid state in quantum solids as solid 4He, where the coexistence of the real space ordering of the lattice structure of the solid and the momentum space ordering of the superfluidity, were discussed based on the Bose Einstein Condensation (BEC) of the imperfections as vacancies, interstitials and other possible excitations in the quantum solids. Whereas new types of superfluidity have been discovered after the above original proposals in different systems. Namely, a real 2 dimensional (2D) superfluid transition has been established both in the theories and experiments for the He monolayer superfluid. A new type of superconductors, initiated by the discovery of the cuprate superconductors, is being discovered with a common feature of the vortex state, involving vortex fluid and vortex solid states, often discussed in connection to the 2D sub-system superfluidity, for example CuO_2 plane electron system for the cuprate high Tc superconductor(HTSC)s. A series of artificial 3D superfluids are being produced out of He monolayer systems. The high temperature transition temperature Tc of the above superconducting materials are being discussed in connection to the large fluctuations associated with some other phase transitions as the antiferromagnetic transition other than that of the low dimensionality of the sub-system as CuO_2 plane for the cuprate.

We review the recent experimental observations of hcp solid ^{4}He using highly sensitive and stable torsional oscillator(TO) techniques under still condition[1, 2, 3] and under DC rotation[4]. TO technique uses an AC oscillation with resonance frequency at around 10^3 Herz. A detailed study of the excitation velocity Vac dependence of the TO responses of hcp He samples at 32 bar and 49 bar pressure showed a unique onset temperature T_o at about 500 mK, below which significant Vac dependence appears, which suggests pre-existing fluctuations in the system and by the AC excitation the fluctuations are reduced. A detailed analysis in terms of tangled quantized vortices lead to the quantitative parameters describing the tangled vortex dynamics and we describe this state as a vortex fluid state[5]. This state is characterized by the non linear rotational susceptibility NLRS spontaneous fluctuations, which can be depressed by strong AC excitations according to log Vac dependence. This dependence was discussed by P.W. Anderson[6] and it describes the depressed fluctuations by the introduction of vortex lines by the strong excitation.

A clear transition was found by the appearance of the hysteretic behavior below a characteristic temperature T_c for the first time in a single sample where vortex fluid state was first observed below T_o and below this T_c a new phase appeared. This phase is characterized by characteristic AC velocities, V_h above which hysteresis appears and V_c. beyond which the hysteretic component is suppressed to zero. We could also evaluate the supersolid density in the absolute unit and from which the extrapolated value of the Josephson's length ξ to zero temperature. This length ξ would be the vortex core diameter. And the critical velocity V_c would be related to $V_c=h/(m_4\ \xi_0\ \pi)$. Our independent observation of V_c and ξ_0 gives us a consistent picture[3]. Further more TO response under DC rotation gave us evidences of quantized vortex lines penetration in the same sample below T_c, where we expect macroscopic coherence of the supersolid state[3].

[1] A. Penzev, Y. Yasuta and M. Kubota, Phys. Rev. Lett. **101**, 065301 (2008).
[2] M. Kubota, N. Shimizu, Y. Yasuta, P. Gumann, S. Nemirovskii, J Low Temp Phys, 158: 572–577 (2010).
[3] N. Shimizu, Y. Yasuta, and M. Kubota, arXiv:0903.1326v3 (2009).
[4] N. Shimizu, et al., Abstract of JPS AutumMeeting 2008, 21pYE-13 (2008).
[5] S. Nemirovskii, N. Shimizu, Y. Yasuta, and M. Kubota, arXiv: 0907.0330v3(2009).
[6]. P. W. Anderson, Nature Physics, Vol. 3, 160 (2007 hhhh)).); ; .

P50

Simultaneous Measurement of Torsional Oscillator and NMR of Extremely Diluted ^{3}He in Solid ^{4}He

R. Toda,[1,2] W. Onoe,[1] P. Gumann,[2] M. Kanemoto, [1] K.Kosaka, [1]
T. Kakuda,[1] Y. Tanaka,[1] and Y. Sasaki[1,2]

[1]*Department of Physics, Graduate School of Science, Kyoto University, Sakyo-ku, Kyoto 606-8502, Japan*
[2]*Research Center for Low Temperature and Materials Sciences, Kyoto University, Sakyo-ku, Kyoto 606-8501, Japan*

Superfluid-like behavior of solid ^{4}He was discovered as missing rotational inertia which is usually referred as non-classical rotational inertia (NCRI) by the torsional oscillator experiment [1]. Since then, a lot of theoretical and experimental studies have been done by many research groups. Among the many experimental results, the most peculiar observation is that the NCRI response and onset temperature are affected strongly by the tiny amount of ^{3}He impurities [2]. The NCRI response disappears when solid ^{4}He contains just a hundred ppm of ^{3}He impurities. This is unreasonably small amount of impurities to destroy the phenomenon if we consider the NCRI as non-magnetic macroscopic phenomenon in solid ^{4}He like superfluid ^{4}He.

In order to study the physics in behind of this peculiar phenomenon, we have developed an apparatus to measure the torsional oscillator response and NMR response for the same solid ^{4}He with dilute ^{3}He impurities. NMR measurement of ^{3}He provides the information on the state of ^{3}He in solid ^{4}He. It is well known that in the solid mixture system, phase separation occurs at low temperature [3]. Below the phase separation temperature T_{PS}, ^{3}He atoms form clusters in solid ^{4}He, and the size of clusters grow up slowly to a few μm in the case of a few % of ^{3}He sample [4]. In our torsional oscillator experiment, commercial grade ^{4}He (0.3 ppm of ^{3}He) at 3.6MPa shows the NCRI fraction of 0.06% at T=0. For the sample of ^{4}He with a few hundred ppm of ^{3}He at 3.6MPa, NCRI response is smashed away. These results are consistent with the observations by other groups. We did not observe any signature on the torsional oscillator frequency near T_{PS}. Thus the phase separation may not be related with NCRI response directly.

We have investigated the NMR properties of ^{3}He with this concentration as well as samples with 300ppm, 100ppm, and 10ppm of ^{3}He. Our results show that three different states of ^{3}He exist in solid ^{4}He below T_{PS}. One corresponds to the isolated ^{3}He atoms in solid ^{4}He. Since it has extremely long longitudinal relaxation time T_1 (over a day) at low temperature, we could not investigate the details of this state. Other two components grow up with time after cooling below T_{PS}. Thus both components of ^{3}He correspond to phase separated clusters in solid ^{4}He. The T_1 values of each component provide a distinction between each components (Fig.1). Both clusters disappear above T_{PS}. However, the (S) component, which is identified by shorter T_1, recovers much faster than the other (L) component, after the solid is cooled down below T_{PS} again. It suggests that the extra trapping potential works in the place where (S) exists, so that the ^{3}He atoms in (S) component stay in the same region even above T_{PS}. Such a trapping potential may come from the macroscopically disordered part of solid ^{4}He.

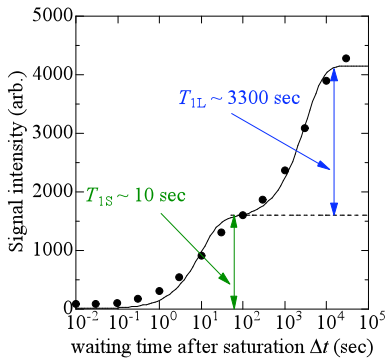

FIG.1: T_1 measurement at 8mK.

Strong ^{3}He impurity effect on NCRI exists below and above T_{PS}. But, it is unlikely that the isolated ^{3}He atoms which locate separately with mean distance of 20 ^{4}He atoms for the case of 100ppm concentration, play a significant role in destroying NCRI response. However, if the NCRI response comes from the disordered part of solid ^{4}He where some ^{3}He atoms are concentrated in, tiny amount of ^{3}He plays a significant role in destroying NCRI response.

[1] E. Kim and M. H. W. Chan, Nature **427**, 255 (2004)
[2] E. Kim, *et. al.*, Phys. Rev. Lett. **100**, 065301 (2008).
[3] D. O. Edwards and S. Balibar, Phys. Rev. B **39**, 4083 (1989)
[4] M. Poole and B. Cowan, J. Low Temp. Phys. **134**, 211 (2004).

*Present address: Department of Physics and Astronomy, Rutgers University, Piscataway, NJ 08854-8019, U.S.A

P51

Successive phase transitions at finite temperatures toward the supersolid state in a three-dimensional extended Bose-Hubbard model

K. Yamamoto,[1] S. Todo,[2,3] and S. Miyashita[1,3]

[1]*Department of Physics, School of Science, The University of Tokyo, 7-3-1 Hongo, Bunkyo-ku, Tokyo 113-0033, Japan,*
[2]*Department of Applied Physics, School of Engineering, The University of Tokyo, 7-3-1 Hongo, Bunkyo-ku, Tokyo 113-0033, Japan,*
[3]*CREST, JST, 4-1-8 Honcho Kawaguchi, Saitama, 332-0012, Japan.*

Since Kim and Chan performed the torsional oscillator experiment on solid Helium 4[1], the studies on the supersolid state have been activated. Supersolid state is characterized by the coexistence of diagonal-long-range order(DLRO) and off-diagonal-long-range order(ODLRO), which corresponds to the solid order and the superfluid order, respectively.

Theoretically, it was shown that the supersolid state can exist in the ground state in the extended Bose-Hubbard model. In this system, we have to set on-site repulsion low enough and set particle density slightly above the half filling, in order to realize the supersolid state. We study the finite temperature properties of the supersolid state, and the effect of on-site repulsion on the coexistence of two orders. We analyzed the extended Bose-Hubbard model on a cubic lattice.

$$H = -t \sum_{<ij>} (a_i^\dagger a_j + a_i a_j^\dagger) + V \sum_{<ij>} n_i n_j + \frac{U}{2} \sum_i n_i(n_i - 1) - \mu \sum_i n_i.$$

Here, t is the hopping parameter between nearest neighbor sites, and V and U represent the nearest-neighbor and on-site repulsion, respectively. μ is the chemical potential. Using a mean-field approximation, we calculate the temperature dependence of the solid and the superfluid order parameters [2]. As a result, we find that the solid fraction and the superfluid fraction compete against each other. The phase diagram in the coordinate of (t/U, T/U) is shown in the figure below. Here we find supersolid phase. The region of the supersolid phase becomes small when the on-site repulsion U is large. Thus, U, i.e. hardness of particles, suppresses the coexistence of the two orders.

[1] E. Kim and M. H. W. Chan, Nature. **427**, 225 (2004).
[2] K. Yamamoto and S. Miyashita, PRB. **79**, 094503 (2009).

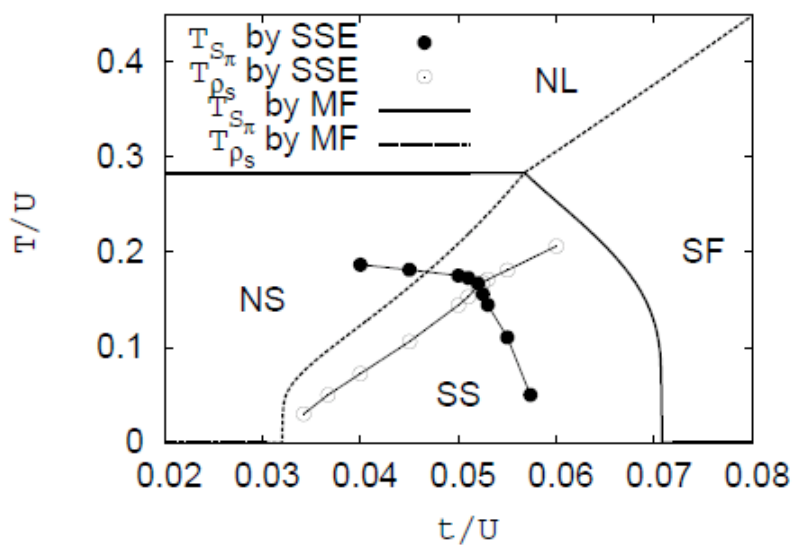

P52

Superflow of one-dimensional supersolid past an obstacle

M.Kunimi, [1] Y.Nagai, [2] and Y.Kato[1,2]

[1]*Department of Basic Science, University of Tokyo, Tokyo 153-8902, Japan*
[2]*Department of Physics, University of Tokyo, Tokyo 113-0033, Japan*

We study dissipationless flow and the critical current of a supersolid in the presence of a potential barrier. The model we consider is the one-dimensional Gross-Pitaevskii(GP) equation with a two-body interaction of finite range. In contrast to the conventional GP equation, this equation has the liquid phase with phonon-roton spectrum at lower density and the solid phase with the nonclassical rotational inertia at higher density.
Numerically solving this equation under the periodic boundary condition in the presence of a potential barrier $U(x) = U_0\theta(d/2 - |x|)$, $\theta(x)$ is the Heaviside's step function, we find that a steady state with dissipationless flow J exists in the liquid phase up to a nonzero critical current J_c. By deriving the formula of the phase shift $\Delta\phi$ between the condensates separated by the barrier, we deduce the Josephson relation $J - \Delta\phi$ in the solid phase for various strengths of potential barrier and two-body interaction.

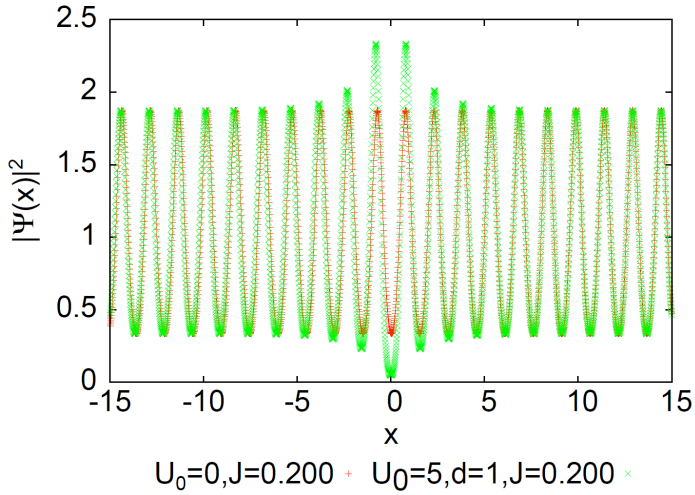

Fig.1. Spatial dependence of the density $|\Psi(x)|^2$ of the condensate wave function.

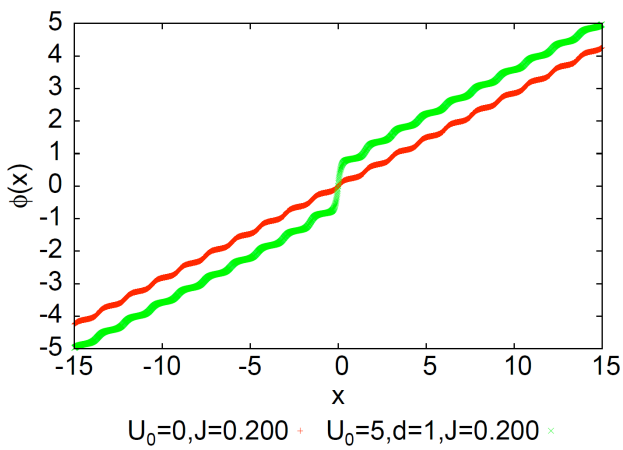

Fig.2. Spatial dependence of the phase $\phi(x)$ of the condensate wave function.

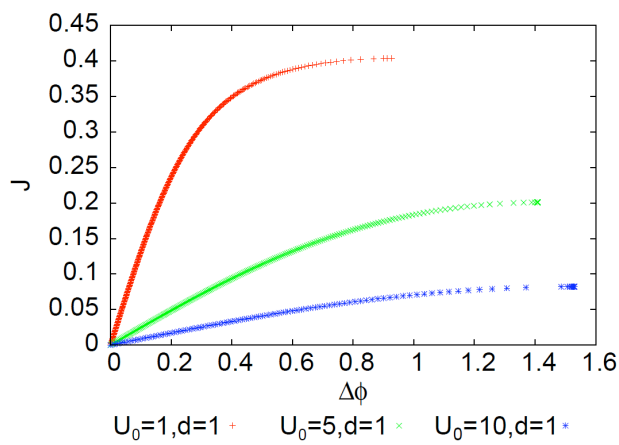

Fig.3. Josephson relation.

[1] Y. Pomeau, and S.Rica, Phys. Rev. Lett. **72**, 2426 (1994).
[2] C. Josserand, Y.Pomeau, and S.Rica, Phys. Rev. Lett. **98**, 195301 (2007).
[3] S. Sepulveda, C.Josserand, and S.Rica, Phys. Rev. B **77,** 054513 (2008).

Supersolid Behaviors in Thin Solid ^{4}He Films Adsorbed on Nanoporous Media

T. Kogure, R. Higashino, H. Yoshimura, Y. Shibayama, K. Shirahama

Dept. of Physics, Keio University, 3-14-1 Hiyoshi, Kohoku-ku, Yokohama 223-8522, Japan

Thin ^{4}He films adsorbed on solid surfaces are a unique model system of two-dimensional (2D) Bosons. The first and partly second atomic layers adjacent to the surface form a solid due to strong attraction from the substrate. The structure of the 2D solid strongly depends on the structure of the underlying substrate, and the areal ^{4}He density, which can be tuned in a wide range. These unique features may enhance the inter-atomic exchange, and hence lead to the intriguing realization of a true supersolid state. To search for the possible supersolid state, we have studied dynamics of 2D solid ^{4}He films on a nanoporous Gelsil glass (pore diameter: 2.5 nm) by a torsional oscillator.

Figure 1 shows a change in frequency from the empty cell background, $\Delta f(T)$, and a corresponding change in dissipation (ΔQ^{-1}) at a coverage n = 17 μmol/m^2. We clearly observed a supersolid-like behavior: The frequency exhibits a positive shift below about 0.6 K associated with a peak in dissipation. The temperature at which the overall phenomena occur decreases as the coverage increases. As a representative we plot the dissipation peak temperature T_p as a function of n. Surprisingly, T_p decreases linearly with n, and approaches 0 K at a "critical coverage" n_c = 21 μmol/m^2, above which the additional ^{4}He atoms form a liquid state exhibiting an ordinary superfluid transition with T_c linearly increasing with n.

This interesting T - n diagram in Fig. 2 strongly suggest an existence of a quantum critical phenomenon (QCP) around n_c and 0 K. Although the origin of the supersolid-like response below n_c is not clear, the QCP may be related to the formation of a gapped localized solid below n_c and an emergence of mobility edge at n_c, which were proposed from heat capacity studies by Reppy and coworkers [1]. The supersolid response also bears a striking resemblance to ultrasound results using a different substrate [2], in which the sound velocity increase was attributed to the slip of the solid film. We speculate that all of these observations are understood by the concept of QCP tuned by atom (or hole) density.

[1] P. A. Crowell *et al.*, PRL **75**, 1106 (1995). [2] Hieda *et al.*, PRL **85**, 5142 (2000).

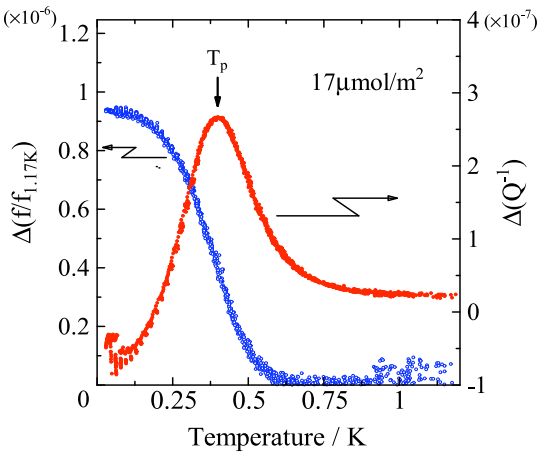

Fig.1: Temperature dependence of frequency and dissipation for coverage of 17 μmol/m^2.

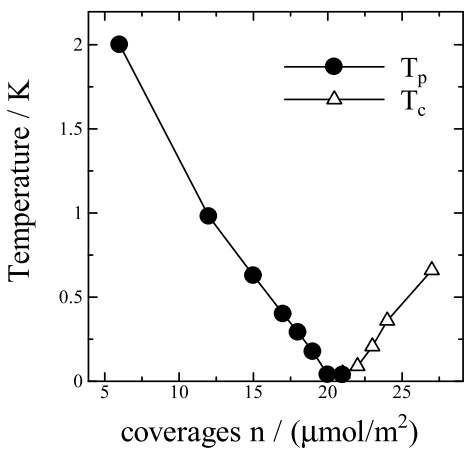

Fig.2: T_p and T_c obtained by the torsional oscillator studies.

P54

Torsional Oscillator Study for ^{4}He Growth on Graphite

A. Koga, Y. Shibayama, and K. Shirahama

Dept. of Physics, Keio University, 3-14-1 Hiyoshi, Kohoku-ku, Yokohama-shi, Kanagawa 223-8522, Japan

Layer by layer growth of solid ^{4}He on graphite is known to occur even below the bulk freezing pressure [1,2]. We aim to utilize this interesting property to study possible supersolidity in the low pressure solid ^{4}He as well as to control the effective pore size of liquid ^{4}He confined in carbon nanotubes.

Here, we study the growth of solid ^{4}He with the torsional oscillator method. We have observed oscillating structures in the amplitude in the range 0.9 K to 0.05 K, that are in line with previous studies indicating two-stage layering transitions below 0.95 K [1]. In addition, frequency shifts coinciding with the second stage of each layering transition suggest that the bulk of each solid layer forms during the second stage.

The search for supersolidity is underway.

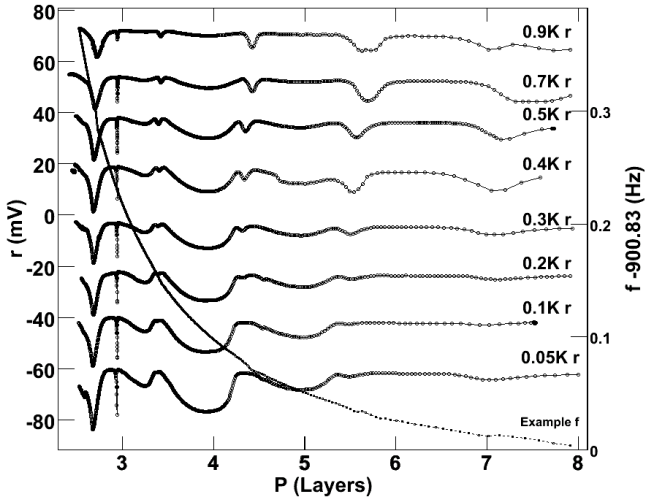

FIG.1: Amplitude (r) and frequency (f) vs. pressure. Example f is data taken at 0.9 K.

[1] M. J. McKenna, T. P. Brosius, and J. D. Maynard, Phys. Rev. Lett. **69**, 3346 (1992).
[2] V. Gridin, J. Adler, Y. Eckstein, and E. Polturak, Phys. Rev. Lett. **53**, 802 (1984).

P55

New dynamics of He-4 films on graphite
−Superfluid dynamics coupled with solid bilayer—

T. Minoguchi

Institute of Physics, University of Tokyo, Komaba 3-8-1, Meguro, Tokyo 153-8902, Japan

Dislocation in solid He-4 attracts much attention in the context of supersolidity. Supersolidity-like behavior is reported also in a two dimensional case, the solid thin layer of He-4 adsorbed on graphite surface. In contrast to it, it has been found in experiment by Hosomi et. al. [1] that the solid thin layer 'sticks' to the graphite surface in the presence of superfluid overlayer, while the solid layer decouples from the substrate if the overlayer is normal fluid [2]. To explain this unexpected observation, I propose a ‘two fluid’ model consisting from a superfluid overlayer and a solid layer containing mobile component (typically edge dislocation). [3] Due to the smoothness of the substrate, the edge dislocation may have dynamics. The dislocation drags, however, the normal fluid component in the superfluid overlayer and hence causes temperature gradient in the superfluid overlayer. It costs energy in proportion to the superfluid density, and the dislocation motion is suppressed. The other interesting possibilities containing crystallization wave [2] will be also suggested.

[1] Y. Shibayama *et al*., J. Phys. **150**, 032096 (2009).

[1] Crowell P A and Reppy J D, *Phys. Rev.* B **53**, 2701 (1996)

[2] Hosomi N, Taniguchi J, Suzuki M and Minoguchi T, *Phys. Rev.* B**79**, 172503 (2009)

[3] Minoguchi T, *J. of Phys.: Conference Series*, **150**, 032060 (2009)

P56

Mechanical Response of ^{4}He films Adsorbed on Graphite with a Quartz Tuning Fork

K. Ideura, H. Nihei, H. Kobayashi, J. Taniguchi and M. Suzuki

Dept. of Applied Physics and Chemistry, University of Electro-Communications, 1-5-1 Chofugaoka, Chofu, Tokyo 182-8585, Japan

We carried out 5 MHz AT-cut quartz-crystal microbalance (QCM) experiments for ^{4}He films adsorbed on Grafoil (^{4}He/Gr) [1-3]. It was found the sliding friction is significantly small in submonolayer films. When the films are two- and three-atom thick, it is found that the film decouples partly below a certain temperature T_S. Above four-atom thick films, the superfluid transition is observed at T_C. Moreover, in the case of superfluid films, the decoupled films below T_S stick again at lower temperature T_D.

It is interesting to clarify the mechanical response of ^{4}He/Gr when an external force acting on films is small. Recently, we have started a QCM experiment for ^{4}He/Gr with a quartz tuning fork of a resonance frequency of 32 kHz.

In this experiment, the observed behavior is clearly different from that of 5 MHz AT-cut QCM experiments. Figure 1 shows the temperature dependence of the resonance frequency for various areal densities. The frequency does not decrease monotonously in proportion to the areal density. Above 22.9 atoms/nm^2, it increases at T_C in cooling, which corresponds to the superfluid transition temperature. T_C shifts to higher temperature with increasing areal density and coincides with a torsional oscillator by Crowell and Reppy [4]. Between 22.9 and 26.7 atoms/nm^2, it was found that the frequency exhibits hysteresis between warming and cooling and that a part of the film remains decoupling above T_C in warming. This suggests that superfluidity changes solidlike layers underneath the superfluid film. This hysteresis smears out when the areal density increases.

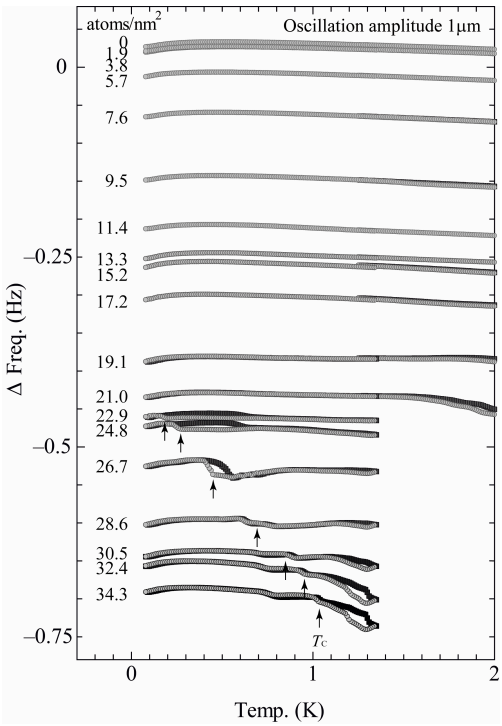

FIG.1: Variation of the resonance frequency for various ^{4}He areal densities as a function of temperature. The resonance frequency is 32 kHz, and the oscillation amplitude is 1μm. Arrows point out the superfluid transition temperature T_C.

[1] N. Hosomi, , A. Tanabe, M. Suzuki, and M. Hieda, Phys. Rev. B, **75**, 064513 (2007).
[2] N. Hosomi, and M. Suzuki, Phys. Rev. B, **77**, 024501 (2008).
[3] N. Hosomi, J. Taniguchi, M. Suzuki, and T. Minoguchi, Phys. Rev. B, **79**, 172503 (2009).
[4] P. A. Crowell and J. D. Reppy, Phys. Rev. B **53**, 2701 (1997).

P57

Superfluid Transition of ^{4}He Film Pressurized by Bulk Liquid ^{3}He

M. Wasai, S. Murakawa, Y. Tamura, Y. Wada, R. Nomura and Y. Okuda

Department of Condensed Matter Physics, Tokyo Institute of Technology, Tokyo, Japan

We measured transverse acoustic impedance Z of normal fluid ^{3}He on a surface coated with a thin ^{4}He film. It is known that ^{4}He thin film enhances the probability of specular scattering of ^{3}He quasiparticles and the specularity depends on the film thickness and the ^{3}He bulk pressure [1,2]. It was found that we can detect the superfluid transition of the ^{4}He film from a change in Z. We measured Z systematically by changing ^{4}He film thickness and bulk ^{3}He pressure.

In the framework of Fermi-liquid theory, Z' is calculated as a function of specularity parameter S [3]. Z' on a partially specular surface is smaller than that on a wall in the diffusive limit. Experimental result is that Z' on coated samples are identical to Z' in pure sample at high temperature and gradually deviates below a particular temperature T_{onset}. One can regard T_{onset} as the superfluid transition temperature of the coated ^{4}He film. The gradual decrease in Z' means that superfluid component in ^{4}He film increases gradually as is expected from the dynamical KT transition at high frequencies. The thicker the film is, the higher T_{onset} is. Increasing the bulk liquid pressure shifted T_{onset} to lower temperature. The T_{onset} 's were ranged in 20 ~ 160 mK depending on the film thickness and bulk pressure. These critical temperatures are much lower than those of the saturated vapor pressure films. Suppression of T_{onset} was probably caused by application of the pressure from a bulk liquid ^{3}He and dissociation of ^{3}He into the ^{4}He film. The result shows that the specularity of ^{3}He quasiparticle scattering is strongly affected by superfluid density of the ^{4}He film.

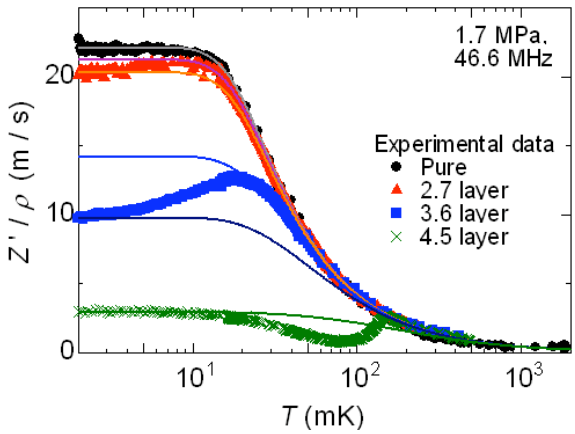

Fig.1: Temperature dependence of Z'. Pressure is 1.7 MPa and measured frequency is 46.3 MHz. Lines are theoretical calculation [3]

[1] S. M. Tolen and J. M. Parpia, Phys. Rev. Lett. **68**, 2810 (1992).
[2] D. Kim, M. Nakagawa, O. Ishikawa, T. Hata , T. Kodama and H. Kojima, Phys. Rev. Lett. **71**, 1581 (1993).
[3] D. Einzel, P. Wölfle and P. J. Hirschfeld, J. Low Temp. Rev. Phys. **80**, 31 (1990).

P58

QCM Study of Superfluid Transition in ^{3}He-^{4}He Mixture Films

T. Oda, M. Hieda, T. Matsushita and N. Wada

Department of Physics, Nagoya University, Furo-cho, Chikusa-ku, Nagoya 464-8602, Japan

There have been a number of experiments exploring the nature of 2D superfluidity and configuration of ^{3}He-^{4}He mixture films on various substrates [1]. It was found that the superfluidity is strongly affected by ^{3}He concentration. At $T = 0$, ^{3}He tends to float on top of ^{4}He and configuration of the mixture films can be viewed as "superfluid sandwich model". Interesting questions still remain, for instance an impurity effect of ^{3}He on 2D quantised vortices in the submonolayer superfluidity [2]. In this poster, we present the results of QCM (quartz crystal microbalance) measurements on flat gold substrate to study on an effect of ^{3}He on the dynamics and configuration of the mixture films.

The three different experimental runs were performed. All superfluid data show the jump of superfluid density σ_s associated with a dissipation peak obeying the Kosterlitz-Thouless theory. In the first two runs, the ^{4}He coverage n_4 was kept constant (■: $n_4 \sim 2.7$layer, ●: $n_4 \sim 3.3$layer) and ^{3}He was incrementally added in the range of $n_3 < 1$layer. As shown in Fig. 1, reductions of the dissipation peak temperature T_p reproduce the torsional oscillator study of Csáthy et al. for porous gold [3]. This depletion of superfluidity is explained by the increase of the localized ^{4}He induced by ^{3}He. In comparison with pure ^{4}He films, we found no effect of ^{3}He on the temperature dependence of the superfluid density σ_s as shown in Fig. 2. The estimated vortex parameter D/a_0^2 (D: diffusion length, a_0: vortex core diameter) is also insensitive to the addition of ^{3}He.

The third run was performed by keeping the constant ^{3}He coverage ($n_3 \sim 1.8$layer) and then adding ^{4}He. Fig. 2 shows that the temperature dependence of σ_s is dramatically changed from that of pure ^{4}He films. The observed increase in σ_s at $T = 0$ indicates that overlayer ^{3}He dissolves into ^{4}He films as the temperature increases. This similar behavior is observed in the mixture films with the 13 overlayers of ^{3}He on Mylar [4]. $n_3 \sim 1$layer is suggested to be a threshold of ^{3}He contribution for σ_s.

[1]R. B. Hallock: Progress in Low Temperature Physics, Elservier Science B. V. , p.322(1995).
[2]H. Cho and G. A. Williams, J. Low Temp. Phys. **110**, 533(1998)
[3]G. A. Csáthy and M. H. W. Chan, Phys. Rev. Lett. **87**, 045301(2001).
[4]D. McQueeney, G. Agnolet and J. D. Reppy, Phys. Rev. Lett. **52**, 1325(1984).

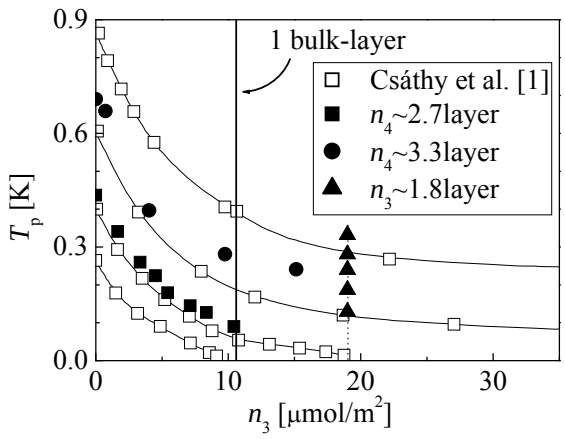

Fig.1: Dissipation peak temperature T_p vs. n_3 for mixture films.

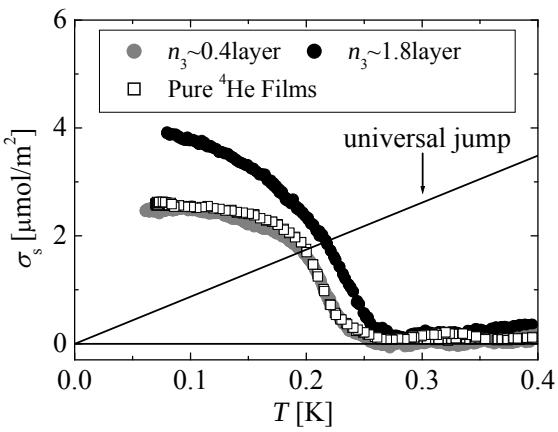

Fig.2: Temperature dependence of superfluid density σ_s for pure ^{4}He films (□) and two mixture films at different n_3 (●: $n_3 \sim 0.4$layer ●: $n_3 \sim 1.8$layer).

P59

Vortex Dynamics of 2D Superfluid in ^{4}He and ^{3}He-^{4}He Films

M. Hieda, T. Oda, T. Matsushita, and N. Wada

Department of Physics, Nagoya University, Furo-cyo, Chikusa-ku, Nagoya 464-8602, Japan

Atomically thin ^{4}He films on various substrates show the Kosterlitz-Thouless (KT) superfluid transition where pairing and unpairing of the 2D quantized vortices play a major role. However, in the submonolayer region of the superfluid, the vortex dynamics has not been revealed enough even for the typical KT transition on flat substrates [1]. In this study, we accurately determined the microscopic vortex parameters (the diffusion constant D, the core diameter a_0) for pure ^{4}He films [2,3] and ^{3}He-^{4}He mixture films on a flat gold substrate, by the frequency dependence of the superfluid onset up to 180MHz, using a quartz crystal microbalance (QCM).

In pure ^{4}He films, the superfluid onset is observed at remarkably higher temperature than the static KT transition temperature T_{KT}, and the observed frequency dependence is well reproduced by the dynamic KT theory close to the high frequency condition, the vortex diffusion length $r_D \approx a_0$ ($r_D \sim$ 14nm at 180MHz). From the frequency dependence of the dissipation peak temperature, the vortex parameter D/a_0^2 is estimated to be 10^9~10^{10} s^{-1} as shown in Fig. 1. We also found the same values on a weak-binding substrate, H_2 (3.3 layers) preplated on gold. These results indicate that the gold substrate is smooth enough for the vortex motion and the vortex diffuses with the largest value $D \sim \hbar/m$ at the quantum diffusion limit [4]. The core diameter a_0 is also estimated to be the same magnitude as the de Broglie wavelength at T_{KT} between 0.1 and 0.9K.

In ^{3}He-^{4}He mixture films, it was found that the superfluidity is strongly affected by ^{3}He concentration [5]. An interesting question is an impurity effect of ^{3}He on the vortices in the submonolayer superfluidity [6]. We performed the QCM study for the mixture films that the ^{4}He coverage n_4 was kept constant ($n_4 \sim 3.3$ layer) and ^{3}He was incrementally added in the range of $n_3 < 1$ layer. In comparison with pure ^{4}He films, we found no effect of ^{3}He on the vortex parameter D/a_0^2.

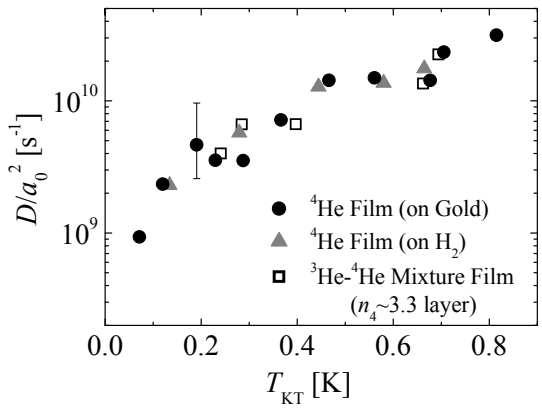

Fig.1 Vortex parameter D/a_0^2 versus T_{KT} for pure ^{4}He films and ^{3}He-^{4}He mixture films with a constant ^{4}He coverage (n_4~3.3 layer). The typical error bar is shown.

[1] H. Yano *et al*., Phys. Rev. B **60**, 543 (1999).
[2] M. Hieda *et al*., J. Phys. Soc. Jpn. **78**, 033604 (2009).
[3] T. Oda *et al*., J. Low Temp. Phys. **158**, 262 (2010).
[4] V. Ambegaokar *et al*., Phys. Rev. B **21**, 1806 (1980).
[5] G. Csáthy and M. H. W. Chan, Phys. Rev. Lett. **87**, 045301 (2001).
[6] H. Cho and G. A. Williams, J. Low Temp. Phys. **110**, 533 (1998).

P60

Numerical Study of Bose-Hubbard Model in Restricted Geometry

M. Tsukamoto, H. Kuroyanagi, and M. Tsubota

[1]*Dept. of Physics, Osaka City University,3-3-138 Sumiyoshi-ku, Osaka 558-8585, Japan*

We perform quantum Monte Carlo simulation of Bose-Hubbard model with site-dependent chemical potentials. This work is motivated by the recent experiments of the ^{4}He confined in various nano-porous media (for example, see [1],[2]). The porous media have the nanometer-size pores and the experimental results depend on the dimensionalities, the randomness, and the sizes of the pores. The system of the ^{4}He confined in the porous media can be described by the Bose-Hubbard model with site-dependent chemical potentials,

$$\mathcal{H} = -J \sum_{\langle i,j \rangle} (\hat{b}_i^\dagger \hat{b}_j + \hat{b}_j^\dagger \hat{b}_i) + \frac{U}{2} \sum_i \hat{n}_i (\hat{n}_i - 1) + \sum_i \mu_i \hat{n}_i$$

where μ_i is the chemical potential depends on site *i*. Here, the chemical potential μ_i plays a role of the confining potential created by the porous media. Using path integral quantum Monte Carlo method, we investigate the above model for various space-dimensions and the distribution of the μ_i. As a result, we find that for three-dimensional system there can exist a state in which the system is locally in Bose-Einstein condensate (BEC) state but has no superfluidity..

In addition, we also discuss the effect of the site-dependent chemical potential in two-dimensional system.

[1] K. Yamamoto, et al., JPSJ **77** 013601 (2008), PRL **100** 195301 (2008).
[2] R. Toda, et al., PRL. **99** 255301 (2007).

P61

Helium Fluid Adsorbed in 1.5 nm One-Dimensional Straight Pores

Taku Matsushita, Jun Miura, Akihisa Ohma, Mitsunori Hieda, and Nobuo Wada

Department of Physics, Graduate School of Science, Nagoya University, Chikusa-ku, Nagoya 464-8602, Japan

When helium atoms are adsorbed in nanopores narrower than characteristic lengths of the He fluid, *eg.* thermal de Broglie wavelength or thermal phonon wavelength, motion in the cross section is not thermally excited, and then, one-dimensional excitations are dominant in the He film. In heat capacity measurments for He adsorbed in 1.8-2.8 nm 1D pores of silicate FSM, we have observed the 1D-2D dimensional crossover of phonons in ^{4}He Bose fluid [1,2], and that of dilute ^{3}He on ^{4}He-preplated pore wall [3,4]. For superfluidity of ^{4}He in these 1D nanopores, obvious decrease of superfluid density is observed between pores 2.2 and 2.8 nm [5,6]. If He atoms still remain fluid in even narrower pores, the 1D states are expected to be observed until higher temperatures. And, when exchange among atoms becomes difficult in sufficiently narrow pores, the He fluid may show essentially different fluid nature from that of He film in wider pores.

In this study, we have measured heat capacities of He adsorbed in straight pores 1.5 nm in diameter, which are narrower pores than those in previous studies, and examined the fluid states. Heat capacity isotherms of ^{4}He atoms adsorbed in 1.5 nm pores are shown in Fig. 1. At coverages below 14.5 μmol/m^2, ^{4}He heat capacity rapidly decreases below a temperature T_L. Since T_L becomes lower with increasing the coverages, it is likely to indicate localization of ^{4}He atoms. At temperatures above T_L, ^{4}He in the nanopore is considered to be a classical fluid described as amorphous-like liquid, similarly to normal fluid ^{4}He. As seen in Fig. 1, small peaks of the isotherms are also observed around 15.5 μmol/m^2. Above the coverage, low-temperature heat capacities do not depends much on the coverage. These small changes of the heat capacity are probably caused by quantum fluid in ^{4}He film outside the nanopore, when the pores are almost filled with ^{4}He. Thus, ^{4}He fluid in 1.5nm is likely to remain classical. Evidence of quantum ^{4}He fluid in 1.5 nm was not observed in this measurement.

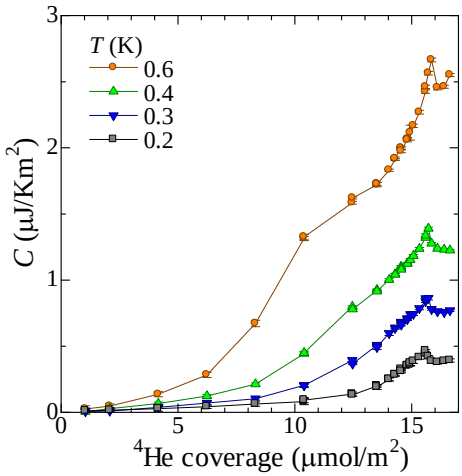

FIG.1: Heat capacity isotherms of pure ^{4}He adsorbed in 1.5 nm pores.

We have also measured specific heats of dilute ^{3}He adsorbed in 1.5 nm pores preplated with ^{4}He. Figure 2 shows the ^{3}He specific heats when the pore wall is preplated with 11.9 μmol/m^2 of ^{4}He. At high temperatures above about 0.5 K, the specific heats are as large as the gas constant R, which indicates that the dilute ^{3}He behaves as gas in 1.5 nm pores. Exponential decreases at low temperatures are likely caused by localization of ^{4}He below T_L. In order to examine low-temperature states of the ^{3}He gas in 1.5 nm pores, measurements of ^{3}He specific heats on thicker ^{4}He layers, where the T_L is much lower, are in progress. Results of these new measurements will be shown together.

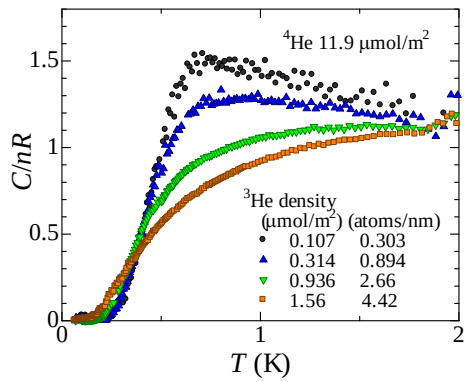

FIG.2: Specific heats of dilute ^{3}He in 1.5 nm pores preplated with ^{4}He (11.9 μmol/m^2).

[1] Y. Matsushita *et al.*, J. Phys. Chem. Solids **66**, 1520 (2005).
[2] Y. Matsushita *et al.*, J. Low Temp. Phys. **150**, 342 (2008).
[3] J. Taniguchi *et al.*, Phys. Rev. Lett. **94**, 065301 (2005).
[4] Y. Matsushita *et al.*, J. Low Temp. Phys. **138**, 211 (2005).
[5] H. Ikegami *et al.*, Phys. Rev. B **76**, 144503 (2007).
[6] Y. Minato *et al.*, in this conference.

P62

Path integral calculation of ^{4}He in quasi-one-dimensional channels

H. Kiriyama[1], J. Taniguchi[1], M. Suzuki[1], and T. Takagi[2]

[1]*Dept. of Appl. Phys. and Chem., Univ. of Electro-Commun., 1-5-1 Chofugaoka, Chofu, Tokyo 182-8585, Japan*
[2] *Dept. of Appl. Phys., Fukui University, 9-1 Bunkyo-3 Fukui-city, Japan*

We have carried out a series of torsional oscillator measurements for liquid ^{4}He confined in a one-dimensional (1D) channel (FSM16). It was found that a rapid increase in the superfluid fraction in the 1D channel is suppressed strongly from the bulk superfluid transition. For 2.8-nm channel, the rapid increase temperature (T_o) at 0.1 MPa is 0.9 K, and is strongly suppressed by pressurization. Moreover, for 2.2-nm channel the rapid increase was not observed clearly (FIG.1). To clarify the properties of ^{4}He in 1D channel, we have performed a numerical calculation of path integral Monte Carlo.

We consider ^{4}He particles confined in cylindrical containers, which are the simplified configuration of FSM16. Both ends of containers are connected by a periodic boundary condition. We adopted three different potentials for the wall of containers: (a) a rigid wall, (b) a geometric corrugation due to hard cores of inert layer, (c) an interaction potential between liquid ^{4}He and inert solid ^{4}He. Inside the containers of (a) and (b), the potential gradient is zero. We used Aziz potential for ^{4}He atomic interaction.

We calculated the energy and the superfluid fraction of ^{4}He in the range of liquid density. Figure 2 shows the diameter dependence of T_{onset}, at which the energy drops due to particle exchanges. As the diameter narrows, T_{onset} for (a) is independent of diameter down to 1.7-nm, and then shifts to lower temperature with further narrowing. Below 0.48-nm channel, we cannot define T_{onset}. For (b) and (c), T_{onset} decreases with narrowing the diameter in the same way as (a), but T_{onset} is suppressed stronger than that for (a). The diameter dependence of T_{onset} is similar to the behavior of T_o observed by a torsional oscillator.

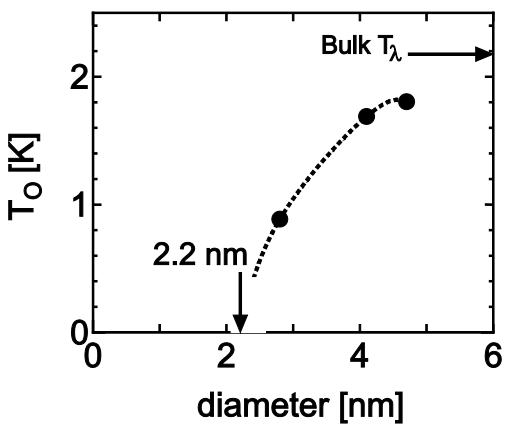

FIG.1: Size dependence of T_o(torsional oscillator measurements).

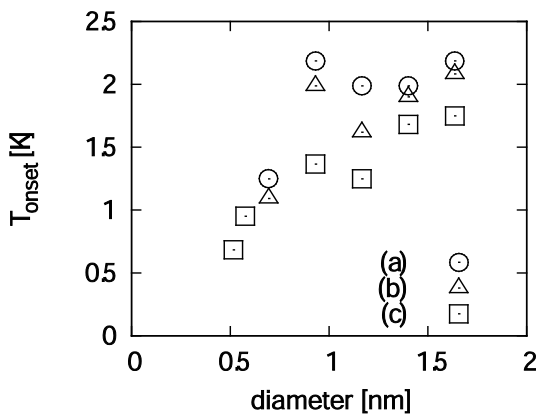

FIG.2: Size dependence of T_{onset} (this calculation).

P63

Quantum Phase Transition of ^{4}He in Nanoporous Gelsil Glass

T. Eggel[1], M. Oshikawa[1] and K. Shirahama[2]

[1]*Institute for Solid State Physics, University of Tokyo, Kashiwa 277-8581, Japan*
[2]*Department of Physics, Keio University, Yokohama-shi, Kanagawa 223-8522, Japan*

In experiments on ^{4}He on nanoporous Gelsil glass with average pore diameter of 2.5 nm [1] a suppression of the λ - transition under pressurization has been observed. The novel feature of this suppression with respect to similar effects in other porous media observed in the past, Vycor glass for example, is that for a pressure of about 3.4 MPa the superfluid transition decreases to zero Kelvin.

We argue that this system indeed exhibits *quantum critical phenomena*. The mapping of the effective model of the system, the 3D quantum rotor model, to a (3+1)D classical model yields a phase boundary between the superfluid and the normal fluid regime of the form $p_c(0)$-$p_c(T)$~T^2. This is in remarkable agreement with experiment (see FIG.1, where we have plotted a fit to the experimentally observed phase boundary). The theory moreover provides expressions for the superfluid density as a function of temperature/pressure which agree very well with the experimental findings.

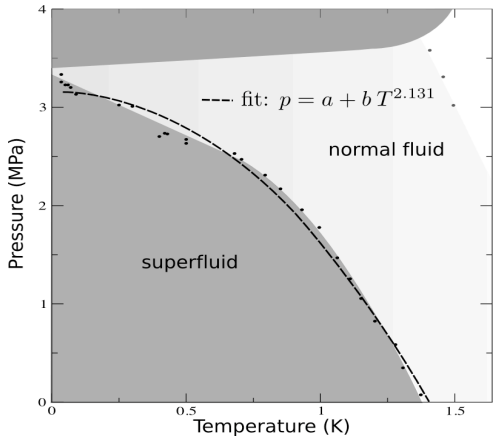

FIG. 1 Phase diagram obtained in [1] displaying the QCP located at around 3.4 MPa and the fit to the phase boundary.

[1] K. Yamamoto *et al*., PRL **100,** 195301 (2008).

P64

Pore-size Dependence of Superfluidity of ^{4}He in 1D-Nanopores FSM

Y. Minato, M. Hieda, T. Matsushita, and N. Wada

Dept. of Physics, Nagoya University, Furo-cho, Chikusa-ku, Nagoya 464-8602, Japan

Superfluid onset observed in 2D-^{4}He films, which is known as KT-transition, is different from λ-transition in 3D bulk liquid. To investigate the possibility of superfluidity in 1D-system, we have studied ^{4}He adsorbed in 1D-nanopores FSM. FSM has channels with uniform diameters d=1.5-4.7nm, and the length ~300nm. ^{4}He films adsorbed on the wall in the channels form a tube. At low coverages, the film is solid. Slightly above the first layer, fluid phase appears on the solid film. At low temperatures, thermal phonon wavelength ($\lambda_{phonon}=hv/k_BT$) exceeds the circumference of ^{4}He fluid tubes in the FSM channels, and then 1D-phonon states can be realized. Heat capacities of ^{4}He adsorbed in FSM with d=1.8-2.8nm pores were explained by the model assuming phonons with continuous 1D-dispersion in the axial direction and discrete energy levels in the azimuthal direction [1,2]. The gap energy to the first excited state in the cross-section Δ was estimated to be Δ/k_B~1K, below which ^{4}He is in 1D-phonon states. In this study, superfluidity in the 1D-phonon states has been examined.

For ^{4}He adsorbed in 1D-nanopores FSM with d=1.5, 1.8, 2.2, 2.8, and 4.7nm, pore-size dependence was studied, which is shown in Fig.1 [3]. Comparing the films with the same superfluid onset temperature (T_{onset}~1K), superfluid densities observed in the 2.8nm and 4.7nm pores are obviously larger than those in the 1.8nm and 2.2nm. To clarify the superfluid behavior between 2.2nm<d<2.8nm, we have measured superfluid density of ^{4}He adsorbed in FSM with d=2.4nm.

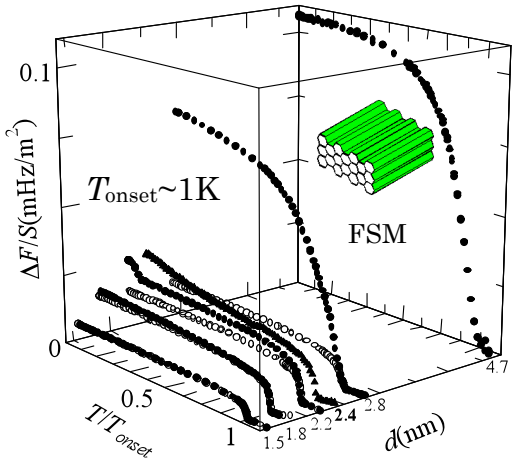

Fig.1
Pore-size dependences of superfluid density measured by the torsional oscillator method (T_{onset}~1K). Open circles show superfluid densities of ^{4}He adsorbed on the outside of the FSM channels.

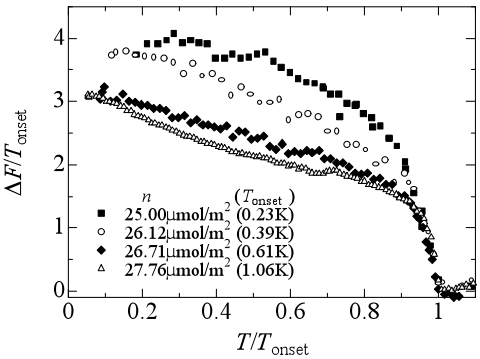

Fig.2
Coverage dependences of the superfluid density (d=2.4nm).

In 2.4nm pores, the superfluid onset is observed above a coverage n=23.0μmol/m^2. When this superfluid onset is explained by KT-transition, the superfluid onset temperatures T_{onset} should be proportional to n. However, dT_{onset}/dn in n>26.0μmol/m^2 becomes larger than that in n<26.0μmol/m^2. The coverage 26μmol/m^2 roughly corresponds to the coverage n_f, up to which ^{4}He films grow uniformly in the channels.

As shown in Fig.2, temperature dependence of superfluid density in 2.4nm pores also changes above 26.0μmol/m^2. At n=25.0μmol/m^2 (T_{onset}=0.23K), it is similar to that of ^{4}He in FSM with d=2.8nm and 4.7nm. On the other hand, in n>26.7μmol/m^2 (T_{onset}>0.6K), superfluid density is suppressed as well as in FSM with d=2.2nm or 1.8nm. This result suggests that ^{4}He in 2.4nm pores is on a boundary between strongly suppressed superfluidity (d=1.8nm and 2.2nm) and KT-like superfluidity (d=2.8nm and 4.7nm).

[1] Y. Matsushita *et al.*, J. Phys. Chem. Solids **66**, 1520 (2005).
[2] Y. Matsushita *et al.*, J. Low Temp. Phys. **150**, 342 (2008).
[3] H. Ikegami *et al.*, Phys. Rev. B **76**, 144503 (2007).

P65

Phase Diagram of ^{4}He Confined in 1D Nano-Porous Media

J. Taniguchi, R. Fujii, H. Kiriyama, H. Ichida, Y. Aoki, and M. Suzuki

[1]*Department of Applied Physics and Chemistry, The University of Electro-Communications, 1-5-1 Chofugaoka, Chofu, Tokyo 182-8585, Japan*

The quantum properties of liquid and solid ^{4}He are altered drastically by confining ^{4}He into nano-porous media whose pore size is from several to ten times as large as the atomic size. We have performed torsional oscillator, ultrasound, freezing pressure, and heat capacity measurements for ^{4}He confined in a FSM16 series, which possess one-dimensional (1D) straight nano-meter size channel.

When liquid ^{4}He is confined in the channel larger than 2.8 nm in diameter, the superfluid was observed at low temperature. The superfluid onset temperature T_o in the 2.8-nm channel is 0.9 K at 0.01 MPa, and is suppressed under the application of pressure. This onset continuously approaches zero at around 2.1 MPa at absolute zero, which suggests a quantum phase transition between the superfluid and non-superfluid states. On the other hand, the heat capacity shows no anomaly at T_o, while it shows a bump at the higher temperature. This demonstrates that the entropy decreases at the higher temperature than T_o. In the pressure region where superfluid disappears, the bump of heat capacity lowers and a hardening in stiffness takes place.

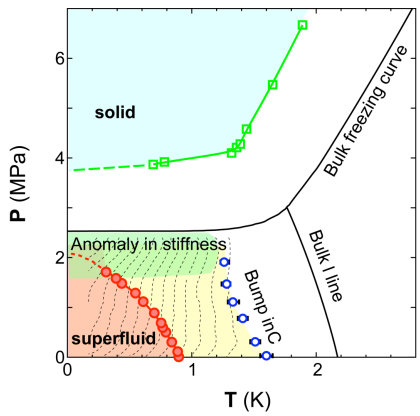

Fig. 1: Pressure-Temperature phase diagram of ^{4}He confined in 1D channel 2.8 nm in diameter. Dotted curves are contour of the change in sound velocity.

P66

State of ^{4}He Adsorbed in Three-Dimensional Nanopores of ZTC with 3D-period 1.4nm

Y. Nakashima, Y. Minato, M. Hieda, T. Matsushita, and N. Wada

Department of Physics, Graduate School of Science, Nagoya University, Nagoya 464-8602, Japan

Recently we have studied superfluidity of ^{4}He film in HMM-2 of which pores 2.7nm in diameter are connected in three-dimension (3D) with the period 5.5nm [1]. The ^{4}He fluid films formed in the 3D pore walls show the evidence of the 3D superfluid transition; the heat capacity shows a sharp peak at the superfluid onset temperature. So as to study the possibility of the quantum fluid state of ^{4}He adsorbed in the 3D pores with the smaller pore diameter and 3D period, we studied ^{4}He adsorbed in ZTC (Zeolite-Templated-Carbon). The new 3D nanopores have the pore diameter 1.2nm, the 3D period 1.4nm, and the porosity 78%. From the pressure isotherms, we observed that the uniform ^{4}He layers are formed up to about 1.4 atomic layers [2].

In this study, we measured heat capacity C of ^{4}He absorbed in 3D nanopore of ZTC as a function of coverage, and obtained heat capacity isotherms as shown in Fig.1. Comparing with the case for HMM-2 [2], we predict the phase diagram of ^{4}He adsorbed in ZTC, as follows. At a lower coverage n than about 15μmol/m^2, the heat capacity decreases below a temperature T_L which is shown with □ in Fig. 2. It suggests a localized state of ^{4}He at the lower temperatures. Minimum of the C-isotherm at n_1=16.5μmol/m^2 indicates the first layer completion. The uniform layer is likely to be formed on the pore walls up to n_f=23μmol/m^2 (n_f/ n_1=1.4 layer). The C-isotherms (Fig. 1) indicate that C increases above n_1 corresponding to the promotion of the second layer. Above n/n_1=1.2 layers, C decreases again. Comparing with the case for HMM-2, we can expect the Bose fluid state above the maximum coverage n_B. The other possibility is a solid or a localized state above the maximum n_{solid}, because the heat capacity becomes small. n_B/n_{solid} is marked with ▲ in Fig. 2. In our torsional oscillator experiment for the present ZTC, we observed the superfluid above n_f. The superfluid onset temperature T_{SF} is shown with ○ in Fig. 2.

To examine if the state above n/n_1=1.2 layers is the Bose fluid, we have to compare the heat capacity between ^{4}He and ^{3}He at the same coverages.

[1] R. Toda *et al.*, P.R.L **99**, 255301(2007).
[2]Y. Kinoshita *et al.*, J.L.T.P **158**, 275 (2010).

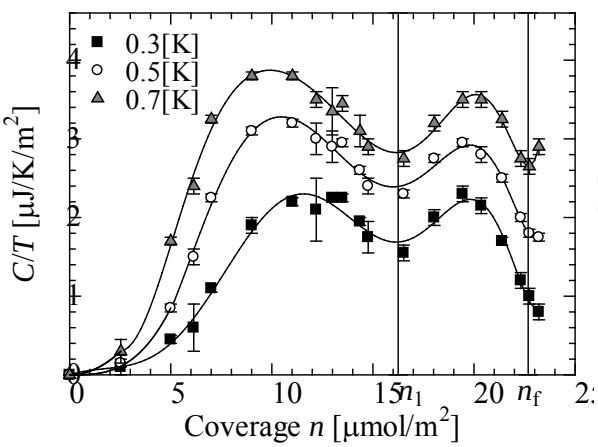

Fig. 1. Heat capacity isotherms of ^{4}He in ZTC.

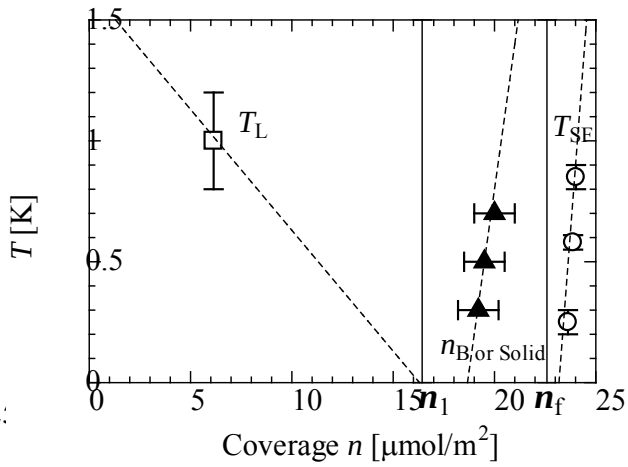

Fig. 2. Predicted phase diagram of ^{4}He adsorbed in ZTC.

P67

Superfluid density of ^{4}He confined in nanopores

K. Yamashita[1] and D. Hirashima[1]

[1]*Depertment of Physics, Nagoya University, Nagoya 464-8602, Japan*

Recently, Ikegami *et al*. [1] and Toda *et al*. [2] succeeded in studying superfluid behavior of ^{4}He films adsorbed on surface of nanopores FSM-16, using a torsional oscillator. They observed finite frequency shift below a finite temperature T_s, which implies that ^{4}He films are in the superfluid state in (quasi-) one dimension. The onset temperature T_s was found to be close to the Kosterlitz-Thouless (KT) transition temperature T_{KT}, which can be estimated by the areal density of ^{4}He atoms. A question is then "why they were able to observe finite superfluid density in q-1D ^{4}He systems below the KT transition temperature". In this study, we answer this question: In (quasi-)1D, superfluid density ρ_s (helicity modulus) is broken down by *phase slippage* below temperatures much lower than T_{KT}. However, it is possible to observe finite superfluid density below the KT transition temperature in a torsional oscillator experiment, because the observed superfluid density ρ_s is likely to be the one that is not affected by phase slippage.

We use the classical ferromagnetic XY model. We are concerned with helicity modulus Y, which represents the rigidity of spin systems and is conventionally related to superfluid density. We are dealing with anisotropic systems of size $\ell_x \times \ell_y$ with $A=\ell_x/\ell_y$ (>1). Figure 1 shows numerical results of helicity modulus Y along x axis in several systems. In the isotopic case, A=1, helicity modulus Y_x has a (universal) jump at $T=T_{KT}\cong 0.9J$. When *aspect ratio* A deviates from unity, Y_x rapidly shifts to low temperature. This is in marked contrast to the finding in the experiments [1,2], where $A\cong 50$. We then have to clarify what is really measured or calculated. This question has actually been discussed by several authors [3].

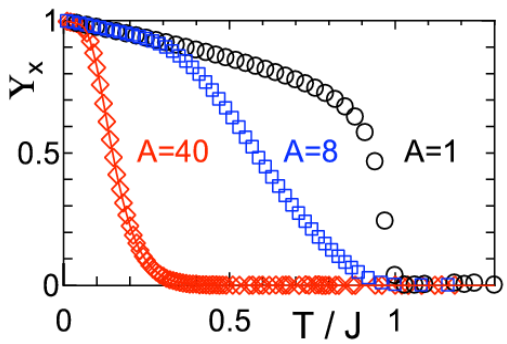

FIG.1: Helicity modulus Y_x in several anisotropic 2D systems.

The reduction of superfluid density is caused by phase slippage in q-1D. States with finite phase slippage in the spin system correspond to the states which has finite superflow in the original boson system. If those states were probed in torsional oscillator experiments, one would observe the reduced superfluid density. However, if only those states without no phase slippage are probed, one can observe finite superfluid density from such a high temperature as the KT transition temperature. That is why finite superfluid density is observed below KT transition temperature in the experiments [1,2].

[1] H. Ikegami *et al*., Phys. Rev. B **76**, 144503 (2007).
[2] R. Toda *et al*.,Phys. Rev. Lett. **99**, 255301 (2007).
[3] T.Minoguchi and Y. Nagaoka, Prog. Theor. Phys. **80**, 397 (1988); J. Machta and R. A. Guyer, J. Low. Temp. Phys. **74**, 231 (1989); N. V. Prokof'ev and B. V. Svistunov, Phys. Rev. B **61**, 11282 (2000)

P68

Quantum Clusters of Helium Formed in Nanocage in Na-Y Zeolite

K. Sahashi, A. Ohma, T. Matsushita, [A]R. Toda, M. Hieda, and N. Wada

Department of Physics, Nagoya University, Furo-cho, chikusa-ku, Nagoya, 464-8602, Japan
[A]Department of Physics, Kyoto University, Kitashirakawa-Oiwake-cho, Sakyo-ku, Kyoto, 606-8501, Japan

We have studied heat capacities of helium confined in nanocages in Na-Y zeolite. Na-Y zeolite has cages 1.3nm in diameter, which are connected through 0.8nm-apertures in the diamond structure. When helium atoms are adsorbed in the cages, helium in the first layer form solid layer. Since the solid layer narrows apertures, helium in the second layer could be confined in each cage, and form a cluster as shown in Fig.1.

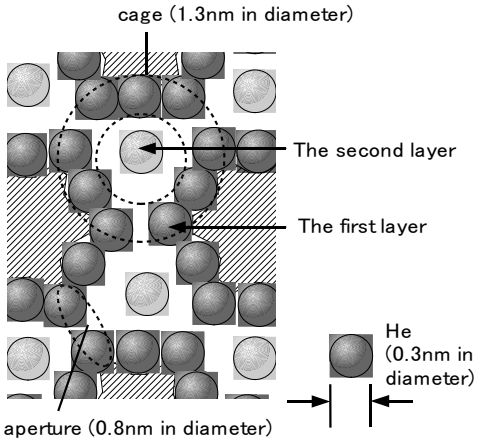

Fig.1 Schematic drawing of helium atoms adsorbed in nanocages in Na-Y

Heat capacity isotherms are shown in Fig.2. The minima about 10.3atoms/cage indicate that the first layer is completed and solidified. At coverages between 13.5 and 17.0atoms/cage, qualitative difference between ^{4}He and ^{3}He heat capacities indicates that the second-layer helium behave as quantum fluid [1]. In this region, ^{3}He heat capacities discontinuously change every 1atom/cages, which suggests that adatoms in the second layer form a quantum cluster confined in each cage [2].

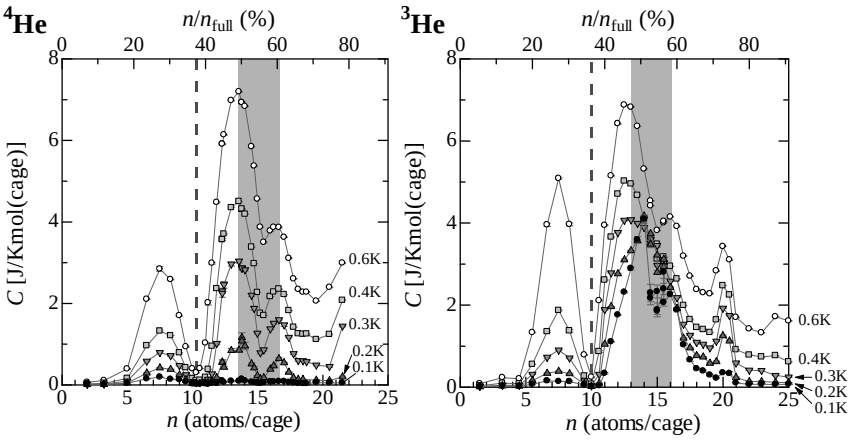

Fig.2 Heat capacities of pure ^{4}He and pure ^{3}He confined in nanocages, where the heat capacity C is for 1 mol of cages.

We also measured the heat capacity of a single ^{3}He atom in a cage coated by the first solid layer of ^{4}He. As seen in Fig.3, ^{3}He specific heat has a peak about gas constant R around 1K. At low temperatures, the specific heat exponentially decreases ($C \sim \exp(-\Delta/k_B T)$). It indicates an energy gap about 3K. This value is comparable to the energy difference between the ground state and the lowest exited state for the ^{3}He free motion in the 0.7nm-cage. On the other hand, a decrease of heat capacity above 2K suggests that the number of exited states is limited.

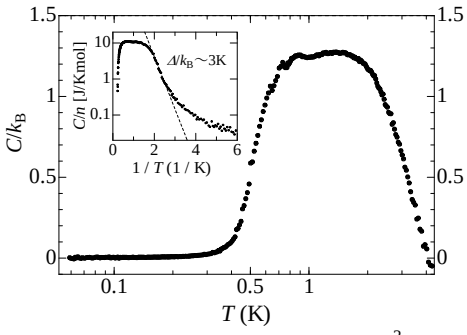

Fig.3 The heat capacity of one ^{3}He atom confined by ^{4}He solid layer in a cage.

[1] T. Matsushita *et al.*, J. Phys. Conf. Ser. **150**, 032055 (2009)
[2] T. Matsushita *et al.*, J. Low Temp. Phys. **158**, 188 (2010)

P69

Size Effect on Superfluid Transition of ^{4}He Films in Thin Porous Gold

S. Kiyota, M. Hieda, T. Matsushita, and N. Wada

Department of Physics, Nagoya University, Furo-cho, Chikusa-ku, Nagoya 464-8602, Japan

The superfluid transition of 2D ^{4}He films shows the Kosteritz-Thouless(KT) transition. However, in case of the ^{4}He films adsorbed on multiple-connected porous substrates, a dimensional crossover from the KT transition (2D-XY) to the 3D-XY system was experimentally observed near the superfluid transition temperature T_c[1,2]. This crossover is thought to be possible since the correlation length ξ exceeds a length scale of the pore connection. An interesting question is a possibility of a finite size effect on the superfluid transition of ^{4}He films due to the restriction of ξ to the direction of the substrate thickness when the multiple-connected porous substrate is very thin. Then we carried out QCM measurements (20MHz) for the three different Porous Gold (PG) substrates with the thickness L=0.5, 1.0, 1.5μm (the pore diameters of 38±4nm, 38±4nm, and 54±11nm respectively) and studied the substrate thickness dependence in the temperature range of 0.7~1.0K.

Figure 1 shows the superfluid density ρ_s versus reduced temperature t=1-T/T_c in a log-log scale at T_c~0.84K. ρ_s agrees with the critical exponent 0.67 of bulk liquid ^{4}He (dashed lines in Fig.1) between ~5×10^{-3}< t <~2×10^{-2} for all PG substrates. This observation qualitatively agrees with the interpretation of a 2D-3D crossover close to T_c reported in the past torsional oscillator study[2]. As T increases towards T_c, ξ deduced from the Josephson's relation grows rapidly in the thin PG substrate. As ξ exceeds ~200nm (=$\xi_{2D\text{-}3D}$), which is approximately equal to the distance of pore connection, the ^{4}He films crossover to the 3D system from the KT transition. As the temperature further approaches to T_c, the deviations from the power law are observed at t~5×10^{-3} equivalent to the length ξ_L. For PG with the thickness L=1.0 and 1.5μm, ξ_L are constant value ~600nm with no dependence on the PG thickness. The deviations are interpreted by the results of macroscopic inhomogeneity of PG. In contrast, for L=0.5μm, the deviation is observed at the smaller length ξ_L~480nm which is almost equal to the PG thickness. This suggests a finite size effect due to the restriction of ξ to the direction of the substrate thickness.

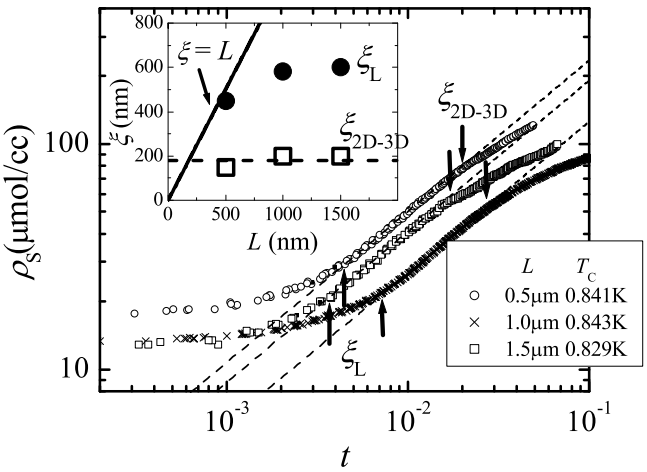

Fig.1 Superfluid density versus reduced temperature at T_c~0.84K. The dashed lines are power law fits to data with the exponent fixed at 0.67. The correlation lengths deviated from the fit, $\xi_{2D\text{-}3D}$ and ξ_L, are plotted versus PG thickness L in the inset.

[1] C.W. Kiewiet, *et al.*, PRL **35**, 1286 (1975)
[2] G.A. Csáthy, *et al.*, PRL **80**, 4482 (1998)

P70

Superfluid ^{4}He in a Porous – Alumina Nanopore Array

Rama Higashino, Koji Yoshimura, Satoshi Murakawa, Yoshiyuki Shibayama, Kensuke Honda*, Keiya Shirahama

Department of Physics, Keio University, Yokohama 223-8522
**Department of Biological Science and Chemistry, Yamaguchi University, Yamaguchi 753-8512*

In the previous work [1] we have revealed that superfluidity of ^{4}He confined in nanopores of 2.5 nm in diameter is strongly suppressed at pressures near the bulk freezing. This rather unexpected result suggests that the superfluid order parameter is suppressed by strongly confining ^{4}He in nanopores of 2 – 3 nm in size, which is an order of magnitude larger than the superfluid coherence length ($\xi \sim 0.3$ nm). This anomalous superfluid suppression is not only interesting as a novel correlation effect of confined Bosons, but also useful in developing a true superfluid Josephson junction. Josephson effect in superfluid ^{4}He has been observed only by using micron-sized apertures in the very vicinity of bulk lambda point (2.17 K), at which ξ becomes comparable to the aperture size [2].

Here we propose a novel Josephson device working at arbitrary temperature based on the superfluid suppression in the nanopores. We employ well – characterized porous alumina (PA), which has a regular array of nanopores (typically 45 nm in size). By controlling an etching process or by laying diamond-like carbon on the PA plate, one may expect to realize a array of hundred millions nanopores of 2 – 5 nm in pore size. As a preliminary test, we examine superfluid properties of ^{4}He in a PA nanopore array (45 nm in pore size) (Fig. 1), by developing an annulus – type torsional oscillator [3]. We will discuss preliminaty results and improvements of the experimental setup that are underway.

[1] K. Yamamoto *et al*., Phys. Rev. Lett. **93,** 075302 (2004); K. Shirahama *et al*., J. Phys. Soc. Jpn. **77** (2008) 111011. [2] E. Hoskinson, R. E. Packard, Phys. Rev. Lett. **94**, 155303 (2005). [3] V. Kotsubo *et al*., Phys. Rev. Lett. **58**, 804 (1987).

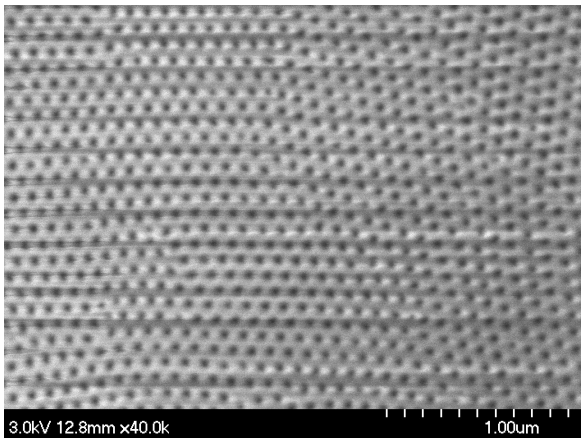

A SEM image of the surface of a porous alumina. The pore size is 45 nm.

P71

Quantum Superfluid Transition of ^{4}He Confined in a Regular Nanoporous Structure

Naoki Yamanaka,[1] Takeshi Kondoh,[1] Yoshihiro Sogabe,[1] Yoshiyuki Shibayama,[1] Shinji Inagaki[2], Keiya Shirahama[1]

[1]*Department of Physics, Keio University, Yokohama 223-8522*
[2]*Toyota Central R & D Labs. Inc., Nagakute-cho 480-1192*

When bosons are subjected to external confinement potential, the ground state can be totally altered from ordinary superfluid state: Mott insulator, Bose glass, and supersolid states are expected. We observed that ^{4}He confined in a nanoporous Gelsil glass (pore size: 2.5 nm) shows a quantum phase (superfluid – nonsuperfluid) transition (QPT) when the pressure is swept around 3.4 MPa and near 0 K. This QPT is closely related to the formation of Localized Bose-Einstein Condensates (LBEC) [1], in which the macroscopic superfluid coherence is destroyed. The LBEC state might be produced by strong confinement of ^{4}He atoms in the nanopores and/or by disorder in the porous structure. The porous structure of Gelsil is inevitably disordered (irregular) and complicated, so the effect of disorder was not clarified. In order to study the effect of disorder, we have examined superfluidity of ^{4}He confined in a regular nanoporous material HMM-3 by torsional oscillator and ultrasound technique.

HMM-3 has a regular 3D porous structure consisting of spherical voids (diameter: 5.1 nm) connected by thin apertures of 2.5 nm in size or less. Figure shows the phase diagram obtained by torsional oscillator, ultrasound and pressure studies. Interestingly, the superfluid Tc drastically decrease and approaches 0 K as the pressure approaches 3.3 MPa, which is very close to the critical pressure observed in the previous Gelsil study. Clearly, ^{4}He undergoes a QPT even in the regular confinement potential, i.e. without disorder. However, thedifference in the shapes of the T_c curves in HMM-3 and Gelsil indicates a significant effect of disorder on the superfluid transition.

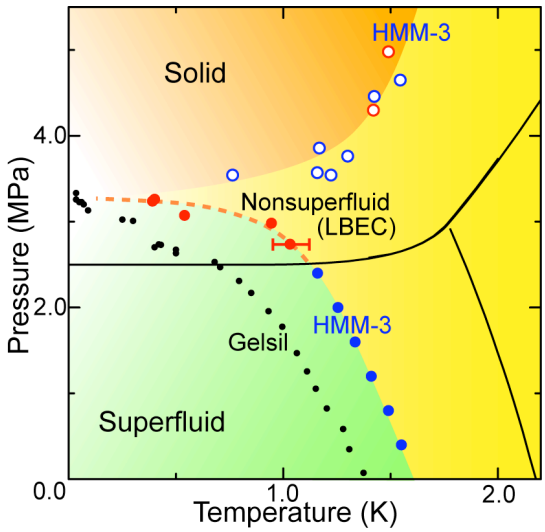

QPT behaviors in the $P-T$ phase diagram: ^{4}He confined in a regular nanoporous material HMM-3 and an irregular porous Gelsil glass [1]. Closed blue and red circles show superfluid T_c measured by a torsional oscillator and ultrasound, respectively.

[1] K. Yamamoto *et al.*, Phys. Rev. Lett. **100** (2008) 195301; J. Phys. Soc. Jpn. 77 (2008) 013601; Phys. Rev. Lett. **93** (2004) 075302; K. Shirahama *et al.*, J. Phys. Soc. Jpn. **77** (2008) 111011.

P72

Quantized Vortices Generated in Turbulent Region of Superfluid ^{4}He at High Temperatures

Y. Nago, T. Ogawa, Y. Miura, K. Obara, H. Yano, O. Ishikawa, and T. Hata

Graduate School of Science, Osaka City University, 3-3-138 Sugimoto, Sumiyoshi-ku, Osaka-shi, Osaka 558-8585, Japan

It is considered that quantum turbulence in superfluid ^{4}He consists of a tangle of quantised vortices and nucleates vortex rings, which propagate in superfluid and can attach to boundaries. We have been studying quantum turbulence in superfluid ^{4}He using a vibrating wire in order to clarify dynamics of vortices in an oscillating turbulent flow. In previous works at 30 mK [1][2], the transition to turbulence triggered by free vortex rings was observed using two vibrating wires: when the generator wire generates turbulence during the detector wire vibrating at high drive in a laminar state, many vortex rings nucleate from the generator, propagate and attach to the detector wire, causing abrupt drop in the velocity of the detector due to the turbulent transition.

At high temperatures, motion of vortices is expected to be greatly different from that at 30 mK because of the normal component: mutual friction due to the normal component disturbs propagating vortex rings. In this work, we performed the experiment for detection of vortices generated in a turbulent flow at 1.2K, corresponding to normal fraction of helium of 3%. We prepared the improved experimental cell of the generator and the detector of vortices: the wires are located close to each other (0.88 mm apart) and in parallel with each other, in order to exactly detect vortices and measure the time of flight of a vortex between both wires.

Figure 1 shows the time development in the peak velocity of the detector. The wire is initially vibrating at the velocity of 200 m/s in a laminar state. After turbulence is generated by the generator at t = 0s, the velocity of the detector drops down to 155 mm/s in Δt = 2.44s. Once the detector enters turbulent state, it keeps in the low velocity during vibration. This result indicates that vortices which are generated from the generator propagate to the detector and expand by oscillation of the detector, causing turbulence. Since vortices are considered to expand within period of the detector oscillation of ~ 1 ms, delay time Δt = 2.44s is corresponding to the time of flight of a vortex triggering turbulence. We measured the time of flight of a vortex for many times and found that the flight time has a distribution from 0.09s to 14.3s. These values are much larger than the time of flight of a vortex ring measured in a previous work at 30 mK [2], which is order of 10 ms. This difference suggests the effect of mutual friction due to the normal component.

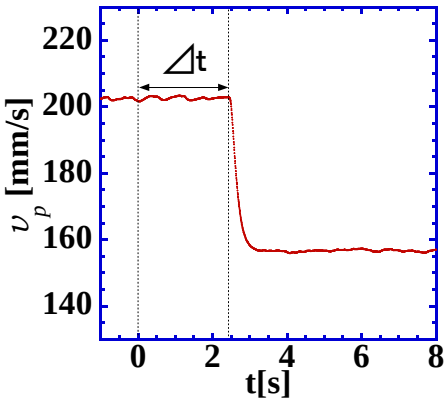

FIG.1: Time development in the peak velocity of the detector at 1.2 K.

[1] R. Goto *et al*., Phys. Rev. Lett., **100,** 045301 (2008)
[2] H. Yano *et al*., J. Phys.:Conf.Series **150**, 032125 (2009).

P73

Generation of Quantum Turbulence in Superfluid ^{4}He using a Quartz Tuning Fork

K. Andachi, Y. Nago, K. Obara, H. Yano, O. Ishikawa, and T. Hata

Graduate School of Science, Osaka City University, 3-3-138 Sugimoto, Sumiyoshi-ku, Osaka-shi, Osaka 558-8585, Japan

Our group has studied quantum turbulence in alternating current by using a vibrating wire. As increasing driving force, the velocity of the wire increases linearly in a laminar state; however, extra damping appears in the response of the wire at velocities above a critical velocity, indicating quantum turbulence generated by a wire. In previous work, we found that the critical velocity obviously depends on the frequency of wires at 50mK, showing that motions of vortices attached to boundaries are characterized by the frequency of boundary flow. We also revealed that the critical velocity v_c for the vibrating wires is proportional to the square root of frequency, fitted to $v_c = 1.8\sqrt{\kappa\omega}$ as shown in Fig.1, where κ and ω are the quantum of circulation and angular frequency, respectively. However it is still unclear how the critical velocity is going to behave for the frequency range higher than 10kHz.

This time we used two quartz tuning forks whose frequencies were 15kHz and 32kHz, in order to investigate the dependence of the critical velocity in the high-frequency oscillation. Furthermore these forks have a very high Q-value (about 1 million) compared with other oscillators such as a vibrating wire (about 1,000~1,500), therefore it seems that they could respond sensitively to the surrounding environment. Based on above written, we carried out experiments as follows.

1: The results measured at 50mK show that the critical velocity increases with increasing frequency as well as the previous data by a vibrating wire, suggesting that unstable motions of attached vortices are affected by frequency of oscillating flow. As a result, we found there exists a relation of $v_c = 0.9\sqrt{\kappa\omega}$ for forks.(Fig.1) We assume that $\sqrt{\kappa\omega}$ would be a characteristic velocity for vortices.

2: A high Q-value of forks enables us to have the exact information of the environment around. In the case of superfluid ^{4}He, when the flow is in a laminar state, the response of forks will only be affected by the elementary excitations responsible for a normal component. Over the wide range of temperature, we measured the temperature dependence of the energy loss $\lambda(T)$ obtained by the relation of $F=\lambda(T)\, v_p$ in a laminar flow (Fig.2), where F and v_p are driving force acting on forks, and velocity of forks, respectively. Consequently, we found that as increase in temperature, $\lambda(T)$ starts from a constant value $\lambda(0)$ due to ^{3}He impurities, then increases in proportion to T^4 mainly by phonons (Ballistic regime), and shifts to Hydrodynamic regime. In addition, we discovered the different behaviors of $\lambda(T)$ in different frequencies. A possible reason will be discussed in the poster.

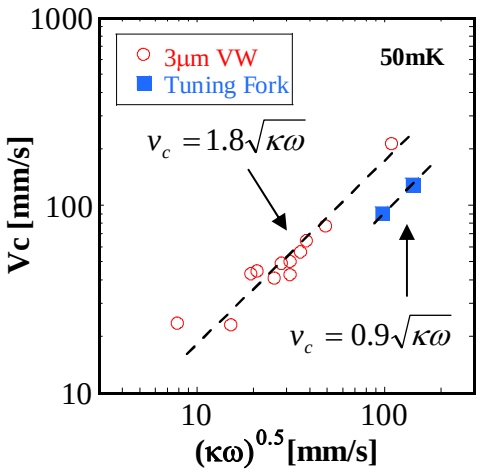

Fig1: Critical velocity v_c of turbulent transition as a function of square root of $\kappa\omega$ at 50mK

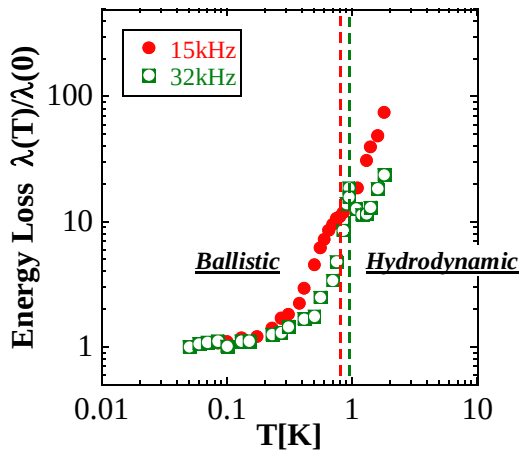

Fig2: Temperature dependence of Energy loss

P74

Direct Energy Cascade in Two-Dimensional Compressible Quantum Turbulence

R. Numasato,[1] M. Tsubota,[1] and V. S. L'vov[2]

[1]*Department of Physics, Osaka City University, Sumiyoshi-ku, Osaka-shi, Osaka 558-8585, Japan*
[2]*Department of Chemical Physics, The Weizmann Institute of Science, Rehovot 76100, Israel*

We study two-dimensional(2D) quantum turbulence(QT) by numerically solving Gross-Pitaevskii(GP) equation. We found *2D-direct energy cascade* with Kolmogorov-Obuckhov incompressible kinetic energy spectrum $E_{\mathrm{kin}}^{\mathrm{i}}(k) \propto k^{-5/3}$ which previously was observed only in 3D turbulence.

Recently, 3DQT has been actively studied in low-temperature physics. Especially, one of the most attractive problems is the analogue between 3DQT and classical turbulence(CT); as one of the typical phenomena the direct energy cascade and the Kolmogorov-Obuckhov's -5/3 law are confirmed in 3DQT too[1-3]. Then, we want to expect this analogue may also hold in 2D case. However, this guess is not necessarily true.

The features of 2DCT is much different from those of 3DCT due to the conservation of enstrophy Ω in 2D incompressible fluids. In 2DCT, while energy is carried to large-scale, enstrophy small-scale[4]. The former energy flow is called *inverse energy cascade*, especially in forced 2DCT. On the other hand, the latter enstrophy flow is called *direct enstrophy cascade*. Energy flow into large-scale causes the self-organization of the system in both forced and decaying 2DCT, i.e. large-scale eddies are formed and finally they grow up to be a vortex dipole.

In 2DQT with GP model, Ω is not conserved because it is proportional to the number of quantized vortex points N_{qv} and N_{qv} is not constant due to the compressibility of Bose-Einstein condensates. Thus, we can expect that incompressible kinetic energy which is responsible for the motion of quantized vortices cascades from large to small scales and the spectrum shows the power law $E_{\mathrm{kin}}^{\mathrm{i}}(k) \propto k^{-5/3}$. Our numerical calculation supports this prediction and we also obtain positive incompressible kinetic enregy flux which proves direct energy cascade. Moreover, long-time calculations tell us that the system finally reaches full thermodynamic equilibrium without quantized vortices. Then, we calculate compressible kinetic energy spectrum and power spectrum of compressible effective velocity field to study equilibrium state.

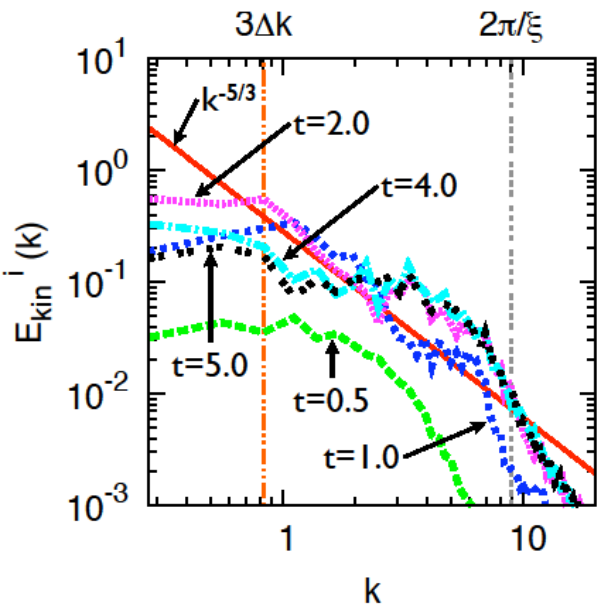

Incompressible kinetic energy spectrum

[1] C. Nore, M. Abid, and M. E. Brachet, Phys. Rev. Lett. **78**, 3896 (1997).
[2] J. Maurer and P. Tabeling, Europhys. Lett. **43**, 29 (1998).
[3] M. Kobayashi and M. Tsubota, Phys. Rev. Lett. **94**, 065302 (2005).
[4] R. H. Kraichnan, Phys. Fluids. **10**, 1417 (1967).

P75

Analysis of vortex line density fluctuations and size distribution of quantum turbulence

Shoji Fujiyama and Makoto Tsubota

Department of Physics, Osaka City University, 3-3-138 Sugimoto, Sumiyoshi-ku, Osaka 558-8585, Japan

The Lancaster group conducted series of experiments of quantum turbulence created by a vibrating grid at low temperature limit[1-3]. The Lancaster group measured the vortex line density fluctuations of the quantum turbulence and found that its spectrum with respect to frequency obeys a power law with the exponent -5/3[3]. Although the power law reminds us of Kolmogorov law-a statistical law with respect to energy observed in wave number space-, its physical meaning has not been given yet.

To investigate the power law of line density fluctuation, we conducted numerical simulations by modeling the experiments by the Lancaster group, obtaining an equilibrium state of quantum turbulence. The spectrum of the line density fluctuations of the simulation obeys power law with the exponent -1.8, the value close to -5/3 in the experiment.

Considering the reason of the line density fluctuations, we concluded that an escape of vortex rings with various sizes from the numerical cell (detection region of vortices in experiments) mainly contributes to the fluctuation. Since the escape rate is expected to be proportional to the density of vortex rings and these with their particular sizes are related to their own time scales by turnover time, the line density fluctuation can be mapped into the vortex size distribution. Accordingly, the size distribution also should obey a power law and the exponent is deduced to be -7/3 from the line density fluctuation spectrum. In fact, the power law of the size distribution is confirmed in the simulation. Interestingly, another power law is also found in the size distribution, which is considered to be the appearance of Richardson cascade process. This idea comes from the belief that the self-similar aspects of the quantum turbulence in wave number space, real space and time space (namely Kolmogorov law, Richardson cascade process and line density fluctuation power spectrum) must be closely connected.

[1] D. I. Bradley *et al*., Phys. Rev. Lett. **95**, 035302 (2005).
[2] D. I. Bradley *et al*., Phys. Rev. Lett. **96**, 035301 (2006).
[3] D. I. Bradley *et al*., Phys. Rev. Lett. **101**, 065302 (2008).

P76

Quantized vortex nucleation by 2D snowballs below the free surface of ^{4}He

D. Takahashi, H. Ikegami, and K. Kono

Low Temp. Phys. Lab., RIKEN, 2-1 Hirosawa, Wako, Saitama 351-0198, Japan

It is possible to create positively or negatively charged ions in liquid He. Such ions provide the only means of studying the Landau critical velocity for emission of rotons and the mechanism of quantum vortex ring creation when they are accelerated to high velocity. In the case of the electron bubble, the creation of vortex rings and the emission of rotons have extensively investigated by the time of flight (TOF) method at low pressure and high pressure of liquid He, respectively. The mechanism of the quantized vortex ring creation is understood as a macroscopic quantum tunneling process below ~ 0.2 K, above which temperature the vortex rings are created by thermally activated process [1].

Ions trapped a few hundred Å below a free He surface form a two-dimensional ion layer. The velocity of ions can be controlled by continuous variation of the electric field along the surface unlike with the TOF method. Therefore, it has an advantage to observe the critical velocity (v_c) associated with both roton emission or vortex ring creation. Here we present transport properties of a two-dimensional snowball system under a high driving electric field.

We measure the I-V characteristic of the two-dimensional snowball system underneath the free surface of helium by means of the Sommer-Tanner method [2] with corbino electrodes. The snowball density (n_i) is ~ 6.6×10^{11} /m^2, as determined by the plasma resonance frequency. The velocity (U_i) is derived from the detected current with $U_i = i/2\pi r_i n_i e$, where r_i and e are the inner corbino radius and elementary charge respectively. As shown in the figure, U_i increases proportionally with the driving voltage at low driving voltage. Then U_i decreases abruptly at a certain threshold voltage and shows non-linear behavior above the threshold. The transition between the linear and non-linear state shows hysteresis. We found that the temperature dependence of U_c is quite unique; U_c at 450 mK is ~31 m/sec, and it decreases with decreasing temperature. However, it is independent of temperature at a value of ~ 18 m/sec below 200 mK.

The observed non-linear transport indicates that a new dissipation mechanism arises at U_c. U_c is sufficiently small (~ 60%) compared to Landau critical velocity for roton emission. The creation of vortex rings could be the origin of the nonlinear behavior. The temperature dependence of U_c could be understood qualitatively as a macroscopic quantum tunneling process including dissipative effect based on the Caldeira-Legget theory [3]. We discuss the details of the experimental procedure and possible explanations for the results.

[1] P. C. Hendry, N. S. Lawson, P. V. E. McClintock, C. D. H. Williams and R. M. Bowley, *Phil. Trans. R. Soc. Lond. A*, **332**, 387-414(1990)
[2] W. T. Sommer and D. J. Tanner, *Phys. Rev. Lett.*, **27**, 1345(1971)
[3] A. O. Caldeira and A. J. Leggett, *Phys. Rev. Lett.*, **46**, 211(1981)

P77

Detection Technique for Kelvin Waves on Vortex Lines in Superfluid ^{4}He

Y. Miura, T. Ogawa, Y. Nago, K. Obara, H. Yano, O. Ishikawa, and T. Hata

Graduate School of Science, Osaka City University, 3-3-138 Sugimoto, Sumiyoshi-ku, Osaka-shi, Osaka 558-8585, Japan

Quantised vortices are known to nucleate at the superfluid transition and remain attached to boundaries. For recent years, our vibrating-wire measurement in superfluid ^{4}He[1] has revealed that bridged vortex lines attached to a vibrating wire cause quantum turbulence. However, the mechanism of turbulence generation due to attached vortex lines has remained an open question up to the present. The numerical simulation[2] predicts that, in an oscillatory flow, the Kelvin waves arise on the bridged vortex lines attached between an oscillating obstacle and surrounding boundaries, becoming unstable to create vortex rings and form turbulence at a sufficiently high flow velocity. We therefore need to observe the Kelvin waves on vortex lines attached to a vibrating wire for approach to the mechanism of turbulence generation. However, many vortex lines are attached to a wire, which makes it difficult to observe the Kelvin waves. Control of attached vortex lines is necessary for improving the sensitivity of the vibrating wire.

In a previous work[3], we covered a vibrating wire with a copper box and cooled the helium liquid slowly from above the lambda temperature to 1.2 K in 2 h, successfully reducing the number of vortices attached to a wire. Moreover, the experiments using vibrating wires with different roughnesses revealed that a vibrating wire with surface roughness of less than ~ 50 nm is efficient for studying the Kelvin waves on vortex lines attached between the wire and surrounding boundaries.

In this presentation, we report the development of detection technique for the Kelvin waves using a vibrating wire with smooth surfaces, a cover box and slow cooling method. The wave length of the Kelvin waves induced by a typical vibrating wire, of which frequency is 100 ~ 10000Hz, is estimated to be order of 10 μm. Therefore, aiming to detect the resonance of the Kelvin waves, we are preparing an experimental cell as follows: we put a boundary near down to the top part of a vibrating wire, expecting that vortex lines easily form bridges between the top part of the wire and the boundary. It is important to adjust the distance between a vibrating wire and a boundary to less than ~ 100 μm for improving the sensitivity of a vibrating wire for the Kelvin waves with the wave length of order of 10 μm. Under this condition, we investigate harmonic modes of the Kelvin wave resonance by continuously changing the distance between the wire and the boundary. A piezoelectric actuator is useful as a movable boundary for adjusting the distance from the wire. We found that a piezoelectric actuator can change the displacement in the range of ~±60 μm in the accuracy of ~ nm at 1.2K, which is enough to detect harmonic modes of the Kelvin waves with the wave length of order of 10 μm. Therefore a piezoelectric actuator is expected to enable us to detect the Kelvin waves on vortex lines by a vibrating wire.

[1] N. Hashimoto, R. Goto, H. Yano, *et al.*, Phys. Rev. B **76**, 020504(R) (2007).

[2] R. Hänninen, M. Tsubota, and W. F. Vinen, Phys.Rev.B **75**,064502(2007).

[3] Y. Nago, Y. Miura, H. Yano, *et al.* , J. Low Temp. Phys. **158**, 443(2010)

P78

Superfluid Properties of Fermi Atoms in Optical Lattices

Y. Fujihara,[1] A. Koga,[2] and N. Kawakami[1]

[1]*Dept. of Physics, Kyoto University, Kyoto 606-8502, Japan*
[2]*Dept. of Physics, Tokyo Institute of Technology, Tokyo 152-8551, Japan*

Superfluidity of fermionic atoms is one of the most fascinating phenomena in optical lattice systems. Recent experiments make it possible to realize a superfluid state in an optical lattice [1], which should certainly stimulate further systematic studies of unconventional superconductivity in the near future. In such optical lattice systems, it is important to consider the effect of a trap potential, which is inherent in the experiments in cold atoms. Therefore the density profiles become nonuniform, and expected superfluid state cannot be characterized by the momenta of the atoms due to the loss of translational symmetry. In addition, it is suggested that a supersolid state, where a density wave state coexists with a superfluid state, may be stabilized in fermionic systems due to the trap potential [2]. Nevertheless, it is still difficult to observe the quantities in a real space such as density distributions, and the effect of the trap potential on the observable quantities.

To this end, we focus on the momentum distributions and the noise correlation functions of fermionic atoms in an optical lattice, and evaluate them for various superfluid states expected in a trap potential. It is shown how the nature of superfluid states is reflected in the observable quantities.

[1] J. K. Chin, *et al*., Nature **443**, 961 (2006).
[2] A. Koga, *et al*., Phys. Rev. A **79**, 013607 (2009).

P79

Polarized superfluid state in a fermionic optical lattice

A. Koga[1] and P. Werner[2]

[1]*Department of Physics, Tokyo Institute of Technology, Tokyo 152-8551, Japan*
[2]*Theoretische Physik, ETH Zurich, 8093 Zürich, Switzerland*

Ultracold atomic systems have attracted much interest since the successful realization of a Bose-Einstein condensate of rubidium atoms [1]. In two-component fermionic systems, interesting phenomena have been observed such as the Mott transition and the BCS-BEC crossover. Furthermore, the observation of a superfluid state with imbalanced spin populations [2] has stimulated further experimental and theoretical investigations on the superfluidity in ultracold fermionic systems.

So far, the superfluid state with imbalanced spin populations has been discussed and various phases have been proposed such as the Fulde-Ferrell-Larkin-Ovchinnikov (FFLO) state and the breached-pair (BP) state [3]. When one considers higher dimensional optical lattice systems, the BP state without momentum dependence, in which both the magnetization and the superfluid order parameter appear, may be one of the appropriate ground states. On the other hand, at finite temperatures, the polarized superfluid (pSF) state is naively expected to be realized below the critical temperature. Therefore, it is interesting to investigate how the pSF state at finite temperatures is connected to the BP state [4].

To make this point clear, we study the attractive Hubbard model in the presence of a magnetic field, which should describe two-component optical lattice systems with imbalanced populations. In this study, to take into account local particle correlations precisely, we combine dynamical mean-field theory with the continuous time quantum Monte Carlo (CTQMC) method [5], which is extended to treat the pSF state in the Nambu formalism [6]. By calculating the superfluid order parameter, the magnetization and the density of states, we discuss how the pSF state is stabilized at low temperatures. The possibility of the BP state is also addressed.

[1] M.H. Anderson, J.R. Ensher, M.R. Matthews, C.E. Wiemann, and E.A. Cornell, Science **269**, 198 (1995).
[2] M.W. Zwierlein *et al.*, Science **311**,492 (2006); G.B. Partridge *et al.*, Science **311**, 503 (2006).
[3] G. Sarma, J. Phys. Chem. Solids **24**, 1029 (1963).
[4] T.-L. Dao, M. Ferrero, A. Georges, M. Capone, and O. Parcollet, Phys. Rev. Lett. **101** 236405 (2008)
[5] A.N. Rubtsov, V.V. Savkin, and A.I. Lichtenstein, Phys. Rev. B **72**, 035122 (2005).
[6] D.J. Luitz and F.F. Assaad, arXiv:0909.2656.

P80

Propagation of second sound in a superfluid Fermi gas in the unitary limit

Emiko Arahata, Tetsuro Nikuni

[1] *Department of Physics, Tokyo University of Science, 1-3 Kagurazaka, Shinjuku-ku, Tokyo, 162-8601, Japan*

We study sound propagation in a uniform superfluid gas of Fermi atoms in the unitary limit. The existence of normal and superfluid components leads to appearance of two sound modes in the collisional regime, referred to as first and second sound. The second sound mode is of particular interest as it is a clear signal of a superfluid component. Using Landau's two-fluid hydrodynamic theory, we calculate hydrodynamic sound velocities and the associated weights in the density response function. The latter is used to calculate the response to a sudden modification of the external potential generating pulse propagation (see Fig.1). The amplitude of a pulse, which is proportional to the weight in the response function, is calculated on the basis of the approach of Nozeres and Schmitt-Rink for the BCS-BEC crossover. We show that, in a superfluid Fermi gas at unitarity, the second-sound pulse is excited with an appreciate amplitude by density perturbations.

[1] E. Taylor, et al., Phys. Rev. A **74**, 063626 (2006).
[2] M. R. Andrews, et al., Phys. Rev. Lett. **78.** 553(1997).

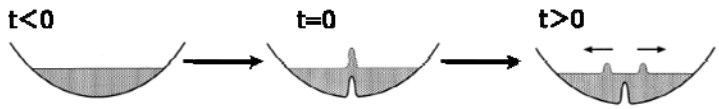

FIG.1: Excitations of wave packets in a superfluid Fermi gas. From[2].

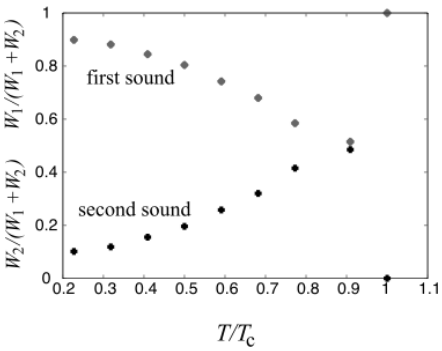

FIG.2: The first sound amplitude $W_1/(W_1 + W_2)$ and the second sound amplitude $W_2/(W_1 + W_2)$ as a function of temperature.

P81

Stability Criterion of Superfluidity with Dynamical Density Fluctuations

Yusuke Kato[1] and Shohei Watabe[2]

[1]*Dept. of Basics Science, The University of Tokyo, 3-8-1, Komaba, Meguro-ku, Tokyo, 153-8902, Japan*
[2]*Institute of Physics, The University of Tokyo, 3-8-1, Komaba, Meguro-ku, Tokyo 153-8902, Japan*

Superfluidity in condensed Bose systems breaks down via various kinds of instability; instability of the excitation spectrum with respect to a flowing condensate (so called the Landau instability) or the emission of topological defects (vortices, solitons). The latter instability has been identified with the saddle-node bifurcation in the context of non-linear physics, through the study of dynamics of the Gross-Pitaevskii equations. If a common aspect of various kinds of instability of superfluidity is clarified, it would provide a crucial step toward a unified understanding of the break-down of superfluidity.

In this presentation, we propose a criterion of stability of superfluidity applicable both to the Landau instability and the saddle-node bifurcation with focusing on dynamical density fluctuations of elementary excitations[1][2]. Within the Gross-Pitaevskii-Bogoliubov theory, we show the validity of our criterion for the Landau instability and the soliton-emission instability. We also show applicability to the Landau instability in the systems with the phonon-roton spectrum.

[1] Y. Kato and S. Watabe, J. Low Temp. Phys. **158**, 92(2010).
[2] S. Watabe, Doctor Thesis (The University of Tokyo, 2010).

P82

Superfluid/ferromagnet/superfluid-junction and π–phase in a superfluid Fermi gas with population imbalance

T. Kashimura[1], S. Tsuchiya[1,2], and Y. Ohashi[1,2]

[1]*Dept. of Physics, Keio University, 3-14-1 Hiyoshi, Yokohama,223-8522, Japan,*
[2]*CREST(JST), 4-1-8 Honcho, Saitama, 332-0012, Japan*

We theoretically propose a method to realize a superfluid/ferromagnet/superfluid (SFS)-junction in a superfluid Fermi gas. To explain our idea in a simple manner, we consider a two-component Fermi gas with population imbalance ($N_\uparrow > N_\downarrow$), described by a one-dimensional attractive Hubbard model. When this model system is in a double-well potential (Fig.1(A)), we show that a part of the excess atoms is localized around the central region in Fig.1(A) under a certain condition, forming a barrier. This barrier region is dominated by atoms with pseudospin-↑, so that it can work as a *ferromagnetic* junction. The resulting system is close to a superconductor/ferromagnet/superconductor-junction discussed in metallic superconductivity, where the so-called π-phase is known to be realized (where the phase of the superfluid order parameter changes by π across the junction). This novel superfluid state is shown to be also possible in the present case, as shown in Fig.1(B), which is a clear evidence of the realization of the SFS-junction in the superfluid Fermi gas. We also show that such an SFS-junction, as well as the π-phase, are possible to realize even in higher-dimensional systems.

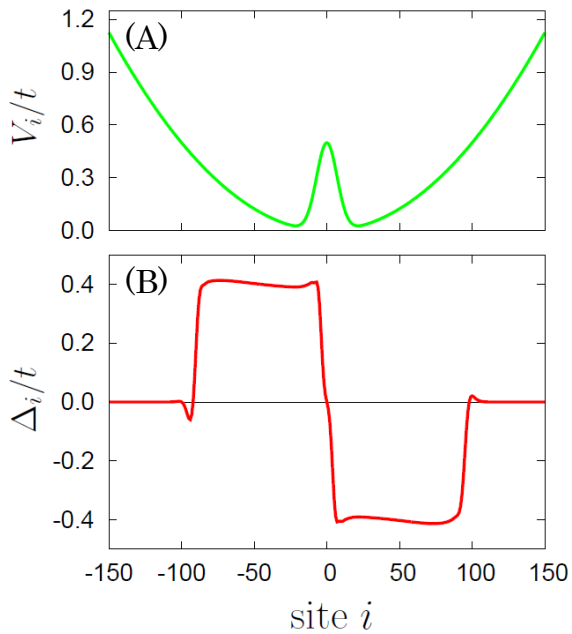

Fig. 1 (A) Model double-well potential *Vi* normalized by nearest-neighbor hopping *t*. The *x*-axis shows the lattice site *i* in the one-dimensional tight-binding model we are using. (B) Spatial variation of the calculated superfluid order parameter *Di* when a part of excess atoms is localized around the central potential in Fig. 1(A). In this calculation, we set $N_\uparrow$=47, $N_\downarrow$=43.

P83

Ferrofluidity in dipolar Bose-Einstein condensates

H. Saito, Y. Kawaguchi,[1] and M. Ueda[1,2]

University of Electro-Communications, Tokyo 182-8585, Japan
[1]*Department of Physics, University of Tokyo, Tokyo 113-0033, Japan*
[2]*Macroscopic Quantum Control Project, ERATO, JST, Tokyo 113-8656, Japan*

When a magnetic liquid (a colloidal suspension of ferromagnetic nanoparticle) is subjected to a magnetic field perpendicular to the surface, the liquid is magnetized and the surface undergoes spontaneous deformation into characteristic patterns shaped like 'horns' growing from the liquid. This surface instability is known as the normal-field or Rosensweig instability [1]. We show that similar phenomena occur in a Bose-Einstein condensate (BEC) of an atomic gas with a dipole-dipole interaction [2].

We consider a system of two-component BECs in a magnetic-field gradient as illustrated in Fig. 1. The two components are phase-separated by the field gradient. We found that the interface between the two components is deformed and a hexagonal pattern emerges as shown in Fig. 2. This pattern formation resembles the Rosensweig pattern on a magnetic-liquid surface.

We show that the hexagonal pattern is formed even in the presence of the superflow. The BEC (off-diagonal order) with the periodic modulation of the density (i.e., diagonal order) offers evidence of supersolidity.

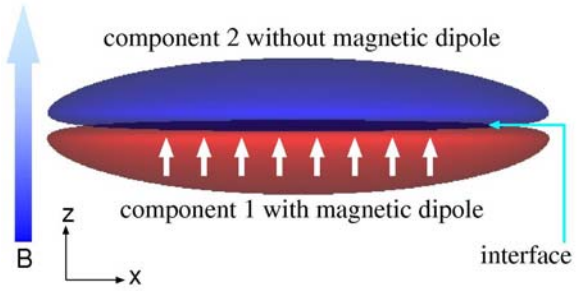

Fig. 1: Schematic illustration of the system.

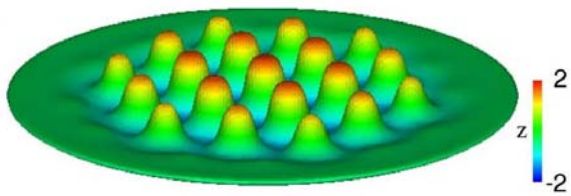

Fig. 2: Isodensity surface of component 1 for a stable state.

[1] M. D. Cowley and R. E. Rosensweig, J. Fluid Mech. **30**, 671 (1967).
[2] H. Saito, Y. Kawaguchi, and M. Ueda, Phys. Rev. Lett. **102**, 230403 (2009).

P84

Vortex Tiling in Spinor Condensates

M. Kobayashi,[1] Y. Kawaguchi,[2] and M. Ueda[2]

[1]*Dept. of Basic Science, University of Tokyo, 3-8-1 Komaba, Meguro-ku, Tokyo 153-8902, Japan*
[2]*Dept. of Physics, University of Tokyo, 7-3-1 Hongo, Bunkyo-ku, Tokyo 113-0033, Japan*

Quantized vortices are topological defects of the superfluid order parameter. For single component Bose-Einstein condensates (BECs), the quantized vortices emerge as phase singularities, and the order parameter vanishes at the core center. However, the situation drastically changes for BECs with the internal degrees of freedom, where the vortex core can be filled with a state having different symmetry. For the case of spin-2 and higher-spin spinor BECs, there are more than two possible candidates of the order parameter in the core, and each order parameter has its own internal spin structure. So, an interesting question arises which we refer to as "vortex tiling" [1], as to how the order parameter of the BEC smoothly connects the spin structure of the vortex core. Furthermore, both order parameter inside and outside the vortex core can have the different discrete symmetries. Such commensurability gives rise to breaking of the rotational symmetry of the vortex, allowing us to probe the symmetry of the order parameter in spin space without the explicit spin-orbit coupling.

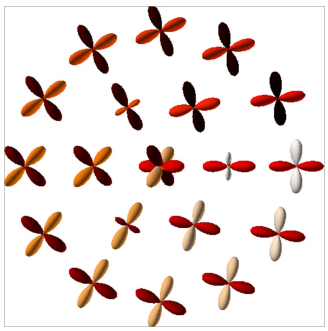

FIG.1: 1/2-1/4 vortex in the biaxial-nematic phase (cloverleaf) with the core of cyclic order (triad).

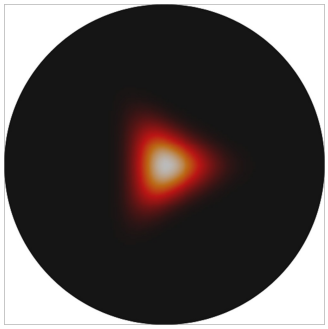

FIG.2: Amplitude of cyclic order in the 1/2-1/4 vortex.

FIG. 1 shows the typical example of the vortex tiling for a 1/2-1/4 vortex with the core of the cyclic order in the biaxial-nematic phase of a spin-2 spinor BEC. Around the vortex, $U(1)$ gauge changes by 2π, and spin rotates by π. While the biaxial-nematic order has the discrete 4th dihedral symmetry, the cyclic order has the tetrahedral symmetry. As a result, the spontaneous breaking of the rotational symmetry occurs and the shape of the core becomes triangle (FIG. 2).

At the vortex core, the cyclic order has the additional degrees of freedom of the coupled spin-gauge $SO(2)$ rotation, which arises the localized Goldstone mode in the vortex core associated twisting excitations along the vortex lines (FIG. 3). Furthermore, this twisting excitation allows the new topological excitations called "vortons" (FIG. 4). Unlike usual vortex rings, the vorton has the quantized circulations not only around the vortex line but also along the vortex ring, and cannot continuously shrink to disappear.

Our predictions for the vortex tiling can be tested experimentally by using a rotating spin-2 ^{87}Rb BEC and enable an experimental realization of the cyclic order parameter.

[1] M. Kobayashi, Y. Kawaguchi, and M. Ueda, arXiv:0907.3761v1.

FIG.3: Twisting wave excited along the vortex with the triangle shape.

FIG.4: Example of vorton excitation. Triangle shape of the vortex core rotates by $8\pi/3$ along the vortex ring.

P85

Textures and Vortices in *d*-Wave Fermi Condensates in Atomic Gases

H. M. Adachi, Y. Tsutsumi, and K. Machida

Dept. of Physics, Okayama University, Okayama 700-8530, Japan

Fundamental properties of superfluids with *d*-wave pairing symmetry are investigated theoretically. We consider neutral atomic Fermi gases in a harmonic trap, the Cooper pairing being produced by a Feshbach resonance via a *d*-wave interaction channel. Our motivation is to provide the physical properties of a *d*-wave superfluid confined by a harmonic potential in order to help identify the *d*-wave nature experimentally, focusing on the order parameter (OP) spatial structures, or, textures at rest and vortices under rotation. A Ginzburg-Landau (GL) functional is constructed which is symmetry-constrained for five components OP. We find stable OP textures and vortices for all three stable known phases [1]. These three phases are the energy minima of the GL functional; the ferromagnetic (FM), polar (PO) and cyclic (CY) phases [1] (FIG. 1) both at rest and under rotation. The three phases are characterized by FM ($|\Theta|=0$, $|\mathbf{f}|\neq 0$), CY ($|\Theta|=0$, $|\mathbf{f}|=0$) and PO ($|\Theta|\neq 0$, $|\mathbf{f}|=0$), here Θ is the orbital singlet pairing amplitude and **f** is the orbital momentum.

We consider a two dimensional system confined by a harmonic trap assuming that the object extend uniformly to the third dimension. Thus, our GL functional is constructed by bulk term [1], gradient term, harmonic trap term and centrifugal potential term. The gradient term is constructed by considering the possible contractions of $(\partial_i B_{jk})^*$ and $(\partial_l B_{mn})$, here B is the symmetric traceless rank-2 tensor. We choose the parameter values β_i (i=1,2,3) which are coefficients of fourth order terms of bulk term to each stable phase.

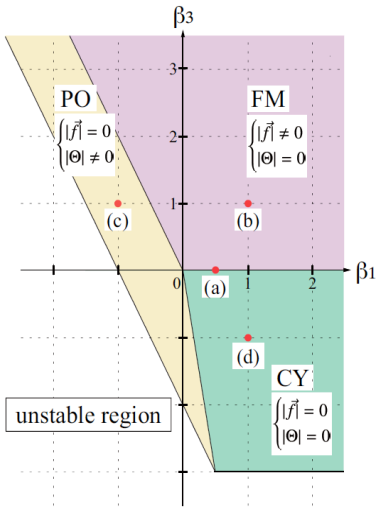

FIG. 1: Phase diagram of the stable phases in uniform system.

In FM phase, we argue the relation between nodal structure and textures of **f**-vector at the boundary region at rest. We conclude that the curving of the **f**-vector is due to the saving of the condensation energy by excluding the point nodes from the condensate like *p*-wave condensates in the trapped system [2]. In PO phase, the half-quantum vortex emerges from the outside under rotation. In CY phase, in particular, we touch upon the stability conditions for a non-Abelian fractional 1/3-vortex in the CY phase under rotation [3] (FIG. 2). It is expected to apply for quantum computation and we propose how to create the intriguing 1/3-vortex experimentally in atomic gases via optical means.

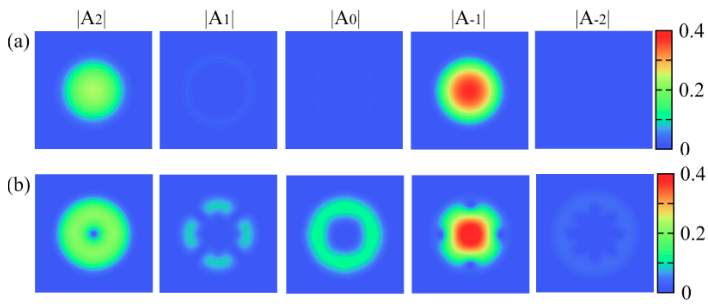

FIG. 2: Contour map of each component in CY phase. (a) There is no 1/3-vortex at rest. (b) 1/3-vortex emerges under rotation.

[1] N. D. Mermin, Phys. Rev. A **9**, 868 (1974).
[2] Y. Tsutsumi and K. Machida, Phys. Rev. A **80**, 035601 (2009); Y. Tsutsumi and K. Machida, J. Phys. Soc. Jpn. **78**, 084702 (2009).
[3] H. M. Adachi *et al.*, J. Phys. Soc. Jpn. **78**, 113301 (2009); H. M. Adachi *et al.*, J. Phys. Soc. Jpn. **79**, No. 4 (2010).

P86

Experimental study on the ground-state phase of ^{87}Rb spin-2 Bose-Einstein condensate

T. Tanabe, Y. Taguchi, M. Kurihara, Y. Suzuki, S. Tojo, and T. Hirano
Department of Physics, Gakushuin University, Mejiro, Toshima-ku, Tokyo 171-8588, Japan

We have experimentally investigated and analyzed the dynamics of ^{87}Rb spin-2 Bose-Einstein condensates (BEC) in an optical trap. Owing to its rich variety of internal degrees of freedom, many interesting dynamics can be observed. The F = 2 BEC is predicted to have a new phase of magnetic ground state (cyclic phase) [1]. It was suggested that the time-evolution measurement initially populated in $|F = 2, m_F = +2\rangle$ and $|F = 2, m_F = -2\rangle$ states in a sufficient low magnetic field can determine the ground-state phase [2]. In the cyclic phase, the $|2,+2\rangle + |2,-2\rangle$ collision produces $|2,0\rangle$ atoms directly, while this collision does not produce $|2,0\rangle$ atoms in the anti-ferromagnetic phase. In our previous study, we observed that $(2,+2)+(2,-2)$ atoms remained in their initial states without producing other spin components [3]. However, we have found that $(2,+2)+(2,-2)$ atoms in an optical trap spatially separated after 100 ms. The separation suggests the difficulty in determining magnetic phases by mixed spin-population measurements. In this study we have implemented on 1D optical lattice in order to suppress this spatial separation.

Figure 1 shows the relative center-of-mass positions of $(2,+2)+(2,-2)$ pair in the 1D optical lattice (circles), and those in the optical trap (squares). We can see that spatial separations between two components are suppressed by the optical lattice. The time dependence of spin populations in the optical lattice at 100mG magnetic field is shown in Figure 2. It is seen that the population of $|2,0\rangle$ atoms remained low. This experimental result suggests the anti-ferromagnetic property. However, due to the presence of a small bias magnetic field, the experimental observation does not exclude the possibility that the ground state phase at zero magnetic fields is cyclic [2]. The spin-population measurements in the optical lattice at lower bias magnetic field will also be reported.

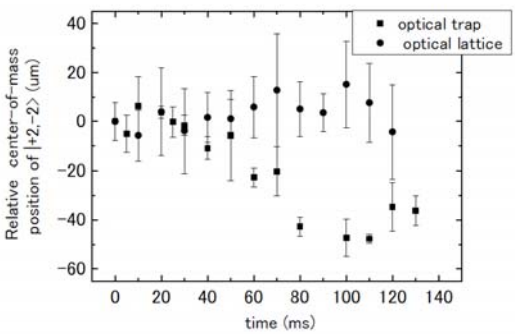

Fig.1: Relative center-of-mass position of |2,+2>+|2,-2> states. Plots represents the average of measurements. Error bars indicate the standard deviation.

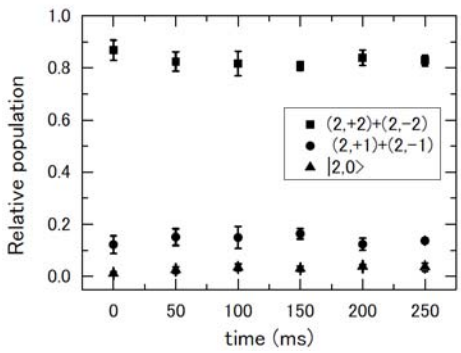

Fig.2: Time-evolution of relative populations of the summation of (2,+2)+(2,-2) atoms (squares), (2,+1)+(2,-1) atoms (circles), and |2,0> (triangle) atoms.

[1] M. Ueda and M. Koashi, Phys. Rev. A **65**, 063602 (2002).
[2] H. Saito and M. Ueda, Phys. Rev. A **72**, 053628 (2005).
[3] S. Tojo *et al*., Appl. Phys. B **93**, 403 (2008).

P87

Mixing dynamics of binary ^{87}Rb Bose-Einstein condensates

Y. Taguchi, T. Tanabe, M. Kurihara, Y. Suzuki, S. Tojo, and T. Hirano

Department of Physics, Gakushuin University, 1-5-1 Mejiro, Toshima-ku, Tokyo 171-8588, Japan

When relative velocity between two Bose-Einstein condensates (BECs) is sufficiently large, it is predict that shear-flow instability arises at the interface between BECs [1]. Miscibility of binary BEC of F = 2 and F = 1 depends on the scattering length. In our previous experiment, we have controlled the scattering length between hyperfine states | F = 2, m_F = -1 > and | 1, 1 > of ^{87}Rb BEC from immiscible to miscible region with Feshbach resonance [2].

Among combinations of F = 2 and F = 1 sublevels, the combination of | 2, -2 > and | 1, -1 > is most sensitive to a magnetic field gradient. Each component is subject to opposite force generated by a magnetic field gradient. As a result, the BECs of | 2, -2 > and | 1, -1 > spatially separate, as was observed in our studies. Then it is possible to make BECs moving opposite directions if we invert a magnetic field gradient. However, the scattering length between | 2, -2 > and | 1, -1 > is uncontrollable. On the other hand, the scattering length between | 2, -2 > and | 1, 0 > can be controlled by Feshbach resonance (these states are expected to be miscible at zero magnetic field [3,4]), and the | 2, -2 > state is sensitive to the magnetic field. In addition, two-body inelastic collision of | 2, -2 > is negligible [5].

We experimentally investigated the dynamics of binary BECs of | 2, -2 > and | 1, -1 > states and | 2, -2 > and | 1, 0 > states. We prepared | 2, -2 > in an optical trap at 20 G of magnetic field. Then half of condensates were transferred to | 1, 0 > by radio-frequency and microwave fields. Magnetic field dependence of atom number of | 2, -2 > and | 1, 0 > is shown in Fig.1. As shown in Fig.1 atom number rapidly decreases near 18.2 G due to Feshbach resonance between | 2, -2 > and | 1, 0 >. Figure 2 shows the time evolution of relative center-of-mass position when a magnetic field gradient was applied. The relative center-of-mass position is the difference between center-of-mass of | 2, -2 > and that of | 1, 0 > after time-of-flight. The result suggests that the binary BEC of | 2, -2 > and | 1, 0 > in the optical trap is spatially separated by a magnetic field gradient. We mix separated binary BEC by opposite magnetic field gradient, and observe mixing dynamics of binary BEC of | 2, -2 > and | 1, 0 >.

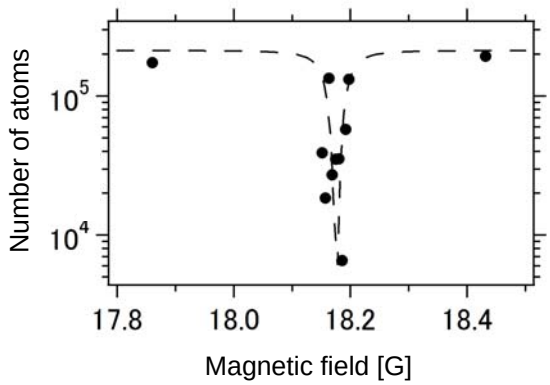

FIG.1: Magnetic field dependence of atom number.

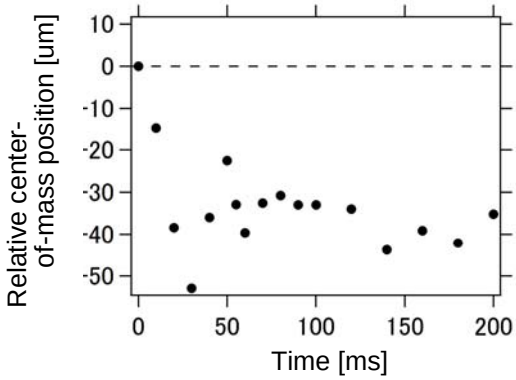

FIG.2: Dependence of relative center-of-mass position on duration time of applied magnetic field gradient.

[1] H. Takeuchi *et al.*, arXiv:0909.2144v1.
[2] S. Tojo *et al.*, 18th International Laser Physics Workshop, 6. 15. 4 (2009).
[3] A. Widera *et al.*, New J. Phys. **8**, 152 (2006).
[4] A. M. Kaufman *et al.*, Phys. Rev. A **80**, 050701(R) (2009).
[5] S. Tojo *et al.*, Phys. Rev. A **80**, 042704 (2009).

P88

Controlling phase separation of binary Bose-Einstein condensates

S. Tojo, T. Tanabe, Y. Taguchi, M. Kurihara, Y. Suzuki, Y. Masuyama, and T. Hirano

Department of Physics, Gakushuin University, Tokyo 171-8588, Japan

Ultracold atomic gases provide an attractive testing ground for studying dynamics of multicomponent quantum fluids. It has been shown that dual-species quantum gases, two- component Bose–Einstein condensates (BECs) comprised of two different hyperfine states, and spinor BECs with different Zeeman sublevels exhibit a rich variety of dynamics [1]. Miscibility between different components is crucially important to the dynamics of muticomponent systems [2]. Feshbach resonance which changes scattering length of corresponding states can control miscibility of two-component BEC [3]. However, there is no report on controlling phase-separation of multi-component BEC in identical species while a magnetic-field Feshbach resonance in mixed hyperfine states was observed at 9.1 G [4]. We have investigated the dynamics of ^{87}Rb binary BEC of $|F=1, m_F=0\rangle$ and $|2,0\rangle$ states (clock states) and $|1,+1\rangle$ and $|2,-1\rangle$ states with Feshbach resonance.

In our experiment, $|2,-2\rangle$ BEC in an optical trap were generated by the crossed far-off resonant laser beams at 3.0G of a homogeneous magnetic field [5,6]. And some part of condensate was transferred to other state by using spin manipulation. We prepared $|2,0\rangle$ and $|1,0\rangle$ state (clock states) or $|2,-1\rangle$ and $|1,+1\rangle$ states using microwave and radio-frequency (rf) fields. In these combinations, especially clock states, the comparison between experimental and theoretical results is easier because of relatively insensitive to the linear Zeeman effect. The power and duration of microwave and rf field were adjusted so that population of F = 1 and F = 2 were equal. After time-evolution at a desired homogeneous magnetic field, the optical trap was turned off and the Stern-Gerlach method was applied in order to separate spin states. Figure 1 shows the absorption images of binary BEC in $|2,-1\rangle$ and $|1,+1\rangle$ states at 50-ms time-evolution. The binary BEC were separating each other with symmetry to avoid overlap when far from Feshbach resonance as shown in Fig.1(a) and (d). Time-evolutions near Feshbach resonance were different as shown in Fig.1(b) and (c) in spite that the number-of-atoms at 9.04 G was almost same as that at 9.16 G. The different miscibility behavior can be caused by the change of scattering length near the Feshbach resonance.

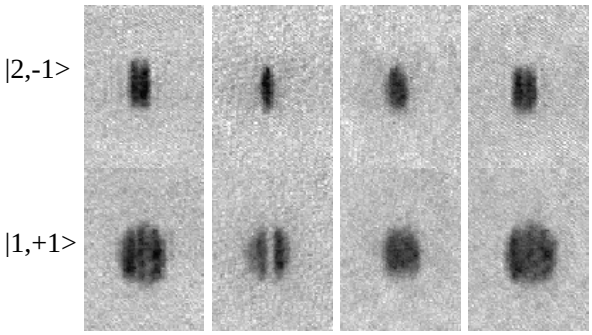

Fig.1: Magnetic field dependence of phase-separations in |2,-1> and |1,+1> states.

[1] For example, A. J. Leggett, Rev. Mod. Phys. **73**, 307 (2001).

[2] D.S. Hall, M.R. Matthews, J.R. Ensher, C.E. Wieman, and E.A. Cornell, Phys. Rev. Lett. **81**, 1539 (1998); K.M. Mertes, J.W. Merrill, R. Carretero-Gonzalez, D.J.Frantzeskakis, P.G. Kevrekidis, and D.S. Hall, *ibid*. **99**, 190402 (2007).

[3] S. B. Papp, J. M. Pino, and C. E. Wieman, Phys. Rev. Lett. **101**, 040402 (2008).

[4] M. Erhard, H. Schmaljohann, J. Kronjäger, K. Bongs, and K. Sengstock, Phys. Rev. A **69**, 032705 (2004).

[5] T. Kuwamoto, K. Araki, T. Eno, and T. Hirano, Phys. Rev. A **69**, 063604 (2004); S. Tojo, A. Tomiyama, M. Iwata, T. Kuwamoto, and T. Hirano, Appl. Phys. B **93**, 403 (2008).

[6] S. Tojo, T. Hayashi, T. Tanabe, T. Hirano, Y. Kawaguchi, H. Saito, and M. Ueda, Phys. Rev. A **80**, 042704 (2009).

P89

Phase separation of multi-component Bose-Einstein condensates induced by a homonuclear Feshbach resonance

R. Shibato,[1] T. Nishimura,[2] T. Watanabe,[1]and T. Suzuki[1]

[1]*Deptment of Physics, Tokyo Metropolitan University, 1-1 Minamioosawa, Hachioji-shi, 192-0397, Japan*
[2]*Division of Advanced Sciences, Ochadai Academic Production,*
Ochanomizu University, Otsuka, Bunkyo-ku, Tokyo 112-8610, Japan

There are much study of multi-component Bose-Einstein Condensations (BECs). One of the reason is that they have rich phase structures because of the interaction between different atoms. We are interested in phase separation phenomena induced by repulsive interaction characterized by the s-wave scattering length. The first observation of phase separation is realized in 1998 with ^{85}Rb -^{87}Rb mixtures [1]. From the realization of Feshbach resonance, it is possible to control the inter-atomic interaction by the magnetic field. This allows us to induce the phase separation state experimentally. Until now, there have been many studies of phase separation induced by Feshbach resonance.

In the present work, we consider homonuclear Feshbach resonance which controls the interaction between same atoms. On the contrary to heteronuclear Feshbach resonance, the phase separation induced by homonuclear Feshbach resonance has not been investigated in detail. We start from two-channel Hamiltonian which includes homonuclear Feshbach molecule's degree of freedom explicitly, and derive two-channel Gross-Pitaevskii (GP) equation to investigate the ground state of the system. Since we want to see how the inter-atomic interaction changes against the number of molecules, we normalize the molecule's degree of freedom into the effective interaction and derive single-channel GP equation. Solving both equations and comparing density profiles, we find no difference between both treatments qualitatively in the case of small number of molecules. Describing the density profile with two-channel GP equation in some molecule number cases, we find the behavior of phase separation (FIG.1). Increasing the number of molecules, one component tend to separate from the center. This result can be interpreted in the term of the effective interaction. Finally, we change the ratio of two atom numbers and show the phase diagram in the plane of molecule number versus atom number ratio.

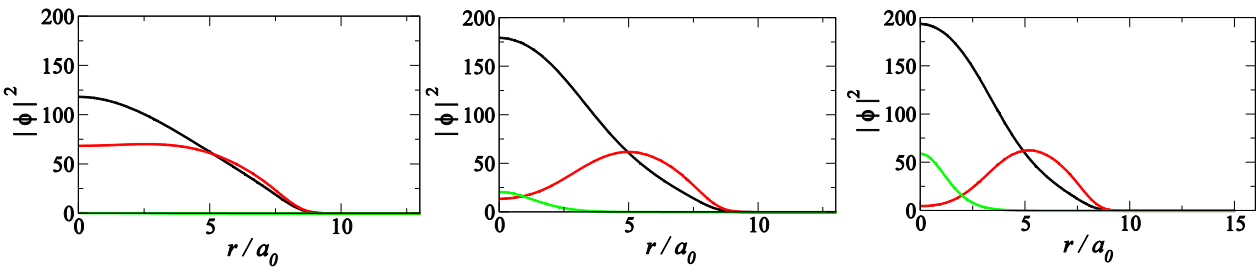

FIG.1: The density profile of two-channel model. We set each number of molecules Nm=100, 1000, 2000, respectively, which can be changed by applying the magnetic field. The number of each atoms is fixed by Na=Nb=100000.

[1] D.S.Hall Phys. Rev. Lett, **81** 1539 (1998)

P90

Cranked-Hartree-Fock-Bogolibov theory for Fragmented Bose-Einstein Condensates

N. Hamamoto,[1] M. Oi,[2] and N. Onishi[3]

[1]*Center for Academic Information Services, Niigata University , 8050 Ikarashi 2-no-cho Niigata 950-2181, Japan*
[2]*Institute of Natural Sciences, Senshu University3-8-1 Kanda Jinbo-cho, Chiyodaku Tokyo 101-8425 , Japan*
[3] *University of Tokyo and Yamanashi University*

Possibility of fragmented Bose-Einstein condensate (FBEC) was discussed first in 1982 by Nozieres et. al. for an infinite system, especially in which several degenerated single-particle states are occupied by a macroscopically large number of Bosons. Their conclusion was, however, that FBEC is quite unstable for *infinite* systems. The realization of BEC in a magneto-optical trap through the laser cooling technique stimulated reinvestigations of the possibility of FBEC for *finite* many-body systems. In fact, Liu et al. performed an exact diagonalization calculation and claimed that a FBEC can be realized for a two-dimensional rotating system in an isotropic harmonic trap [1].

We applied the cranked Hartree-Fock-Bogoliubov (HFB) theory, which was originally developed for nuclear rotation of Ferimi systems, to the study of the yrast state of rotating ultra-cold Bose gases [2]. The cranked HFB is a variational theory with a trial function of a form of $N\exp(1/2 f_{ab} c_a^+ c_b^+)$. Unlike the widely-used Gross-Pitaevskii approach (GPA), the HFB wave function is able to describe fragmented condensates. The ansatz in GPA looks better than the one in HFB from a viewpoint of the variational theory, but it is just a 'pseudo-paradox' as pointed out by Leggett [3]. In fact, two-body correlations and the Fock term are missing in GPA. These entities are important to make it possible to cross over naturally from BEC to super-fluidity.

Although the pseudo-potential of a delta-function type has to be used in GPA, more elaborate finite-range interactions should be responsible for the structure of BEC in reality. With this point of view, we developed a method called the ``valence field expansion", to expand realistic interactions suitable for the mean-field theory. With this approach, we can calculate the yrast state of interacting Bose gases efficiently. As the first step, the valence field expansion is applied to the δ type potential in the deformed trap, in order to check whether our method functions properly. In our poster presentation, a new result is presented to show that the yrast state undergoes a transition from the fragmented BEC to the single BEC, as the trapping potential is deformed. We give an explanation to the transition mechanism through a concept of symmetry breaking and restoration by the trapping potential and the repulsive two-body force.

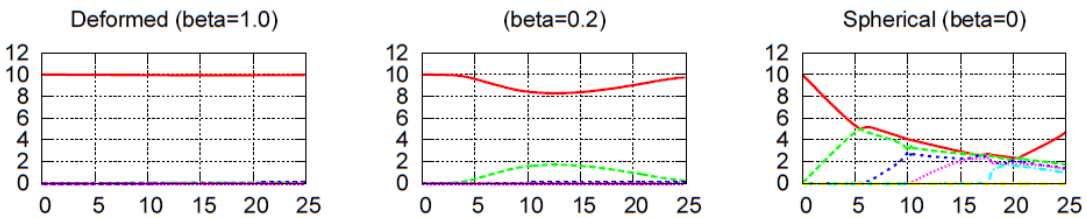

The inverse participation as a function of angular momentum for rotating Bose gases (N=10). Fragmented- and single-BEC appear in the spherical (right) and deformed (left) trap, respectively.

[1]Xia-Ji. Liu *et. al.* Phys. Rev. Lett. **87** 030404 (2001)
[2] N.Hamamoto, M.Oi, N. Onishi, Phys. Rev. A **75**, 063614 (2007)
[3]A.J.Leggett, New J. Phys. **5** 103.1 (2003)

P91

Effect of confinement geometry on imbalanced Fermi condensates

Masaki Tezuka,[1*] Youichi Yanase,[2] and Masahito Ueda[3]

[1]*Dept. of Physics, Kyoto University, Kitashirakawa, Sakyo-ku, Kyoto-shi, Kyoto 606-8502, Japan*
[2]*Department of Physics, Niigata University, 2-8050 Igarashi, Nishi-ku, Niigata 950-2181, Japan*
[3]*Department of Physics, The University of Tokyo, 7-3-1 Hongo, Bunkyo-ku, Tokyo 113-0033, Japan*

Superfluids of ultracold Fermi atomic gases with population difference between two hyperfine species have been realized, but there have been a debate over the role of the trap anisotropy. Results from the MIT [1] and Rice [2] groups have shown significant differences over the validity of local density approximation (LDA) and the upper bound of the imbalance ratio P (P is the ratio of the population difference to the total population) for condensation to occur, the Chandrasekhar-Clogston limit P_{CC}.

In the MIT experiment the density profiles of both majority and minority atoms obey LDA, and the CC limit was observed. In the Rice experiment with a more elongated trap and fewer atoms, the minority atom cloud was markedly deformed, and no CC limit was found. While it has been proposed that a phenomenological surface tension [3, 4] or an non-equilibrium scenario [5] can reproduce the deformation in the Rice experiment, how to reconcile the apparently contradicting experimental results without free parameters has been a target of heated debate.

By solving the Bogoliubov-de Gennes equations with coupling-constant renormalization appropriate for an elongated trapped system with a chemical potential difference [6], we show that P_{CC} does not increase with the trap aspect ratio λ. This is also confirmed by our simulation based on the real-space self-consistent T-matrix approximation (RSTA) [7]. Moreover, while the deformation of the cloud shape from that expected within LDA from the trap shape increases, it stays minor for extreme values of λ. This finding indicates that, despite the apparent discrepancy between the MIT and Rice experiments over the value of P_{CC} and the breakdown of local density approximation, the equilibrium state of the system for the aspect ratio in the Rice experiment would be closer to that of MIT, which is consistent with the recent experimental results of the ENS group [8].

[1] G. B. Partridge *et al*., Phys. Rev. Lett. **97**, 190407 (2006) and references therein.
[2] Y.-I. Shin *et al*., Nature **451**, 689 (2008) and references therein.
[3] T. N. De Silva and E. J. Mueller, Phys. Rev. Lett. **97**, 070402 (2006).
[4] M. Haque and H. T. C. Stoof, Phys. Rev. Lett. **98**, 260406 (2007).
[5] M. M. Parish and D. A. Huse, Phys. Rev. A **80**, 063605 (2009).
[6] M. Tezuka and M. Ueda, arXiv:0811.1650 .
[7] Y. Yanase, J. Phys. Soc. Japan. **73**, 1000 (2004).
[8] S. Nascimbene *et al.*, Phys. Rev. Lett. **103**, 170402 (2009).

* tezuka@scphys.kyoto-u.ac.jp

P92

Quantum-Quench Dynamics of Ultracold Fermions in Optical Superlattice

N. Kawakami,[1] A. Yamamoto,[2] and M. Yamashita[3]

[1]*Department of Physics, Kyoto University, Kyoto 606-8502, Japan*
[2]*Department of Applied Physics, Osaka University, Suita, Osaka 565-0871, Japan*
[3]*NTT Basic Research Laboratories, NTT Corporation, Atsugi, Kanagawa 243-0198, Japan*

We study the time-dependent dynamical properties of two-component ultracold fermions in a one-dimensional optical superlattice by applying the adaptive time-dependent density matrix renormalization group to a repulsive Hubbard model with an alternating superlattice potential [1]. We clarify how the time evolution of local quantities occurs when the superlattice potential is suddenly changed to a normal one (see Fig.1). For a Mott-type insulating state at quarter filling, the time evolution exhibits a profile similar to that expected for bosonic atoms, where atom correlation effects are less important. On the other hand, for a band-type insulating state at half filling, the strong repulsive interaction induces an unusual pairing of fermions, resulting in some striking properties in time evolution, such as a paired fermion co-tunneling process and the suppression of local spin moments. We further address the effect of a confining potential, which causes spatial confinement of the paired fermions.

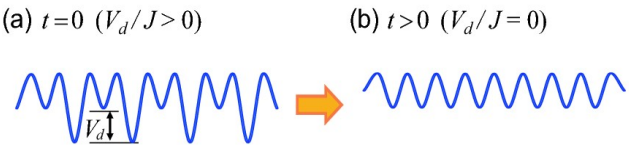

Fig.1: Schematic diagrams of nonadiabatic control of one-dimensional optical superlattice: (a) an initial two-site periodic superlattice with a large potential difference V_d and (b) a normal lattice after a sudden disappearance of V_d for t>0.

Shown in Fig. 2 are some examples of the obtained results: time-dependent local quantities for even and odd sites at half filling. For small repulsive interactions U, all the quantities exhibit characteristic oscillations, reflecting a specific atom configuration of the initial state. When the interaction increases, the oscillations are gradually suppressed. In particular, the variance of spin fluctuations is considerably decreased as U increases, in contrast to the naive expectation that the local spins are developed with increasing U. In this case, the repulsive interaction produces atom pairs, which can hop around the lattice only through a co-tunneling process. This kind of unusual pairing was demonstrated experimentally for bosonic systems, and is expected to be observed for fermionic systems. It is quite interesting to study what happens for such a metastable paired state if we take into account three dimensionality.

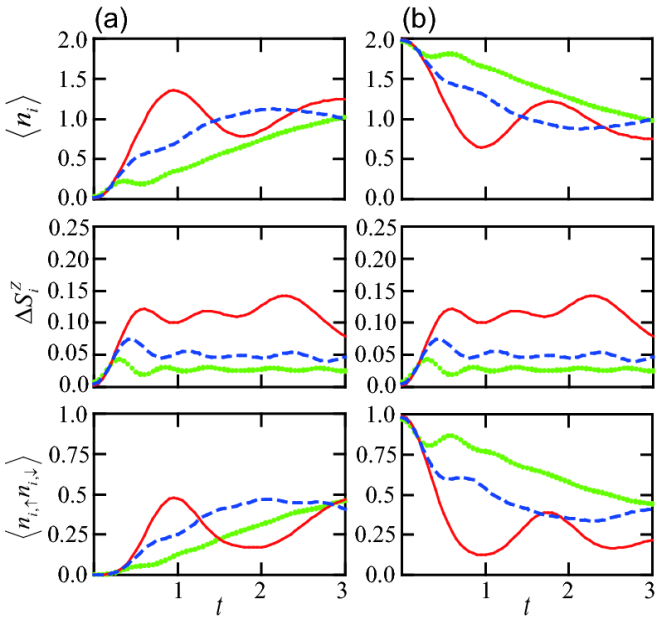

Fig.2: Time dependence of the local quantities for several choices of on-site interaction U for the system at half filling with L=36 and N=18. Plots of the local density , the variance of local spins and the double occupancy from top to bottom. The on-site interaction is chosen as U=1 (solid line), 5 (dashed line), and 9 (dotted line) at (a) i=18 and (b) i=19.

[1] A. Yamamoto *et al.*, J. Phys. Soc. Jpn. **78**, 123002, 124001 (2009)

P93

Equilibrium Properties of a Trapped Dipolar Fermion at Finite Temperatures

Y. Endo,[1] T. Miyakawa,[2] and T. Nikuni[1]

[1]*Department of Physics, Tokyo University of Science, 1-3 Kagurazaka, Shinjuku-ku, Tokyo, Japan, 162-8601*
[2]*Faculty of Education, Aichi University of Education, 1 Hirosawa, Igaya-cho, Kariya, Aichi, Japan, 448-8542*

There is a growing interest in dipolar gases since the realization of Bose-Einstein Condensate (BEC) of ^{52}Cr atoms, which have a large magnetic dipole moment, was experimentally observed [1]. The anisotropic and long-range nature of the dipole-dipole interaction gives rise to rich properties in both equilibrium and dynamics of dipolar gases. On the other hand, a number of experiments proceed energetically toward the realization of creating heteronuclear Fermi polar molecules whose large electric dipole moment brings a strong dipole-dipole interaction [2].

Unlike the dipolar BEC, the dipolar Fermi gas does not interact via s-wave collision and it has both Hartree direct and Fock exchange energies of the dipole-dipole interaction in the mean-field description which reflects the anti-symmetric many-body wave function, and the anisotropic nature of the interaction causes Fermi surface deformation through the Fock exchange energy.

So far most of studies of the dipolar Fermi gas mainly concentrated on zero-temperature properties of the gas and there are few theoretical works on finite temperature. In contrast, despite many groups are conducting the experiments energetically, no groups have succeeded in cooling down polar molecules to their quantum-degenerate region. It is thus important to investigate the temperature range in which the effect of the dipole-dipole interaction can be appreciable. For this reason, we concentrate on the properties of dipolar Fermi gas at finite temperatures.

We study equilibrium properties of a dipolar Fermi gas at finite temperatures. We introduce a variational ansatz for the phase space distribution function, which can describe the deformation in both real and momentum spaces. As in the case at zero-temperature, the anisotropic nature of the dipole-dipole interaction leads to deformation in momentum and real spaces and the partially attraction of the interaction causes instability of the gas against collapse [3]. In addition, we find that the dipolar Fermi gas is compressed in the momentum space with increasing electric dipole moment. We also examine the stability of the system with varying the temperature, trap aspect ratio and the dipole moment and we found that the stable region expands at finite temperatures (FIG.1). These results are useful when the polar molecules are cooled down in experiments. In addition, we also revealed that the deformation in both momentum and real spaces can be observed at high-temperature regime with the larger electric dipole moment and the higher trap frequency.

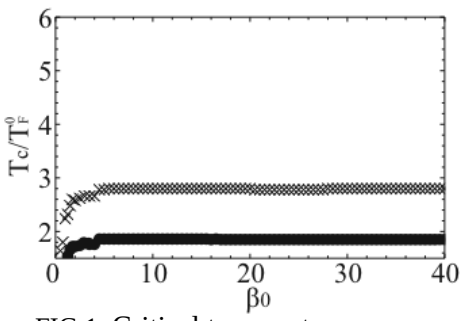

FIG.1: Critical temperature as a function of the trap aspect ratio for the dipole moment p = 3.0 (filled circles) and p = 5.0 (cross mark).

[1] A. Griesmaier, et. al. Phys. Rev. Lett. 94, 160401 (2005).
[2] K. K. Ni, et. al. Science 322, 231 (2008).
[3] T. Miyakawa, et. al. Phys. Rev. A 77, 061603 R (2008).

P94

Three-component Fermionic Atoms in Optical Lattices

S. Suga[1,2] and K. Inaba[3,4]

[1]*Department of Materials Science and Chemistry, University of Hyogo, Himeji 671-2280, Japan*
[2]*Department of Applied Physics, Osaka University, Suita, Osaka 565-0871, Japan*
[3]*NTT Basic Research Laboratories, NTT Corporation, Atsugi 243-0198, Japan*
[4]*JST, CREST, Chiyoda-ku, Tokyo 102-0075, Japan*

Recent progress in the study of cold atoms is remarkable. Research on cold fermionic atoms has been extended to topics that are not found in ordinary condensed matter physics. Recently, a balanced population of attractive ^{6}Li fermionic atoms with three kinds of internal degrees of freedom was successfully created [1,2]. For the attractive three-component (colors) fermionic atoms in optical lattices, it was shown theoretically that atoms with two of the three colors form Cooper pairs, yielding a color superfluid (CSF) [3]. As the strength of the attractive interaction increases, there is a quantum phase transition from the CSF state to the trionic state, where three atoms with different colors form singlet bound states. In contrast to the detailed investigations for zero-temperature properties, little information is available about the finite-temperature properties.

For repulsive three-component fermionic atoms with isotropic interactions on a square lattice, it was shown theoretically that the color density-wave (DW) state appears at half filling, where pairs of atoms with two of the three colors and atoms with the third color occupy different sites alternately [4]. Repulsive ^{173}Yb fermionic atoms were successfully cooled to form degenerate Fermi gases [5]. Since its nuclear spin is I=5/2, ^{173}Yb atoms may be a candidate for realizing three-component repulsive fermionic atoms in optical lattices. In real systems, the interactions are not necessarily isotropic. However, our knowledge of the anisotropic interaction effects are still insufficient.

Motivated by these situations, we investigate three-component fermionic atoms in optical lattices. For the attractive interaction system, we investigate finite-temperature properties using a self-energy functional approach [6]. As the strength of the attractive interaction increases in the low temperature region, we observe a second order transition from a Fermi liquid (FL) to a CSF. In the strong attractive region, we observe a first order transitions from a CSF to a trionic state. A crossover between a FL and a trionic state is observed in the high temperature region. We present a phase diagram covering zero to finite temperatures as shown in the figure. We also demonstrate that the CSF transition temperature is enhanced by the anisotropy of the attractive interaction.

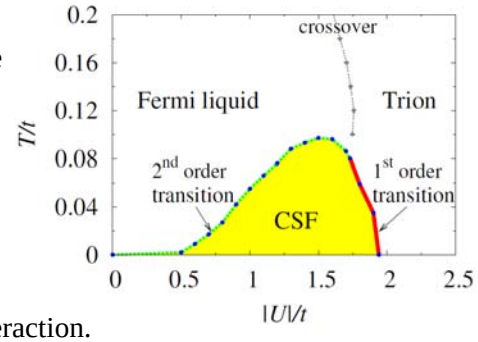

For the repulsive interaction system, we investigate the anisotropic interaction effects using a two-site dynamical mean field theory [7]. Depending on the anisotropy of the repulsive interactions, either a color DW state or a color selective antiferromagnetic (CSAF) state appears at half filling. In the latter state, atoms with two of the three colors occupy different sites alternately and atoms with the third color are itinerant throughout the system. We calculate the order parameters of both states across the SU(3) isotropic point. We find a hysteresis as a function of the anisotropy of the repulsive interaction, implying a discontinuous quantum phase transition. We confirm that the energies of both states cross at the SU(3) point. The results indicated that, when the interactions are isotropic, the color DW state and the CSAF state are degenerate. The results are discussed using an effective model: a Falicov-Kimball model.

[1] T. B. Ottenstein, *et al*, Phys. Rev. Lett. **101**, 203202 (2008).
[2] J. H. Huckans, *et al*, Phys. Rev. Lett. **102**, 165302 (2009)
[3] A. Rapp, *et al*, Phys. Rev. Lett. **98**, 160405 (2007); Phys. Rev. B. **77**, 144520 (2008)
[4] C. Honerkamp and W. Hofstetter, Phys. Rev. Lett. **92**, 170403 (2004).
[5] T. Fukuhara, *et al*, Phys. Rev. Lett. **98**, 030401 (2007).
[6] K. Inaba and S. Suga, Phys. Rev A **80**, 041602(R) (2009).
[7] S. Miyatake, K. Inaba and S. Suga, Phys. Rev. A **81**, (2010) accepted as Rapid Communication.

P95

Excitation Spectrum of a Bose-Bose mixture in an Optical Lattice

T. Ozaki, I. Danshita, and T. Nikuni

[1]*Department of Physics, Tokyo University of Science, 1-3 Kagurazaka, Shinjuku-ku, Tokyo, 162-8601, Japan*

Systems of ultracold Bosonic atoms in an optical lattice have attracted attention to study strongly correlated quantum matter. One of the most interesting phenomena exhibited by ultracold Bosonic atoms in an optical lattice is superfluid (SF) to Mott insulator (MI) phase transition, as experimentally observed [1]. The properties of this system can be well captured by Bose-Hubbard model.

Adding the second atomic species, the system can exhibit rich quantum phases. Theoretically, in addition to the ordinary SF phase and MI phase, supersolid, pair superfluid and counterblow superfluid (CFSF) phases have been predicted to exist [2]. Recently, some experimental groups have been experimentally realized two-component ^{87}Rb [3] and ^{87}Rb-^{41}K [4] mixtures trapped in an optical lattice. However, the predicted quantum phases have not been found experimentally.

We study the properties of a Bose-Bose mixture in an optical lattice at zero temperature by using Bose-Hubbard model for Bose-Bose mixtures. Especially, we consider the case of repulsive inter-species interaction. First, we obtain the ground-state phase diagram using the Gutzwiller mean-field approach. We determine the phase boundaries between different phases, such as MI phase, SF phase and CFSF phase. Second, we use the dynamical Gutzwiller approach to calculate excitation spectrum to identify the quantum phases. We derive the expression for Bogoliubov equations, and calculate the excitation spectrum in different phases.

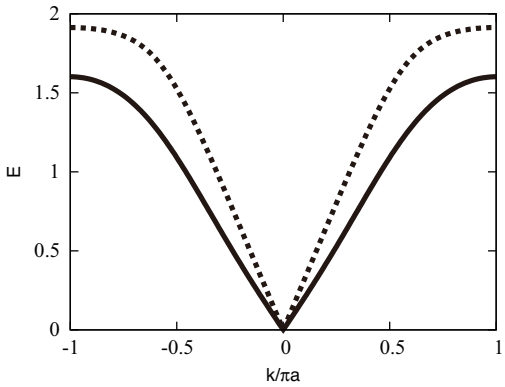

Fig. 1. Excitation spectrum in the SF phase.

[1] M. Greiner *et al.*, Nature, **415**, 39 (2002)
[2] A. Kuklov *et al.*, Phys. Rev. Lett. **92**, 050402 (2004).
[3] A. Widera *et al.*, Phys. Rev. Lett. **100**, 140401 (2008).
[4] J. Catani *et al.*, Phys. Rev. A, **77**, 011603(R) (2008).

P96

Tunneling Problems of Excitations in Spin-1 Bose-Einstein Condensates

Shohei Watabe[1] and Yusuke Kato[2]

[1]*Institute of Physics, The University of Tokyo, 3-8-1, Komaba, Meguro-ku, Tokyo 153-8902, Japan*
[2]*Dept. of Basics Science, The University of Tokyo, 3-8-1, Komaba, Meguro-ku, Tokyo, 153-8902, Japan*

Features of quantum many-body systems appear in non-uniform systems. In a weakly interacting condensed Bose system, an excitation in the low energy limit shows the total transmission against a potential barrier [1]. A single particle obeying the Schrodinger equation shows the total reflection in the low energy limit, contrary to the excitation in the weakly interacting condensed Bose system. To understand this phenomenon in detail, it is needed to study the tunneling problems of excitations in Bose-Einstein condensates (BECs) in more general situations.

With these backgrounds, we study tunneling problems of excitations in spin-1 BECs [2,3]. We found that all excitations except a quadrupolar spin mode in the ferromagnetic phase show the total transmission against the potential barrier. Extending the problem to that of reflection and refraction in junction of BECs with different densities, we obtained transmission and reflection coefficients of the Bogoliubov excitation and of the spin wave in the ferromagnetic phase. The Bogoliubov excitation shows the partial transmission with refraction, showing the Brewster's law studied in the electromagnetic waves [3,4]. The spin wave in the ferromagnetic phase shows the partial transmission without refraction. We show that these transmission and reflection coefficients are written in terms of amplitudes of order parameters in the asymptotic regime, which are independent of the potential barrier.

[1] D. L. Kovrizhin, Phys. Lett. A **287**, 392 (2001). Yu. Kagan, D. L. Kovrizhin, and L. A. Maksimov, Phys. Rev. Lett. **90**, 130402 (2003).
[2] S. Watabe, and Y. Kato, J. Low Temp. Phys. **158**, 23 (2010).
[3] S. Watabe, and Y. Kato, Phys. Rev. A **78,** 063611 (2008).
[4] S. Watabe, Doctor Thesis (The University of Tokyo, 2010).

P97

Interface instabilities in two-component Bose-Einstein condensates

Naoya Suzuki, Kazuki Sasaki, and Hiroki Saito

Department of Applied Physics and Chemistry,
University of Electro-Communications, Tokyo 182-8585, Japan

We study interfacial instabilities in phase-separated two-component Bose-Einstein condensates. There are various interfacial instabilities in classical fluids, among which we focus on the Kelvin-Helmholtz (KH) instability and the Rayleigh-Taylor (RT) instability.

The KH instability occurs when there is shear flow between two fluids, which is closely related to various phenomena, such as wind-generated ocean waves, flapping flags, and billow clouds. The KH instability in superfluid ^{3}He has been observed. Here, we propose possible experimental setups for observing the KH instability in a trapped BEC. We consider axisymmetric interface in counterrotating two-component BECs in a pancake-shaped trap, in which the KH instability is observed as axisymmetry breaking. The snapshots of the dynamics are shown in Fig. 1.

The RT instability occurs at the interface between two fluids, when one fluid is pushing the other fluid. For example, when oil heavier than water is floating above water, their interface is deformed by the RT instability. Figure 2 shows a two-component BEC, in which one component is pushed to the other. We see a mushroom-cap pattern formed by the RT instability.

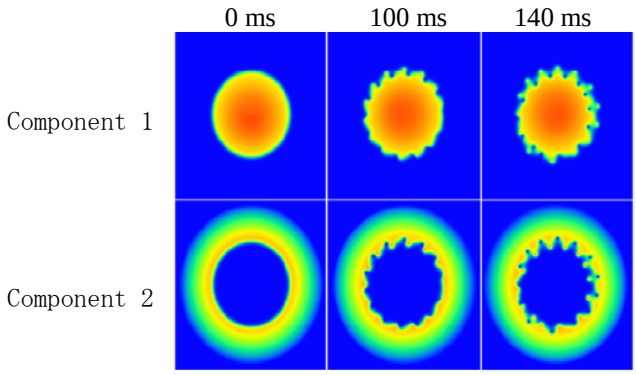

Fig. 1: The Kelvin-Helmholtz instability in quasi-2D BECs, where component 2 is rotating.

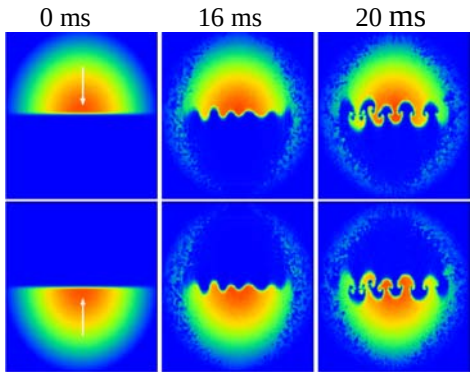

Fig. 2: Interface pattern formed by the Rayleigh-Taylor instability. Component 1 is pushed upward by field gradient.

[1] H. Takeuchi, N. Suzuki, K. Kasamatsu, H. Saito, and M. Tsubota, arXiv:0909.2144

[2] K. Sasaki, N. Suzuki, D. Akamatsu, and H. Saito, Phys. Rev. A **80**, 063611 (2009)

P98

Transmission properties of Bogoliubov excitations near and at the critical current state

Daisuke Takahashi and Yusuke Kato

Department of Basic Science, University of Tokyo, Tokyo 153-8902, Japan

The condensate wavefunction described by Gross-Pitaevskii equation (nonlinear Schrödinger equation) has supercurrent solutions across a potential barrier, if the velocity (or equivalently, magnitude of the current) of the condensate is less than a critical value, which should be determined from the shape of potential. We refer the state with maximum supercurrent as “critical current state”. Near the critical current state, it is known that various kinds of physical quantities, e.g., magnitude of complex eigenvalue of Bogoliubov equations in unstable stationary state, or period of soliton emission in non-stationary state, obey some scaling laws[1,2]. These scaling properties are understood by bifurcation theory of dynamical systems, and the critical current state is identified as a bifurcation point.

In the presence of potential barrier and the condensate current stated above, we have studied the transmission and reflection problems of Bogoliubov excitations[3,4], particularly focusing on the critical current state. We have exactly proved the disappearance of perfect transmission in the critical current state, and clarified that its physical origin is the emergence of zero-energy density fluctuation [5]. Furthermore, we recently have found that transmission coefficient near the critical current state shows scaling properties. In our poster, we discuss these recent developments on transmission and reflection properties of Bogoliubov excitations.

[1] C.-T. Pham and M. Brachet, Physica D **163**, 127 (2002).
[2] V. Hakim, Phys. Rev. E **55**, 2835 (1997).
[3] Yu Kagan, D. L. Kovrizhin, and L. A. Maksimov, Phys. Rev. Lett. **90**, 130402 (2003).
[4] I. Danshita, N. Yokoshi, and S. Kurihara, New J. Phys. **8**, 44 (2006).
[5] D. Takahashi and Y. Kato, J. Phys. Soc. Jpn. **78**, 023001 (2009); J. Low Temp. Phys. **158**, 65(2010).

P99

Thermalization of Atom-Molecule Bose gases in a Double-Well Potential

A. Motohashi, T. Nikuni

[1]*Dept. of Physics, Faculty of Science, Tokyo University of Science, 1-3 Kagurazaka, Shinjuku-ku, Tokyo, Japan*

Bose-Josephson junction(BJJ) is one of ideal experimental setup for macroscopic quantum phenomena, which is an isolated quantum system[1]. In this study, we investigate the dynamics of a two-component Bose-Josephson junction composed of atom-molecule mixture gases. Increasing atom-molecule internal tunneling strengths, we show that this system exhibits non-periodic chaotic motions in a semi-classical limit. In this chaotic system, the level statistics of quantum counterpart represents a wigner distribution[2].

Recently, M. Rigol *et al*. showed that quantum chaotic dynamics in a generic quantum system is related to thermalization[3]. However, they do not fully investigate the effect of quantum fluctuations.

In BJJ, the strength of quantum fluctuations can be controlled by changing the total particle number. We investigate the influence of quantum fluctuations on quantum chaos and thermalization.

[1] M. Albiez *et al*., Phys. Rev. Lett. **95**, 010402 (2005).
[2] A. Motohashi and T. Nikuni, J. Low Temp. Phys. **158**, 72 (2010).
[3] M. Rigol *et al*., Nature 452, 854-858 (2008)

P100

D-branes in Bose-Einstein condensates

K. Kasamatsu,[1] H. Takeuchi,[2] M. Nitta,[3] and M. Tsubota[2]

[1]*Department of Physics, Kinki University, Higashi-Osaka, 577-8502, Japan*
[2]*Department of Physics, Osaka City University, Sumiyoshi-Ku, Osaka 558-8585, Japan*
[3]*Department of Physics, and Research and Education Center for Natural Sciences, Keio University, Hiyoshi 4-1-1, Yokohama, Kanagawa 223-8521, Japan*

Dirichlet (D-) branes were found as non-perturbative solitonic states of string theory, on which open fundamental strings can terminate with the Dirichlet boundary condition. Here, we show that wall-vortex composite solitons, analogues of D-brane, can be realized in rotating phase-separated two-component Bose-Einstein condensates (BECs) and they are experimentally observable. The structure is analyzed by the generalized nonlinear sigma model for the pseudospin of this system [1]. The domain wall is identified as a D2-brane to which vortices are attached via `tHooft-Polyakov monopoles (hedgehogs), namely, *boojums*, a point defect at the interface with well-defined boundary conditions [2].

[1] K. Kasamatsu, M. Tsubota, M. Ueda, Phys. Rev. A **71**, 043611 (2005).
[2] G. E. Volovik: *The Universe in a Helium Droplet* (Clarendon Press, Oxford, 2003)

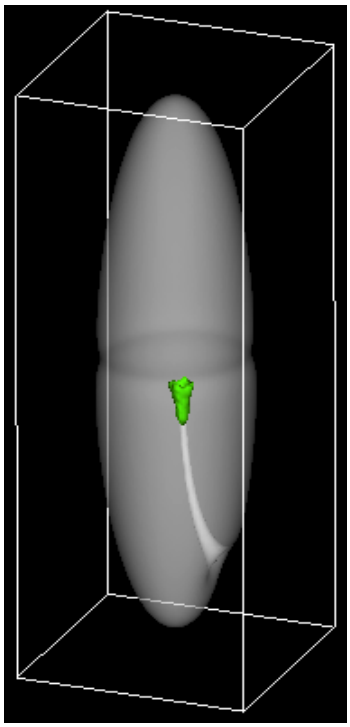

FIG.1: D-brane soliton in two-component BECs

P101

Efimov physics with three lithium atoms

Pascal Naidon[1], Masahito Ueda[1,2]

[1]ERATO Macroscopic Quantum Project, JST Tōkyō, 113-8656, Japan
[2]Department of Physics, University of Tōkyō, 7-3-1 Hongō, Bunkyō-ku 113-0033, Japan

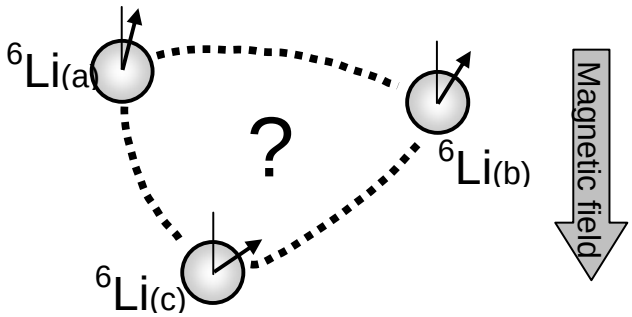

Nuclear physicist Vitaly Efimov predicted 40 years ago remarkable universal properties of the three-body systems with very strong short-range interaction, in particular the existence of special 3-body bound states whose binding mechanism cannot be explained classically. A few years ago the existence of those states were finally discovered in cold atomic gases. In particular, the case of a 3-component fermionic lithium 6 gas revealed several interesting Efimov features [1,2,3] which we analysed. While those features are qualitatively consistent with the universal predictions, they also present some non-universal deviations.

References

[1] T. B. Ottenstein et al., Phys. Rev. Lett. **101**, 203202 (2008).
[2] J. H. Huckans et al., Phys.Rev.Lett.**102,** 165302 (2009).
[3] P. Naidon & M. Ueda, Phys. Rev. Lett. **103** 073203 (2009).

P102

Kelvin Helmholtz Instability in Atomic Bose-Einstein Condensates

Hiromitsu Takeuchi,[1] Naoya Suzuki,[2] Kenichi Kasamatsu,[3] Hiroki Saito,[2] Makoto Tsubota[1]

[1]*Department of Physics, Osaka City University, Sumiyoshi-ku, Osaka 558-8585, Japan*
[2]*Department of Applied Physics and Chemistry, University of Electro-Communications, Tokyo 182-8585, Japan*
[3]*Department of Physics, Kinki University, Higashi-Osaka, Osaka 577-8502, Japan*

Interface between two fluids with a sufficiently large relative velocity is dynamically unstable to form wavy patterns. This instability is known as the Kelvin-Helmholtz instability (KHI) [1], which is closely related to various phenomena, such as wind-generated ocean waves, flapping flags, billow clouds, and sand dunes. Because of its broad applicability, KHI has been discussed for different types of flows including quantum fluids [2].

In this work, KHI in superfluid is theoretically studied and numerically examined in phase-separated two-component Bose-Einstein condensates (BECs) with shear flow [3]. The dynamic and thermodynamic stability of the shear flow states are investigated with the Bogoliubov-de Gennes models, compared with an analytic model. The nonlinear dynamics is revealed by numerically solving the GP equations. When the relative velocity between the two condensates exceeds the critical velocity for dynamic instability, the interface modes with complex frequencies are amplified leading to the formations of singly-quantized vortices. Such a nonlinear dynamics is quite different from that in KHI in classical fluid.

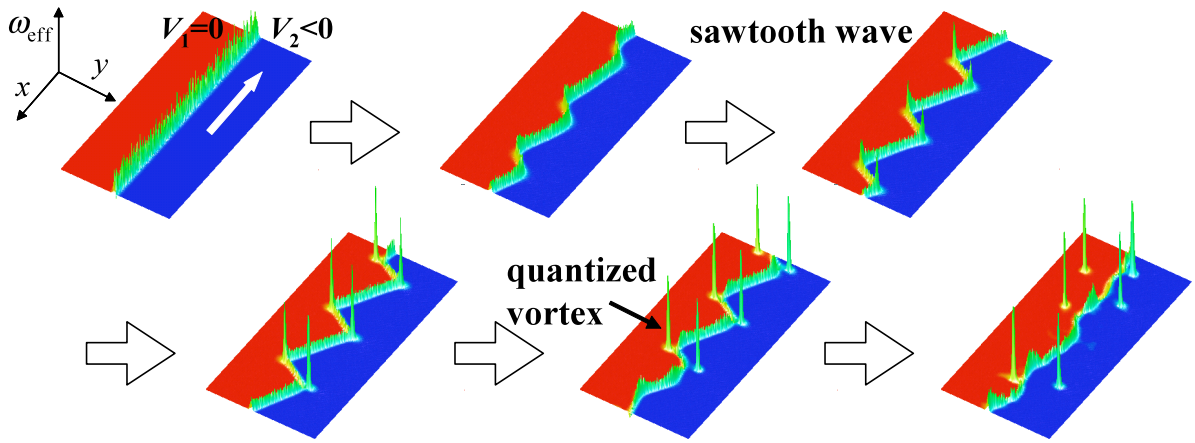

FIG 1: Nonlinear dynamics of KHI in a two-component BEC. The height and color show the vorticity w_{eff} and the density difference between the two condensates, respectively.

[1] See, for example, P. K. Kundu and I. M. Cohen, *Fluid Mechanics*, 4th ed. (Academic Press, New York, 2008).
[2] R. Blaauwgeers, V. B. Eltsov, G. Eska, A. P. Finne, R.P. Haley, M. Krusius, J. J. Ruohio, L. Skrbek, and G. E.Volovik, Phys. Rev. Lett. **89**, 155301 (2002).
[3] Hiromitsu Takeuchi, Naoya Suzuki, Kenichi Kasamatsu, Hiroki Saito, Makoto Tsubota, arXiv:0909.2144.

P103

Theory of photoemission spectroscopy of Fermi gases in the BCS-BEC crossover

S. Tsuchiya,[1,2] R. Watanabe,[1] and Y. Ohashi[1,2]

[1]*Dept. of Physics, Keio University, 3-14-1 Hiyoshi, Kohoku-ku, Yokohama-shi, Kanagawa 223-8522, Japan*
[2]*JST(CREST), 4-1-8 Honcho, Saitama 332-0012, Japan*

We address recent photoemission experiments on ultracold Fermi gases by the JILA group. Extending the recently developed T-matrix approximation for a homogeneous Fermi gas [1], we investigate strong-coupling effects on single-particle excitation spectra in trapped Fermi gases in the BCS-BEC crossover. We calculate the momentum-resolved tunneling current into another hyperfine state, as well as the single-particle spectral weight (SW) and density of states (DOS) including effects of trapping potentials by a local density approximation. We clarify the spatial and temperature dependence of SW and DOS, and find that they exhibit the pseudogap behavior around the center of the trap. We find the spatially averaged spectral weight shows a very good agreement with the measured excitation spectra. We also discuss interpretations of experimental results.

[1] S. Tsuchiya *et al*., Phys. Rev. A **80**, 033613 (2009).

P104

Ultracold Fermi Gases of Ytterbium in Optical Lattices

Shintaro Taie,[1] Seiji Sugawa,[1] Rekishu Yamazaki,[1,2] and Yoshiro Takahashi[1,2]

[1]*Department. of Physics, Kyoto University, Kitashirakawa Oiwake-cho, Sakyo-ku, Kyoto 606-8502, Japan*
[2]*JST-CREST, 4-1-8 Honcho Kawaguchi, Saitama 332-0012, Japan*

The achievement of quantum degeneracy in ultracold atomic gases has opened a new research field of quantum many-body physics. They not only serve as quantum simulators of theoretical models in condensed matter physics, but also are the promising systems to investigate the novel quantum physics, where there is no counterpart in the traditional condensed matters.

Ytterbium (Yb) has no electronic spin in the ground state, and therefore, its spin degree of freedom originates from the nuclear spin *I*. The collisional properties of ultracold atoms are mainly determined by the electronic states of two colliding atoms, thus Yb has the same scattering length independent of its nuclear spin states. In this case, the symmetry of the spin space of Yb is extended from the usual SU(2) to SU(2*I*+1) symmetry. Recently, such systems attract theoretical interests and the presence of various quantum phases are predicted [1]. Two fermionic isotopes of Yb (^{171}Yb: I=1/2, ^{173}Yb: I=5/2) are the good candidates for investigating these novel quantum phases where the spin degree of freedom plays an essential role.

We carry out the series of experiments on the ultracold Fermi gases of ytterbium in the optical lattices. First, we study the behavior of ^{171}Yb in a three-dimensional optical lattice. The scattering length of ^{171}Yb equals -0.15nm and can be regarded as “non-interacting” system. As the lattice depth is increased, the quasimomentum distribution of ^{171}Yb fills up the entire 1st Brillouin zone and thus the system exhibits insulating behavior. Furthermore, the dynamics of ^{171}Yb in an optical lattice is also investigated. In the presence of gravity, a pure ^{171}Yb gas in the lattice shows clear Bloch oscillations. On the contrary, in the mixture with ^{173}Yb which strongly interacts with ^{171}Yb ($a_{171\text{-}173}$=-30.6nm), the strong suppression of Bloch oscillations is observed. Interpretation of the results, including the formation of the confinement-induced molecule due to the presence of the lattice, is discussed.

As the first step toward the experimental study of Fermi gases with the SU(6) symmetry, we are currently working toward the realization of an SU(6) Mott insulator of ^{173}Yb. The double occupancy measurement via photoassociation in the lattice is showing a sign of the formation of the incompressible Mott plateau. Further exploration is needed for the confirmation.

In this poster, we will report the latest results of these experiments.

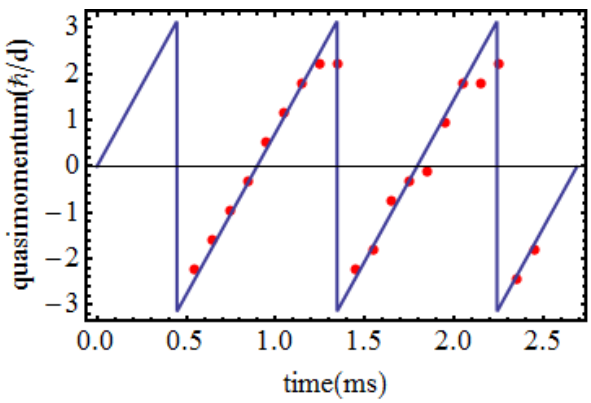

Fig.1 The Bloch oscillation of ^{171}Yb in quasimomentum space. The characteristic saw-shape oscillation is clearly visible.

[1] M. Hermele, *et al*., PRL **103**, 135301 (2009); A. V. Gorshkov, *et al*., arXiv:0905.2610 (2009); M. A. Cazalilla, et al., N. J. Phys **11**, 103033 (2009).

P105

Frictional Motion of Superfluid ^{3}He Normal Fluid Component in Aerogel

K. Obara[1], C. Kato[1], T. Matsukura[1], H. Yano[1], O. Ishikawa[1], T. Hata[1], S. Higashitani[2] and K. Nagai[2]

[1]*Department of Physics, Osaka City University, Sumiyoshi-ku, Osaka 558-8585, Japan*
[2]*Faculty of Integrated Arts and Sciences, Hiroshima University,Kagamiyama 1-7-1, Higashi-Hiroshima 739-8521, Japan*

We have studied the superfluidity of liquid ^{3}He in the high porosity (99.0%) aerogel as an impurity by means of the fourth sound resonance method. The fourth sound is a compression wave propagating through the *superleak* that blocks the motion of the normal fluid component due to its finite viscosity and allows only the superfluid component to pass through. The superfluid density fraction can be obtaind directry from the resonance frequency. At the same time, the fourth sound resonance can drive the normal fluid motion slightly in order to compensate the total pressure gradient and rises the energy loss, which can be obtaiend from the shape of the resonance spectrum.

As shown in FIG 1(A), both transition temperature and the superfluid fraction has been found to be suppressed because of the pair breaking effect. The density of states of quasiparticles (DOS $n(\varepsilon)$) was calculated by using well known Abrikosov-Gor'kov's formula, revealing the finite density of states well below the gap edge. This isolated impurity band is the one of the significant point for the higher porosity aerogel: the impurity band for 98% aerogel extends up to the gap edge [1]. Despite the finite energy gap, the superfluid density fraction is not unity at $T = 0$. From the resonance spectra, we found that the energy loss Q^{-1} in the resonator including aerogel is smaller than that of in pure superfluid resonator, as show in FIG.1 (B). This is puzzling in following two sense: first, the amount of normal fluid component ρ_n in the aerogel is larger than pure ^{3}He. And second, since the viscosity η is protpotional to the viscous mean free path of the quasiparticles, the effective viscosity should decrease. Therefore, the viscous penetration depth $\sqrt{2\eta/\rho_n\omega}$ should shrink and the effective amount of the movable normal fluid component should increase in the aerogel compared with pure ^{3}He. As a consequence, the flow field of the normal fluid component $\boldsymbol{v}_n$ changes from palabolic (Hagen-Poiseuille type) to flat (like Drude's electron in conventional metals) [2]. Taking these effects into the hydrodynamic theory[3], the energy loss in the aerogel should be larger than pure case. The next question is why not the first sound resonace have been realized but the fourth sound inspite of the short penetration depth? To solve the questions above, we propose that the dissipation mechanism changes from the conventional viscous type to the frictional type whose origin is the momentum transfer from quasiparticles to the aerogel. The drag force $\boldsymbol{F}_d$ acting on the normal fluid component motion and the energy loss due to its drag can be written as[4],

$$\boldsymbol{F}_d = \lim_{|\boldsymbol{v}_a|\to 0}\frac{\rho_n}{\tau_f}(\boldsymbol{v}_n - \boldsymbol{v}_a)\ ,\ \ Q^{-1} = \left(\frac{\rho_n}{\rho_s}\right)\omega\tau_f,$$

here, $\boldsymbol{v}_a$ is the velocity of the aerogel strands. This is not the surface effect but the bulk effect. The temperature dependence of the frictional relaxation time τ_f that we measured is well reproduced by the numerical calculation qualitatively, holding our proposal. We found that the relaxation time becomes very short at the lowest temperature, revealing that the residual normal componentis tightly bounded to the aerogel chains by the frictional force.

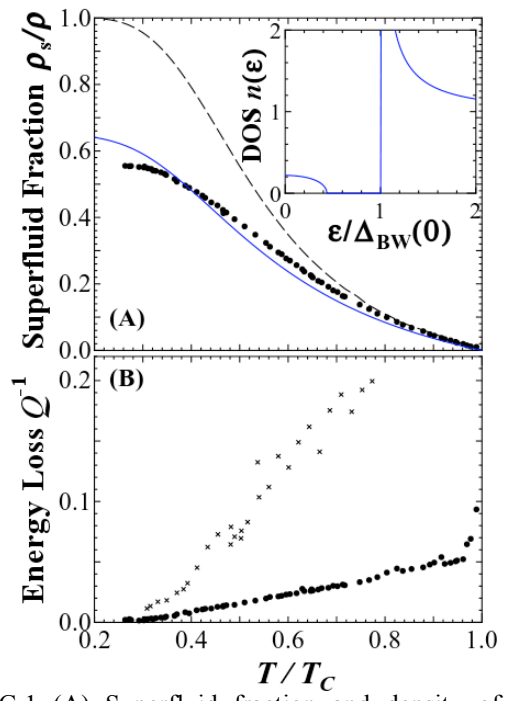

FIG.1 (A) Superfluid fraction and density of states. Tc = 2.20 mK. Solid and dashed line represents numerical calculation using AG formula and pure ^{3}He, respectively. (B) Energy loss of the 4th Sound resonance in aerogel. The x symbol shows the pure case.

[1] P. Sharma and J. Sauls, J. Low Temp. Phys. **125**, 115 (2001), [3] H.H. Jensen, et.al., J. Low Temp. Phys. **51**, 81 (1983)
[2] D. Einzel, et.al., Phys. Rev. Lett., 81, 3896 (1998), [4] S. Higashitani, et. al., Phys. Rev. B **71**, 134508 (2005)

P106

Phase Separation in A-like and B-like Phase of Superfluid ^{3}He in Aerogel

R. Kado [A], R. Toda [B, C], M. Kanemoto [B], W. Onoe [B], T. Kakuda [B], Y. Tanaka [B], K. Obara [A], H. Yano [A], O. Ishikawa [A], T. Hata [A], and Y. Sasaki [B, C]

[A] *Graduate School of Science, Osaka City University, Osaka 558-8585, Japan.*
[B] *Department of Physics, Graduate School of Science, Kyoto University, Kyoto 606-8502, Japan.*
[C] *LTM Center, Kyoto University, Kyoto 606-8502, Japan.*

Superfluid ^{3}He immersed in aerogel is attracting interests of researchers to study the effect of impurity scattering in the novel spin pairing system. Previously, we observed that the A-like and the B-like phase appear at 2.4 MPa in 97.5 % porosity cylindrical aerogel. On cooling, the A-like phase is converted into the B-like phase gradually within the range of a few hundreds μK. By applying a field gradient, which changes as a function of square of radius, we found that the A-like phase located on the rim of cylinder, while the B-like phase located on the central part as a column.

To further clarify this coexistent state, we started an MRI study at Kyoto University as collaboration between Kyoto and OCU, on superfluid 3He in 98.0% porosity cylindrical aerogel at 2.4 MPa. The similar coexistent state as that in 97.5 % porosity aerogel is observed. Through the MRI measurements, we find that there is an unexpected bulk liquid between aerogel and surrounding glass tube, which are supposed to have no gap between them. A distribution of A-like phase and B-like phase in this experiment different from the previous OCU result with 97.5% aerogel. The A-like phase located on the central part as a column, while the B-like phase located on the rim of cylinder. We considered that the reason of this difference is from the different boundary condition.

P107

Fourth Sound Resonance of Superfluid ^{3}He in Slab Geometry

C. Kato, S. Sasamoto, K. Obara, H. Yano, O. Ishikawa, and T. Hata

Graduate School of Science, Osaka City University, Osaka 558-8585, Japan

We are now performing the fourth sound resonance experiment of superfluid 3He confined in the slabs between parallel plates. The fourth sound is a compression wave propagating through the superleak that blocks the motion of the normal fluid component due to its finite viscosity and allows only the superfluid component to pass through. In an ideal superleak, the normal fluid component is completely rocked, so that only the superfluid component is able to move. In this sense, the fourth sound resonance is non-dissipative. But in a reality, the viscosity is not high enough to rock the normal fluid completely, so that the normal fluid component is able to move slightly and its minute oscillation causes the energy loss. The energy loss of the resonance can be obtained from the shape of the resonance spectrum.

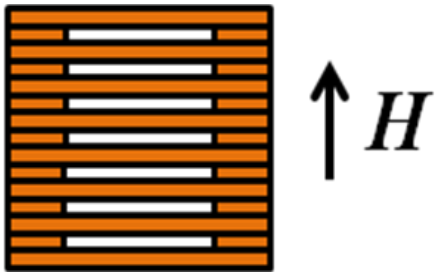

FIG.1: Schematic draw of section of parallel plate. Sound oscillation propagates in a direction normal to paper. Thickness of each slab is 12 or 25 μm.

In order to study an anisotropic superfluid ^{3}He-A, it is important to investigate the spatial variations of the ℓ-vector which is the order parameter of ^{3}He-A that is called the ℓ-texture. The ℓ-texture is not uniquely defined in a free space without any field. But there are some possible constraints that are able to give artificially; first is the geometrical restriction that the ℓ-vector must align its orientation normal to the wall. Second is that the ℓ-vector tends to be perpendicular to the magnetic field. So we have developed the slab geometry between the parallel plates as shown schematically in Fig. 1. The thickness of each slab is 12 or 25 μm, which is enough wider than the superfluid coherence length. Neither the superfluid transition temperature nor the superfluid density are supposed to be suppressed. The magnetic field ***H*** is fixed normal to the slab. It means that there is an orientational competition: the steady state of ℓ-vector orientation at the middle of the slab is non-trivial. There was a fourth sound resonance experiment using the slab geometry[1], but they could not show the energy loss because the quality of the resonance spectrum is not high enough. We have developed the high sensitivity transducer and have got over this problem.

Although there is a theoretical treatment describing the energy loss of the fourth sound in B phase[2], there is none in A phase. This work becomes the pioneering work previous to the theory. Since the fourth sound resonance can drive the normal fluid component directly, it is possible to study the interaction between the ℓ-vector and the normal-fluid flow by changing the direction of the magnetic field. We will show the preliminary result at the poster session.

[1] H. Kojima *et.al.*, J. Low Temp. Phys. **21**, 283 (1975)
[2] H. H. Jensen *et.al.*, J. Low Temp. Phys. **51**, 81 (1983

P108

Measurements of Transverse Acoustic Impedance of Superfluid ^{3}He in Non-Unitary Phases at High Magnetic Fields

S. Murakawa[1], A. Yamaguchi[2], M. Arai[1], M. Wasai[1], Y. Aoki[1], H. Ishimoto[2], R. Nomura[1], and Y. Okuda[1]

[1]*Department of Condensed Matter Physics, Tokyo Institute of Technology, 2-12-1 O-okayama, Meguro-ku, Tokyo 152-8551, Japan*
2Institute for Solid State Physics, University of Tokyo, 5-1-5 Kashiwanoha, Kashiwa-shi, Chiba 277-8581, Japan

Recently, the surface state of unconventional superfluids and superconductors attracts a lot of interests. In the vicinity of a surface in such materials, the surface density of state is drastically modified from the bulk one and unique surface quasiparticle states are formed near the Fermi energy. Among such unconventional pairing systems, superfluid ^{3}He is an ideal experimental substance to study the surface states, because it is an established spin triplet *p*-wave superfluid and a "super-clean" system whose bulk properties and symmetry of the order parameters are well understood. Surface states of superfluid ^{3}He in B phase have been studied using transverse acoustic impedance Z measurements [1].

We extended that measurement to high magnetic fields up to 13 T to study the surface states of superfluid ^{3}He in non-unitary phases called A_1 and A_2 phases. A_1 phase appears between T_{c1} and T_{c2}, and A_2 phase below T_{c2}. Figure 1 shows the temperature dependence of the real (Z') and the imaginary part (Z'') of the transverse acoustic impedance. The characteristic temperature dependence of Z in A_1 phase was very similar to that in A phase under zero magnetic field. At the lowest frequency, the sharp decrease of Z'' appeared near the transition temperature of each phase. As the measuring frequency becomes higher, the transition point became barely observable only with a tiny kink. We define the temperature corresponding to the kink as T_k. The higher the frequency is, the lower T_k is.

The field dependence of Z'' is shown in Fig. 2. In A_1 phase, all data points fall on a single universal curve even though the magnetic field is different. The saturation values at the lowest temperature are field independent in A_2 phase. This independence is expected from a simple weak-coupling theory. However, the magnitude of the decrease in the A_2 phase is much smaller than that in the A_1 phase, while they are expected to behave similarly in the weak-coupling theory. To understand the present experimental findings, we may have to take into account the coupling between the two order parameters.

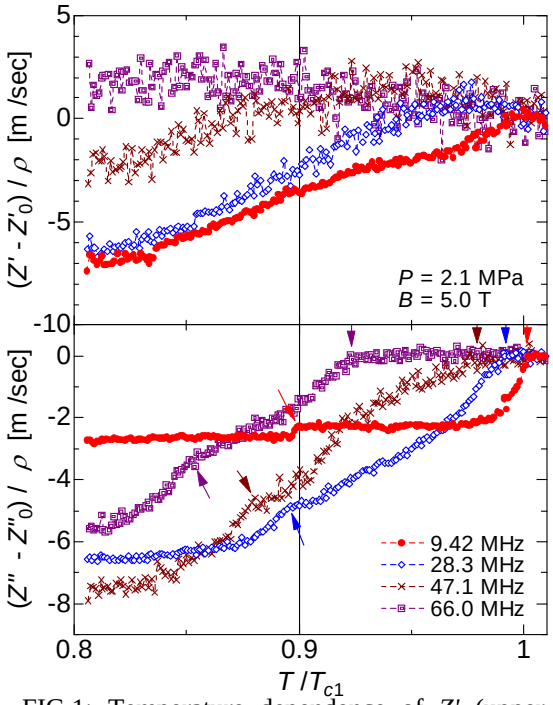

FIG.1: Temperature dependence of Z' (upper panel) and Z'' (lower panel). The deviations from the normal state value Z_0 are plotted. ρ is the density of ^{3}He. The horizontal axis is normalized by T_{c1}. The vertical line corresponds to T_{c2}. The arrows indicate T_k.

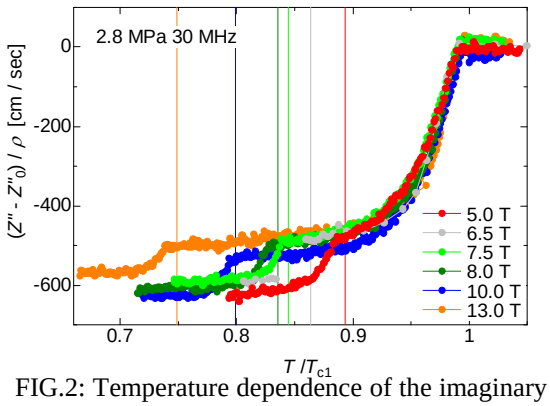

FIG.2: Temperature dependence of the imaginary part of Z in the various magnetic fields. The vertical lines are corresponding to T_{c2}.

[1] Y. Aoki *et al.*, Phys. Rev. Lett. **95**, 075301 (2005);
M. Saitoh *et al.*, Phys. Rev. B **74**, 220505(R) (2006);
Y. Wada *et al.*, Phys. Rev. B **78**, 214516 (2008);
S. Murakawa *et al.*, Phys. Rev. Lett. **103**, 155301 (2009)

P109

Magnetic Field Dependence of Dissipative Flow in Superfluid ^{3}He Films

M. Saitoh,[1, 2] . H. Ikegami,[1] and K. Kono[1]

[1]*Low Temp. Phys. Lab., RIKEN, 2-1 Hirosawa, Wako-shi, Saitama, 351-0198, Japan*
[2]*Institute of Physics and TIMS, University of Tsukuba, 1-1-1 Tennodai, Tsukuba-shi, Ibaraki, 305-8571, Japan*

In films of liquid ^{3}He with a thickness of ~ 1 μm, spatially inhomogeneous superfluid state is predicted [1]. To investigate the ^{3}He films for the thickness where the novel phase is expected, we have measured the dissipative flow in ^{3}He films for a thickness range from 0.6 to 1.5 μm at 0 and 0.3 T using inter-digitated capacitors (IDCs). The flow from the bulk liquid to the upper IDC is induced by an electrostatic force by ramping applied dc voltage V to the capacitor. The amount of liquid ^{3}He on the IDC can be known from its capacitance.

In zero field, as shown in Fig. 1, we observed two distinct driving rate (R_d) dependence of the dissipative flow. Similar R_d dependence of the dissipative flow was not observed in the magnetic field of 0.3 T where A phase is considered stable. These results suggest that the two distinct dissipation is related to the B phase films.

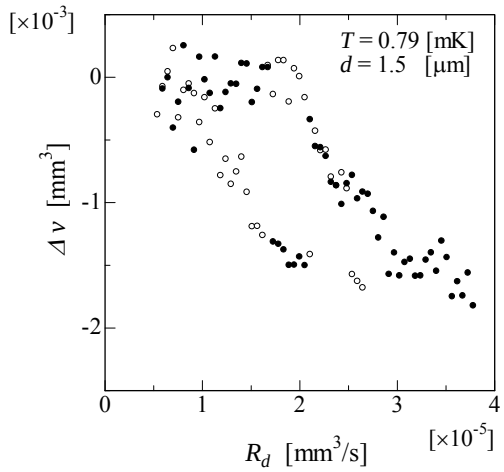

FIG.1: Driving rate dependence of dissipative flow in superfluid ^{3}He film at thickness of 1.5 μm in magnetic field of 0 T. The vertical axis represent the magnitude of the dissipative flow expressed by the volume difference (Δv), of liquid ^{3}He on upper IDC, between the measured volume and equilibrium volume, caused by the each driving.

[1] A. B. Vorontsov and J. A. Sauls, Phys. Rev. Lett. **98**, 045301 (2007).

P110

Singular and Half-Quantum Vortices in Superfluid ^{3}He-A between Parallel Plates

T. Kawakami, Y. Tsutsumi, and K. Machida

Department of Physics, Okayama University, Okayama 700-8530

Majorana zero energy modes have been widely discussed in various research fields. In condensed-matter physics, certain types of vortices in *p*-wave neutral Fermion or chiral *p*-wave superconductors contain the Majorana zero energy bound state at the vortex core. Then these vortices obey non-Abelian statistics [1]. In particular, the interest is the possible application to quantum computing, based on the fact that a pair of Majorana zero energy modes is intrinsically entangled and topologically protected from external disturbances.

Theoretical investigations are devoted to finding these modes in superconductors and neutral Fermion superfluids in ^{3}He and cold atoms. The *p*-wave superfluids in neutral atomic gases have yet been realized experimentally. The physical parameter of the ^{3}He is more favorable than one of the superconductors. The ^{3}He-A phase is the most concrete examples of chiral *p*-wave superfluidity. In this respect, the ^{3}He-A phase is a prime candidate for testing the Majorana zero energy modes.

To realize the Majorana zero energy modes in ^{3}He-A phase system, the *l*-vectors must be aligned with certain direction in the whole system. This condition can be realized in experiments in parallel plate geometry performed by Yamashita *et al.* [2]. We consider stability of the textures that have the Majorana zero energy modes in this system by means of phenomenological Ginzburg-Landau (GL) theory. Our GL free energy is taken into account of the condensation energy, the gradient energy, the dipole interaction, and the interaction with the external field. Then we will present the regions where Majorana zero energy modes appear quantitatively.

We consider the following three cases distinguished by the direction of the external magnetic field [3,4,5]. In the cases 1 and 2, the directions of an external magnetic field are parallel and perpendicular to the plate. In the case 3, the direction of an external magnetic field is tilted to the plate. In the cases 1 and 2, we conclude that the Majorana zero energy modes exist in the vortex core of the singular and half-quantum vortex. On the other hands, in the case 3, we obtain the singular vortex texture shown in Fig. 1 and the existence of the Majorana zero energy modes is non trivial.

[1] D.A. Ivanov Phys. Rev. Lett. **86**. 268 (2000).
[2] M. Yamashita *et al*., Phys. Rev. Lett. **101**, 025302 (2008).
[3] Y. Tsutsumi *et al*., Phys. Rev. Lett. **101**. 135302 (2008).
[4] T. Kawakami *et al*., Phys. Rev. B **79**. 092506 (2009).
[5] T. Kawakami *et al.,* arXiv: 0912.308 (submitted to J. Phys. Soc. Jpn.).

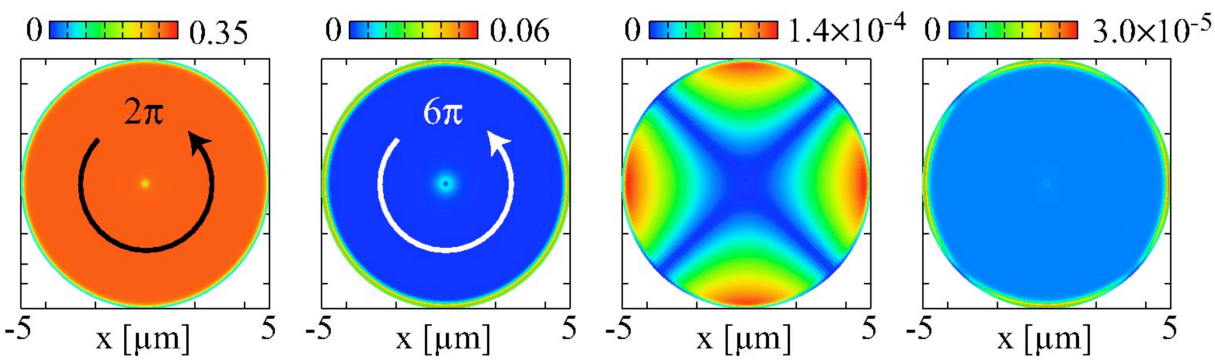

FIG. 1: Obtained order parameter amplitude (a) $|A_{\sigma\sigma,+}|$, (b) $|A_{\sigma\sigma,-}|$, (c) $|A_{\uparrow\downarrow,+}|$, and (d) $|A_{\uparrow\downarrow,-}|$ for R=5 μ m, T=0.95T_c, H=2 mT, the angle between the *z*-direction and the external field $\theta_H = \pi/18$. The spin quantization axis is chosen to be perpendicular to the bulk *d*-vector. The spatial structure of the $A_{\uparrow\downarrow,+}$ shows that the *d*-vector oscillates along the quantization axis.

P111

Decaying Process of Persisitent Precessing Domain in Superfluid ^{3}He-B

M. Kanemoto,[1] R. Toda,[1,2] W. Onoe,[1] T. Kakuda,[1] Y. Tanaka,[1] and Y. Sasaki[1,2]

[1]*Department of Physics, Graduate School of Science, Kyoto University, Sakyo-ku, Kyoto 606-8502, Japan*
[2]*Research Center for Low Temperature and Materials Sciences, Kyoto University, Sakyo-ku, Kyoto 606-8501, Japan*

Since the discovery of superfluid ^{3}He in 1971, various experiments have performed to reveal the wonderful nature of this remarkable quantum condensate. Among those activities, NMR experiments were by far effective in extracting precise information on the internal degree of freedom of the order parameter. Spin dynamics of superfluid ^{3}He was well explained by the Leggett equations and their extensions including Leggett-Takagi relaxation mechanism and spin wave effect. The effect of spin supercurrent was first observed as an anomalous spin relaxation in pulsed NMR experiment. In 1984 Moscow group discovered remarkable state, where macroscopic and outstandingly long-lived coherence of the transverse magnetization was kept in the significant part of the sample cell. Later they named this phenomenon as Homogeneous Precessing Domain (HPD). The HPD was explained as the macroscopically coherent precession of spins achieved by spin supercurrent. In 1992, another macroscopically coherent state was discovered by Bunkov and Lancaster group[1]. This state, called as Persistent Induction Signal, appeared near the lowest achievable temperatures which could be achieved only by Lancaster style double cell. Later they named this phenomenon as Persistent Precessing Domain (PPD). They found that the PPD has extremely long life, which was as long as 2000 sec at the lowest achievable temperature [2], in the case where the PPD was formed apart from the cell wall[3]. Bonkov and Volovik showed that this signal was coming from a standing spin wave trapped in a dipole potential formed by texture and precessing magnetization, which acted as a close analogue of the Q ball, and argued that these macroscopically coherent precession could be described as Bose-Einstein condensation of magnons[4].

We have obtained the PPD signal from different geometry. A liquid ^{3}He sample of 2.9 MPa in a single cylindrical sapphire cell attached below massive sintered silver heat exchangers was cooled down to about 300 μK. Static magnetic field of 0.16 T as well as linear field gradient was applied perpendicular to the cylinder axis. After an excitation pulse of 30 degree in typical, we could observe a long-lived free induction signal, whose frequency was at the lowest resonance frequency in the sample cell under the same field gradient. The obtained signals hold all the feature of the PPD signal. Since we could adjust the angle between the direction of field gradient G and static magnetic field B, we could change the location of PPD in the cell. When G was perpendicular to B, the PPD stayed apart from the cell wall and survived for a long time. When G was parallel to B, the PPD touched to the wall and decayed much faster. At the intermediate angle between G and B, we observed a two-stage fast and slow decay. The fast decay was attributed to the surface induced relaxation. We understood that the shape of the PPD is a sort of curved board standing parallel to the vertical cell wall. By adjusting a strength of G, we could change the thickness of the board as 1/G. Since the measured time constant of the slow decay was proportional to 1/G, we understood that the relaxation mechanism of this free standing PPD was working not in the bulk but at the surface of the PPD. Since the temperature dependence of this slow time constant was rather strong, the relaxation mechanism was possibly related to the orbital motion in the PPD and a drag from the stationary orbital component outside of the PPD.

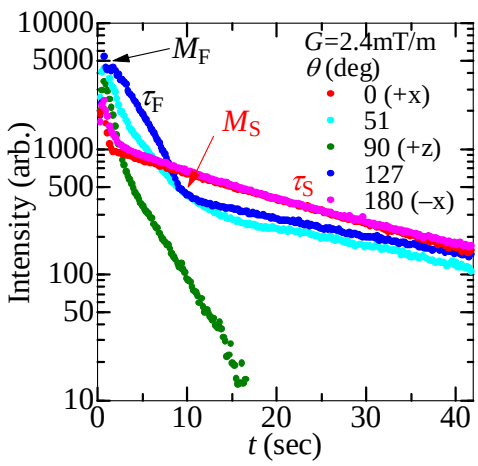

[1] Yu.M. Bunkov, S.N. Fisher, A.M. Guenault, and G.R. Pickett, Phys. Rev. Lett. **69**, 3092 (1992)
[2] S.N. Fisher *et. al.*, J. Low Temp. Phys. **121**, 303 (2000)
[3] D.I. Bradley *et. al.*, J. Low Temp. Phys. **134**, 351 (2004)
[4] Yu.M. Bunkov and G.E. Volovik, Phys. Rev. Lett. **98**, 265302 (2007)

P112

Surface Andreev Bound States in Superfluid ^{3}He-B

T. Mizushima and K. Machida

Department of Physics, Okayama University, Okayama 700-8530, Japan

Much attention has been given in recent years to topological insulators (TI) and topological superfluids (TS) in various physics systems with time reversal symmetry. Both the topological materials involve a gapful excitation in the bulk, while a topologically protected gapless dispersion appears in the edge of the systems as a consequence of the surface Andreev bound state (SABS). The remarkable fact is that the SABS is describable with the time reversal invariant or helical Majorana quasiparticle representation [1]. In contrast to time reversal symmetry breaking systems, however, the SABS in the TI and TS does not give rise to the net mass flow along the edge, which is canceled out by the time reversal counterparts.

The superfluid ^{3}He-B phase is known to be a typical and only example of the topological superfluid. In ^{3}He-B with diffusive surfaces, the existence of the SABS has recently been realized in experiments through anomalous behaviors on the transverse acoustic impedance [2] and surface specific heat [3]. In addition, the recent development of experimental technique enables to enhance the specularity in quasiparticle scattering by the wall [4].

Here, the aim in this work is to clarify the direct signatures of the SABS in ^{3}He-B with a specular surface, based on the full numerical calculation of the Bogoliubov-de Gennes equation. Due to the gapless spectrum of the SABS, the density of states near the surface turns out to be linear on the energy. As seen in Fig.1(a), it is demonstrated that this provides a power low behavior of the low-temperature heat capacity, similar to superconductors with a line node. In addition, we investigate the unconventional property of the SABS through the spin relaxation of the electron bubbles injected the vicinity of the surface, whose idea were originally proposed in Ref. [5]. Here, the full numerical calculation of the spin-spin correlation function reveals the strong anisotropy of the spin relaxation time of the injected electrons, which is consistent with the theoretical prediction based on the Majorana representation of low-lying quasiparticle states [5,6]. In addition to the *Ising*-like anisotropy on spin dynamics, it is revealed that the temperature dependence exhibits a power low behavior in low temperature regime, when the Zeeman field is parallel to the wall. The preliminary result is displayed in Fig.1(b), where for simplicity the local relaxation process of the electron spins is assumed. The more realistic situation, such as the non-local process due to the magnetic dipole interaction, will be taken into account in future study.

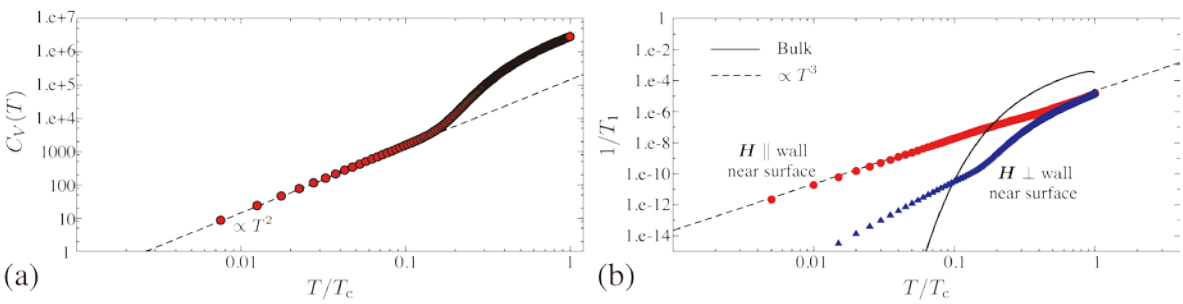

Fig.1: (a) Temperature dependece of the heat capacity in superfluids 3He B-phase with a specular boundary. (b) Temperature dependence of the spin relaxation time of the electrons induced near the surface (circles and triangles) and the bulk (solid curve). The circles (triangles) correspond to the case where the applied Zeeman field is parallel (perpendicular) to the wall.

[1] X.L. Qi, T.L. Hughes, S. Raghu, and S.C. Zhang, Phys. Rev. Lett. **102**, 187001 (2009).
[2] Y. Aoki, et al., Phys. Rev. Lett. **95**, 075301 (2005).
[3] H. Choi, J.P. Davis, J. Pollanen, and W.P. Halperin, Phys. Rev. Lett. **96**, 125301 (2006).
[4] S. Murakawa et al., Phys. Rev. Lett. **103**, 155301 (2009).
[5] S.B. Chung and S.C. Zhang, Phys. Rev. Lett. **103**, 235301 (2009).
[6] Y. Nagato, S. Higashitani, and K. Nagai, J. Phys.SocJpn. **78**, 123603 (2009).

P113

Surface Majorana Cone of the Superfluid ^{3}He B Phase on a Partially Specular Wall

S. Murakawa, Y. Wada, M. Wasai, K. Akiyama, Y. Tamura, M. Saitoh, Y. Aoki, R. Nomura, and Y. Okuda

Department of condensed Matter Physics, Tokyo Institute of Technology, 2-12-1Ookayama, Meguro-ku, Tokyo 152-8551, Japan

In the vicinity of a surface of unconventional superfluids and superconductors, the density of states is modified from the bulk one and an additional low energy state is formed within the energy gap Δ.. This new state is called surface Andreev bound states (SABS) and is the universal feature in such systems. For example, the zero bias conductance peak of superconductors is an manifestation of SABS. Recently, it is pointed out that SABS of 3He-B is recognized as the surface Majorana fermion [1,2].

Superfluid ^{3}He is the spin-triplet *p*-wave superfluid and a "super-clean" system whose bulk parameter is well investigated. Thus, it should be a model system to study such a surface state.

SABS is strongly affected by the surface condition, as shown in Fig.2 [3]. By changing the specularity parameter from diffusive one (S =0) to specular (S = 1), SABS band width Δ^* becomes broader and zero energy state density decreases. In the limit of S = 1, the density of states has the linear dependence with respect to energy, which reflects the Majorana cone in the quasi-particle dispersion relation.

We have found that transverse acoustic impedance Z of liquid ^{3}He is a good probe to study the surface state of superfluid ^{3}He. Surface condition can be controlled *in situ* by coating the surface with ^{4}He. At S = 0, anomalies, indicated by downward arrows in Fig. 2, are observed near the transition temperature, which comes from Δ^* [4,5]. That is the first observation of the SABS band of superfluid ^{3}He. As increasing S, those anomalies are shifted to higher temperature [6]. That is the evidence of the broadening of SABS towards specular surface condition [3]. In S > 0.5, we observed new peaks, indicated by upward arrows in Fig.2 [7]. Those peaks are interpreted by the change of density of state with respect to S [7,8]. For S > 0.5, the states near the fermi energy decrease and SABS have a peak structure at higher energy. This change of SABS is the origin of new peaks. Therefore, growth of new peaks strongly suggests the Majorana cone at the specular limit.

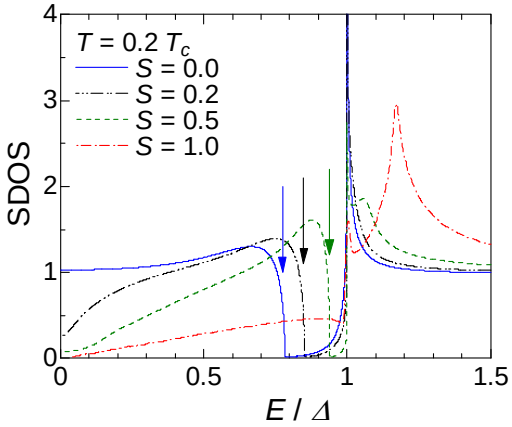

FIG.1: Surface density of states of the BW state as a function of energy for typical surface conditions. The arrows indicate the band edge energy Δ^*[3].

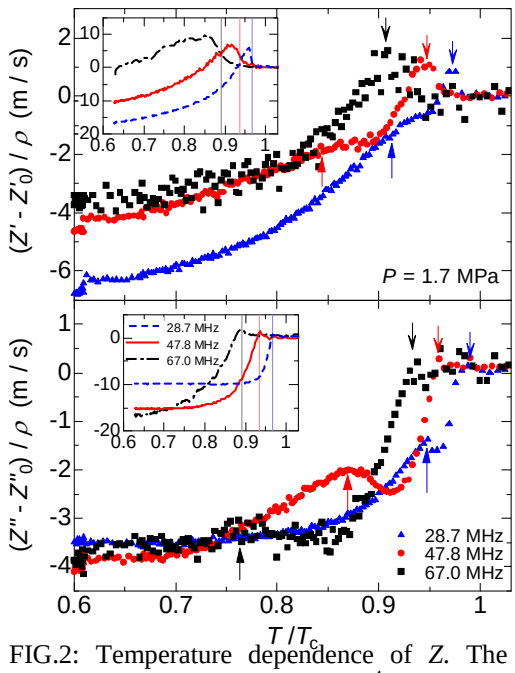

FIG.2: Temperature dependence of Z. The surface is coated with 3.6 layers ^{4}He and S = 0.53. The insets are the results of pure sample at S = 0[7].

[1] A. Schnyder *et al.*, Phys. Rev. B **78**, 195125 (2008).
[2] X.-L. Qi *et al.*, Phys. Rev. Lett. **102**, 187001 (2009).
[3] Y. Nagato *et al.*, J. Low Temp. Phys, **149**, 294 (2007)
[4] Y. Aoki *et al.*, Phys. Rev. Lett. **95**, 075301 (2005)
[5] M. Saitoh *et al.*, Phys. Rev. B **74**, 220505(R) (2006)
[6] Y. Wada *et al.*, Phys. Rev. B **78**, 214516 (2008)
[7] S. Murakawa *et al.*, Phys. Rev. Lett. **103**, 155301 (2009)
[8] K. Nagai *et al.*, J. Phys. Soc. Jpn. **77**, 111003 (2008).

P114

Stable Textures and Majorana Zero Modes in Trapped *p*-Wave Resonant Superfluidity of Atomic Fermi Gases

Y. Tsutsumi, T. Mizushima, and K. Machida

Department of Physics, Okayama University, Okayama 700-8530, Japan.

Recently, there has been much attention paid to *p*-wave resonant superfluidity in alkaline atomic Fermi gases, such as ^{6}Li and ^{40}K, both experimentally and theoretically. In the system, since the population of atoms in each hyperfine spin state can be controlled by using the rf field, the spin degrees of freedom are frozen, and hence only the orbital degrees of freedom remain active. Because of this degrees of freedom, the *p*-wave resonant superfluidity shows different features from F=1 spinor Bose-Einstein condensates. In addition, since the atomic gases are confined in a trap potential, boundary conditions imposed on them are different from that on the superfluid ^{3}He in a container. One of our aims is to find stable spatial structures of the order parameter, that is, orbital textures, by a trap potential, such as cigar or pancake shape. Furthermore, spinless chiral *p*-wave superfluidity can form vortices involving zero energy Majorana bound states. It is proposed that the spinless chiral *p*-wave superfluid of atomic Fermi gases with Majorana zero modes can be utilized for quantum computations. Another our aim is to determine conditions for Majorana zero modes to exist.

In this work, we show the energetically favored textures and vortex states by employing the Ginzburg-Landau (GL) framework. This framework is applicable to superfluid of atomic Fermi gases with a harmonic trap potential under $k_B T_c >> \hbar\omega$, where T_c and ω are the transition temperature and the trap frequency, respectively. The GL free energy functional consists of bulk condensation energy up to fourth orders of order parameter and gradient energy with three independent terms. In addition, the GL free energy functional includes contribution of an external rotation and a trap potential.

When the atomic gases are confined in the cigar shape trap potential, the *l*-vectors, which direct to a point node of order parameter, follow the circumference of the condensates (Fig.1). In contrast, the atomic gases are confined in the pancake shape trap potential flattened in the *x*-*y*-plane, the *l*-vectors align toward the *z*-direction [1]. Therefore, the chiral *p*-wave superfluidity, which is suitable for Majorana modes to exist, is realized in a quasi-two dimensional (quasi-2D) trap potential. Under this situation, we obtain a phase diagram of the vortex structures for trap frequency (ω) vs rotation frequency (Ω) (Fig.2). Majorana modes are found to accompany only a singular vortex in the region S [2]. We suggest the use of a quasi-2D square well potential for confinement, which is also used in the superfluid ^{3}He confined in parallel plates, to be utilized for a quantum computer.

[1] Y. Tsutsumi and K. Machida, Phys. Rev. A **80**, 035601 (2009); J. Phys. Soc. Jpn. **78**, 084702 (2009).
[2] Y. Tsutsumi and K. Machida to be published in J. Phys. Soc. Jpn. **79**, No. 3 (2010).

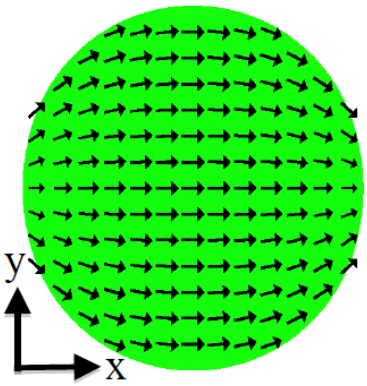

FIG.1: Cross section of the stable texture in a cigar shape trap potential elongated toward the *z*-direction. Arrows show the *l*-vectors.

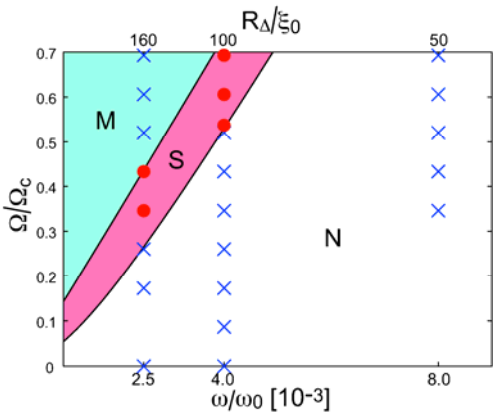

FIG.2: Phase diagram of the vortex structures. The region N is the nonvortex structure, S is the singular vortex structure where Majorana zero modes exist, and M is the multiple vortex structure.

P115

Zero Energy Majorana States in Spinless Chiral *p*-wave Superfluids with Plural Vortices

T. Mizushima and K. Machida

Department of Physics, Okayama University, Okayama 700-8530, Japan

A *spinless* chiral *p*-wave superfluid may be an effective model that describes the low energy properties of various *p*-wave superfluids without time reversal symmetry, *e.g.*, *p*-wave resonant Fermi gases [1], half-quantum vortices in spinful systems [2], and superfluid-ferromagnet insulator junctions formed on the topological insulator [3]. Using this model with singular vortices, the low energy excitations are found to consist of the vortex core bound state and edge bound state. The noticeable consequence is that the lowest eigenenergy can be zero when the vorticity is odd. The zero energy state (ZES) is composed of the equivalent contributions from the particle and hole, and thus its creation is describable with a self-Hermitian operator, called the Majorana fermion. The linear combination of two Majorana operators may restore the fermionic commutation relation, called the complex fermion. As a consequence of the non-local occupation of the complex fermion states, their host vortices obey neither Fermi nor Bose statistics, called the non-abelian statistics [2]. For instance, a discrete set of the unitary group, which manipulates the occupation of the ZES, can be implemented by the braiding operations of four vortices.

The aims in this work are to clarify the low energy quasiparticle structures and the splitting of the zero energy Majorana states in spinless *p*-wave superfluids with plural vortices. While this system will offer the promising method of the fault-tolerant quantum computation, it has recently been revealed that the intervortex tunneling and thermal fluctuations of vortices give rise to the decoherence of the topological qubit [4]. In the dilute limit of vortices, it is confirmed numerically that there exists a single ZES for odd vorticity and none for even vorticity [5,6]. This is contrast to the Atiyah-Singer index theorem for the relativistic Dirac Hamiltonian. It is also revealed that in two-vortex systems, the interference between two core-localized Majorana states lifts the degenerate zero energy exponentially on the vortex separation. In particular, the splitting energies oscillate rapidly on the Fermi wavelength in the weak coupling regime, as seen in Fig. 1. We extend this argument to the strong coupling regime. Here, the wave function of the ZES turns out to be describable with the modified Bessel function, which makes the rapid oscillation of the splitting eigenenergies smooth. It was proposed in Ref. [7] that the continuous manipulation of the topological state can be realized by braiding three vortices, in contrast to a discrete set of the unitary group in four-vortex systems. Neverthless, the stability of the zero energy Majorana state in three-vortex systems has never been studied so far. Hence, we will expand the argument in two-vortex systems into three-vortex systems, where a pair of edge- and core-localized Majorana states is found to always survive in the zero energy regardless of the vortex separation.

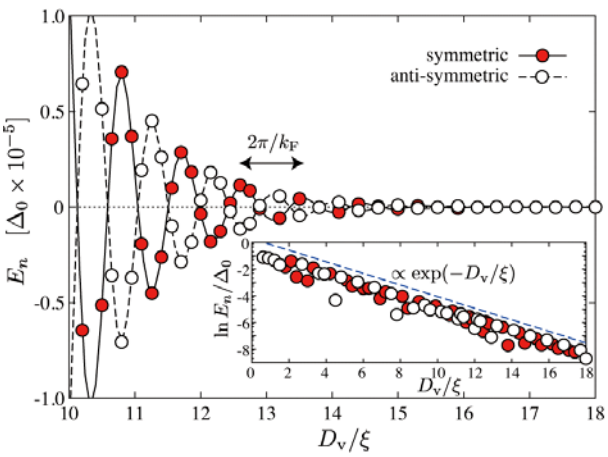

Fig.1: Lowest eigenenergies as a function of vortex distance in two-vortex systems. The inset shows the positive eigenenergies with the logarithmic scale.

[1] T. Mizushima, M. Ichioka, and K. Machida, Phys. Rev. Lett. **101**, 150409 (2008).
[2] D. Ivanov, Phys. Rev. Lett. **86**, 268 (2001).
[3] Y. Tanaka, T. Yokoyama, N. Nagaosa, Phys. Rev. Lett. **103**, 107002 (2009).
[4] M. Cheng, R. Lutchyn, V. Galitski, and S. Das Sarma, Phys. Rev. Lett. **103**, 107001 (2009).
[5] V. Gurarie and L. Radzihovsky, Phys. Rev. B 75, 212509 (2007).
[6] T. Mizushima and K. Machida, arXiv:1001.5325.
[7] T. Ohmi and M. Nakahara, arXiv:0906.4444.

P116

Low temperature magnetization hysteresis anomalies in Sr_2RuO_4

Y. Karaki, K. Kuga, H. Nema, M. Kubota, Y. Uwatoko, S. Kittaka[1] and Y. Maeno[1]

Institute for Solid State Physics, University of Tokyo, Kashiwanoha 5-1-5, Kashiwa, Chiba 277-8581, Japan
[1]Department of Physics, Graduate School of Science, Kyoto University, Kyoto 606-8502, Japan

We measured the hysteresis of magnetization curve in Sr_2RuO_4 down to 24mK using a DC SQUID and a dilution refrigerator to study the anomalous pinning caused by the domain separating degenerate states expected in the superconductor with broken time-reversal symmetry. The sample is an annealed single crystal with a size of 1.3x3x1.2 mm^3 (the sample along the c-axis is 1.2 mm long). The results in the field parallel to c-axis are shown in Fig. 1. At temperatures below Tc(~1.5K) to 60mK, there is no anomaly on the magnetization. The magnetization curve expands as decreasing temperature as expected from the temperature dependence of the critical current. Below ~50mK three anomalies are observed. Firstly, the magnetization curves exhibit a sequence of zigzag oscillations with kinks. Tenya *et al.* has observed same anomaly at rather high temperatures up to 200 mK[1]. Secondly, diamagnetization at the negative field side(opposite to the direction of the initial ramping field) increases. Thirdly, the hysteresis ΔM drastically decreases below 50mK around zero field as shown in Fig. 2. Relaxation of the remnant magnetization of Sr_2RuO_4 measured by Dumont and Mota shows that the creep rate of vortex becomes very small at same temperature range[2]. They explain that the domain wall prevents vortex flow as discussed by Sigrist and Agterberg[3]. Our results also can be explained by the presence of the domain with the impermeable wall. If vortices can not enter the domain, the density inside of the domain becomes lower than outside. Thus, the anomalous diamagnetization and the decrease of ΔM can be explained. However, as shown in Fig. 3 no anomaly is observed the magnetization in the field perpendicular to the c-axis. Two-dimensional superconductivity in Sr_2RuO_4 may explain the observed anisotropy.

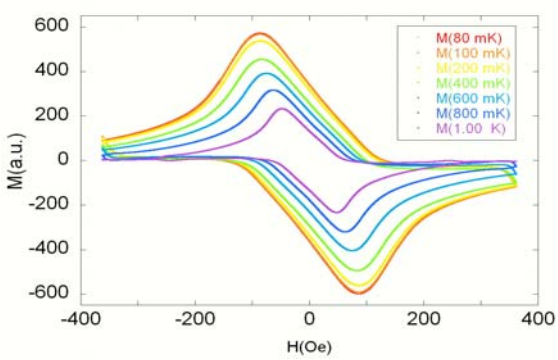

FIG.1: Magnetization curves for H//c at temperatures from 1.0 K to 80 mK.

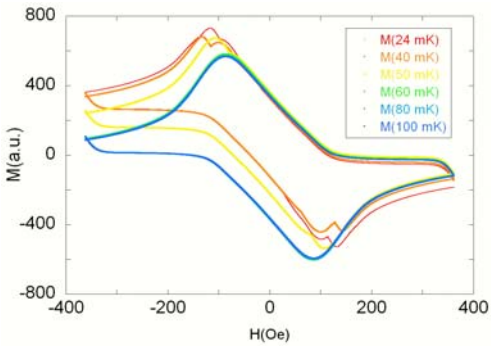

FIG 2: Magnetization curves for H//c at temperatures from 1.36 K to 23 mK.

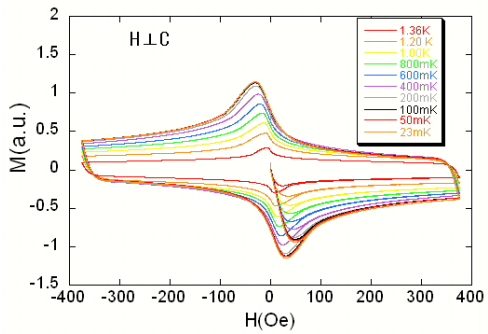

FIG 3: Magnetization curves for H ⊥c at temperatures 1.36 K to 24 mK.

[1] K. Tenya *et al.*, Physica B **403,** 1101(2008)
[2] E. Dumont and A. C. Mota, Phys. Rev. B **65**, 144519(2002)
[3] M. Sigrist and D. F. Agterberg, Prog. Theor. Phys. **102**, 965 (1999)

P117

Effects of spin-orbit interaction on magnetism and spin-triplet superconductivity in Sr_2RuO_4

T. Nomura,[1] and H. Ikeda[2]

[1]*Synchrotron Radiation Research Center, Japan Atomic Energy Agency, Hyogo 679-5148, Japan*
[2]*Department of Physics, Graduate School of Science, Kyoto University, Kyoto 606-8502, Japan*

We will discuss comprehensively the effects of spin-orbit coupling on the magnetic properties and the ***d***-vector state of Sr_2RuO_4 from a viewpoint of microscopic theory. We use a three-band Hubbard model and a seven-band *d-p* model which include the realistic multi-band electronic structure of Sr_2RuO_4 and the on-site Coulomb integrals *U* (intra-orbital), *U*' (inter-orbital), *J* (Hund's coupling), and *J*' (pair-hopping).

For the magnetic properties, we study the anisotropy of magnetic susceptibility within the random phase approximation (RPA). The obtained magnetic anisotropy is qualitatively consistent with experimental results, i.e., the *c*-axis component of magnetic susceptibility is larger than the *ab*-plane one ($\chi_c(\boldsymbol{q},\omega) > \chi_{ab}(\boldsymbol{q},\omega)$) due to the effect of spin-orbit interaction among the Ru4*d*ε states. We will discuss also the effects of oxygen 2*p* orbitals by comparing the results for the Hubbard model with those for the *d-p* model. Results of NMR relaxation rate $1/T_1T$ will be also presented.

For the spin-triplet superconductivity, the effective pairing interaction is evaluated within the third order perturbation expansion in the on-site Coulomb integrals. The band-, frequency-, and momentum-dependences of the superconducting order parameter are determined by solving the Eliashberg equation numerically. The spin-orbit interaction term among the Ru4*d*ε states is fully included (i.e., not included perturbatively, as in other previous studies, but included in the unitary matrix for band diagonalization). The anisotropy of the ***d***-vector is investigated by comparing the eigenvalues of the linearized Eliashberg equation for various ***d***-vector states. By taking full account of the hybridization among the Ru4*d*ε orbitals, we find that the degeneracy among the five ***d***-vector states is completely lifted. Within the realistic strength of the spin-orbit coupling (～0.05eV), the anisotropy of the ***d***-vector is expected to be very small. The most favorable ***d***-vector state is the Eu state ($\boldsymbol{d}(\boldsymbol{k})=k_x\boldsymbol{z}, k_y\boldsymbol{z}$, this state corresponds to the chiral state) or the A1u state ($\boldsymbol{d}(\boldsymbol{k})=k_x\boldsymbol{x}+k_y\boldsymbol{y}$, an analogous state to the BW state of superfluid ^{3}He), depending on the strength of the spin-orbit coupling and the *yz-xz* orbital hybridization. These two states could compete with each other and are possibly almost degenerated at low temperatures. Thus the chiral state (Eu state with ***d***//*c*) is not so robustly favorable against the A1u state as suggested in previous microscopic theories.

P118

Magnetization and Magnetocaloric Studies on the Spin-Triplet Superconductivity in Sr_2RuO_4

K. Tenya,[1] Y. Shimura,[2] T. Sakakibara,[2] M. Yokoyama,[3] H. Amitsuka,[4] K. Deguchi[5] and Y. Maeno[6]

[1]*Faculty of Education, Shinshu University, Nagano 380-8544, Japan.*
[2]*Institute for Solid State Physics, University of Tokyo, Kashiwa 277-8581, Japan.*
[3]*Faculty of Science, Ibaraki University, Mito 310-8512, Japan.*
[4]*Department of Physics, Hokkaido University, Sapporo 060-0810, Japan.*
[5]*Department of Physics, Nagoya University, Nagoya 464-8602, Japan.*
[6]*Department of Physics, Kyoto University, Kyoto 606-8502, Japan.*

Since the discovery of the superconductivity with internal degree of freedom, the layered ruthenate Sr_2RuO_4 has been attracting great interest among various unconventional superconductors. From the experimental results on μSR, NMR Knight shift and polar Kerr effect [1−3], Sr_2RuO_4 is evidenced to be a 2D spin-triplet superconductor with chiral ***d***-vector. In order to investigate the chiral-superconducting properties, detailed magnetization and magnetocaloric measurements have been performed on the single crystals Sr_2RuO_4 for the field parallel to the principal axes.

Anomalous features of the magnetization are found at small fields, which is slightly larger than the lower critical field H_{c1}, for H // [001] in the superconducting mixed state: The magnitude of the hysteretic magnetization strongly depends on the field-gradient in the field region below about 0.1 kOe while no anomaly is observed in the equilibrium magnetization. Above 0.4 K a small peak structure of the hysteretic magnetization is observed around 0.1 kOe, as shown in FIG. 1 [4]. Here the upper limit field below which the hysteretic magnetization depends on the field-gradient is denoted as H_R. At temperatures below 0.2 K, successive and tiny flux-jumps of the hysteretic magnetization are observed below H_R.

In the magnetocaloric effect measurements at the zero-field temperature of 0.27 K, divergent behavior of the temperature is observed around 0.12 kOe below which the magnetization depends on the field-gradient (FIG.2). A kink structure is also observed at around 0.67 kOe which corresponds to the upper critical field H_{c2} at 0.27 K.

Possible origins for the anomalous behaviors in Sr_2RuO_4 are discussed.

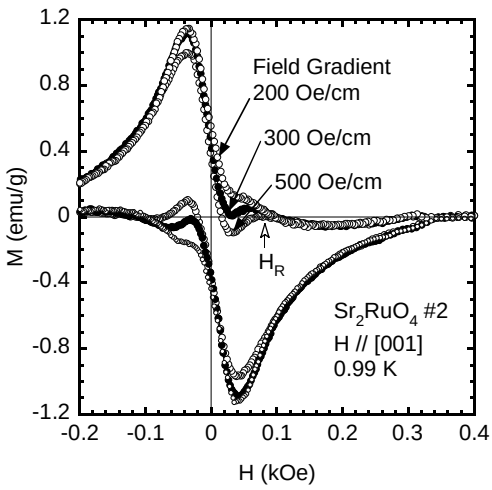

FIG.1: Magnetization curves of Sr_2RuO_4 for H // [001] under various field-gradients.

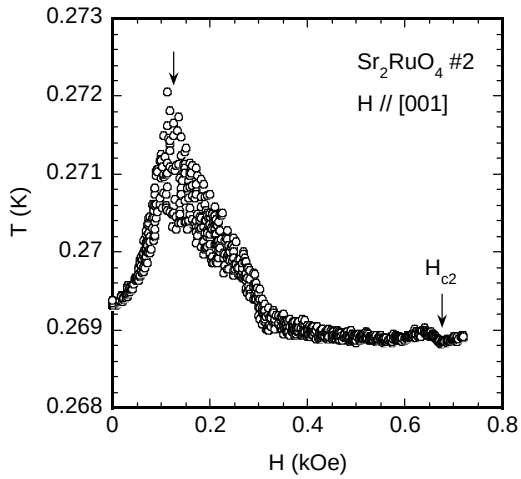

FIG.2: Field dependence of the temperature in the adiabatic Sr_2RuO_4 single crystal in the increasing-field process for H // [001].

[1] G. M. Luke *et al.*, Nature (London) **394** (1998) 558. [2] K. Ishida *et al.*, Nature (London) **396** (1998) 658.
[3] J. Xia *et al.*, Phys. Rev. Lett. **97** (2006) 167002. [4] K. Tenya *et al.*, Physica **B403** (2008) 1101.

P119

Nuclear-Magnetic-Resonance Measurements on Sr_2RuO_4 in a precisely Controlled Magnetic Field

Kenji Ishida[1,2], Hiroshi Murakawa[1,*], Yoshihoko Ihara[1], Z. Q. Mao[1,$], and Yoshiteru Maeno[1]

[1]*Department of Physics, Graduate School of Science, Kyoto University, Sakyo-ku, Kyoto 606-8502, Japan*
[2]*TRIP-JST, Sanban-cho bldg.5, Sanbancho, Chiyoda, Tokyo 102-0075, Japan*

In the presentation, we review our nuclear magnetic resonance (NMR) and nuclear quadrupole resonance (NQR) studies using high-quality single-crystal Sr_2RuO_4 under a precisely controlled magnetic field [1]. We have performed Knight-shift measurement on spin-triplet superconductor Sr_2RuO_4 under various magnetic fields to determine the ***d***-vector direction, which is perpendicular to the spin direction of the Cooper pair. We employed the ^{101}Ru nuclear quadrupole resonance (NQR) to measure the Knight shift under small fields. Application of small fields splits the NQR signal, and the Knight shift is derived from the interval between two split peaks. We reported the Knight-shift results along the c-axis (K_c) and the RuO_2 plane (K_{ab}) in the superconducting (SC) state in small fields obtained by this technique [2,3]. The decrease of the Knight shift was not found in any field direction below T_c within the experimental accuracy. This result suggests that the spins of the SC pair directs to the applied magnetic fields in the measured fields (order of several hundred Oe), and implies that the spin-orbit interaction, which locks the ***d***-vector to a crystal lattice, is so weak that the ***d*** vector can be rotated by small applied magnetic fields.

We have also performed ^{17}O-NMR to measure linewidth and the nuclear spin-lattice relaxation rate ($1/T_1$) in magnetic fields exactly parallel to the RuO_2 plane within the accuracy of 0.5 degree. The ^{17}O-NMR linewidth in the normal state was approximately 5 Oe in ~6 kOe. Appreciable change of the linewidth has not been detected in the SC state. The temperature dependence of $1/T_1$ of ^{17}O in ~6 kOe and zero fields is shown. The implication of these results is discussed.

[1,*]*Present address:Multiferroics Project, ERATO, Japan Science and Technology Agency (JST), Tokyo 113-8656, Japan*
[1,$]*Department of Physics, Tulane University, New Orleans, Louisiana 70118, USA*

[1] K. Ishida, H. Murakawa, H. Mukuda, Y. Kitaoka, Z. Q. Mao, and Y. Maeno, *J. Phys. Chem. Solids* **69**, 3108 (2008).

[2] H. Murakawa, K. Ishida, K. Kitagawa, Z. Q. Mao, and Y. Maeno, *Phys. Rev. Lett.* **93**, 167004 (2004).

[3] H. Murakawa, K. Ishida, K. Kitagawa, H. Ikeda, Z. Q. Mao, and Y. Maeno, *J. Phys. Soc. Jpn.* **76**, 024716 (2007).

P120

ab initio calculation of *d*-vector in spin-triplet superconductor Sr_2RuO_4

H. Ikeda

Dept. of Physics, Kyoto University, Kyoto 606-8502, Japan

The most promicing superconducting pairing state in Sr_2RuO_4 has been considered to be the spin-triplet $k_x \pm ik_y$ wave state. However, the possibility seems to be inconsistent with some behaviors under in-plane magnetic field; the Pauli-limitting like behavior and almost isotropic behavior of the critical magnetic field H_{c2}. In addition, the importance of the k_z dispersion and k_z dependence of the spin-orbit coupling has been indicated from the first-principle band structure calculation. [2]

We here investigate an effective three-dimensional Hubbard model obtained from the first-principle band structure within the third-order perturbation. Such three-dimensionality has not been considered seriously so far. We will report *ab* initio evaluation of *d*-vector with the effect of the spin-orbit coupling.

[1] K. Machida and M. Ichioka, Phys. Rev. B**77**, 184515 (2008).
[2] M.W. Haverkort *et al.*, Phys. Rev. Lett. **101**, 026406 (2008).

P121

Enhancement of T_c to 3 K by applying uniaxial pressure to Sr_2RuO_4

S. Kittaka,[1] H. Taniguchi,[1] S. Yonezawa,[1] H. Yaguchi,[2] and Y. Maeno[1]

[1]*Department of Physics, Graduate School of Science, Kyoto University, Kyoto, Japan*
[2]*Department of Physics, Faculty of Science and Technology, Tokyo University of Science, Chiba, Japan*

The layered perovskite ruthenate Sr_2RuO_4, for which convincing evidence has been accumulated in favor of spin-triplet superconductivity [1], has an undistorted tetragonal structure. The intrinsic superconducting transition temperature T_c of Sr_2RuO_4 was revealed to be 1.5 K for crystals with the best quality. Surprisingly, the onset T_c of Sr_2RuO_4 is enhanced up to slightly above 3 K in the Sr_2RuO_4-Ru eutectic system [2], while hydrostatic pressure [3] as well as a small amount of impurities or defects [1] is known to suppress its T_c. The mechanism of the enhancement of T_c in the Sr_2RuO_4-Ru eutectic system has been unresolved for more than ten years since its discovery. An important hint for clarifying this mechanism is the fact that the 3-K superconductivity occurs in the Sr_2RuO_4 side near the Sr_2RuO_4-Ru interface. This hint implies that the origin of the enhanced T_c is related to the change in the Sr_2RuO_4 region near the interface. One of possible changes is an anisotropic distortion of Sr_2RuO_4 induced by the presence of Ru inclusions [4].

In order to obtain insight into the mechanism of the enhancement of T_c, we have investigated uniaxial pressure effects on superconductivity of pure Sr_2RuO_4 and the Sr_2RuO_4-Ru eutectic system through the AC and DC magnetic susceptibility measurements. We revealed that uniaxial pressures in all of the applied directions strongly enhance the volume fraction of the 3-K superconductivity in the Sr_2RuO_4-Ru eutectic system [5]. Unexpectedly, the onset T_c of *pure* Sr_2RuO_4 was revealed to be immediately enhanced from 1.34 K to 3.2 K by a very low uniaxial pressure along the *c* axis of as small as 0.2 GPa (Fig. 1) [6]. This drastic increase in T_c cannot be explained by the uniaxial pressure effect with the elastic limit [7, 8]. We speculate that a qualitative change in the electronic structure of Sr_2RuO_4 arises at relatively low uniaxial pressure and generates superconductivity with the enhanced T_c. The present results suggest that *pure* Sr_2RuO_4 intrinsically has two superconducting phases with T_c =1.5 K and with varying T_c up to 3.2 K, depending on anisotropic distortions in its crystal structure.

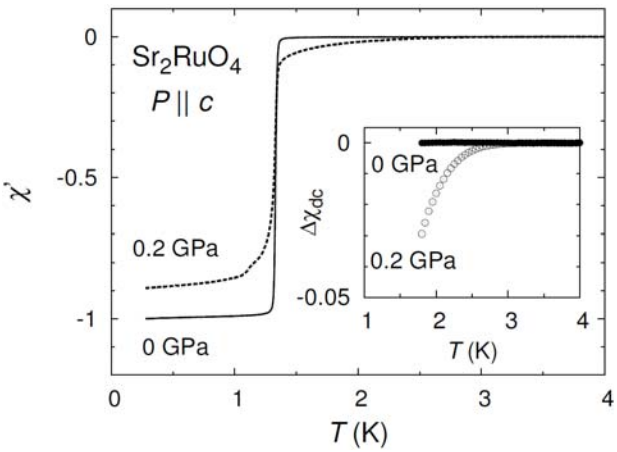

Fig. 1: Temperature dependence of the real part χ' of the AC susceptibility of pure Sr_2RuO_4 under uniaxial pressure along the *c* axis. Inset represents the DC susceptibility normalized by the ideal value for the full Meissner state without the demagnetization correction.

[1] A. P. Mackenzie and Y. Maeno, Rev. Mod. Phys. **75**, 657 (2003).
[2] Y. Maeno *et al*., Phys. Rev. Lett. **81**, 3765 (1998); T. Ando *et al*., J. Phys. Soc. Jpn. **68**, 1651 (1999).
[3] N. Shirakawa *et al*., Phys. Rev. B **56**, 7890 (1997); D. Forsythe *et al*., Phys. Rev. Lett. **89**, 166402 (2002).
[4] Y. A. Ying *et al*., Phys. Rev. Lett. **103**, 247004 (2009).
[5] S. Kittaka *et al*., J. Phys. Soc. Jpn. **78**, 103705 (2009).
[6] S. Kittaka *et al*., submitted to Phys. Rev. Lett.
[7] N. Okuda *et al*., J. Phys. Soc. Jpn. **71**, 1134 (2002).
[8] T. Nomura and K. Yamada, J. Phys. Soc. Jpn. **71**, 1993 (2002).

P122

Surface Impedance of Spin-triplet NS junctions

Y. Asano,[1] Y. Tanaka,[2] and A. A. Golubov[3]

[1] *Department of Applied Physics and Center for Topological Science & Technology, Hokkaido University*
[2] *Department of Applied Physics, Nagoya University, Nagoya 464-8603, Japan*
[3]*Faculty of Science and Technology, University of Twente, 7500 AE, Enschede, The Netherland*

The clear distinction between the spin-singlet superconductor and spin-triplet one is a difficult issue in condensed matter experiments even now. We think of several experimental methods for this purpose: the nuclear magnetic resonance, the muon spin rotation, the critical magnetic field H_{C2} beyond the Pauli limit, the Josephson π-junctions, the thermal conductivity, and the detection of multiple-phases by the spin susceptibility and the specific heat. For instance, the unchanged Knight-shift across the critical temperature T_C suggests the spin-triplet superconductivity. This result, however, is not the sufficient condition for the spin-triplet superconductivity because the spin-singlet superconductivity with the strong spin-orbit coupling may also explain the unchanged Knight-shift.

To distinguish spin-triplet from spin singlet, we have proposed conductance spectroscopy of superconducting T-shaped junction. According to the theoretical calculation, a large zero-bias peak is expected in dIdV-conductance for spin-triplet junction, whereas small zero-bias dip is expected in the case of spin-singlet. Odd-frequency Cooper pairs in a metal of the T-shaped junction causes the anomalous zero-bias peak structure in spin-triplet junction. Although the experimental signal would be very clear depending on the pairing symmetry, it is still difficult to make electric contact between a metal and a spin-triplet superconductor Sr_2RuO_4.

Surface impedance ($Z=R+iX$) well reflects the pairing symmetry of superconductor. For instance, it is possible to know the nodes in the pairing function from temperature dependence of the real part R (surface resistance) and the imaginary part X (reactance). In this research, we consider a proximity structure, where a normal metal surrounds a superconductor. By solving the Maxwell equation with assuming the penetration of odd-frequency pairs, we have phenomenologically shown that odd-frequency property drastically affect the surface impedance. A relation $R<X$ usually holds in spin-singlet proximity structure for all temperature below Tc. However this relation is expected to be reverse in spin-triplet proximity structure. In the presentation we will discuss results of microscopic calculation on the basis of quailclassical Green function theory.

P123

Interference between Sr_2RuO_4 and *s*-wave superconductors

R. Nakagawa[1], T. Nakamura[1], T. Yamagishi[1], Y. A. Ying[2], S. Yonezawa[1], T. Terashima[3] and Y. Maeno[1]

[1]*Dept. of Physics, Kyoto University, Oiwake-cho, Kitashirakawa, Sakyou-ku, Kyoto 606-8502, Japan*
[3]*Department of Physics, Pennsylvania State University, University Park, PA 16802-6300, USA*
[3]*LTM Center, Kyoto University, Yoshidahon-cho, Sakyou-ku, Kyoto 606-8501, Japan*

There exists strong experimental evidence in favor of spin-triplet *p*-wave superconductivity in Sr_2RuO_4 (T_c = 1.5 K) [1]. A eutectic system Sr_2RuO_4-Ru exhibits a broad superconducting transition around Ru-inclusions with an onset ~ 3 K, called 3-K phase, although T_c of Sr_2RuO_4 and Ru are 1.5 K and 0.5 K respectively. This superconductivity above 1.5 K is also considered as *p*-wave and the mechanism of enhancement of T_c is intriguing [2].

In order to clarify the superconducting parity of Sr_2RuO_4, we fabricated proximity junctions with Sr_2RuO_4 and Pb, which is a conventional superconductor with T_c = 7.2 K. Since the cleaved *ab* surface of Sr_2RuO_4 shows high contact resistance, the junctions were fabricated with Sr_2RuO_4-Ru eutectic single crystals, and Pb and Sr_2RuO_4 are connected well electrically through Ru-inclusions. In such junctions, anomalous temperature dependence of the critical current is observed [3, 4]. This behavior has been theoretically interpreted by the interference between superconducting wave functions of Pb and Sr_2RuO_4 having different parities [5]. However, the roles of Ru inclusions or the 3-K phase superconductivity were not explicitly considered theoretically, nor precisely characterized experimentally.

In order to clarify the contribution of the 3-K phase superconductivity, we constructed various junctions with Sr_2RuO_4-Ru eutectic crystals. Surprisingly, the Pb/Ru/Sr_2RuO_4 junction with a single Pb electrode exhibited anomalous behavior of I_c just like the one observed in Pb/Sr_2RuO_4/Pb junctions (Fig.1, 2). This result indicates existence of a new mechanism that can cause I_c anomaly. We propose that a topological change in the wave function of the 3-K phase superconductivity is driven by the competition between the induced s-wave order parameter in Ru and the *p*-wave order parameter of the bulk Sr_2RuO_4 and plays a key role to explain the observed behavior of $I_c(T)$.

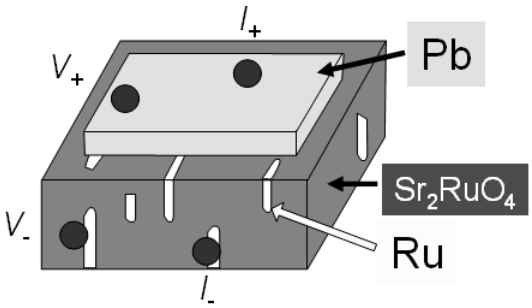

Fig. 1. Schematic of a Pb/Ru/Sr_2RuO_4 junction. The junction contains many Ru inclusions with the size of ~1 × 10 × 30 (μm)^3, which are embedded in the eutectic crystal of Sr_2RuO_4-Ru. The Pb film with the thickness of ~1μm was deposited by thermal evaporation method.

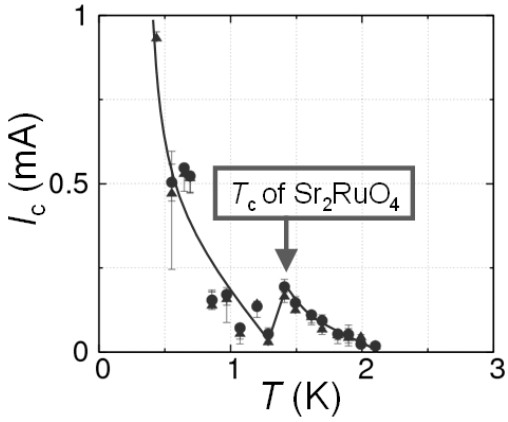

Fig. 2. Temperature dependence of the critical current in the Pb/Ru/Sr_2RuO_4 junction. I_c increases with lowering temperature. Just below T_c of Sr_2RuO_4, however, I_c exhibits a sharp decrease and then a sharp increase again below 1.2 K.

[1] A. P. Mackenzie and Y. Maeno, Rev. Mod. Phys. **75**, 657 (2003).
[2] M. Sigrist and H. Monien, J. Phys. Soc. Jpn. **70**, 2409 (2001).
[3] R. Jin, Yu. Zadorozhny, Y. Liu, D. G. Schlom, Y. Mori and Y. Maeno, Phys. Rev. B **59**, 4433 (1999)
[4] R. Nakagawa, T. Nakamura, T. Terashima, S. Yonezawa and Y. Maeno, to appear in Physica C (2010).
[5] C. Honerkamp and M. Sigrist, Prog. Theor. Phys. **53**, 100 (1998).

P124

Microscopic Theory of D-vector in Spin Triplet Superconductors

Y. Yanase

Dept. of Physics, Niigata University, 8050 Ikarashi, Nishi-ku, Niigata 950-2181, Japan

The multi-component order parameter in spin-triplet superconductors/superfluid, called d-vector, has been intensively investigated for a long time. The heavy fermion superconductors UPt_3 and Ube_{13} are the first promising candidates for the spin triplet superconductor and vast studies in 80's were devoted to explore the pairing state in these materials. The discovery of superconductivity in transition metal oxide Sr_2RuO_4 led to more detailed and precise theoretical treatments of the d-vector. The field of spin triplet superconductivity has been also extended to the other heavy fermion superconductors including UGe_2, URhCe, UCoGe, $CePt_3Si$, and $PrOs_4Sb_{12}$.

The physics of d-vector has been investigated on the basis of the phenomenological theory [1], but the microscopic mechanism to determine the structure of d-vector remained unclear. Recent developments in the theory of multi-orbital superconductors have made it possible to study the d-vector from the microscopic point of view. In this presentation, I will talk about our microscopic studies on the d-vector in the family of Sr_2RuO_4 [2,3] and the non-centrosymmetric superconductor $CePt_3Si$ [4].

We show the several exact rules for the d-vector. The direction and anisotropy of the d-vector are determined by the crystal structure, local orbital of electrons, and the symmetry of Cooper pairs, independent of the details of electron correlation. The results are summarized in Table I [2,4,5]. We investigate the pairing state of Sr_2RuO_4 in the magnetic field on the basis of the Table I [3]. The second superconducting phase of Sr_2RuO_4 at high magnetic fields and low temperatures is identified to be the non-unitary state, which is similar to the A_1 phase in ^{3}He.

In this presentation, I will also discuss the roles of the directional disorder, such as the stacking faults in Sr_2RuO_4 and $CePt_3Si$ [6]. It is shown that the d-vector in some centrosymmetric spin triplet superconductors is determined by the random spin-orbit coupling arising from the disorders. For the eutectic crystal of Sr_2RuO_4 the superconducting state with time-reversal symmetry, which is different from the chiral superconducting state in the bulk, is predicted.

Crystal	Tetragonal		Hexagonal			Non-centro. systems	Disorder (Stacking fault)
Local orbital	d_{xy}	d_{yz} d_{zx}	E_g		A_{1g}		
Sym. of SC	P-wave		P	F	P, F		
d-vector	d//c	d//ab	d//ab	both	both	d//g(k)	d//ab
Anisotropy	$O(\lambda^2/E_F^2)$	$O(\lambda/E_F)$	$O(\lambda/E_F)$	$O(\lambda^2/E_F^2)$	$O(\lambda^2/E_F^2)$	$O(1)$	$O(\bar{\alpha}^2/E_F T_{c0})$

Table I: Summary of the d-vector. The structure of d-vector is determined by the crystal structure, local electron orbital, and the symmetry of superconductivity.

[1] M. Sigrist and K. Ueda, RMP 63, 239 (1991).
[2] Y. Yanase and M. Ogata, JPSJ 72, 673 (2003).
[3] M. Udagawa, Y. Yanase, and M. Ogata, JPSJ 74, 2905 (2005).
[4] Y. Yanase and M. Sigrist, JPSJ 76, 043712 (2007); JPSJ 77, 124711 (2008) .
[5] Y. Yanase, M. Mochizuki, and M. Ogata, JPSJ 74, 430 (2005).
[6] Y. Yanase, In preparation.

P125

Interplay between Antiferromagnetism and Superconductivity in the Two-Dimensional Hubbard model within a Variational study

Kenji Kobayashi[1] and Hisatoshi Yokoyama[2]

[1]*Department of Natural Science, Chiba Institute of Technology, Shibazono, Narashino 275-0023, Japan*
[2]*Department of Physics, Tohoku University, Sendai 980-8578, Japan*

The proximity of antiferromagnetic and superconducting phases is a feature universal to all cuprate superconductors, and seems to be essential to clarify the interplay between antiferromagnetism (AF) and superconductivity (SC). This feature has been noticed again by a recent NMR experiment showing the coexistence of the two phases in a single CuO_2 plane in the Hg-based multi-layered cuprate [1]. In this presentation, we study the interplay between AF and SC in the Hubbard model on a square lattice with a diagonal transfer t', which is useful in linking weak and strong coupling (t-J-model) regimes. A variational Monte Carlo method we use is a rare approach to consider the whole range of the model parameters with quantitative reliability, and can treat the local correlation exactly. As in the preceding work [2], we simultaneously introduce the following improvements into the wave function: (1) Coexistence of AF and d-wave singlet gaps that enables us to directly check the cooperation or competition between them. (2) Band renormalization effect owing to electron correlation within the fourth-neighbor hoppings. (3) Refined doublon-holon correlation factors, which control the effect of Mott transition near half filling more precisely. Applying this wave function to the Hubbard model, it is found that the stable state changes with the value of U/t, t'/t, and doping rate δ. For the extremely large value of U/t, a coexisting state is realized for $t'/t \geq -0.15$, whose range of doping rate extends as t'/t increases. In this region, the δ dependence of SC and AF orders is similar to that of the t-J model as a whole. In contrast, for t'/t=-0.3, AF and SC states are mutually exclusive, and a coexisting state does not appear. As U/t decreases, the area of pure AF extends, and that of coexisting state shrinks. As a result, the coexisting state disappears for t'/t = -0.15 and U/t=12, probable values for hole-doped cuprates. The resultant phase diagram has a feature different from that of the t-J model, especially in the under-doped regime, and the coexisting state is restricted to the extremely large values of U/t and low densities for hole-doped cuprates.

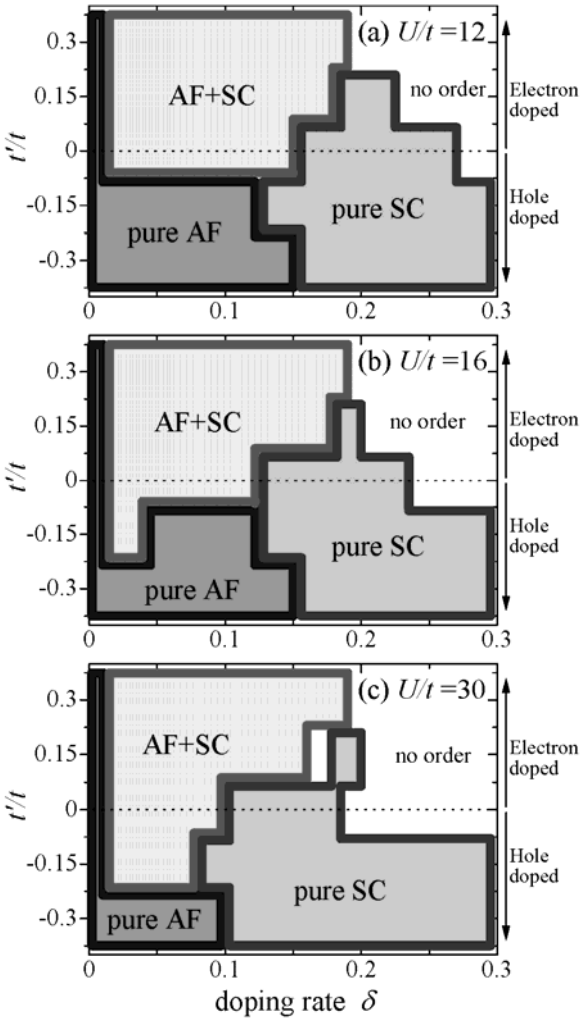

FIG.1: Phase diagrams constructed within the present wave function.

[1] H. Mukuda *et al.*, Phys. Rev. Lett. **96**, 087001(2006); H. Mukuda *et al.*, J. Phys. Soc. Jpn. **77**, 124706(2008).
[2] K. Kobayashi and H. Yokoyama, J. Phys. Chem. Solids **69**, 3274(2008); K. Kobayashi and H. Yokoyama, Physica C **469**, 974(2009).

P126

STM/STS Studies of Superconducting Ultra-Thin Indium Films on Graphite

S. Matsuo, N. F. Kawai, T. Matsui, and Hiroshi Fukuyama

Department of Physics, The University of Tokyo, 7-3-1 Hongo, Bunkyo-ku, Tokyo 113-0033, Japan

We will show experimental plan and some preliminary results of scanning tunneling microscopy and spectroscopy (STM/STS) measurements on superconducting ultra-thin indium islands grown on a highly oriented pyrolytic graphite (HOPG) surface.

Superconductivity is still one of major research disciplines in physics and engineering after the BCS theory succeeded in microscopic explanation of this phenomenon more than fifty years ago. Recent progress in nanotechnology enables us to fabricate superconductors in nanometer scale or reduced dimensions and to measure their local electronic properties in similar or even smaller scales with STM/STS. For example, the layer-by-layer oscillation of the superconducting transition temperature was observed in ultra-thin lead films fabricated on silicon substrate as a function of the film thickness [1]. In lead nano-islands on silicon, it was found that the superconducting energy gap reduces diminishingly as the island size decreases [2] and that a single vortex penetrates into an island [3]. The availability of atomically flat film surfaces was crucial for those kinds of quantitative STS measurements. So far, there are few similar experiments on different superconducting materials from lead nor those indicating the two-dimensional character of the phase transition.

We have started STM/STS experiments for ultra-thin indium islands fabricated on a HOPG surface using our ultra-low temperature STM/STS [4]. This apparatus has the capability of sample preparation in ultra-high vacuum at arbitrary temperatures between 7 and 1300 K. The film is deposited on the substrate at room temperature under an ultra-high vacuum condition. The typical radius and thickness of the islands are measured with STM *in situ* as 60 nm and 6 nm, respectively. We expect to obtain thinner and more uniform islands by annealing the islands at an elevated temperature after the deposition. STM/STS measurements of the energy gap and vortices in each island are planned to be done at low temperatures.

[1] Y. Guo *et al*., Science **306**, 1915 (2004).
[2] C. Brun *et al*, Phys. Rev. Lett. **102**, 207002 (2009).
[3] T. Nishio *et al,* Phys. Rev. Lett. **101**,167001 (2008).
[4] H. Kambara, T. Matsui, Y. Niimi, and H. Fukuyama, Rev. Sci. Instrum. **78**, 073703 (2007).

P127

Superconductivity in the noncentrosymmetric system $Li_2(Pd_{1-x}Pt_x)_3B$

M. Kriener,[1] G. Eguchi,[1] D. C. Peets,[1] S. Harada,[2] Sk. Md. Shamsuzzaman,[2] Y. Inada,[3] G.-q. Zheng,[2] Y. Maeno[1]

[1]*Dept. of Physics, Kyoto University, Kyoto, Japan*
[2]*Department of Physics, Okayama University, Okayama, Japan*
[3]*Faculty of Education, Okayama University, Okayama, Japan*

Most superconductors known to date crystallize in a structure which obeys inversion symmetry. In such materials the Cooper pair wave function has to be spin singlet (triplet) if their parity is even (odd). In contrast the lack of inversion symmetry can lead to an admixture of spin-singlet and triplet states depending on the strength of parity violating antisymmetric spin-orbit coupling [1]. This scenario is suggested to apply for the series $Li_2(Pd_{1-x}Pt_x)_3B$ which crystallize in the noncentrosymmetric cubic space group $P4_332$. A change of the pairing state from mostly spin singlet in Li_2Pd_3B to mostly spin triplet in Li_2Pt_3B was proposed based on penetration-depth and specific-heat measurements [2-4]. This scenario got further support by an NMR study [5].

Recent contradictory results of two different specific-heat studies [3, 6] motivated us to carry out a detailed AC susceptibility and specific-heat study on newly prepared polycrystalline samples of $Li_2(Pd_{1-x}Pt_x)_3B$ for x = 1, 0.9, and 0.84 by an arc-melting method. The superconducting transition temperatures T_c of these samples are slightly higher than reported previously, indicating high quality. From AC susceptometry in zero and various finite magnetic fields H–T phase diagrams were constructed. The critical temperatures and upper critical field strengths are T_c = 3.1K, H_{c2} = 1.7T (x = 1); 3.3K, 1.7T (x = 0.9); and 3.2K, 1.7T (x = 0.84), respectively.

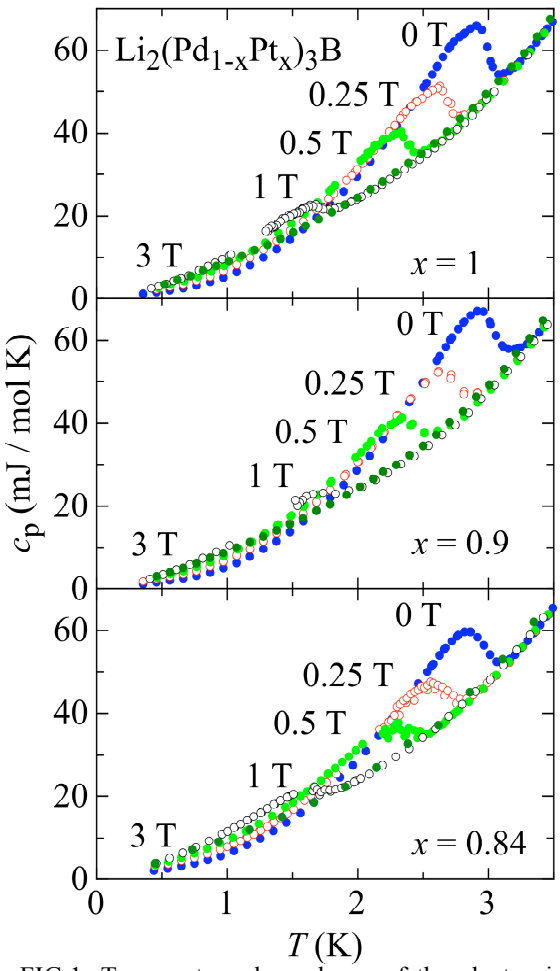

FIG.1: Temperature dependence of the electronic specific heat c_{el}/T of $Li_2(Pd_{1-x}Pt_x)_3B$ for (a) x = 1, (b) 0.9, and (c) 0.84 in various magnetic fields.

The transition temperatures deduced from the specific-heat measurements are in good agreement with those obtained from AC susceptibility. In zero magnetic field all three samples exhibit a clear jump-like anomaly at T_c, see Fig. 1. Upon increasing magnetic field strength, the superconducting transitions shift to lower temperatures and smear out but remain visible up to fields larger than 1T, in agreement with the aforementioned upper critical field values. In this presentation, we will introduce this interesting substitution series and discuss our recent AC susceptibility and specific-heat data in terms of a possible mixing of spin-singlet and spin-triplet states.

[1] S. Fujimoto, J. Phys. Soc. Jpn. **76**, 051008 (2007).
[2] H.Q. Yuan *et al.*, Phys. Rev. Lett. **97**, 017006 (2006).
[3] H. Takeya *et al.*, Phys. Rev. B **72**, 104506 (2005) and **76**, 104506 (2007), Phys. B **403**, 1078 (2008).
[4] R. Khasanov *et al.*, Phys. Rev. B **73**, 214528 (2006).
[5] M. Nishiyama *et al.*, Phys. Rev. Lett. **98**, 047002 (2007).
[6] P.S. Häfliger *et al.*, J. Supercond. Nov. Magn. **22**, 337 (2009)

P128

The Noncentrosymmetric *d*-Electron Superconductors $CaIrSi_3$ and $CaPtSi_3$

G. Eguchi[1], **D.C. Peets[1]**, M. Kriener[1], S. Maki[2], E. Nishibori[2], H. Sawa[2], and Y. Maeno[1]

[1]*Department of Physics, Graduate School of Science, Kyoto University, Kyoto, Japan*
[2]*Department of Applied Physics, Graduate School of Engineering, Nagoya University, Nagoya, Japan*

Most known superconducting materials have an inversion centre in their crystal structure. In superconductors lacking this symmetry element, parity is not a meaningful label, and "singlet" and "triplet" designations cannot strictly be applied to the order parameter. Interactions such as spin-orbit which violate parity and thus mix singlet and triplet channels can be significant, and can lead to a variety of highly unconventional electronic properties and phases [1]. Several such properties have been observed in *f*-electron systems, but not in *d*-electron systems, and it would desirable to disentangle the *f*-electron physics from the noncentrosymmetric physics.

A variety of $AMSi_3$ superconductors (A = Ca, Sr, Ba; M a *d*-block transition metal) crystallizing in the noncentrosymmetric *I4mm* space group were recently discovered [2] (see Fig. 1 for crystal structure). Little work has been done on this family of materials, and it is not yet known whether they exhibit any of the highly unconventional physics possible in noncentrosymmetric systems.

After verifying the existence and superconductivity of $CaIrSi_3$ using another preparation technique, samples of $CaIrSi_3$ and $CaPtSi_3$ were prepared by arc melting, and specific heat and AC susceptibility measurements were performed to characterize the superconducting state and check for unconventional behaviour. Following an introduction to the physics of noncentrosymmetric superconductivity, the preparation, characterization, superconducting properties and *H-T* phase diagrams of these two compounds will be presented.

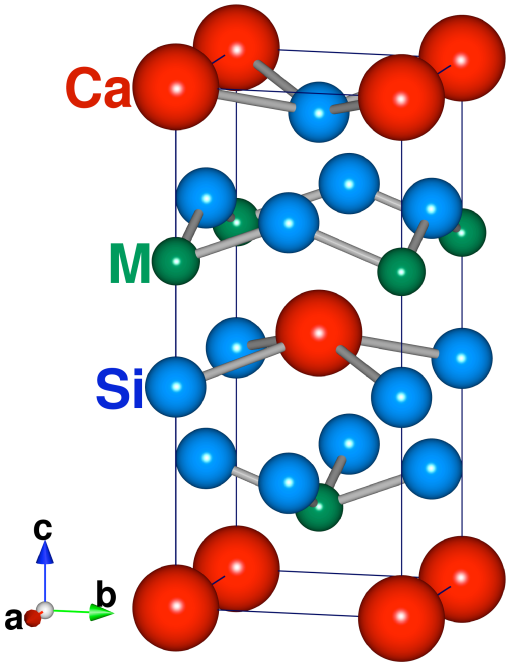

Figure 1: Crystal structure of $CaMSi_3$. The Ca-Si-Si-M stacking along the *c*-axis precludes inversion symmetry.

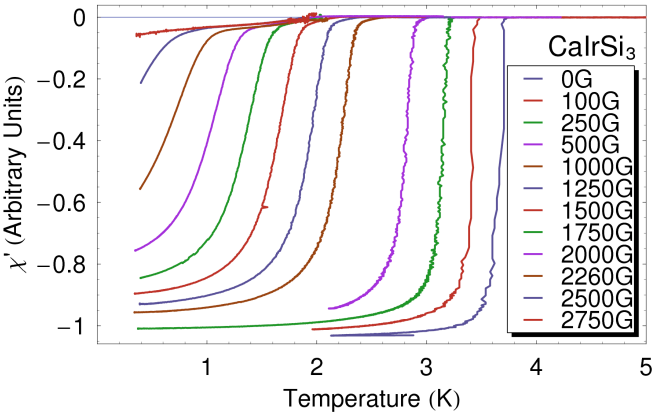

Figure 2: AC susceptibility χ' of $CaIrSi_3$ in various fields.

[1] S. Fujimoto, J. Phys. Soc. Jpn. **76**, 051008 (2007)
[2] S. Oikawa *et al*, talk 23pQC-1 at JPS fall meeting 2008

P129

Theoretical study on the field dependence of the FFLO state

K. Suzuki[1], N. Nakai[2,3], M. Ichioka[1], K. Machida[1]

[1]*Dept. of Physics, Okayama University, 3-1-1 Tsushimanaka, Kita-ku, Okayama-shi, Okayama 223-8522, Japan*
[2]*CCSE, Japan Atomic Energy Agency, 6-9-3 Higashi-Ueno Taito-ku, Tokyo 110-0015, Japan*
[3]*CREST(JST), 4-1-8 Honcho, Kawaguchi, Saitama 332-0012, Japan*

By the quasiclassical Eilenberger theory we investigate the field dependence of the Flude-Ferrell-Larkin-Ovchinnikov(FFLO)[1,2] state with also including orbital depairing effect by vortices. Especially we consider the LO state, in which the order parameter modulates with changing its sign in real space. We assume that the Fermi surface is spherical and that a pairing interaction is isotropic. We set initial conditions that the nodal plane of the LO state is perpendicular to the vortex line and that vortices form triangular lattices. And we calculate Eilenberger equations self-consistently in each field and some periods of the LO state. With self-consistent solutions we calculate the free energy and physical quantities such as paramagnetic moment for each parameter. Comparing free energies we estimate the stable LO state.

As shown in Fig.1, from developments of q-vector, which is the momentum of Cooper pairs for the center-of-mass, a phase transition from the Abrikosov states to the LO state seems to be the second-order transition. We show that q-dependence of the order parameter in Fig.2. Each order parameter is normalized by their maximum value and period. From Fig. 2 we can see that the order parameter with large q-vector is almost sinusoidal, but that the order parameter with small q-vector is not sinusoidal.

[1] P. Fulde and R. A. Ferrell, Phys. Rev. **135**, A550 (1964).
[2] A. I. Larkin and Y. N. Ovchinnikov, Sov. Phys. JETP **20**, 762 (1965)

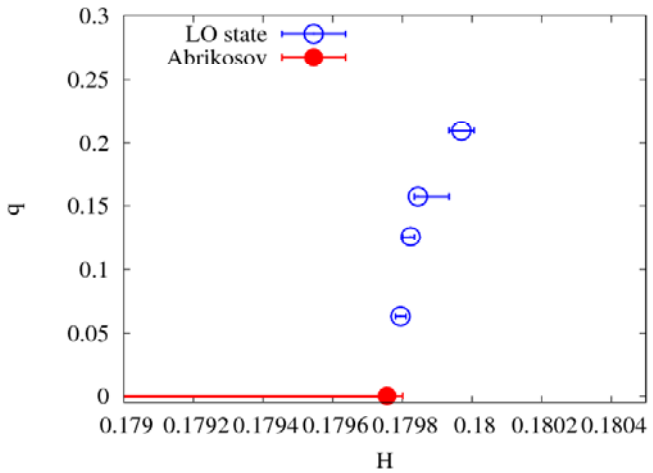

Fig.1. The field dependence of the q-vector. q is 2π/L, where L is the wave length of the LO state in z-direction.

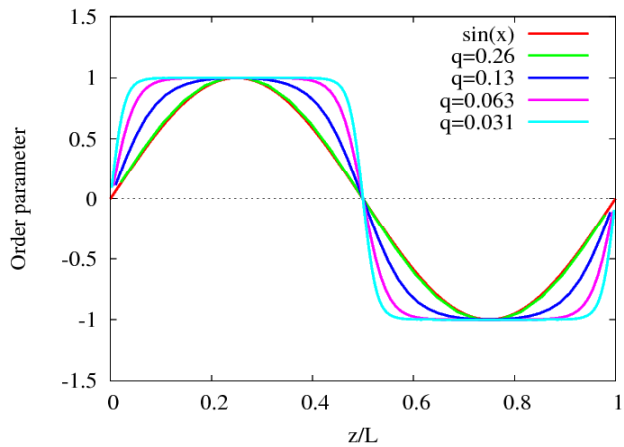

Fig.2. The order parameters in a place away enough from vortex core are plotted. The maximum values of each order parameter are normalized.

P130

Meissner Effect of the Odd-Frequency Superconductivity

Y. Fuseya and K. Miyake

Dept. of Materials Engineering Science, Osaka University, Tyonaka, Osaka 560-8531, Japan

The odd-frequency superconductivity is the novel class of superconductivity, of which pairing correlations are odd in frequency, as introduced originally by Berezinskii [1] and more recently by Balatsky and Abrahams [2]. Recent theoretical studies demonstrated the possible existence of the odd-frequency superconductivity in a wide variety of systems [3-6].

On the other hand, there still remains a fundamental problem: the negative sign problem in the Meissner effect. For the odd-frequency pairing, the Meissner kernel has an opposite sign from the conventional (even-frequency) pairing within the approximation that only considers the contribution of quasi-particle (coherent part), i.e., without any fluctuations or correlations. According to our previous study, however, some strong fluctuations are needed to realize the odd-frequency superconductivity [4]. Therefore, we should consider adequately the contribution of the fluctuations (or the incoherent part).

In the present work, we investigate the Meissner effect with considering the corrections of spin fluctuations. It is found that the Meissner kernel becomes positive sign with moderate strength of spin fluctuations.

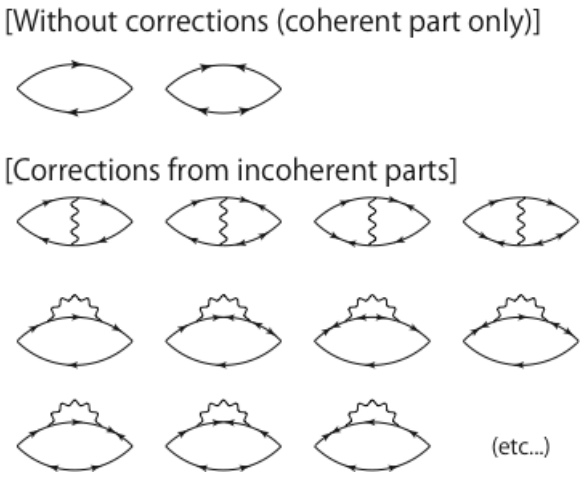

Feynman diagrams that contribute to the Meissner effect.
(upper) Contributions from the coherent part previously considered.
(lower) Contributions from the incoherent part considerd in the present work.

[1] V. L. Berezinskii: JETP Lett. **20** (1974) 287.
[2] A. Balatsky, E. Abrahams: Phys. Rev. B **45** (1992) 13125.
[3] M. Vojta and E. Dagotto: Phys. Rev. B **59** (1999) R713.
[4] Y. Fuseya, H. Kohno, K. Miyake: J. Phys. Soc. Jpn. **72** (2003) 2914.
[5] K. Yada et al.: arXiv: 0806.4241.
[6] K. Shigeta et al.: Phys. Rev. B **79** (2009) 174507.

P131

Magnetic Field Induced Crossover in the Yb-based Heavy-Fermion System α-$YbAlB_4$

N. Horie[1], T. Tomita[1], K. Kuga[1], Y. Matsumoto[1], C. Petrovic[1,2], and S. Nakatsuji[1]

[1] *Institute for Solid State Physics, Univ. of Tokyo, Kashiwa, 277-8581, Japan.*
[2]*Brookhaven National Laboratory, NY, 11973-5000, US.*

The Yb-based heavy fermion (HF) system, α-$YbAlB_4$, is isostoichiometric to the centrosymmetric HF superconductor β-$YbAlB_4$ [1,2] and it has a noncentrosymmetric crystal structure. Recently these systems were revealed to be in intermediate valence states by photoemission spectroscopy[3]. Although some of the physical properties were reported for α-$YbAlB_4$ [4, 5], there has been no detailed low-temperature study particularly using high quality samples. Recently, we have succeeded in growing pure single crystals with RRR over 100 using an Al flux method. Here, we present our results of the resistivity, specific heat and magnetization measurements at low temperatures under magnetic fields. Our results indicate a Fermi Liquid ground state in α-$YbAlB_4$ under ambient pressure and zero magnetic field, in contrast with the non-Fermi-liquid state found in β-$YbAlB_4$ [1].

Moreover, a magnetic-field induced crossover is observed in α-$YbAlB_4$. Magnetization curve shows the slope change at 3T as one can see in inset of Fig.1, indicating a metamagnetic transition. Interestingly, corresponding changes under magnetic fields are also observed in the specific heat C_m/T, the differential susceptibility *dM/dH* and the magnetoresistance. We will discuss the origin of these effects, taking account of their similarity to the crossover observed in $YbRh_2Si_2$ [6] and other metamagnetic transitions seen in the HF systems.

This work is performed in collaboration with Y. Matsuda, Y. Shimura, T. Sakakibara at ISSP, Univ. of Tokyo.

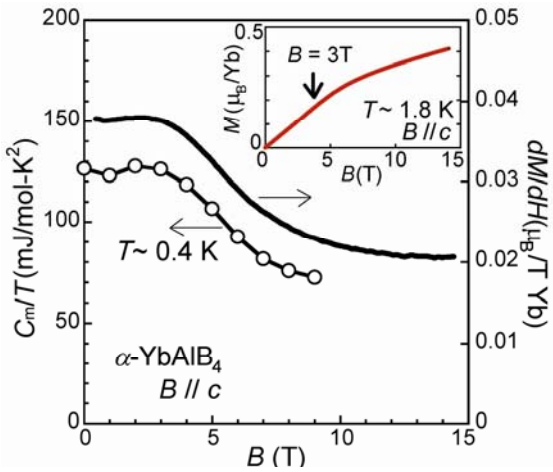

Fig. 1: Magnetic field dependence of C_m/T obtained at ~ 0.4 K and differential susceptibility *dM/dH* at ~ 1.8 K. Inset: Magnetization measured under fields along *c*-axis at ~ 1.8 K.

[1] S. Nakatsuji, K.Kuga, Y. Machida, T. Tayama, T. Sakakibara, Y. Karaki, H. Ishimoto, S. Yonezawa, Y. Maeno, E. Pearson, G. G. Lonzarich, L. Balicas, H. Lee, and Z. Fisk, *Nature Phys.* **4**, 603 (2008).
[2] K. Kuga, Y. Karaki, Y. Karaki, Y. Matsumoto, Y. Machida, and S. Nakatsuji, *Phys. Rev.Lett.* **101**, 137004(2008).
[3] M. Okawa, M. Matsunami, K. Ishizaka, R. Eguchi, M. Taguchi, A. Chainani, Y. Takata, M. Yaba shi, K. Tamasaku, Y. Nishino, T. Ishikawa, K. Kuga, N. Horie, S. Nakatsuji, and S. Shin, *preprint at* arXiv:0906.4899.
[4] Z. Fisk, K. N. Yang, M. B. Maple, H. R. Ott, In *Valence Fluctuations in Solids*; L. M. Falicov, W. Hanke, M. B. Maple, Eds.; North-Holland Publishing Company: New York, 1981;pp 345-347.
[5] Robin T. Macaluso, Satoru Nakatsuji, Kentaro Kuga, Evan Lyle Thomas, Yo Machida, Yoshiteru Maeno, Zachary Fisk, and Julia Y. Chan, *Chem. Mater.* **19**, 1918 (2007).
[6] Y. Tokiwa *et al.*, *Phys. Rev. Lett.* **94**, 226402(2005).

P132

Heat Capacity Study of the Quasi-One-Dimensional Organic Superconductor $(TMTSF)_2ClO_4$ in Accurately Aligned Magnetic Fields

S. Yonezawa,[1] Y. Maeno,[1] K. Bechgaard,[2] and D. Jérome[3]

[1]*Deptartment of Physics, Graduate School of Science, Kyoto University, Kyoto, Japan*
[2]*Department of Chemistry, Oersted Institute, Copenhagen, Denmark*
[3]*Laboratoire de Physique des Solides, Université Paris-Sud, Orsay, France*

The molecular salt $(TMTSF)_2X$ (X = ClO_4, PF_6, etc.) is the first reported organic superconductor discovered in 1980 [1,2], and its fascinating physical properties have kept attracting much attention throughout this 30 years. Here, we present results of our recent specific heat study with improved techniques, providing new insights on the superconducting (SC) state of $(TMTSF)_2ClO_4$.

The TMTSF family is one of the most archetypal quasi-one-dimensional (Q1D) conductor with the highest conductivity along the *a* axis. Its electronic structure and its Fermi surface are very simple in spite of its complex crystal structure [3]. This simplicity, as well as availability of very clean single crystals, provides us good opportunities to deeply study the intrinsic SC phenomena in Q1D systems both experimentally and theoretically.

In fact, it has been revealed that the superconductivity in $(TMTSF)_2X$ is highly unconventional with sign changes on the SC gap [4,5]. Another example is that the onset of superconductivity determined from resistivity measurements survives up to above 5 T [6-8]. This field is much larger than the Pauli limiting field H_P ~ 2.5 T, where ordinary singlet pairs would be unstable due to the Zeeman effect. Thus possibility of triplet pairing or FFLO state has been discussed [9]. However, several pieces of important information on the SC state, such as the SC gap structure and the SC symmetry, are still controversial [10].

We developed a small heat capacity measurement apparatus with high resolution (~ 0.1 nJ/K @ 1 K) based on a modification of the ac method. This technique allows us to study the heat capacity of one single crystal of $(TMTSF)_2ClO_4$, as shown in Fig. 1. We also measure the specific heat in magnetic fields whose direction is precisely controlled with respect to the crystalline axes. The obtained data suggest that $(TMTSF)_2ClO_4$ is a singlet superconductor with line nodes on its SC gap. Comparison between the SC phase diagram deduced from the present specific heat measurement and those obtained from previous resistivity measurements are also discussed.

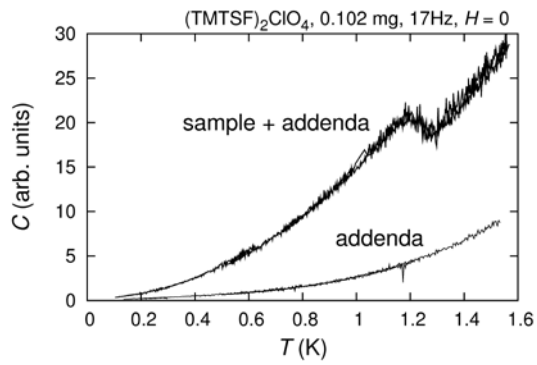

FIG.1: Temperature dependence of the heat capacity of one single crystal of $(TMTSF)_2ClO_4$ (0.102 mg) plus the addenda (background). The heat capacity of the addenda alone is also presented.

[1] D. Jérome *et al.*, J. Phys. Lett. **41**, 95 (1980).
[2] K. Bechgaard *et al.*, Phys. Rev. Lett. **46**, 852 (1981).
[3] D. L. Pevelen *et al.*, Eur. Phys. J. B **19**, 363 (2001)
[4] M. Y. Choi *et al.*, Phys. Rev. B **25**, 6208 (1982);
[5] N. Joo *et al.*, Europhys. Lett. **72**, 645 (2005).
[6] I. J. Lee *et al.*, Phys. Rev. Lett. **78**, 3555 (1997).
[7] J. I. Oh and M. J. Naughton, Phys. Rev. Lett. **92**, 067001 (2004).
[8] S. Yonezawa *et al.*, Phys. Rev. Lett. **100**, 117002 (2008); J. Phys. Soc. Jpn. **77**, 054712 (2008).
[9] For example, A. G. Lebed, JETP Lett. **44**, 114 (1986); N. Dupuis and G. Montambaux, Phys. Rev. B **49**, 8993 (1994).
[10] For example, M. Takigawa *et al.*, J. Phys. Soc. Jpn. **56**, 873 (1987); S. Belin and K. Behnia, Phys. Rev. Lett. 79, 2125 (1997); I. J. Lee *et al.*, Phys. Rev. Lett. **88**, 017004 (2001); J. Shinagawa *et al.*, Phys. Rev. Lett. **98**, 147002 (2007).

P133

Effect of Long-Range Impurity Potential on Superconductivity

A. Okada and K. Miyake

Graduate School of engineering Science, Osaka University, Osaka 560-8531, Japan

The transition temperature (T_c) of the unconventional superconductivity in $CeCu_2Ge_2$ takes the maximum at pressure around P_v where valence of Ce ion changes drastically [1]. Onishi and Miyake proposed the critical valence fluctuations as its mechanism on the basis of an extended periodic Anderson model with Coulomb repulsion between conduction and f-electron [2]. On the basis of the same model, the experimental result that the residual resistivity ρ_0 has a large maximum near P_v was also explained [3]. The reason why ρ_0 has the large maximum is that impurity potential becomes long-range around P_v because of renormalization effect of the critical valence fluctuations. For the impurity having short-range potential, the impurity-concentration dependence of T_c was revealed and described by Anderson theorem for isotropic superconductivity and Abrikosov-Gor'kov (AG) formula for anisotropic superconductivity.

Then, we investigate the case in which impurity potential is screened Coulomb type as a simple model of long-range potential and the scattering is elastic. We treat the screening factor η in the potential as the distance from the critical point and calculate the impurity-concentration dependence of T_c for several η. It is revealed that η determines whether the dependence is affected by the symmetry of superconductivity or not. In the case of $\eta << 1$, T_c of s-wave superconductivity is also suppressed by impurity following the AG formula as p-, d-wave superconductivity. On the other hand, when η is not so small, the reduction of T_c is depends on the symmetry of superconductivity. The superconductivity having lower symmetry is more robust for impurity than the higher one.

A secret of the present result is that long-range impurity potential gives a vertex correction for the pair susceptibility cancelling the effect of self-energy correction. For $\eta << 1$, because the vertex correction is much smaller than self-energy correction, any superconductivity follows the AG formula in which not the vertex correction but the self-energy correction contributes.

References
[1] D. Jaccard *et al*.: Physica B **259-261** (1999) 1.
[2] Y. Onishi and K. Miyake : J. Phys. Soc. Jpn. **69** (2000) 3955.
[3] K. Miyake and H. Maebashi : J. Phys. Soc. Jpn. **71** (2002) 1007.

P134

Pr site imperfection effect and doping effect on the spontaneous internal fields in the heavy fermion superconductor $PrOs_4Sb_{12}$

Y. Aoki,[1] A. Imamura, [1] R. Miyazaki, [1] T. Saito, [1] I. Umegaki, [1] R. Higashinaka, [1] Y. Tunashima, [1] H. Sato[1] T. Fukuhara,[2] H. Sugawara,[3] D. E. MacLaughlin,[4] Lei Shu,[4] W. Higemoto,[5] K. Ohishi,[5] R. H. Heffner, [5] A. Koda,[6] R. Kadono, [6] and A. D. Hillier[7]

[1] *Department of Physics, Tokyo Metropolitan University, Hachioji-Shi, Tokyo 192-0397 Japan*
[2] *Department of Liberal Arts and Sciences, Toyama Prefectural University, Kosugi, Toyama 939-0398*
[3] *Department of Physics, Kobe University, Kobe 657-8501, Japan*
[4]*Department of Physics, University of California, Riverside, California 92521 USA*
[5]*Japan Atomic Energy Research Institute, Tokai 319-1195, Japan*
[6]*Meson Science Laboratory, KEK, Tsukuba, Ibaraki 305-0801, Japan*
[7]*ISIS Facility, Rutherford Appleton Laboratory, Chilton, Didcot, Oxfordshire OX11 0QX, United Kingdom*

The filled skutterudite $PrOs_4Sb_{12}$ is the first Pr-ion-based heavy-fermion superconductor [1] and the anomalous physical quantities reported so far indicates the superconducting state being unconventional one [2]. The appearance of internal fields in the superconducting state indicating broken time reversal symmetry in the superconducting state is one of the most interesting features [3]. In order to investigate the doping effect on this feature, muon spin relaxation (μSR) experiments are going on $(Pr_xLa_{1-x})Os_4Sb_{12}$ and $Pr(Os_xRu_{1-x})_4Sb_{12}$ systems [4]. It has been found that the internal fields are rapidly suppressed for the latter case. This finding will be discussed in connection with the 4f-electron crystalline-electric-field (CEF) singlet-triplet low energy splitting Δ, which is modified by the doping.

Another interesting finding is that Pr-site deficiency can be controlled by changing the heat treatment process in growing single crystals by the flux method [5]. The superconducting transition temperature T_c (as well as the upper critical field H_{c2}) rapidly decreases with decreasing the Pr-site occupancy x (determined by EPMA), in comparison with those observed in $(Pr_xLa_{1-x})Os_4Sb_{12}$ [6,7]. In $Pr_xOs_4Sb_{12}$, from the specific heat and magnetic susceptibility measurements, the 4f-electron CEF energy splitting Δ decreases rapidly with decreasing x, while almost no change appears in Δ for $(Pr_xLa_{1-x})Os_4Sb_{12}$. This observation supports that the CEF excitations of 4f-electrons play a major role for the realization of the unconventional superconductivity in $PrOs_4Sb_{12}$ [8,9].

[1] E.D. Bauer *et al*., Phys. Rev. B **65,** 100506(R) (2002).
[2] For a review, see Y. Aoki *et al*., J. Phys. Soc. Jpn. **76,** 051006 (2007).
[3] Y. Aoki *et al*., Phys. Rev. Lett. **91**, 067003 (2003).
[4] For a preliminary report, see L. Shu et al., J. Magn. Magn. Mat. **310** (2007) 551.
[5] Y. Aoki et al. Physica C (2010) to appear.
[6] C. R. Rotundu, *et al*. Phys. Rev. B **73**, 014515 (2006).
[7] M. Yogi *et al*., J. Phys. Soc. Jpn. **75**, 124702 (2006).
[8] T. Namiki *et al*., J. Phys. Soc. Jpn. **76**, 093704(2007).
[9] J. Chang *et al*., Phys. Rev. B **76**, 220510(2007).

P135

Heavy Fermion Superconducting Properties of the Filled Skutterudite $Pr(Os_{1-x}Ru_x)_4Sb_{12}$

R. Miyazaki,[1] Y. Aoki,[1] R. Higashinaka,[1] H. Sugawara[2] and H. Sato[1]

[1]*Dept. of Physics, Tokyo Metropolitan University, 1-1 Minamiosawa, Hachioji, Tokyo 192-0397, Japan*
[2]*Department of Physics, Kobe University, 1-1 Nada-ku, Kobe, Hyogo 675-8501, Japan*

Filled skutterudite compound $PrOs_4Sb_{12}$ exhibits unconventional properties in the superconducting state, for example, heavy fermion (HF) superconductivity with relatively high transition temperature T_c = 1.85 K, possible existence of multiple superconducting phases, time reversal symmetry breaking and multiband nature of the superconductivity. It is an interesting question whether these unconventional features are associated with the anharmonic oscillations (rattling) of Pr ions and 4f-electron quadrupolar excitons.

Since $PrRu_4Sb_{12}$ is a conventional BCS superconductor, it is important to investigate the physical properties of the alloy series $Pr(Os_{1-x}Ru_x)_4Sb_{12}$. In this series, it was reported that the transition temperature T_c has a minimum near x = 0.6. To clarify the origin of this behavior, we have measured specific heat and susceptibility of $Pr(Os_{1-x}Ru_x)_4Sb_{12}$ to investigate the x dependences of the excitation energies of the anharmonic oscillations of Pr ions and the 4f-electron quadrupolar excitons. Figure.1 shows the x dependences of the rattling energy Θ_E and the quadrupolar exciton energy Δ_1. While Θ_E exhibits almost no x dependence, Δ_1 increases with x, resulting in a crossing of the two energy levels at around x = 0.6. This level crossing indicates a possible bound state formation between rattling and quadrupolar excitation which may suppress superconductivity at around x = 0.6.

From low temperature specific heat along with a thermodynamical analysis, the electronic specific heat coefficient γ and $\alpha = \Delta_{sc}/k_BT$, where Δ_{sc} represents superconducting gap energy, have been extracted as shown in Fig.2. Both of the quantities show significant changes in low x regions.

These findings suggest that the 4f-electron quadrupolar excitons are responsible for the strong coupling nature of the superconductivity in $PrOs_4Sb_{12}$.

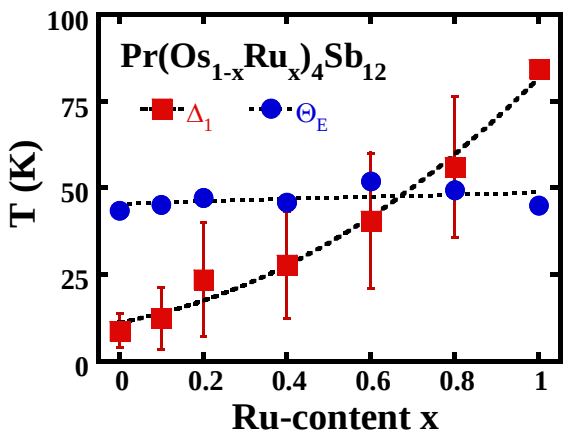

Figure 1. x dependences of 4f-electon quadrupolar exciting energy Δ_1 and rattling energy Θ_E. A level crossing appears at around x = 0.6 between the two energy levels.

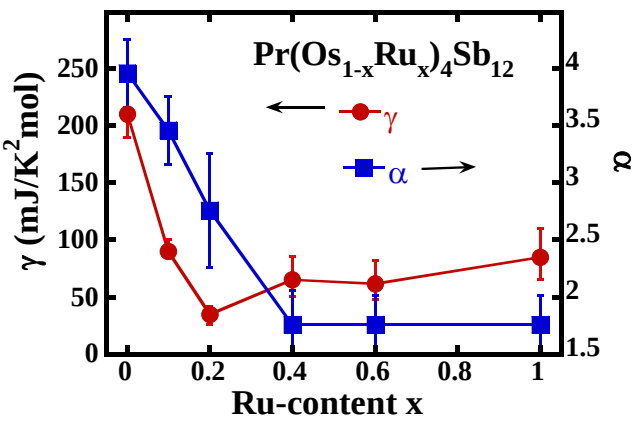

Figure 2. x dependences of electronic specific heat coefficient γ and $\alpha = \Delta_{sc}/k_BT$, where Δ_{sc} is the superconducting gap energy.

P136

Noncontact Friction by Low Temperature Lateral Force Microscopy

Kohta Saitoh, Yoshiyuki Shibayama and Keiya Shirahama

Dept. of Physics, Keio University, 3-14-1 Hiyoshi, Kohoku-ku, Yokohama-shi, Kanagawa 223-8522, Japan

Scanning probe microscopy (SPM) is one of the possible techniques that can work at very low temperatures. Low temperature SPMs allow us to explore nano scale quantum phenomena that are never unveiled by macroscopic measurement. We develop a frequency modulation-atomic force microscope (FM-AFM) using a quartz tuning fork as a force sensor. The AFM has been tested down to 1.3 K [1]. As a first application of the low temperature AFM, we investigate surface friction in the region at which a tip and a sample do not contact (‘Noncontact friction’).

Noncontact friction is one of the interesting topics in nano scale frictional study (‘Nanotribology’). Some experiments using an ultrasensitive cantilever show the existence of the noncontact friction [2]. The measured friction coefficient is 10^{-15}～10^{-13} kg/s, and the origin of this friction is regarded as a fluctuating electromagnetic field between the tip and the sample [3]. This phenomenon is, however, not fully understood and still controversial.

We oscillate the quartz tuning fork with the tip parallel to the sample surface (‘Lateral force microscopy’) at low temperatures. A thermal fluctuation and a viscosity of adsorbates are negligible at low temperatures. $NbSe_2$ is employed as a sample because of its excellent surface quality. The origin of the tip-sample distance is defined by a tunneling current measurement. Fig. 1 shows a frequency shift and energy dissipation between the tip and the sample as a function of the tip-sample distance at 4.2 K. The frequency and the dissipation have increased in a long range, and the dissipation has switched to a decrease near the sample surface. The long range behavior in the dissipation is similar to the noncontact friction observed by Stipe *et al*. The friction coefficient converted from the dissipation, however, is at least 10^{-5} kg/s and much larger than that of Stipe *et al.* The origin of this noncontact friction therefore cannot be explained by the fluctuating electromagnetic field. The increase in the frequency and a peak in the dissipation are similar to Debye relaxation. The behavior therefore can be explained by relaxation time depending on the tip-sample distance. Measurements of sample dependence are underway.

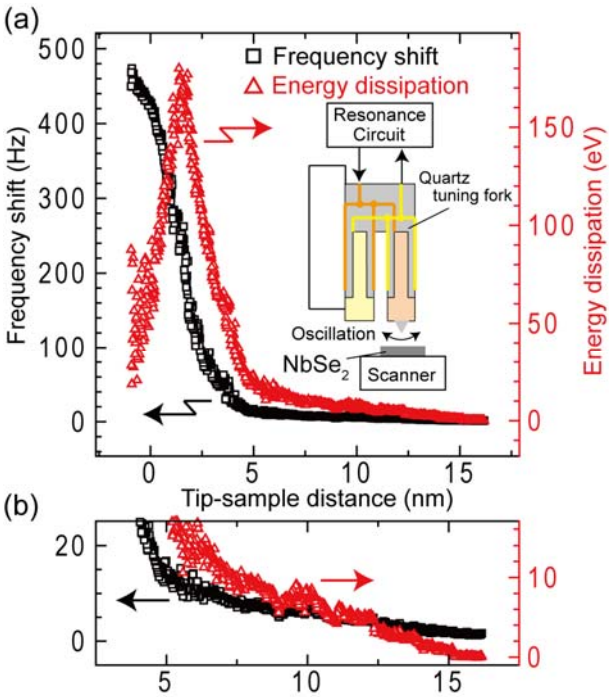

Fig. 1: (a)The frequency shift and the energy dissipation on $NbSe_2$ as a function of the tip-sample distance at 4.2 K. The inset is the principle of lateral force microscopy. (b)The expansion from 5 nm to 15 nm.

[1]K. Saitoh *et al.*, *J. Low. Temp. Phys*. **150**, 561 (2008); *J. Phys. Conf. Series*.**150**, 012039 (2009).

[2]B. C. Stipe *et al*., *Phys. Rev. Lett.* **87**, 096801 (2001).

[3]A. I. Volokitin and B. N. J. Persson, *Rev. Mod. Phys.* **79**, 1291 (2007).

P137

Development of MRI Microscope

T. Ueno,[1] T. Mizusaki,[2,3] and A. Matsubara[3]

[1]*Graduate School of Medicine, Kyoto University, 53 Kawaharacho, Shogoin, Sakyo-ku, Kyoto-shi, Kyoto 606-8507, Japan*
[2]*Toyota Physical and Chemical Research Institute, 41-1 Aza Yokomichi, Oza Nagakute, Nagakute-cho, Aichi-gun, Aichi 480-1192, Japan*
[3]*Reaserch Center for Low Tempearature and Materials Sciences, Kyoto University, Oiwakecho, Kitashirakawa, Sakyo-ku, Kyoto-shi, Kyoto 606-8502, Japan*

We have been developing an ultra high resolution MRI, "MRI microscope"[1]. The ultimate goal of our MRI microscope is to achieve 1 μm × 1 μm two dimensional spatial resolution comparable to optical microscopes. In order to obtain high resolution, lower temperature, higher magnetic field and stronger magnetic field gradients are necessary.

At low temperature and with strong magnetic field gradients, fast spin diffusion decreases signal to noise ratio. Shorter pulse interval is required so as to suppress spin diffusion effect, however, it causes a new problem that spin echo signal come to be mingled with FID signal of 2nd excitation pulse. Quadrature phase-shift keying (QPSK) technique is employed to solve the problem. Besides, at low temperature, dipole field becomes large because of strong magnetization. If dipole field is inhomogeneous, multiple spin echoes (MSE) are generated and original signal is distorted. High magnetic homogeneity is needed so as not to generate MSE. Furthermore, the high magnetic field environment may put a new limitation on MRI due to large nonlinear quantum effect of ^{3}He. At ultra low temperature and with higher magnetic field, Leggett-Rice effect makes nuclear spins of liquid ^{3}He coherent, spin wave excited and MRI images could be blurred as a result.

We constructed the MRI Microscope using a magnetic field of 7.2 T, with tri-axial magnetic field gradients of 2.0 T/m, Helmholtz transmitter coil of 5 mm diameter and 2.5 mm gap whose magnetic homogeneity in visualization area is 99.99%. We visualized the pure liquid ^{3}He in a 230 μm diameter tube to study the effect of nonlinearity on the MRI Microscope at low temperature and in high magnetic fields. An MRI image was obtained at 0.22 MPa, 1 K with 1.8 μm × 1.8 μm pixel size. At 65 mK, the MRI image became more blurred. We speculate that it was caused by large spin diffusion and nonlinearity.

We will apply this MRI microscope to image the vortex lattice of rotating superfluid ^{3}He-A phase, where the core structure does not have cylindrical symmetry if it is the double core vortex and the triangular lattice is deformed due to the uni-axial symmetry of the A phase.

[1] M. Hachiya *et al.*, J. Low Temp. Phys. **158**, 697 (2010).

P138

Dielectric breakdown accompanied by structural change in a Mott insulator Ca_2RuO_4

Mariko Sakaki, Yohei Yamauchi, Yûsaku Kimura and Fumihiko Nakamura

ADSM, Hiroshima University, Higashi-Hiroshima 739-8530, Japan.

We introduce a unique dielectric breakdown phenomenon in a 4d electron Mott insulator Ca_2RuO_4. Application of quite small electric-field of E_{th}~40V/cm induces the transition from the Mott insulating to the quasi two-dimensional metallic state at 295K. The breakdown phenomenon is accompanied by a structural transition and is understood as bulk transition. However, the value of E_{th}~40V/cm is too small to be interpreted in terms of well-known models such as Zener breakdown. We expect that a physics covered from equilibrium to nonequilibrium natures allows us to understand our findings.

P139

Transport Properties of Sr_2RuO_4 Microdevices

S. Kashiwaya,[1] H. Kambara,[1] H. Kashiwaya, [1] T. Matsumoto, [1] T. Furuta, [2] H. Yaguchi,[2] Y. Tanaka,[3] and Y. Maeno[4]

[1] *National Institute of Advanced Industrial Science and Technology (AIST), Tsukuba 305-8568*
[2] *Department of Physics, Faculty of Science and Technology, Tokyo University of Science, Noda 278-8510*
[3] *Department of Applied Physics, Nagoya University, Nagoya 464-8603*
[4] *Department of Physics, Kyoto University, Kyoto 606-8502*

Strontium ruthenate Sr_2RuO_4 (SRO) has been accepted as one of the most plausible candidates for spin-triplet chiral *p*-wave state ($p_x \pm ip_y$) with broken time reversal symmetry based on various experimental tests[1]. Several peculiar properties, such as chiral domain, edge states formation and the stable existence of half flux quanta, are theoretically predicted for the chiral *p*-wave superconductors. Examining these properties using microfabricated devices of SRO are important issues for superconducting physics. On the other hand, superconducting SRO films have not been successfully synthesized because of extremely fragility of the superconductivity for defects and impurities. Therefore, superconducting device fabrication using conventional lithography method cannot be applied for SRO. Here we report the development of microdevice fabrication of SRO using focused ion beam (FIB) from single crystals and the transport properties observed in these microdevices.

Fabricated SRO-based devices are shown in the figures1. We carefully evaluated the degradation due to Ga ion radiation during the fabrication process. The minimum device size based on the present process was about 2 mm, which suggests the degraded layer of 1mm thickness inevitably exists at the etched surface. However, the observation of superconductivity in micro-fabricated devices indicates that the damage is restricted to the surface area and that the crystallinity inside the devices keeps high quality. Various peculiar transport properties, such as chiral domain motion [2], possible edge channel formation and the Josephson effect, have been observed in these devices. Details of these results will be presented.

[1] A. P. Mackenzie and Y. Maeno, Rev. Mod. Phys. **75**, 657 (2003).
[2] H. Kambara, S. Kashiwaya, H. Yaguchi, Y. Asano, Y. Tanaka, and Y. Maeno, Phys. Rev. Lett. **101**, 267003 (2008).

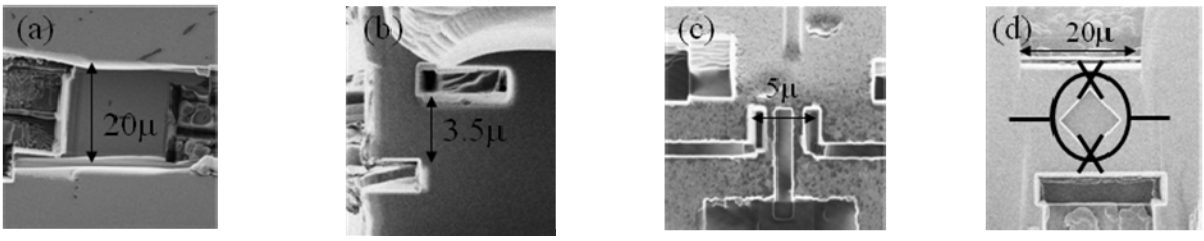

FIG.1: (a) A scanning ion microscope image of microbridge of Sr_2RuO_4 to detect the edge states formation. (b) c-axis weak link bridge to estimate the anisotropy and the Josephson effect, (c) T-shaped junction to detect the proximity effect and the odd frequency Cooper pairs, (d) DC-SQUID to detect the half flux quantum..

List of Participants

List of Participants

(registered until February 23)

Adachi, Hiroki M.	Okayama University	hiroki@mp.okayama-u.ac.jp	P85
Akiyama, Koki	Tokyo Institute of Technology	tsunays@yahoo.co.jp	
Aoki, Yuji	Tokyo Metropolitan University	aoki@tmu.ac.jp	P134
Arahata, Emiko	Tokyo University of Science	a1208702@rs.kagu.tus.ac.jp	P80
Arai, Toshikazu	Kyoto University	toshikaz@scphys.kyoto-u.ac.jp	P9
Arikawa, Mitsuhiro	University of Tsukuba	arikawa@sakura.cc.tsukuba.ac.jp	P3
Asano, Yasuhiro	Hokkaido University	asano@eng.hokudai.ac.jp	P122
Bagnato, Vanderlei S.	IFSC, Univeristy of Sao Paulo	vander@ifsc.usp.br	O2
Balibar, Sébastien	ENS and CNRS	balibar@lps.ens.fr	O11
Chung, Suk Bum	Stanford University	sbchung@stanford.edu	O35
Ebisawa, Hiromichi	Tohoku University	ebi@mail.tains.tohoku.ac.jp	
Eggel, Thomas E.	University of Tokyo	et@issp.u-tokyo.ac.jp	P63
Endo, Yuki	Tokyo University of Science	a1208705@rs.kagu.tus.ac.jp	P93
Fisher, Shaun N.	Lancaster University	s.fisher@lancaster.ac.uk	O34
Fujihara, Yusuke	Kyoto University	fujihara@scphys.kyoto-u.ac.jp	P78
Fujiyama, Shigeki	RIKEN	fujiyama@riken.jp	P29
Fujiyama, Shoji	Osaka City University	fujiyama@sci.osaka-cu.ac.jp	P75
Fukuda, Akira	Hyogo College of Medicine	fuku@hyo-med.ac.jp	P5
Fukuyama, Hidetoshi	Tokyo University of Science	fukuyama@rs.kagu.tus.ac.jp	
Fukuyama, Hiroshi	The University of Tokyo	hiroshi@phys.s.u-tokyo.ac.jp	O23
Fuseya, Yuki	Osaka University	fuseya@mp.es.osaka-u.ac.jp	P130
Giamarchi, Thierry	University of Geneva	Thierry.Giamarchi@unige.ch	O16
Golov, Andrei I.	The University of Manchester	golov@man.ac.uk	O3
Golubov, Alexander A.	University of Twente	a.a.golubov@utwente.nl	O44
Hamamoto, Nobukuni	Niigata University	hamamoto@cais.niigata-u.ac.jp	P90
Harada, Taiyo	Nagoya University	mikan_f5pnn@yahoo.co.jp	P39
Hatsugai, Yasuhiro	University of Tsukuba	y.hatsugai@gmail.com	O29
Hayashi, Masahiko	Akita University	m-hayashi@ed.akita-u.ac.jp	P20
Hieda, Mitsunori	Nagoya University	hieda@cc.nagoya-u.ac.jp	P59
Higashitani, Seiji	Hiroshima University	seiji@minerva.ias.hiroshima-u.ac.jp	O39
Higo, Tomoya	The University of Tokyo	higo@issp.u-tokyo.ac.jp	P45
Hirano, Takuya	Gakushuin University	takuya.hirano@gakushuin.ac.jp	O32
Hirashima, Dai	Nagoya University	dai@slab.phys.nagoya-u.ac.jp	O10
Ho, Tin-Lun	The Ohio State University	jasontlho@gmail.com	O31
Horie, Naoki	The University of Tokyo	horie@issp.u-tokyo.ac.jp	P131
Iinuma, Satoshi	Keio university	fr050111@z6.keio.jp	
Ikeda, Hiroaki	Kyoto university	hiroaki@scphys.kyoto-u.ac.jp	P120
Imada, Masatoshi	The University of Tokyo	imada@ap.t.u-tokyo.ac.jp	O15
Imamura, Takeo	Tokyo Metropolitan University		
Ishida, Kenji	Kyoto University	kishida@scphys.kyoto-u.ac.jp	P119
Ishikawa, Osamu	Osaka City University	ishikawa@sci.osaka-cu.ac.jp	O36
Ishimoto, Hidehiko	RIKEN	ishimoto@issp.u-tokyo.ac.jp	P32
Ishizuka, Hiroaki	The University of Tokyo	ishizuka@aion.t.u-tokyo.ac.jp	P16
Iye, Yasuhiro	The University of Tokyo	iye@issp.u-tokyo.ac.jp	
Kado, Ryusuke	Osaka City University	kadoryu@sci.osaka-cu.ac.jp	P106

Kambara, Hiroshi	Advanced Industrial Science and Technology (AIST)	h.kambara@aist.go.jp	O42
Kaneko, Ryui	The University of Tokyo	rkaneko@solis.t.u-tokyo.ac.jp	P48
Kanemoto, Masatomo	The University of Kyoto	kanemoto@scphys.kyoto-u.ac.jp	P111
Kanoda, Kazushi	University of Tokyo	kanoda@ap.t.u-tokyo.ac.jp	P27
Karaki, Yoshitomo	University of Tokyo	karaki@issp.u-tokyo.ac.jp	P116
Kasamatsu, Kenichi	Kinki University	kenichi@phys.kindai.ac.jp	P100
Kashimura, Takashi	Keio University	t.kashimura@a3.keio.jp	P82
Kashiwaya, Satoshi	National Institute of Advanced Industrial Science and Technology	s.kashiwaya@aist.go.jp	P139
Kato, Chiaki	Osaka City University	c.kato@sci.osaka-cu.ac.jp	P107
Kato, Yusuke	The University of Tokyo	yusuke@phys.c.u-tokyo.ac.jp	P81
Kawai, Naoki F.	The University of Tokyo	kawai@kelvin.phys.s.u-tokyo.ac.jp	P1
Kawakami, Norio	Kyoto University	norio@scphys.kyoto-u.ac.jp	P92
Kawakami, Takuto	Okayama University	kawakami@mp.okayama-u.ac.jp	P110
Kim, Eun-Seong	KAIST	eunseong@kaist.edu	O12
Kiriyama, Hajime	The University of Electro-Communications	kiriyama@phys.uec.ac.jp	P62
Kittaka, Shunichiro	Kyoto University	kittaka@scphys.kyoto-u.ac.jp	P121
Kiyota, Shuichiro	Nagoya University	kiyota.shuuichiro@g.mbox.nagoya-u.ac.jp	P69
Kobayashi, Hajime	University of Electro-Communications	hajime@phys.uec.ac.jp	P56
Kobayashi, Keigo	Kyushu University	kobayashi@stat.phys.kyushu-u.ac.jp	P42
Kobayashi, Kenji	Chiba Institute of Technology	koba@sun.it-chiba.ac.jp	P125
Kobayashi, Michikazu	The University of Tokyo	michikaz@cat.phys.s.u-tokyo.ac.jp	P84
Kobayashi, Shingo	Tokyo Institute of Technolory	shingo@cat.phys.s.u-tokyo.ac.jp	
Koga, Aaron M.	Keio University	aaronkoga@z2.keio.jp	P54
Koga, Akihisa	Tokyo Institute of Technology	koga@phys.titech.ac.jp	P79
Kogure, Takayuki	Keio University	kogure@a5.keio.jp	P53
Kohno, Masanori	National Institute for Materials Science	KOHNO.Masanori@nims.go.jp	P44
Kono, Kimitoshi	RIKEN	kkono@riken.jp	
Koshio, Akane	Gakushuin Univercity	koshio@qo.phys.gakushin.ac.jp	
Kriener, Markus	Kyoto University	mkriener@scphys.kyoto-u.ac.jp	P127
Kubo, Kenn	Aoyama Gakuin University	kubo@phys.aoyama.ac.jp	
Kubota, Minoru	The University of Tokyo	kubota@issp.u-tokyo.ac.jp	P49
Kunimi, Masaya	The University of Tokyo	kunimi@vortex.c.u-tokyo.ac.jp	P52
Leggett, Anthony J.	University of Illinois at Urbana-Champaign	aleggett@illinois.edu	O33
Lhuillier, Claire	University Pierre and Marie Curie	claire.lhuillier@upmc.fr	O27
Machida, Kazushige	Okayama University	machida@mp.okayama-u.ac.jp	
Machida, Masahiko	Japan Atomic Energy Agency	machida.masahiko@jaea.go.jp	O5
Maeno, Yoshiteru	Kyoto Univerisity	maeno@scphys.kyoto-u.ac.jp	O41
Marmorini, Giacomo	Keio University	giacomo@phys-h.keio.ac.jp	
Masaki, Akiko	Tokyo Metropolitan University	masaki-akiko@ed.tmu.ac.jp	P26
Masumoto, Ryota	Tokyo Institute of Technology	masumoto.r.ac@m.titech.ac.jp	P36
Masutomi, Ryuichi	The University of Tokyo	masutomi@phys.s.u-tokyo.ac.jp	P30
Masuyama, Yuta	Gakushuin University	masuyama@qo.phys.gakushuin.ac.jp	
Matsui, Kouta	The University of Tokyo	kmatsui@kelvin.phys.s.u-tokyo.ac.jp	
Matsui, Tomohiro	The University of Tokyo	matsui@kelvin.phys.s.u-tokyo.ac.jp	P2
Matsumoto, Yosuke	The University of Tokyo	matsumoto@issp.u-tokyo.ac.jp	P25

Matsuo, Sadashige	The University of Tokyo	matsuo@kelvin.phys.s.u-tokyo.ac.jp	P126
Matsushita, Taku	Nagoya University	matsushita@cc.nagoya-u.ac.jp	P61
Minato, Yusuke	The University of Nagoya	minato.yusuke@b.mbox.nagoya-u.ac.jp	P64
Minoguchi, Tomoki	The University of Tokyo	mino@phys.c.u-tokyo.ac.jp	P55
Misawa, Takahiro	The University of Tokyo	misawa@solis.t.u-tokyo.ac.jp	P24 P43
Miura, Takehide	Aoyama Gakuin University	raumiemi@gmail.com	P37
Miura, Yukie	Osaka City University	miuray@sci.osaka-cu.ac.jp	P77
Miwa, Izumi	Gakushuin University	miwa@qo.phys.gakushuin.ac.jp	
Miyagawa, Kazuya	University of Tokyo	kazuya@ap.t.u-tokyo.ac.jp	O20
Miyake, Kazumasa	Osaka University	miyake@mp.es.osaka-u.ac.jp	O40
Miyamoto, Noboru	Tokyo Metropolitan University	miyamoto-noboru@ed.tmu.ac.jp	
Miyazaki, Ryoichi	Tokyo Metropolitan University	miyazaki-ryoichi@ed.tmu.ac.jp	P135
Mizusaki, Takao	Toyota Physical and Chemical Research Institute	mizusaki@scphys.kyoto-u.ac.jp	
Mizushima, Takeshi	Okayama University	mizushima@mp.okayama-u.ac.jp	P112 P115
Momoi, Tsutomu	RIKEN	momoi@riken.jp	O26
Mori, Shigeo	Osaka Prefecture University	mori@mtr.osakafu-u.ac.jp	
Morikawa, Tomoki	Kyoto University	morikawa@scphys.kyoto-u.ac.jp	P8
Morishita, Masashi	University of Tsukuba	morishit@sakura.cc.tsukuba.ac.jp	P33 P34
Motohashi, Atsushi	Tokyo University of Science	j1208710@ed.kagu.tus.ac.jp	P99
Motome, Yukitoshi	The University of Tokyo	motome@ap.t.u-tokyo.ac.jp	O17
Murakawa, Satoshi	Keio university	murakawa@phys.keio.ac.jp	P108 P113
Nagai, Katsuhiko	Hiroshima University	nagai@minerva.ias.hiroshima-u.ac.jp	
Nago, Yusuke	Osaka City University	ynago@sci.osaka-cu.ac.jp	P72 P73
Naidon, Pascal	The University of Tokyo	pascal@cat.phys.s.u-tokyo.ac.jp	P101
Nakagawa, Ryoji	Kyoto University	nakagawa@scphys.kyoto-u.ac.jp	P123
Nakamikawa, Kyoya	The University of Tokyo	nakamikawa@aion.t.u-tokyo.ac.jp	P15
Nakamura, Fumihiko	Hiroshima University	fumihiko@hiroshima-u.ac.jp	O43
Nakamura, Sachiko	The University of Tokyo	nakamura@kelvin.phys.s.u-tokyo.ac.jp	P35
Nakashima, Yuna	The University of Nagoya	nakashima.yuna@a.mbox.nagoya-u.ac.jp	P66
Nakatsuji, Satoru	The University of Tokyo	satoru@issp.u-tokyo.ac.jp	O19
Negishi, Yuu	Keio University	y.n@a6.keio.jp	
Nishi, Kazuhisa	Toyohashi University of Technology	nishi@eco.tut.ac.jp	
Nomura, Kiyohide	Kyushu University	knomura@stat.phys.kyushu-u.ac.jp	P12
Nomura, Ryuji	Tokyo Institute of Technology	nomura@ap.titech.ac.jp	O38
Nomura, Takuji	Japan Atomic Energy Agency	nomurat@spring8.or.jp	P117
Numasato, Ryu	Osaka City University	numasato@sci.osaka-cu.ac.jp	P74
Obara, Ken	Osaka City Universirty	obara@sci.osaka-cu.ac.jp	P105
Oda, Takuya	The University of Nagoya	oda.takuya@a.mbox.nagoya-u.ac.jp	P58
Ogata, Masao	University of Tokyo	ogata@phys.s.u-tokyo.ac.jp	O24
Oi, Makito	Senshu University	m.oi@isc.senshu-u.ac.jp	
Okada, Akihisa	Osaka University	okada@blade.mp.es.osaka-u.ac.jp	P133

Okamoto, Kiyomi	Tokyo Institute of Technology	kokamoto@phys.titech.ac.jp	P41
Okamoto, Tohru	The University of Tokyo	okamoto@phys.s.u-tokyo.ac.jp	
Okuda, Yuichi	Tokyo Institute of Technology	okuda@ap.titech.ac.jp	O6
Onishi, Naoki	University of Tokyo and Yamanashi University	onishi@sunny.ocn.ne.jp	
Onoda, Shigeki	RIKEN	s.onoda@riken.jp	P19
Osheroff, Douglas D.	Stanford University	osheroff@stanford.edu	O22
Ozaki, Takeshi	Tokyo University of Science	j1209702@ed.kagu.tus.ac.jp	P95
Peets, Darren C.	Kyoto University	dpeets@scphys.kyoto-u.ac.jp	P128
Phuc, Nguyen T.	The University of Tokyo	littlefutt_85@yahoo.com	
Sahashi, Kazuhiro	The University of Nagoya	sahashi.kazuhiro@g.mbox.nagoya-u.ac.jp	P68
Saito, Hiroki	The University of Electro-Communications	hsaito@pc.uec.ac.jp	P83
Saitoh, Kohta	Keio University	kotas@phys.keio.ac.jp	P136
Saitoh, Masamichi	University of Tsukuba	saitoh@lt.px.tsukuba.ac.jp	P109
Sakai, Shiro	Vienna University of Technology	sakaishiro@gmail.com	P13
Sakai, Toru	JAEA	sakai@spring8.or.jp	P47
Sakaki, Mariko	Hiroshima University	M085386@hiroshima-u.ac.jp	P138
Sasaki, Kohei	The University of Tokyo	sasaki@dolphin.phys.s.u-tokyo.ac.jp	P4
Sasaki, Yutaka	Kyoto University	sasaki@scphys.kyoto-u.ac.jp	O13
Sato, Daisuke	The University of Tokyo	sato@kelvin.phys.s.u-tokyo.ac.jp	P31
Sato, Masahiro	RIKEN	sato-m@riken.jp	P40
Saunders, John	Royal Holloway University of London	j.saunders@rhul.ac.uk	O21
Sawada, Anju	Kyoto University	sawada@ltm.kyoto-u.ac.jp	P7
Sebastian, Suchitra	University of Cambridge	ses59@cam.ac.uk	O18
Sekine, Sawako	Gakushuin University	sekine@qo.phys.gakushuin.ac.jp	
Shibato, Ryosuke	Tokyo Metropolitan University	shibato-ryosuke@ed.tmu.ac.jp	P89
Shibayama, Yoshiyuki	Keio University	yshibaya@phys.keio.ac.jp	O14
Shinaoka, Hiroshi	The University of Tokyo	shinaoka@issp.u-tokyo.ac.jp	P21
Shirahama, Keiya	Keio University	keiya@phys.keio.ac.jp	O7 P70
Suga, Seiichiro	University of Hyogo	suga@eng.u-hyogo.ac.jp	P94
Suzuki, Kenta M.	Okayama University	kenta@mp.okayama-u.ac.jp	P129
Suzuki, Masaru	University of Electro-Communications	suzuki@phys.uec.ac.jp	O8
Suzuki, Naoya	University of Electro-Communications	suzuki@hs.pc.uec.ac.jp	P97
Taguchi, Yoshihisa	Gakushuin University	tagtone@gmail.com	P87
Taie, Shintaro	Kyoto University	taie@scphys.kyoto-u.ac.jp	P104
Takagi, Takeo	University of Fukui	takagi@apphy.u-fukui.ac.jp	O25
Takahashi, Daisuke	RIKEN	dtakahashi@riken.jp	P76
Takahashi, Daisuke	The University of Tokyo	takahashi@vortex.c.u-tokyo.ac.jp	P98
Takahashi, Kota	Kyushu University	takahashi@stat.phys.kyushu-u.ac.jp	P38
Takayoshi, Shintaro	The University of Tokyo	shintaro@issp.u-tokyo.ac.jp	P10
Takenaka, Koshi	Nagoya University	takenaka@nuap.nagoya-u.ac.jp	
Takeuchi, Hiromitsu	Osaka City University	hiromitu@sci.osaka-cu.ac.jp	P102
Tamura, Masafumi	Tokyo University of Science	qra_tam@ph.noda.tus.ac.jp	P46
Tanabe, Tatsuyoshi	Gakushuin University	tanabe@qo.phys.gakushuin.ac.jp	P86
Tanaka, Yukio	Nagoya University	ytanaka@nuap.nagoya-u.ac.jp	O45
Taniguchi, Junko	The University of Electro-Communications	tany@phys.uec.ac.jp	P65

Tenya, Kenichi	Shinshu University	tenya@shinshu-u.ac.jp	P118
Tezuka, Masaki	Kyoto University	tezuka@scphys.kyoto-u.ac.jp	P91
Toda, Ryo	Kyoto University	rftoda@scphys.kyoto-u.ac.jp	P50
Tojo, Satoshi	Gakushuin University	satoshi.tojo@gakushuin.ac.jp	P88
Tsubota, Makoto	Osaka City University	tsubota@sci.osaka-cu.ac.jp	O1
Tsuchiya, Shunji	Keio University	tsuchiya@rk.phys.keio.ac.jp	P103
Tsukamoto, Mitsuaki	Osaka City University	mitsuaki@sci.osaka-cu.ac.jp	P60
Tsunetsugu, Hirokazu	University of Tokyo	tsune@issp.u-tokyo.ac.jp	O28
Tsutsumi, Yasumasa	Okayama University	tsutsumi@mp.okayama-u.ac.jp	P114
Udagawa, Masafumi	The University of Tokyo	udagawa@ap.t.u-tokyo.ac.jp	P11
			P22
Ueda, Masahito	The University of Tokyo	ueda@phys.s.u-tokyo.ac.jp	O30
Ueno, Tomohiro	Kyoto University	ueno@hs.med.kyoto-u.ac.jp	P137
Wada, Nobuo	Nagoya University	nwada@cc.nagoya-u.ac.jp	O9
Wasai, Masahiro	Tokyo Institute of Technology	wasai.m.aa@m.titech.ac.jp	P57
Watabe, Shohei	The University of Tokyo	watabe@vortex.c.u-tokyo.ac.jp	P96
Watanabe, Ryota	Keio University	fr042323@z3.keio.jp	
Watanabe, Shinji	Osaka University	swata@mp.es.osaka-u.ac.jp	P23
Yaguchi, Hiroshi	Tokyo University of Science	hy@ph.noda.tus.ac.jp	
Yamaguchi, Akira	University of Hyogo	yamagu@sci.u-hyogo.ac.jp	O37
Yamaji, Youhei	The University of Tokyo	yamaji@solis.t.u-tokyo.ac.jp	P28
Yamamoto, Atsushi	Osaka University	yamamoto@tp.ap.eng.osaka-u.ac.jp	
Yamamoto, Keisuke	The University of Tokyo	yamamoto@spin.phys.s.u-tokyo.ac.jp	P51
Yamanaka, Naoki	Keio University	nyam@z5.keio.jp	P71
Yamashita, Kouhei	Nagoya University	kouhei@s.phys.nagoya-u.ac.jp	P67
Yanase, Youichi	Niigata University	yanase@phys.sc.niigata-u.ac.jp	P124
Yano, Hideo	Osaka City University	hideo@sci.osaka-cu.ac.jp	O4
Yasunaga, Masashi	Osaka City University	yasunaga@sci.osaka-cu.ac.jp	
Yokoyama, Hisatoshi	Tohoku University	yoko@cmpt.phys.tohoku.ac.jp	P14
Yonezawa, Shingo	Kyoto University	yonezawa@scphys.kyoto-u.ac.jp	P132
Yoshioka, Yu	Osaka University	yoshioka@blade.mp.es.osaka-u.ac.jp	P18
Yoshitake, Junki	The University of Tokyo	yoshitake@aion.t.u-tokyo.ac.jp	P17
Zheng, Yangdong	Kyoto University	yd_zheng@ltm.kyoto-u.ac.jp	P6

International Symposium on Physics of New Quantum Phases in Superclean Materials (PSM2010)

国際シンポジウム「スーパークリーン物質で実現する新しい量子相の物理(PSM2010)」

Published : March 8, 2010

Publisher : Hiroshi Fukuyama, The University of Tokyo
7-3-1 Hongo, Bunkyo-ku, Tokyo 113-0033, Japan

Editors : Osamu Ishikawa, Osaka City University
Tomohiro Matsui, The University of Tokyo

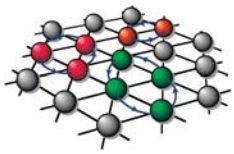

Cover layout : Kayoko Ogita
Cover photo : YAKEI JAPAN Masamitsu Kimura

PSM2010 Time Table

Time	March 8 (Mon)	March 9 (Tue)	March 10 (Wed)	March 11 (Thu)	March 12 (Fri)	Time
9:00		9:00 Registration				9:00
		9:30 Opening	**S 5** 9:30 M. Imada	**S 9** 9:30 M. Ueda	**S12** 9:30 Y. Maeno	
10:00		**S 1** 9:50 M. Tsubota 10:20 V. Bagnato	10:00 T. Giamarchi 10:30 Y. Motome	10:00 T-L. Ho 10:30 T. Hirano	10:00 H. Kambara 10:20 F. Nakamura	10:00
		10:50-11:10 Break	10:50-11:10 Break	10:50-11:10 Break	10:40-11:00 Break	
11:00		**S 2** 11:10 A. Golov 11:40 H. Yano	**S 6** 11:10 S. Sebastian 11:40 S. Nakatsuji	**S10** 11:10 A. Leggett (PSM lecture) 11:50 S. Fisher	**S13** 11:00 A. Golubov 11:30 Y. Tanaka	11:00
12:00		12:00 M. Machida 12:20 Y. Okuda	12:00 K. Miyagawa 12:20 J. Saunders	12:20 S-B. Chung	11:50-12:20 Closing	12:00
13:00		12:50-14:10 Lunch	12:50-14:10 Lunch	12:50-14:00 Lunch		13:00
14:00		**S 3** 14:10 K. Shirahama 14:40 M. Suzuki	**S 7** 14:10 D. Osheroff (PSM lecture) 14:40 H. Fukuyama	**S11** 14:00 O. Ishikawa 14:30 A. Yamaguchi 14:50 R. Nomura		14:00
15:00		15:00 N. Wada 15:30 D. Hirashima	15:10 M. Ogata 15:30 T. Takagi	15:10 S. Higashitani 15:30 K. Miyake		15:00
16:00		15:50-16:20 Break	15:50-16:20 Break			16:00
		S 4 16:20 S. Balibar 16:50 E-S. Kim	**S 8** 16:20 T. Momoi 16:50 C. Lhullier	16:30 meeting at Osanbashi Terminal		
17:00		17:20 Y. Sasaki 17:40 Y. Shibayama	17:20 H. Tsunetsugu 17:40 Y. Hatsugai	17:00-19:00 Banquet (Yokohama Bay Dinner Cruise)		17:00
18:00	18:00-20:00 Registration and Welcome Party	**P 1** 18:00-20:00 Poster Session (odd numbers)	**P 2** 18:00-20:00 Poster Session (even numbers)			18:00
19:00						19:00
20:00						20:00